CHARACTERIZATION OF PEDIATRIC OCULAR MATERIAL PROPERTIES FOR IMPLEMENTATION IN FINITE ELEMENT MODELING

by

Jami Marie Saffioti

A dissertation submitted to the faculty of
The University of Utah
in partial fulfillment of the requirements for the degree of

Doctor of Philosophy

Department of Mechanical Engineering

The University of Utah

August 2014

The University of Utah Graduate School

STATEMENT OF DISSERTATION APPROVAL

The dissertation of **Jami Marie Saffioti**

has been approved by the following supervisory committee members:

Brittany Coats	, Chair	**6/9/2014** Date Approved
Kenneth Monson	, Member	**6/9/2014** Date Approved
Andrew Merryweather	, Member	**6/9/2014** Date Approved
Kenneth L. DeVries	, Member	**6/9/2014** Date Approved
Robert Hoffman	, Member	**6/10/2014** Date Approved

and by **Tim Ameel**, Chair of

the Department of **Mechanical Engineering**

and by David B. Kieda, Dean of The Graduate School.

ABSTRACT

Abusive head trauma (AHT) is a prominent cause of death and disability in children in the United States. Retinal hemorrhage (RH) is often used to diagnose AHT, but injury mechanisms and thresholds are unknown. One goal of our research is to develop a finite element (FE) model of the human infant eye to evaluate changes in retinal stress and strain during infant head trauma. However, there are no published data characterizing age-dependent material properties of ocular tissues.

To characterize age and strain-rate dependent properties, we tested sclera and retina from preterm, infant, and adult sheep according to two uniaxial tensile test protocols. In general, scleral strength decreased with age, whereas no age effect was found for the retina. Sclera and retina had a stiffer elastic response when tested at higher strain-rates. Anterior sclera was stiffer than posterior sclera.

In preparation to collect human tissue, viable storage techniques and postmortem time frames for material testing were determined. Pediatric scleral specimens were evaluated up to 24 hours postmortem. Retinal and scleral fresh, frozen-then-thawed, and fixed specimens were also evaluated. Adult sclera maintains its integrity for 24 hours, but immature sclera softened after 10 hours postmortem. Freezing then thawing had minimal effect on the material properties of retina and sclera suggesting this may be a suitable shipping method for the pediatric ocular tissues.

The mechanical data were used to determine appropriate constitutive models for

the sclera and retina. The material models were implemented into a FE model of the eye and validated against experimental ocular inflation tests. Finally, a whole model was generated to represent an infant eye subjected to shaking. Vitreoretinal interaction parameters were varied to analyze the changes in retinal stress and strain. Interaction parameters minimally affected retinal stress and strain. Overall, the equatorial retina experienced the greatest stress and strain. Stress and strain increased with the addition of shaking cycles. The anterior retina experienced greater strain than the posterior region after the first cycle and for the remaining rotation sequence. With additional refinement, these models will be valuable to investigate potential injury mechanisms of RH and potentially differentiate abuse-related RH.

TABLE OF CONTENTS

ACKNOWLEDGEMENTS

This dissertation work was by no means a sole effort. I must recognize key people who have contributed a great deal of support throughout this project. First, I would like to express my gratitude for the guidance provided by my graduate advisor, Brittany Coats. Thank you, Brittany, for all of your patience and devotion to my work and success. I have matured as an engineer and developed a new work ethic under your supervision.

Next, I would like to recognize my fellow peers in the Pediatric Injury Biomechanics Laboratory. It has been an honor to work alongside such a brilliant and motivated research group. Not only will I remember my lab members as amazing colleagues, but I have gained lifelong friends.

Thank you, MarJanna Dahl and the rest of the Albertine Laboratory for providing assistance in obtaining all of our ocular specimens. And a huge 'thank you' to the Knights Templar Eye Foundation for their funding support.

Last, but most important, I want to acknowledge my family for the abundance of love and care they have given me throughout this program. Although they may not fully understand my research, they understood my frustration at times and never stopped encouraging me to persevere and do the best that I could. I love you, Mama, Dad, Darren and Jonathan, so very much. And of course, I love you, Joe. You are my rock and have kept me focused on the end goal of all of our hard work and efforts.

INTRODUCTION

Abusive Head Trauma

Abusive head trauma (AHT) is a leading cause of death and disability in children in the United States.[3,5,6,17] During diagnosis of AHT, intracranial and intraocular hemorrhages are carefully considered for their consistency with the provided medical history. Retinal hemorrhage (RH), bleeding from the blood vessels in the retina, is commonly present with AHT (Figure 1). RH injuries have been reported in 78-85% of AHT cases.[13,14] However, RH has also been reported in 0-20% of accidental trauma cases[14] and since the underlying injury mechanism of RH is unclear, presence of RH cannot definitely discern abuse.

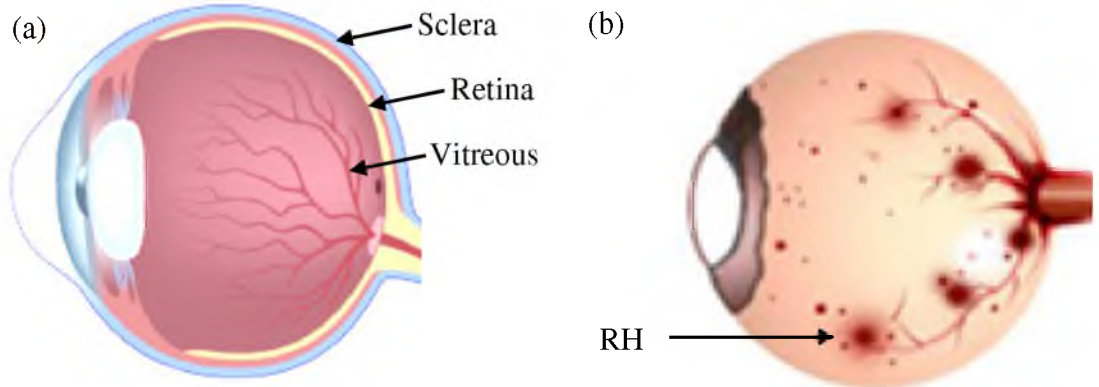

Modified image from – www.alilamedicalimages.com

Modified image from – dontshake.org.

Figure 1: Ocular anatomy and abuse-related injury. (a) The sclera is the tough, outer-protective layer of the eye. The retina is the layered tissue lining the inner surface that houses the photoreceptor cells used for vision. Immediately interior to the retina is the vitreous. (b) Retinal hemorrhage is the condition in which bleeding occurs in the retina, and is commonly associated with abusive head trauma.

Etiology of RH typically identified with AHT cases is widespread, multilayered RH, with bilateral formation (RH occurring in both right and left sides).[2,9,11,15,20] RH from nonabusive cases are typically identified as fewer in number and unilateral.[1] The exact mechanism for RH is unknown. One theory, however, is that during rapid head rotations, the vitreous, lying immediately inside and firmly attached to the retina, pulls on the retina, causing retinal traction or vitreoretinal detachment. Unfortunately, the only research to date are clinical epidemiology studies and witness accounts, which do not offer any evidence regarding the biomechanics of RH. A thorough understanding of ocular mechanics and RH injury mechanisms will be invaluable to clinical diagnoses, proper legal rulings, and prevention of repeated abuse incidences.

Computational Modeling

Finite element (FE) modeling may be a useful tool for analyzing the mechanical responses of the pediatric eye during traumatic events. Models may shed light on injury thresholds and mechanisms of RH, and provide data that can assist clinicians in differentiating injuries from accidental and abusive head trauma. Through computational modeling we will be able to better assess retinal stress and strain experienced during kinematic loading conditions.

Currently, there are two FE models of the pediatric eye in the literature. Hans et al. generated a pediatric eye model comparing the retinal force experienced from shaking to that of an impact pulse. Their results suggest that shaking alone is capable of causing retinal stresses high enough for RH.[10] The other FE model by Ranganrajan et al. had a simplified ocular geometry and was used to evaluate the influence of the vitreous and

extraocular fat on retinal stress and stress distribution. The prescribed angular acceleration was similar to shaking. They concluded that accurately modeling the vitreous has a significant influence on the retina, and that peak stresses occurred in the posterior retina.[18] In both of these studies, ocular material property data were based on adult material properties, and the potential for mechanical changes in the developing eye was neglected.

The primary reason current pediatric eye models use adult ocular material property data is due to its absence in the literature. To date, there are only two studies investigating changes in ocular properties with age. Krag et al. previously characterized the age-related mechanical differences in human anterior lens capsule from donors 7 months to 98 years old, and found a decrease in strength with age.[12] Curtin et al. assessed differences in the mechanical response of premature, child (4 - 6 years old) and adult human sclera and found that the adult posterior sclera is more extensible than the younger groups. An inverse age-relation was seen for the anterior and equatorial sclera.[4] These studies, and other studies conducted in our lab, indicate that there are developmental changes in many ocular tissues, and pediatric ocular tissues must be mechanically characterized in order to build accurate FE models for pediatric vision research.

Research Objective

In this study, we set out to develop the first pediatric eye FE model that incorporates age-appropriate material property data. Vitreous has been characterized previously in our lab, so our efforts were focused on characterizing the pediatric sclera and retina. The sclera is the strong outer layer of the eye (Figure 1). Its function is to protect the eye by providing resistance to intraocular pressure, and more importantly, retinal deformation. The retina is

the innermost layer of the eye and houses the light-sensitive, photoreceptor cells used for vision. The biomechanical behavior of ocular tissues is likely complex with both hyperelastic and viscoelastic material responses. Careful consideration of these characteristics must be taken into account when exploring the mechanical nature of ocular tissues through experimental testing.

The ultimate goal of this dissertation research was to mechanically characterize the age-dependent material properties of the sclera and retina in order to determine appropriate constitutive models to implement into a FE model of the infant eye for assessing retinal stress and strain. To achieve this goal, we performed material property testing (Chapters 1, 2), assessed storage and testing time frames for the collection of pediatric ocular specimens (Chapter 3), developed and validated a computational model of the pediatric eye (Chapter 4), and used the data to generate an overall infant eye model to investigate the influence of vitreoretinal adhesion on retinal stress and strain (Chapter 5). Combined, these studies significantly advance the state of knowledge of pediatric ocular mechanics, and lend insight into mechanical parameters influential in predicting retinal stress and strain from repetitive head trauma.

Chapter Structure

Chapter 1 details the collection and preparation, mechanical testing procedures, as well as data processing and analysis of ovine scleral samples. Human pediatric ocular tissues are limited, so ovine ocular tissue were selected to evaluate a potential age, strain, and strain-rate dependent response. Ovine sclera from premature, infant (3 days – 6 weeks), and adult ($\geq$ 4 years) human-equivalent age groups were tested in uniaxial tension

according to two testing protocols. A small strain and low strain-rate test protocol was implemented to measure the scleral response to physiologic increased intraocular pressure. A large strain and high strain-rate test protocol was implemented to measure the scleral response to trauma. To evaluate possible regional effects on the material properties, tissue was tested from the anterior and posterior regions of the sclera.

Chapter 2 describes the collection, testing, and analysis of ovine retinal samples. Age and strain-rate dependent material properties were evaluated in retina from immature (0– 6 weeks) and mature ($\geq$ 4 years) ovine eyes. Specimens were tested according to high and low strain-rate uniaxial tension protocols.

Material property testing is ideally conducted immediately postmortem to reflect the truest physiologic mechanical response for that specimen. Human ocular tissues are difficult to obtain. They may only be available 24-72 hours postmortem, and require shipping from multiple eye banks located across the country. To date, there are no known studies assessing the effect of postmortem time (PMT) on pediatric material properties. Furthermore, it is unclear what storage/shipping parameters are suitable, if any. In preparation for the collection of human ocular specimens, we sought to determine a viable time period and shipping strategy for material testing. Therefore, in ***Chapter 3***, we characterized the effect of PMT and storage condition on the mechanical response of sclera and retina from immature and mature ovine eyes. Sclera was tested up to 24 hours postmortem, and differences were assessed among fresh, frozen then thawed, and fixed sclera and retina. These findings will guide the mechanical testing protocols when pediatric eye tissue becomes available from human donors.

In ***Chapter 4,*** the material property data detailed in Chapters 1 and 2, and measured

from other studies conducted in our lab were used to determine age-appropriate constitutive models for the sclera, retina, and vitreous. We then generated and validated a finite element model of the infant ovine eye by predicting scleral surface strains in a simulation of experimental ocular inflation. The model's anatomical geometry, material models, meshes, and boundary conditions were defined based on *ex vivo* measurements, as well as data found in previous literature. This validated model progressed the design of an entire infant eye model investigating retinal stress due to rapid head rotations.

In ***Chapter 5***, a whole ovine infant eye model was generated to simulate a traumatic shaking event. Given the likely importance of vitreoretinal (VR) adhesion in evaluating the theory of VR traction as a cause of RH, VR adhesion parameters were varied and changes in distribution and magnitude of retinal stress and strain were compared. This is the first immature eye model to incorporate age-dependent mechanical properties, and serves to more closely approximate the retinal stress and strain due to repetitive head rotations compared to existing models.

Additional refinement of the model will result in an advanced tool to provide insight into injury mechanisms and prediction of RH. ***Chapter 6*** summarizes the key findings of this research, as well as limitations and suggestions for future work.

References

1. Betchel, K., Stoessel, K., Leventhal, J.M., Ogle, E., Teague, S.L., Banyas, B., Allen, K., Dziura, J., Duncan, C., Characteristics that distinguish accidental from abusive injury in hospitalized young children with head trauma. Pediatrics, 2004. 114(1): p. 165-168.

2. Binnenbaum, G., Mirza-George, N., Christian, C.W., Forbes, B.J. Odds of abuse associated with retinal hemorrhages in children suspected of child abuse. Journal of the American Association for Pediatric Ophthalmology and Stribismus, 2009. 13(3): p. 268-272.

3. Brenner, R.A., Overpeck, M.D., Trumble, A.C., DerSimonian, R., Berendes, H. Deaths attributable to injuries in infants, United States, 1983-1991, Pediatrics, 1999. 103(5 Pt 1): p. 968-974.

4. Curtin, B.J., Physiopathologic Aspects of Scleral Stress-Strain. Tr. Am. Ophth. Soc., 1969. 67: p. 417-461.

5. Duhaime, A.C., Gennarelli, T.A., Thibault, L.F., Bruce, D.A., Margulies, S.S>, Wiser, R. The shaken baby syndrome: a clinical, pathological, and biomechanical study. Journal of Neurosurgery, 1987. 66(3): p. 409-415.

6. Duhaime, A.C., Christian, C.W., Rorke, L.B., Zimmerman, R.A. Nonaccidental head injury in infants—the "shaken baby syndrome". The New England Journal of Medicine, 1998. 338(25): p. 1822-1829.

7. Gilles, E.E., McGregor, M.L., Levy-Clarke, G. Retinal hemorrhage symmetry in inflicted head injury: a clue to pathogenesis? Journal of Pediatrics, 2003. 143(4): p. 494-499.

8. Girard, M.J.A., Suh, J.-K.F., Hart, R.T., Burgoyne, C.F., Downs, J.C., Effects of storage time on the mechanical properties of rabbit peripapillary sclera after enucleation. Current Eye Research, 2007. 32(5): p. 465-470.

9. Green, M.A., Lieberman, G., Milroy, C.M., Parsons, M.A. Ocular and cerebral trauma in non-accidental injury in infancy: underlying mechanisms and implications for paediatric practice. British Journal of Ophthalmology, 1996. 80(4): p. 282-287.

10. Hans, S.A., Bawab, S.Y., Woodhouse, M.L., A finite element infant eye model to investigate retinal forces in shaken baby syndrome. Graefe's Archives for Clinical and Experimental Ophthalmology, 2009. 247(4): p. 561-571.

11. Kivlin, J.D. Manifestations of the shalen baby syndrome. Curr Opin Ophthalmology, 2001. 12(3): p. 158-163.

12. Krag, S., Olsen, T., Andreassen, T. Biomechanical characteristics of the human anterior lens capsule in relation to age. Investigative Ophthalmology & Visual Science, 1997. 38(2): p.357-363.

13. Levin, A.V., Retinal Hemorrhage in Abusive Head Trauma. Pediatrics, 2010. 126(5): p. 961-970.Levin, A.V., Christian, C.W. The eye examination in the evaluation of child abuse. Pediatrics, 2010. 162(2): p. 376-380.

14. Maguire, S.W., Watts, P.O., Shaw, A.D., Holden, S., Taylor, R.H., Watkins, W.J., Mann, M.K., Tempest, V., Kemp, A.M., Retinal haemorrhages and related findings in abusive and non-abusive head trauma: a systemic review. Eye, 2012. 27(1): p. 28-36.

15. Morad, Y., Kim, Y.M., Armstrong, D.C., Huver, D., Mian, M., Levin, A.V. Correlation between retinal abnormalities and intracranial abnormalities in the shaken baby

syndrome. American Journal of Ophthalmology, 2002. 134(3): p. 354-359.

16. Moran, P.R. (2012) Characterization of the vitreoretinal interface and vitreous in the porcine eye as it changes with age (Master's thesis). Retrieved from http://content.lib.utah.edu/cdm/ref/collection/etd3/id/1932

17. Overpeck, M.D., Brenner, R.A., Trumble, A.C., Trifiletti, L.B., Berendes, H.W. Risk factors for infant homicide in the United States. The New England Journal of Medicine, 1998. 339(17): p. 1211-1216.

18. Rangarajan, N., Kamalakkhannan, S., Hasija, V., Shams, T., Jenny, C., Serbanescu, I., Ho, J., Rusinek, M., Levin, A., Finite element model of ocular injury in abusive head trauma. Journal of the American Association for Pediatric Ophthalmology and Stribismus, 2009. 13(4): p. 364-369.

19. Sebag, J. Ageing of the vitreous. Eye (Lond), 1987. 1(Pt 2): p. 254-262.

20. Sturm, V., Knecht, P.B., Landau, K., Menke, M.N. Rare retinal hemorrhages in translational accidental head trauma in childrens. Eye (Lond), 2009. 23(7): p. 1535-1541.

CHAPTER 1

CHARACTERIZATION OF AGE, REGION, AND STRAIN-DEPENDENT MATERIAL PROPERTIES OF OVINE SCLERA

1.1 Abstract

There is a paucity of infant eye material property data and as yet there are no thorough investigations characterizing the age-dependent material properties of sclera. To quantify the effect of age on the mechanical response of sclera, we tested tissue from the anterior and posterior regions of preterm, infant, and adult ovine eyes. Two strain-dependent uniaxial tensile tests were implemented to assess the mechanical response to different loading conditions. Differences were statistically tested by comparing the stress relaxation constants and material properties across age, region, and strain-rate. Young's modulus was significantly larger for preterm and infant sclera than adult sclera at high strain-rates. At low strain-rates, only the modulus of posterior sclera significantly decreased with age. The ultimate stress was also age-dependent with the adult posterior sclera having a significantly lower average ultimate stress than both the preterm and infant posterior sclera when tested at low strain-rates. Similar age-dependent trends were seen for both anterior and posterior sclera when tested at high strain-rates. Stress relaxation constants were assessed at high strain-rates and the preterm sclera experienced the highest

stresses, which again decreased with age. In the region study, anterior sclera was stiffer and had higher ultimate stress than posterior sclera for all age groups tested at the low strain-rate, but only adult anterior sclera was stiffer than posterior sclera at the high strain-rate. However, at the high strain-rate, posterior sclera interestingly was stiffer than anterior sclera for the preterm and infant groups. At the high strain-rate, anterior sclera had higher stress constants than posterior sclera for all age groups. In the strain-rate study, sclera tested at the high strain-rate generally had greater elastic modulus and ultimate stress than sclera tested at the low strain-rate. The results from our region and strain-rate analyses agree with the existing literature that the anterior sclera exhibits a stiffer elastic response than posterior and that sclera is stiffer at higher strain-rates. Our trend with age, on the other hand, contrasts ophthalmic experience that adult sclera feels stiffer than pediatric. This contradiction is likely explained by the structural rigidity of sclera. The thicker adult tissue would qualitatively feel stiffer than the thinner pediatric sclera. The data herein show that there are age-related mechanical differences of ovine sclera that are age-dependent. Similar differences are likely to be found in human pediatric and adult sclera.

1.2 Introduction

Finite element (FE) analysis may be a useful tool in understanding the mechanical response of the infant eye and assist in the prediction of ocular injuries from accidental or abusive head trauma. However, current FE models of the pediatric eye are based on adult material properties with little or no consideration for changes during maturation.[17,26] There are limited data thoroughly characterizing the age-dependent material properties of ocular tissues. Age-related changes in the anterior lens capsule from donors 7 months to 98 years

old have been reported showing a decrease in strength with age.[19] Curtin et al. investigated mechanical properties of human sclera which included preterm, toddler, and adult tissue.[6] In this study, a static load-dependent tensile test was implemented to measure the strain response of the sclera at given stresses. However, the infant age group was not investigated and the premature tissue was only evaluated for anterior sclera. Studies in our lab indicate that there are early developmental changes in the vitreous[20] which suggests that age-dependent changes in other ocular tissues must be considered.

The sclera is the tough outer membrane which protects the eye and helps maintain globe shape by providing resistance to forces such as intraocular pressure. It is a major load bearing, connective tissue and is likely an essential component to most computational models of the eye. Scleral mechanics has been thoroughly characterized for the adult and elderly population with much of eye research focusing on ocular diseases such as macular degeneration and glaucoma.[4,5,7,8,10,12-18,22,24,25,28,29] The posterior sclera is the thickest region, becoming noticeably thinner towards the equator of the eye and slightly thickening again near the front of the eye. Studies reporting regional differences in the mechanical properties of adult sclera have shown a stiffer anterior sclera compared to the equatorial and posterior sclera, with posterior sclera exhibiting the least stiff response. These data infer the sclera is a region-dependent material.[11] Rate-dependence has been previously assessed in adult sclera and the results show that the modulus increased at higher strain-rates.[11] Direction has no significant effect on scleral mechanics and the sclera may be regarded as an isotropic material.[4] Structural changes in sclera with age suggest that material properties of sclera are age-dependent, but there is a paucity of infant eye material property data in the literature to support the assertion. The scleral extracellular matrix is

composed predominantly of type I collagen. Elastin may guide some of the viscoelastic response of sclera, but type I collagen and glycosaminoglycans (GAGs) are said to be the most influential constituents because they act as load bearing structures and dampening mechanisms, respectively.[1] GAGs are hydrophilic and thought to control tissue hydration. With age, there is a degradation of collagen and GAGs and the sclera becomes increasingly dehydrated.[2] These age-related changes in the scleral extracellular matrix highlight the inadequacies of using adult material properties in infant eye computational models.

For this study, we assessed region and strain-rate dependent material properties in the sclera in addition to age-related changes. Ocular specimens from premature, infant (3 days – 6 weeks), and adult ($\geq$ 4 years) sheep were tested according to uniaxial tensile test protocols in which anterior and posterior regions of the sclera were subjected to either a low or high strain test. An ovine animal model was selected because its ocular anatomy closely resembles the human eye sharing common major components. The similarities in mass, geometry, and physiology in the ovine eye to the age-equivalent human eye makes this a good animal model to observe mechanical differences throughout development. The availability of animal ocular tissue allows for a more thorough evaluation of age, rate, and region dependence of material properties.

1.3 Material and Methods

1.3.1. Tissue collection and sample preparation

Newborn lamb and mature sheep whole eyes were obtained immediately postmortem from nonocular studies being conducted at the University of Utah. From this group we received lamb eyes from newborns delivered prematurely (128-136 days

gestation) and from normal birth (~150 days gestation). Lambs were survived from 3 days up to 6 weeks and age was determined based on development rather than birth. Eyes were tested immediately (<1 hour postmortem) or stored in phosphate buffered saline (PBS) at 2°C and tested within 6 hours postmortem. Prior to testing, enucleated eyes were transferred to a petri dish for dissection. An aqueous environment of PBS was maintained throughout dissection to prevent the ocular tissues from drying out. The extraocular muscles and soft tissues were trimmed from the eye and discarded, and the optic nerve was severed at the optic nerve scleral junction. Each eye was carefully bisected sagittally into nasal and temporal halves (Figure 2a). Sclera was isolated by removing all intraocular tissues with tweezers. The resulting hemisections of sclera were placed on a cutting board. Anterior and posterior scleral samples were cut from each ocular half (Figure 2b) using a custom made dog-bone cutting die (Figure 2c). Tissue thickness was measured using an optical microscope at 1x magnification (SZX16, Olympus, Center Valley, PA). Tissue specimens were often naturally curved when cut.

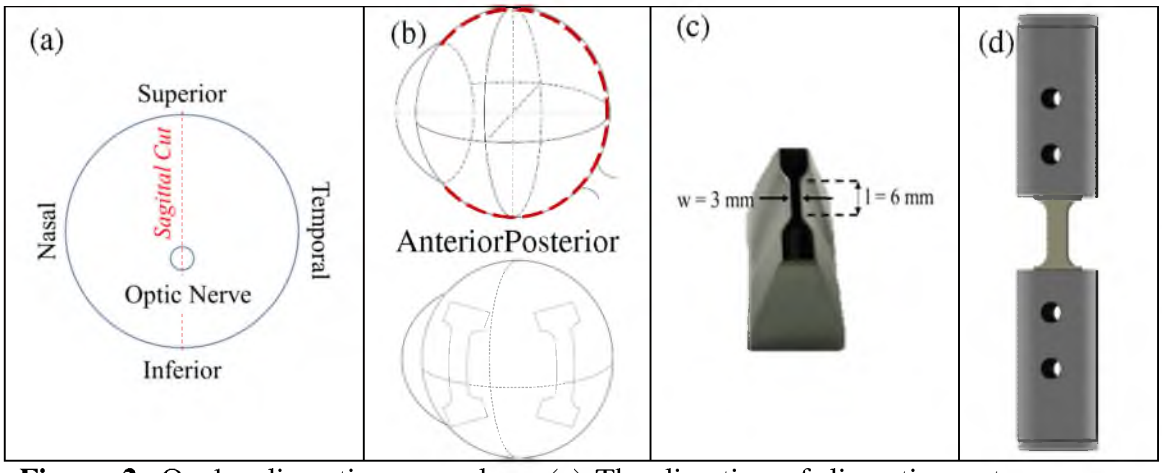

Figure 2: Ocular dissection procedure. (a) The direction of dissection cut on an eye globe. (b) The eye was bisected and scleral samples were taken from the anterior and posterior regions of each half. (c) A custom dog bone cutting die was used to cut scleral samples. (d) Tissue samples were aligned in custom screw-driven grips.

They were placed on a pair of flat tweezers. The surface tension created from the moist tissue caused the tissue to flatten (without any pressure) onto the tweezers. Note that the tweezers were not compressed at all. They merely acted as a means to transport the tissue. Three thickness measurements were taken by imaging one side of the tissue. The tissue was rotated 180 degrees to visualize the other side and an additional three thickness measurements were taken (Figure 3). The six thickness measurements were taken for each tissue sample at the center and each end of the gage length of both sides. The average of these six measurements was recorded for every sample. Width (3 mm) and gage length (6 mm) were determined by the dog-bone shape of the tissue sample. The scleral sample was aligned in custom screw-driven clamps (Figure 2d) that were fixed to a material test system (Model 5943, Instron, Norwood, MA) equipped with a 1-kN or 500-g load cell (LSB210, Futek, Irvine, CA) for high and low strain tests, respectively.

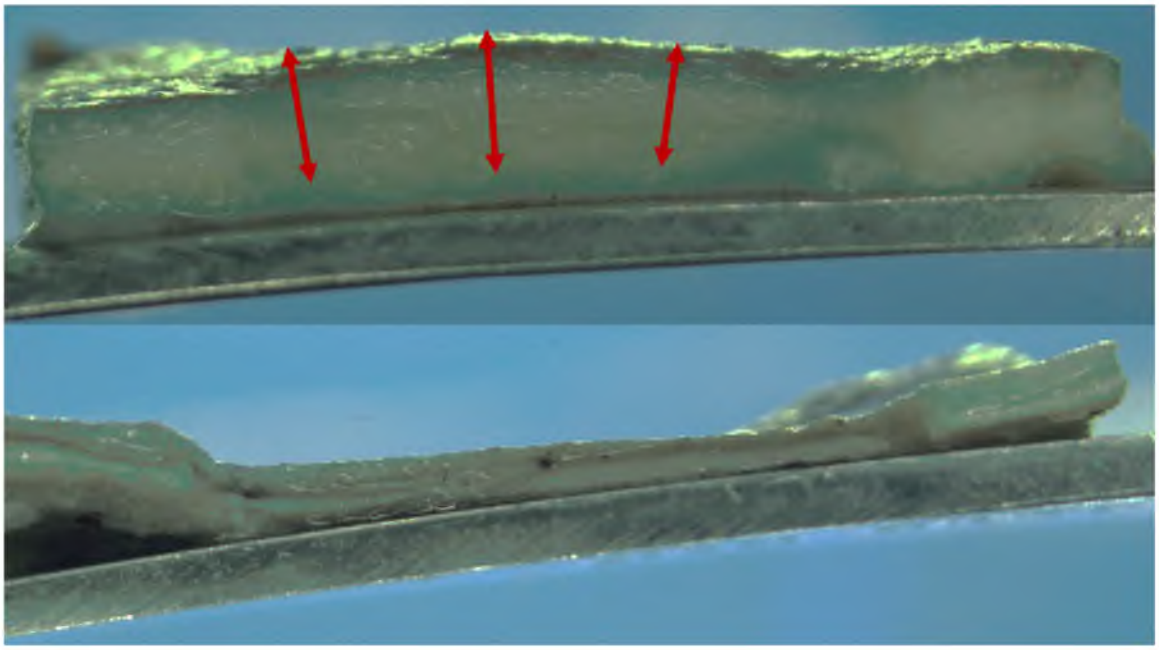

Figure 3: Scleral samples were placed on a thin metal sheet and turned on its side to measure tissue thickness (posterior on top, anterior on bottom).

1.3.2. Mechanical testing

Scleral samples were subjected to one of two uniaxial tensile test protocols in order to quantify strain and strain-rate dependent behavior (Figure 4). A low strain protocol was implemented to characterize the mechanical response of ocular tissues under normal physiologic intraocular pressure.[16] A high strain protocol was implemented to characterize the mechanical response of ocular tissues during high rate, high strain trauma. All tests were performed in an environmental bath filled with PBS at room temperature. Studies have shown significant differences in mechanical testing of sclera in different environments,[4] thus we implemented the most physiologic environment we could.

1.3.2.1 Low strain-rate. Each tissue was subjected to ten cycles of preconditioning from 0 to 1% strain at a strain-rate of 0.01 s^{-1}. Specimens were allowed to recover for 60 s and then subjected to tensile ramp to failure at 0.01 s^{-1}.

1.3.2.2 High strain-rate. Each tissue was subjected to ten cycles of preconditioning from 0 to 5% strain at a strain-rate of 0.05 s^{-1}. Specimens were allowed to recover for 60 s and then a stress relaxation test was performed by applying 25% strain and holding for 900 s. The tissue was allowed to recover for 60 s, and then subjected to tensile ramp to failure at 0.1 s^{-1}.

The raw load and displacement data were sampled at 10 Hz and extracted to calculate engineering stress and strain. A custom Matlab (Mathworks, Natick, MA) code was implemented for scleral analysis and plotting which can be seen in Appendices A and B. Stress was calculated by dividing the current force by the reference cross-sectional area. Strain was calculated by dividing displacement of the Instron crosshead by the original gage length. Each tissue was preloaded to approximately 0.08 N to remove any slack in

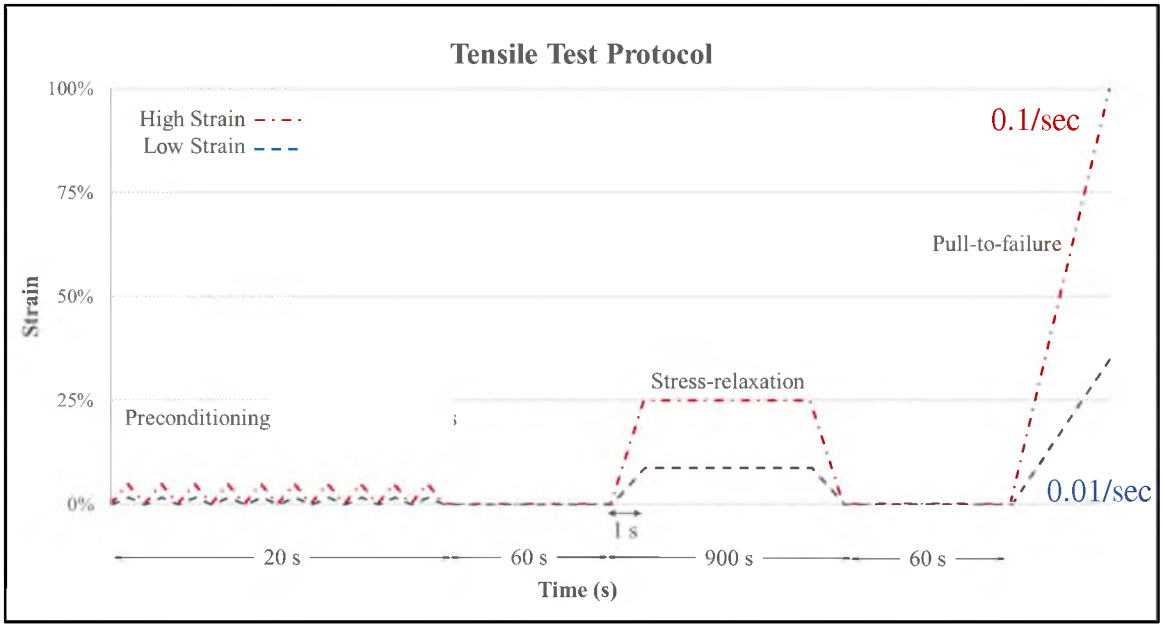

Figure 4: The strain-dependent uniaxial tensile test protocol consisted of preconditioning, stress relaxation, and pull-to-failure.

the tissue sample. Stress relaxation data for each specimen were fit to a two-term generalized Maxwell model [Eq.1].[27] A least-squares curve-fitting technique in Matlab was used to solve for equilibrium stress (σ_e), intermediate stresses (σ_1, σ_2), and the decay (τ_1, τ_2) constants. Instantaneous stress (σ_i) was defined as the sum of the equilibrium and intermediate stresses [Eq. 2]. The strain length of the toe region (ε_{toe}), elastic modulus (E), ultimate stress (σ_{ult}), and ultimate strain (ε_{ult}) were extracted from each pull-to-failure test. ε_{toe} was defined as the strain achieved at the end of the nonlinear elastic response during pull-to-failure. Young's modulus was defined as the slope of the linear region during pull-to-failure. The ultimate stress and strain were the maximum stress and strain achieved by the specimen.

1.3.3. Statistical analysis

Age, region, and strain-rate were analyzed independently for this study. A one-way analysis of variance (ANOVA) was used to determine if age significantly affected tissue thickness. One-way ANOVAs were also used to determine if (1) age significantly affected the relaxation constants (τ_1, τ_2, σ_i, σ_e, σ_1, σ_2) and material properties (ε_{toe}, E, σ_{ult}, ε_{ult}), (2) region significantly affected the relaxation constants (τ_1, τ_2, σ_i, σ_e, σ_1, σ_2) and material properties (ε_{toe}, E, σ_{ult}, ε_{ult}), and (3) strain-rate significantly affected the material properties (ε_{toe}, E, σ_{ult}, ε_{ult}). A p-value of 0.05 was used to define significance. A Tukey's Honestly Significant Difference test with a p-value of 0.05 was used post-hoc to test for significant differences within the one-way analysis of variance. The scleral data which were analyzed in Matlab were implemented into statistical software (JMP, Cary, NC) and can be seen in Appendix D.

$$\sigma(t) = \sigma_e + \sum_{j=1}^{2} \sigma_j e^{-\frac{t}{\tau_j}} \quad (1)$$

$$\sigma_i = \sigma_e + \sigma_1 + \sigma_2 \quad (2)$$

1.4 Results

The posterior sclera was significantly thicker than anterior sclera for all age groups ($p<0.05$). Scleral thickness significantly increased with age ($p<0.005$) as the mature sclera was roughly 1.65 and 2.45 times greater than the infant and preterm sclera, respectively (Table 1). Scleral thickness was significantly different between all age groups (Figure 5).

Table 1: Average ± standard deviation for regional scleral thickness (mm) in each age group. The number of specimens for each group is provided in parentheses.

Preterm	Anterior (n=32)	0.39±0.08	Posterior (n=30)	0.86±0.20
Infant	Anterior (n=21)	0.54±0.16	Posterior (n=21)	1.28±0.35
Adult	Anterior (n=26)	0.93±0.21	Posterior (n=26)	2.16±0.36

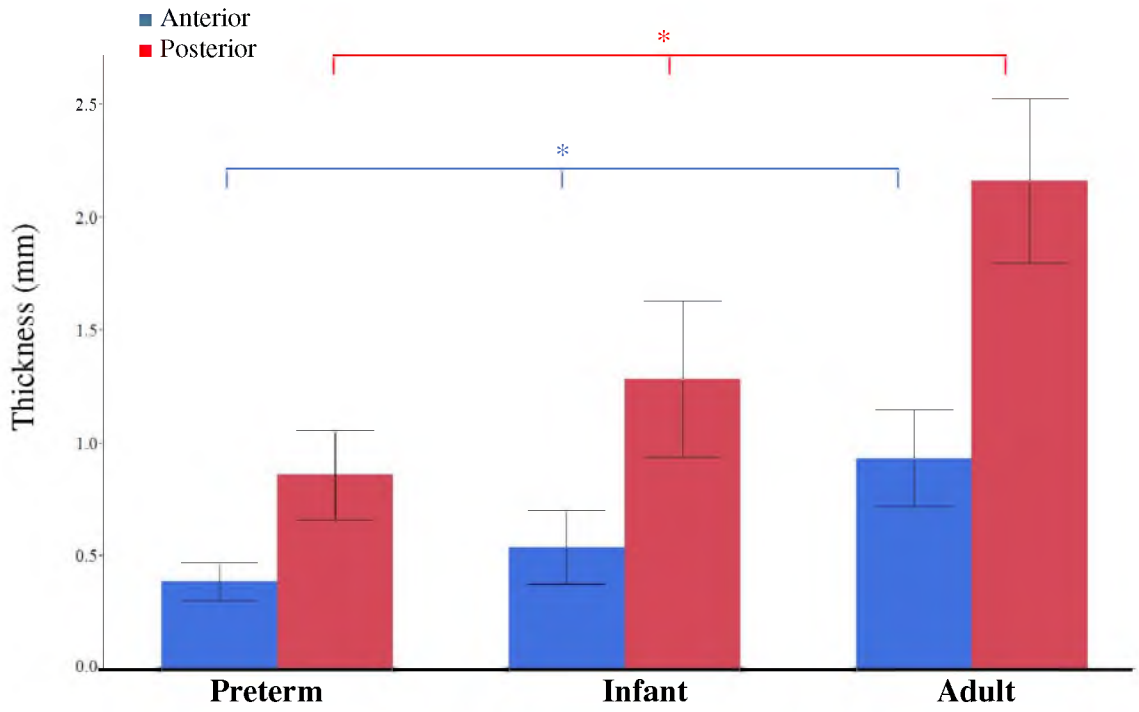

Figure 5: Average and standard deviation for sclera thickness of preterm, infant, and adult anterior and posterior sclera. * $p<0.005$

All scleral samples had a good overall fit to the second order Maxwell model (Figure 6). Average goodness of fits for preterm, infant, and adult specimens were 0.95, 0.98, and 0.97, respectively. In order to obtain adequate data resolution of tensile tests at low strain, the 500-g (~4.9 N) load cell was used. The ultimate force measured during the low strain-rate pull-to-failure, which immediately followed stress relaxation, occasionally exceeded the load cell limits. As a result, ultimate stress and strain were not reported for these tests. Additional pull-to-failure samples were tested to replace the removed data.

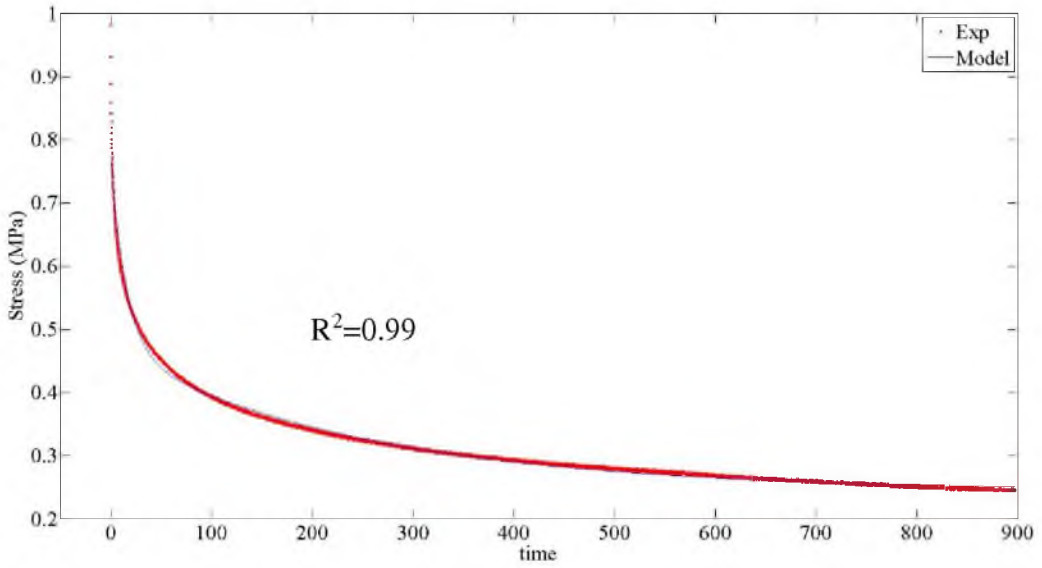

Figure 6: Representative curve fit of stress relaxation data to the second order Maxwell model for infant sclera.

1.4.1 Age

The Young's modulus and stress constants of the preterm sclera were generally greater than the infant and adult groups. The scleral material properties at the low strain-rate can be seen in Table 2. The scleral material properties at the high strain-rate can be seen in Table 4.

1.4.1.1 Low strain-rate. The strain length of the toe region (ε_{toe}) and Young's modulus (E) of the preterm anterior sclera were generally larger than the infant and adult anterior sclera but no significant differences were found. ε_{toe} of the preterm posterior sclera was significantly longer ($p<0.005$) than the adult posterior sclera (Figure 7). ε_{toe} decreased with age for both anterior and posterior sclera but was only statistically significant between adult and preterm posterior sclera. The Young's modulus of the posterior sclera decreased with age and was significantly different ($p<0.05$) between all three age groups (Figure 8). The preterm anterior sclera generally had a higher Young's modulus and ultimate stress

Table 2: Average ± standard deviation of material properties for preterm, infant, and adult anterior and posterior sclera tested at low strain-rate. Similar symbols (*,†) in each row indicate groups that were significantly different than each other ($p<0.05$).

	Low Strain-rate					
	Preterm		*Infant*		*Adult*	
	Anterior	Posterior	Anterior	Posterior	Anterior	Posterior
ε_{toe}	0.25 ± 0.29	0.25 ± 0.04 *	0.13 ± 0.03	0.20 ± 0.06	0.06 ± 0.03	0.13 ± 0.06 *
E (MPa)	20.35 ± 20.71	17.22 ± 4.00 *	9.58 ± 4.75	9.35 ± 4.63	10.17 ± 12.52	2.49 ± 4.58 *
σ_{ult} (MPa)	5.70 ±5.62	4.62 ± 1.4 *	2.09 ± 0.61	2.69 ± 1.65 †	1.81 ± 3.11	0.72 ± 1.09 *†
ε_{ult}	0.46 ± 0.11	0.57 ± 0.12	0.42 ± 0.07	0.48 ± 0.16	0.53 ± 0.33	0.49 ± 0.14

than the infant and adult anterior sclera yet no statistically significant differences were found due to large variability. The adult posterior sclera had a significantly lower ultimate stress than the preterm ($p<0.05$) and infant ($p<0.0005$) posterior sclera (Figure 9). No statistically significant differences were found for the ultimate strain of sclera tested at low strain-rate (Figure 10).

The low strain-rate pull-to-failure responses for all scleral specimens can be seen in Figure 11. As mentioned earlier, not all tissues reached failure due to the limits of the low force load cell. Figure 12 includes only the scleral trials that achieved failure at the low strain-rate, and the additional pull-to-failure specimens tested. The averaged responses across age and region for trials that achieved failure can be seen in Figure 13. Stress for every age and region combination was averaged at every 0.1 mm/mm strain increment up to 1 mm/mm. Preterm sclera exhibits the stiffest response and greatest ultimate stress. Infant sclera responded similar to adult at low strain-rates.

1.4.1.2 High strain-rate. The stress relaxation constants for sclera tested at the high strain level can be seen in Table 3. All stress constants (σ_i, σ_1, σ_2, σ_e) for the preterm posterior sclera were significantly higher than both the infant ($p<0.05$) and adult ($p<0.001$) posterior sclera. The preterm anterior sclera also experienced higher stresses than the

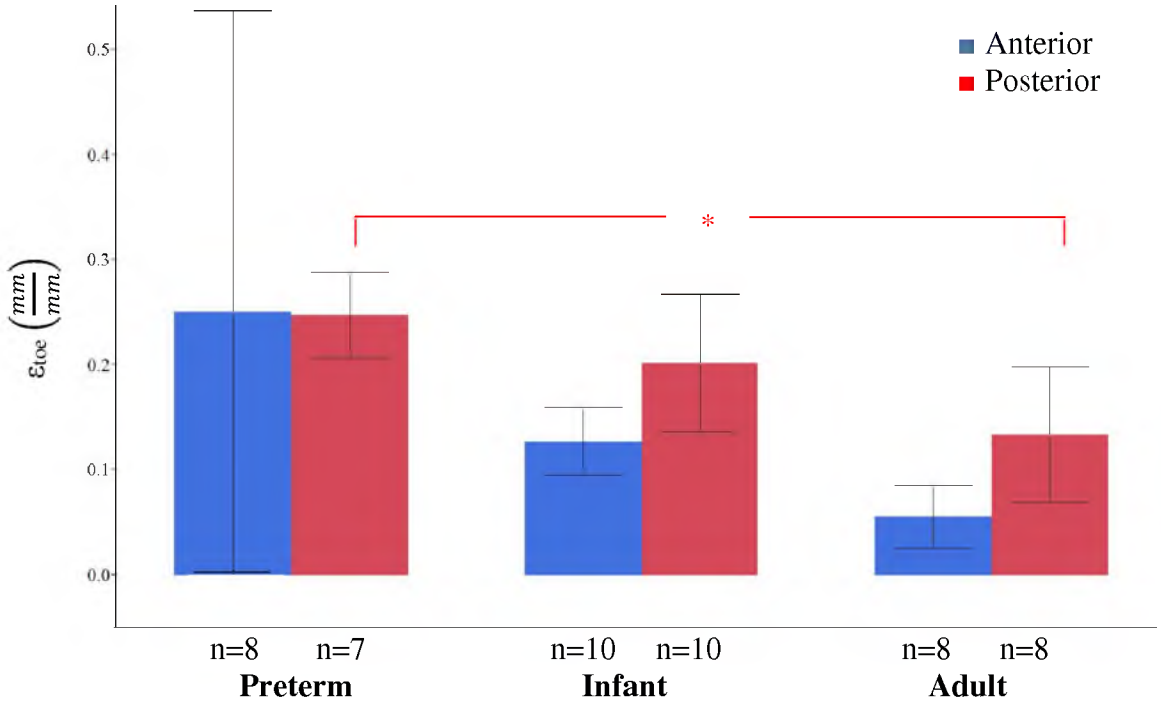

Figure 7: Average and standard deviation for toe region across age and region for sclera tested at low strain. * $p<0.01$

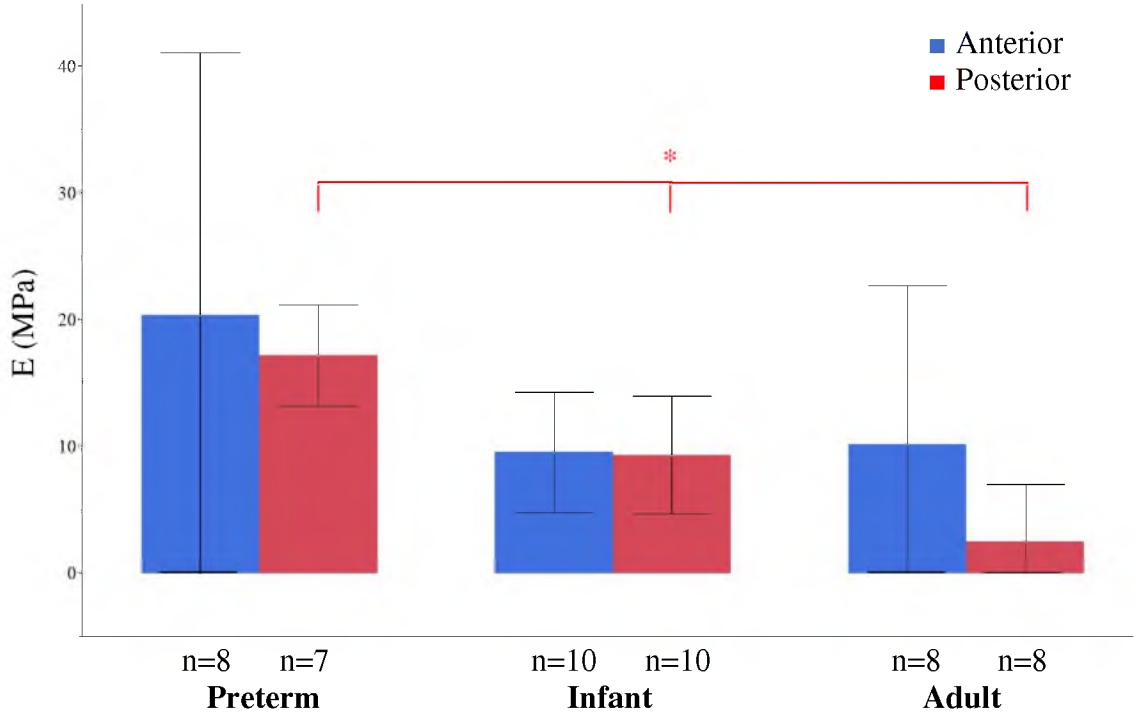

Figure 8: Average and standard deviation for Young's modulus across age and region for sclera tested at low strain. * $p<0.01$

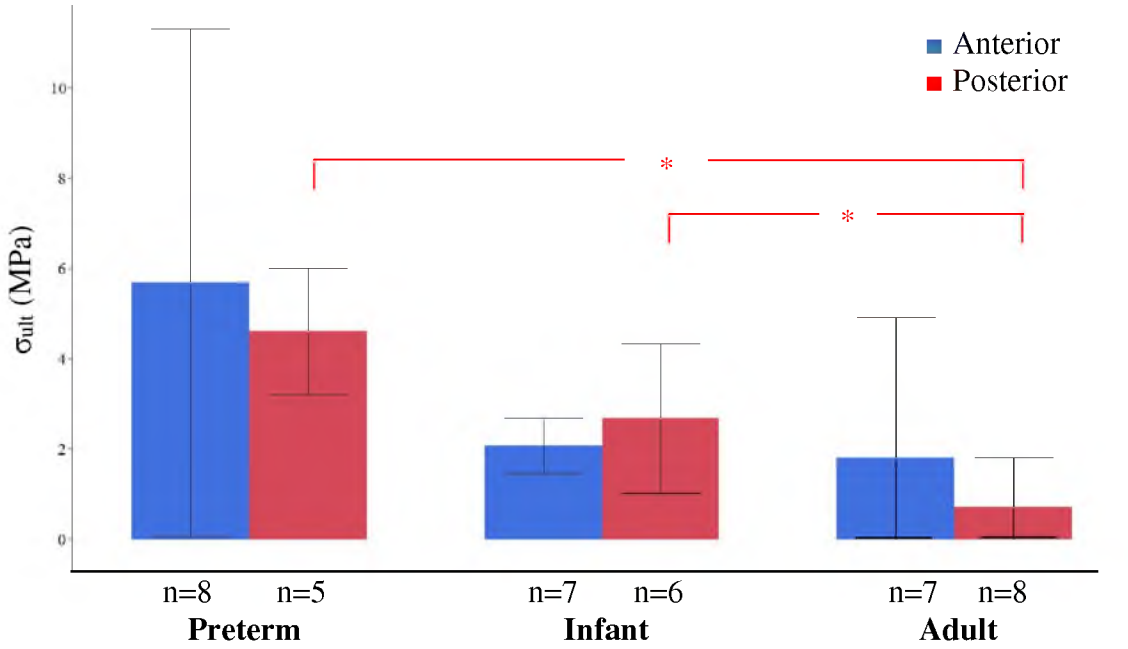

Figure 9: Average and standard deviation for ultimate stress across age and region for sclera tested at low strain. * p<0.005

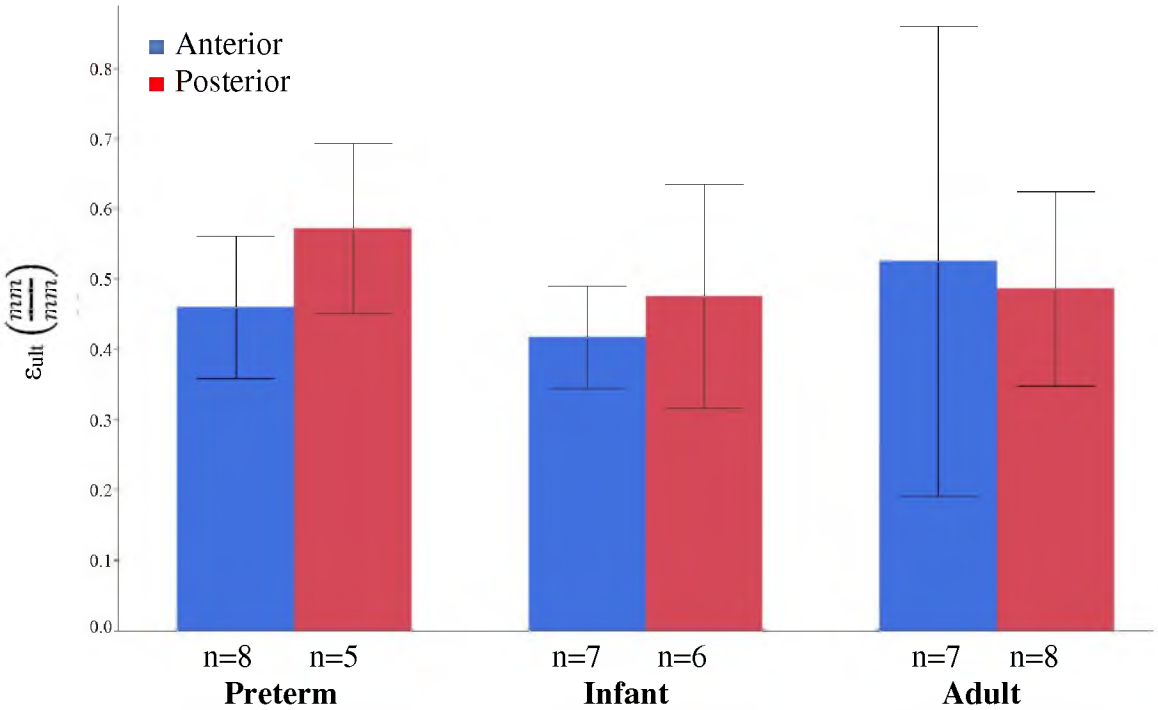

Figure 10: Average and standard deviation for ultimate strain across age and region for sclera tested at low strain. * p<0.05

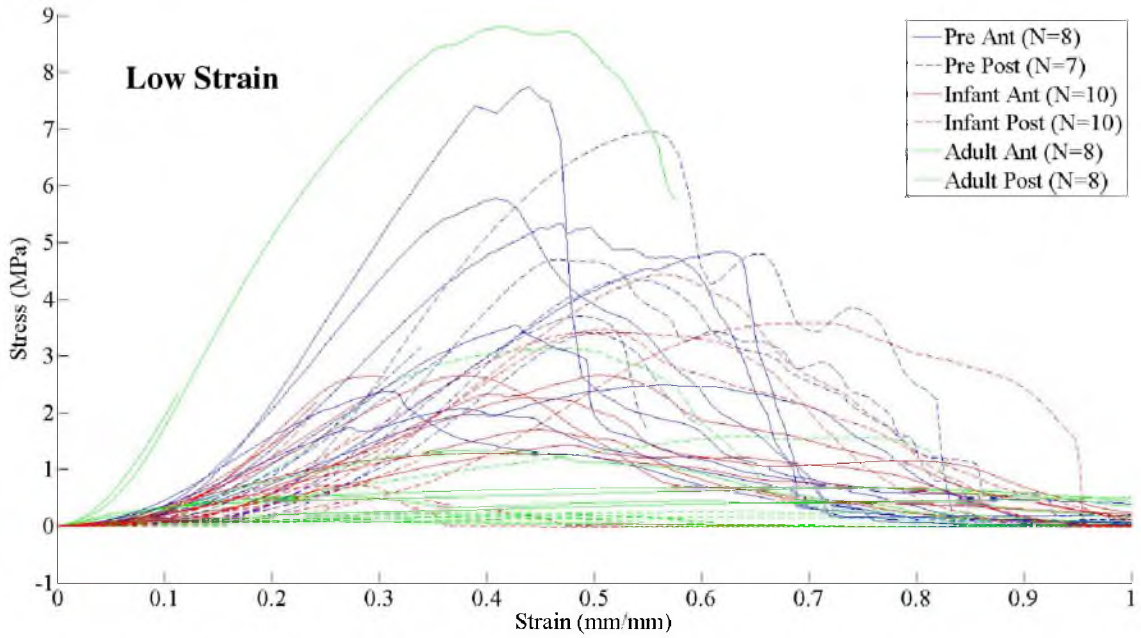

Figure 11: Pull-to-failure response of all included trials at low strain-rate across age and region.

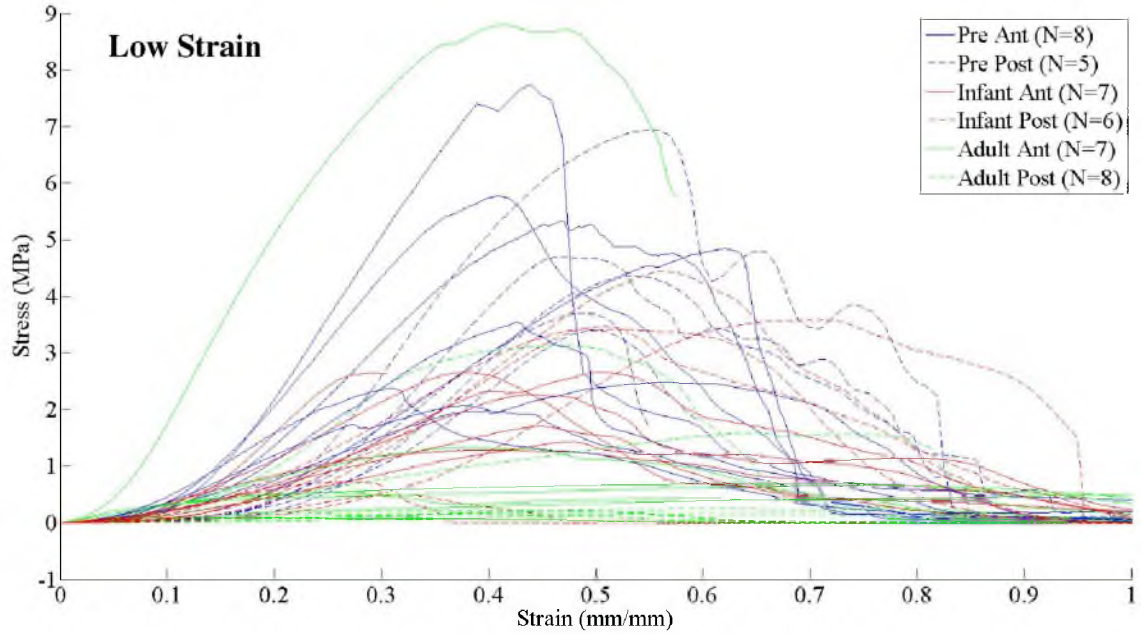

Figure 12: Pull-to-failure response at low strain-rate across age and region, excluding trials that do not fail.

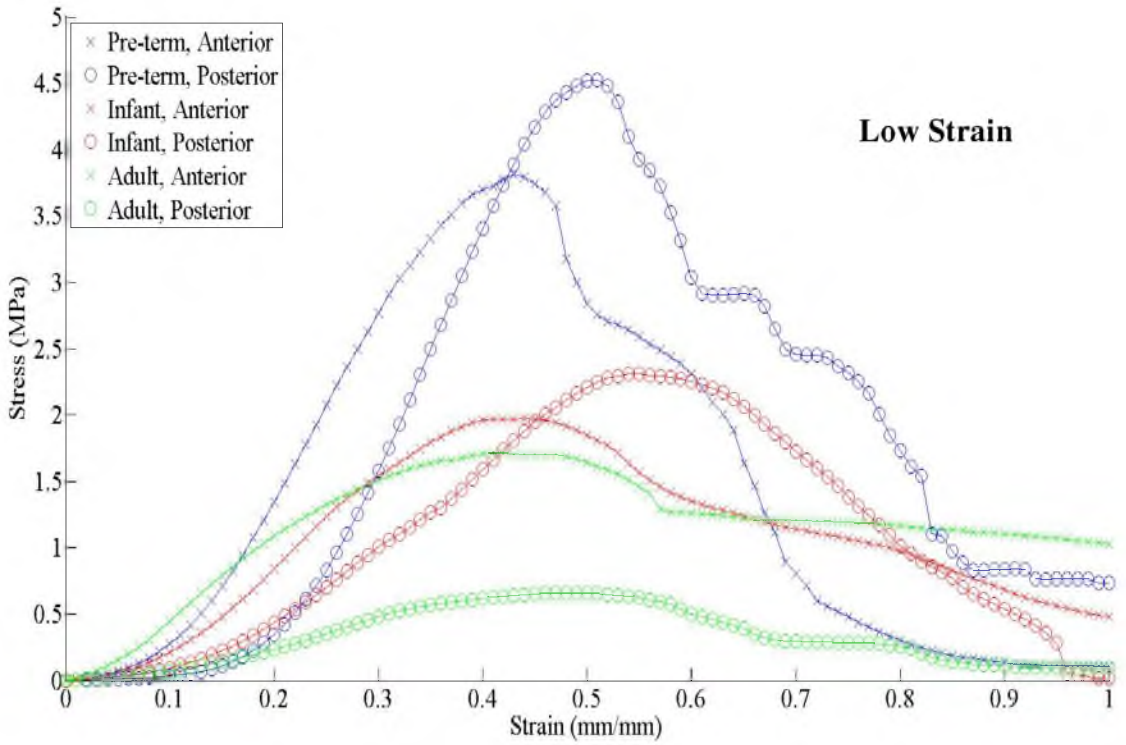

Figure 13: Average pull-to-failure response at low strain-rate across age and region.

infant and adult anterior sclera. No significant age differences were found for the anterior sclera tested at high rate (Figure 14).

The preterm anterior sclera had a significantly higher immediate and long-term decay time than the adult anterior sclera ($p<0.005$). The immediate decay time constant of the adult posterior sclera was significantly lower than the preterm and infant posterior sclera ($p<0.003$). The long-term decay time of the adult posterior sclera was significantly lower than the infant posterior sclera ($p<0.02$) (Figure 15, Figure 16). The high strain relaxation responses can be seen in Figure 17 and the averaged responses with age and region can be seen in Figure 18. Preterm sclera experiences the highest stresses and most rapid decay rates, then infant and adult. No significant differences in the ε_{toe} of anterior sclera were found among the three ages (Figure 19).

Table 3: Average ± standard deviation of stress relaxation constants for preterm, infant, and adult anterior and posterior sclera tested at high strain. Similar symbols (*,†,ǂ,§) in each row indicate groups that were significantly different than each other ($p<0.05$).

	High Strain					
	Preterm		*Infant*		*Adult*	
	Anterior	Posterior	Anterior	Posterior	Anterior	Posterior
σ_i (MPa)	1.78 ± 1.37	1.39 ± 0.72 *†	1.26 ± 0.65	0.61 ± 0.44 *	0.84 ± 0.61	0.14 ± 0.04 †
σ_1 (MPa)	0.45 ± 0.39	0.33 ± 0.18 *†	0.27 ± 0.13	0.17 ± 0.11 *	0.13 ± 0.09	0.03 ± 0.01 †
σ_2 (MPa)	0.71 ± 0.50	0.54 ± 0.25 *†	0.57 ± 0.32	0.27 ± 0.19 *	0.54 ± 0.44	0.07 ± 0.03 †
σ_e (MPa)	0.62 ± 0.49	0.52 ± 0.31 *†	0.40 ± 0.23	0.18 ± 0.15 *	0.17 ± 0.11	0.03 ± 0.01 †
τ_1 (sec)	309.13 ± 118.71 *†	243.93 ± 33.50 ǂ	214.98 ± 29.51 *	237.64 ± 39.25 §	120.74 ± 90.65 †	144.43 ± 49.73 ǂ§
τ_2 (sec)	12.44 ± 4.45 *†	10.60 ± 3.28 ǂ§	7.38 ± 2.85 *	11.56 ± 3.23 ǂ	3.49 ± 3.54 †	6.09 ± 2.95 §

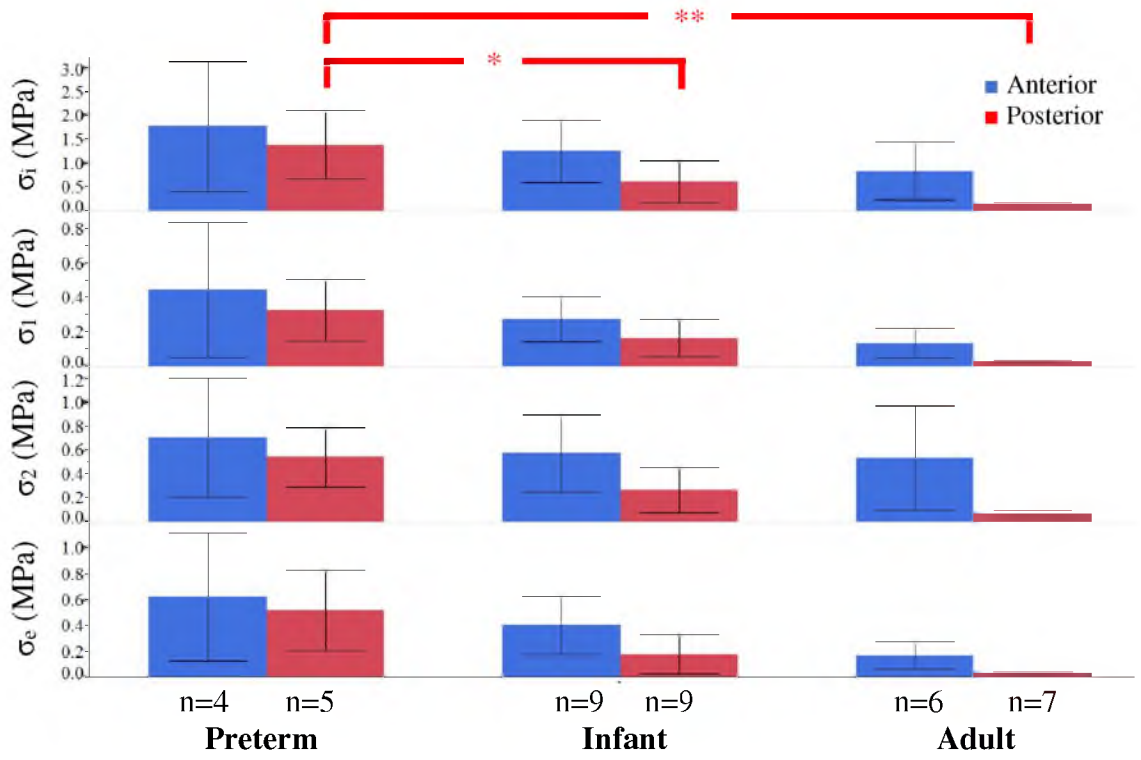

Figure 14: Average and standard deviation for stress constants across age and region for sclera tested at high strain. The thick red lines indicate significance across all stress constants for posterior sclera. ** $p<0.001$ * $p<0.05$

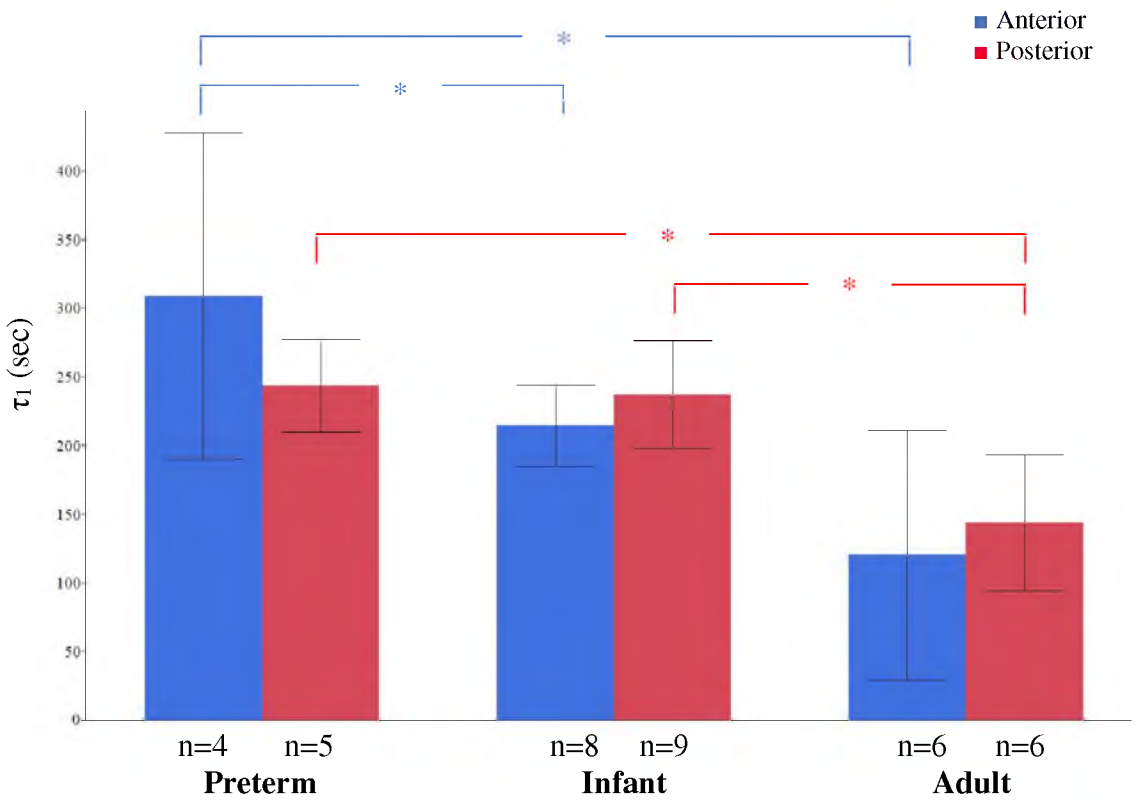

Figure 15: Average and standard deviation for immediate decay time across age and region for sclera tested at high strain. * $p<0.05$

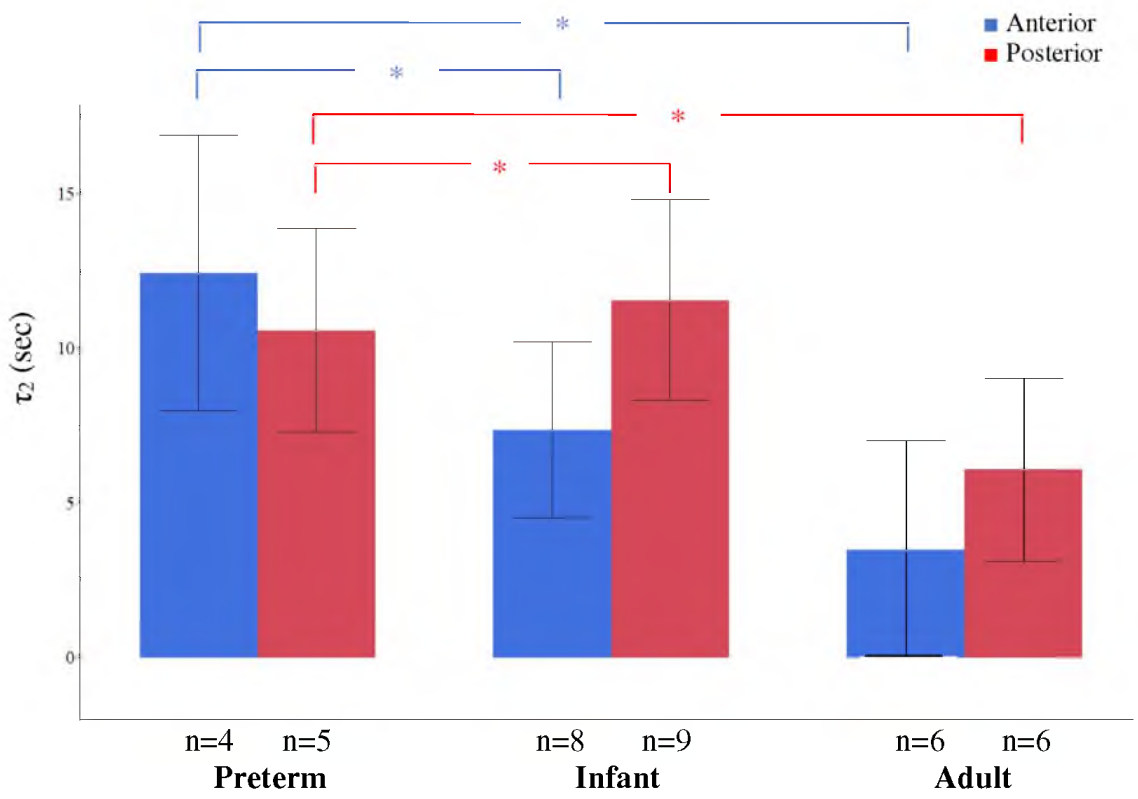

Figure 16: Average and standard deviation for long-term decay time across age and region for sclera tested at high strain. * $p<0.05$

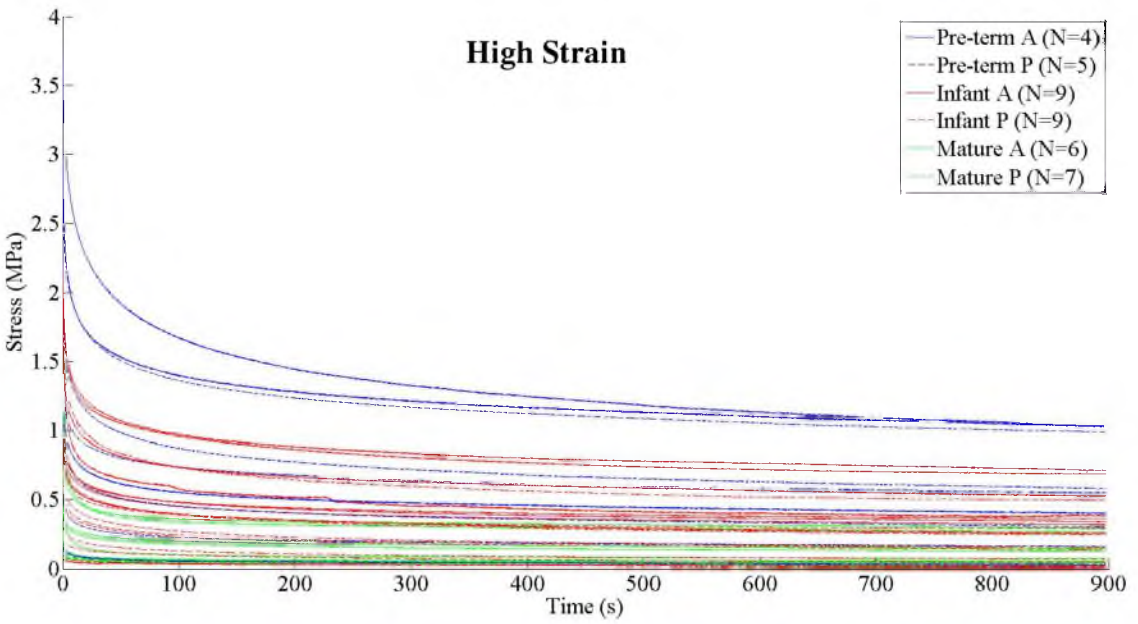

Figure 17: Relaxation response of all scleral trials at high strain across age and region.

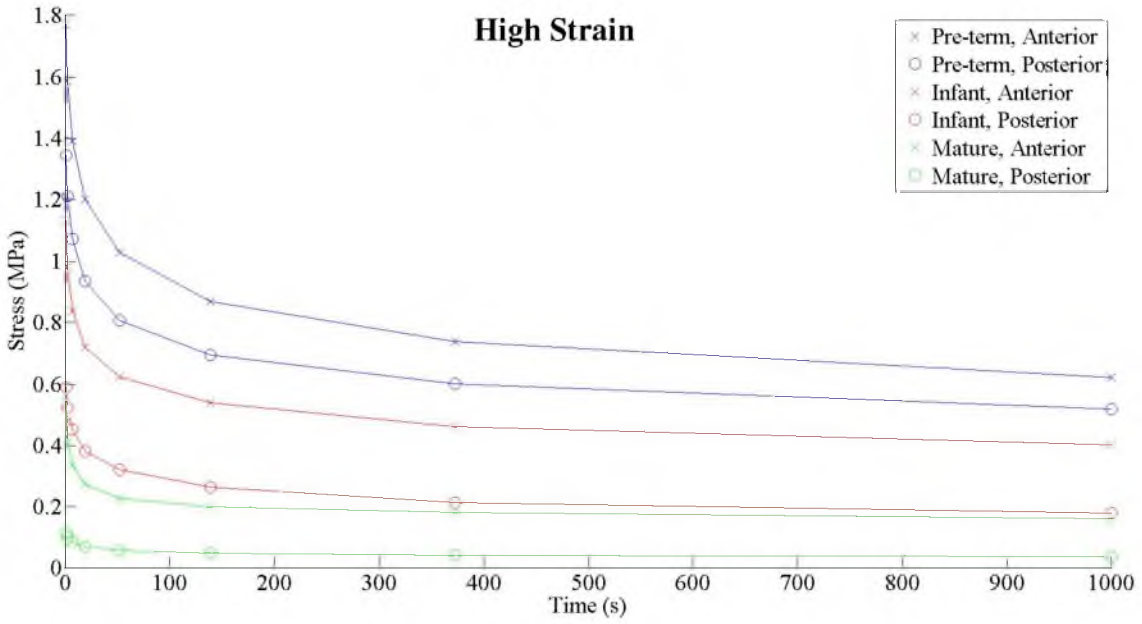

Figure 18: Averaged relaxation responses at high strain across age and region.

Pull-to-failure data for sclera tested at the high strain level can be seen in Table 4. The E of the preterm anterior sclera was significantly higher than the adult anterior sclera ($p<0.05$). The ε_{toe} of the preterm posterior sclera, however, was significantly shorter than the ε_{toe} of the infant posterior sclera ($p<0.03$). The preterm ε_{toe} was also smaller than adult, but a larger variation in the toe region of adult posterior sclera posterior sclera precluded significance. The E of the adult posterior sclera was significantly less ($p<0.02$) than both the preterm and infant posterior sclera (Figure 20). The adult anterior sclera had a significantly lower ultimate stress than both the preterm and infant anterior sclera ($p<0.02$). The ultimate stress of the infant posterior sclera was significantly larger ($p<0.002$) than the adult posterior sclera (Figure 21). No age effect was found for the ultimate strain of sclera (Figure 22). The high strain-rate, pull-to-failure responses for all scleral specimens can be seen in Figure 23 and the averaged responses with age and region can be seen in Figure 24. Stress was averaged up to 100% strain in increments of 10% strain.

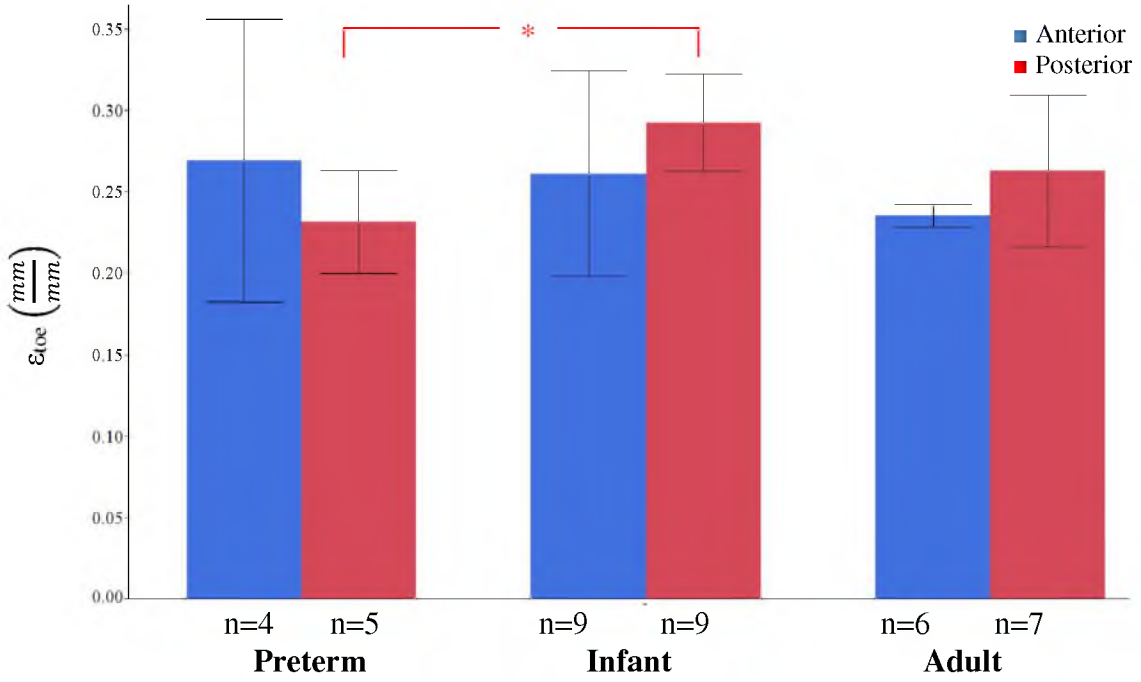

Figure 19: Average and standard deviation for toe region across age and region for sclera tested at high strain-rate. * $p<0.05$

Table 4: Average ± standard deviation of material properties for preterm, infant, and adult anterior and posterior sclera tested at high strain-rate. Similar symbols (*,†,ǂ) in each row indicate groups that were significantly different than each other ($p<0.05$).

	High Strain-rate					
	Preterm		*Infant*		*Adult*	
	Anterior	Posterior	Anterior	Posterior	Anterior	Posterior
ε_{toe}	0.27 ± 0.09	0.23 ± 0.03 *	0.26 ± 0.06	0.29 ± 0.03 *	0.24 ± 0.01	0.26 ± 0.05
E (MPa)	20.62 ± 6.30 *	21.55 ± 9.42 †	18.00 ± 5.74	19.82 ± 7.02 ǂ	10.86 ± 5.70 *	6.36 ± 7.89 †ǂ
σ_{ult} (MPa)	4.47 ± 1.60 *	4.16 ± 1.27 ǂ	3.74 ± 1.20 †	5.32 ± 1.58 ǂ	1.63 ± 1.01 *†	1.68 ± 2.22
ε_{ult}	0.52 ± 0.10	0.45 ± 0.09	0.58 ± 0.13	0.59 ± 0.07	0.54 ± 0.15	0.62 ± 0.22

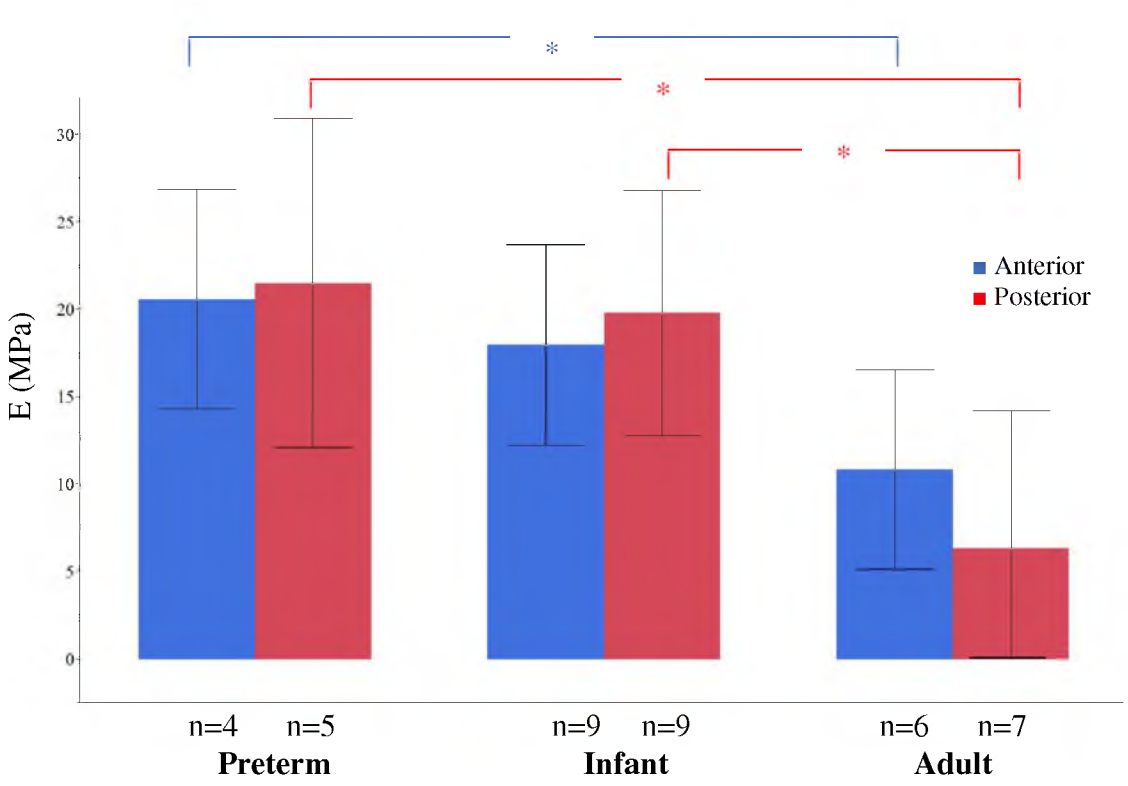

Figure 20: Average and standard deviation for Young's modulus across age and region for sclera tested at high strain-rate. * $p<0.05$

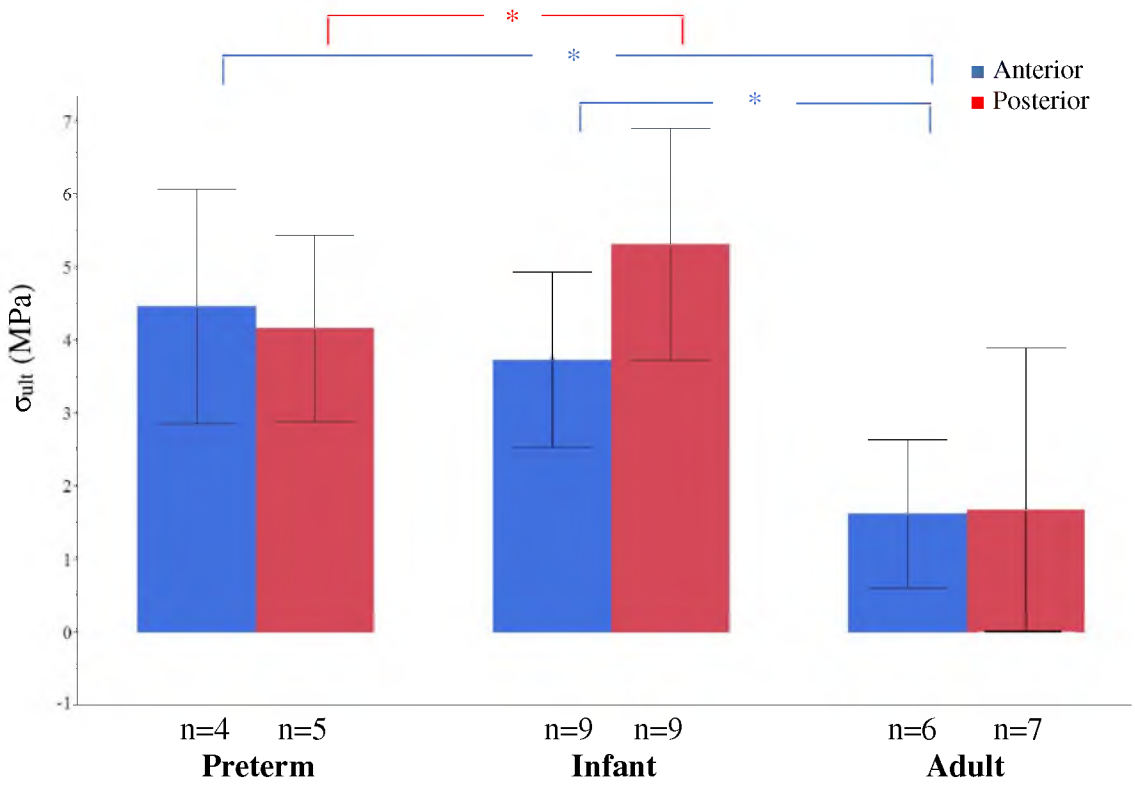

Figure 21: Average and standard deviation for ultimate stress across age and region for sclera tested at high strain-rate. * $p<0.05$

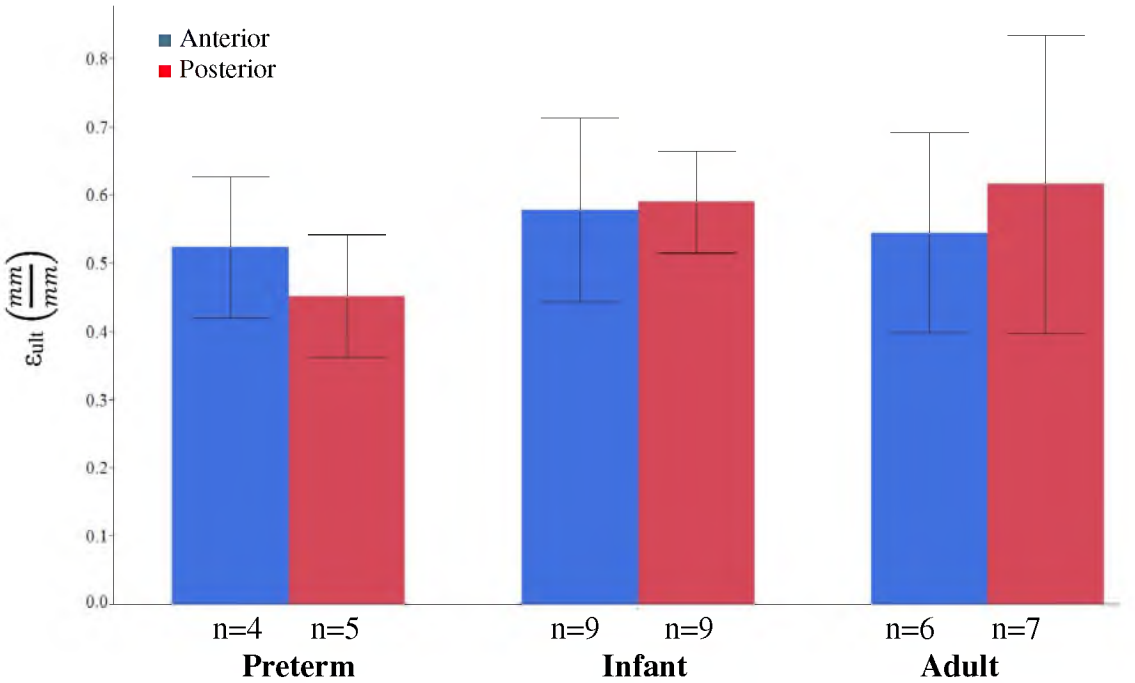

Figure 22: Average and standard deviation for ultimate strain across age and region for sclera tested at high strain.

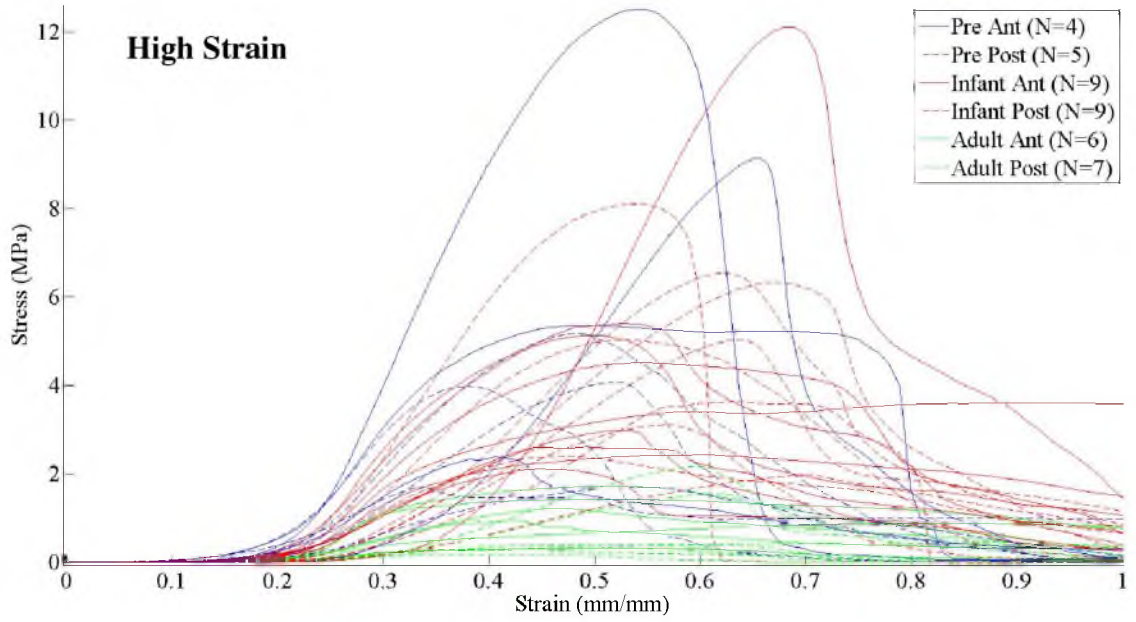

Figure 23: Pull-to-failure response of all included trials at high strain-rate across age and region.

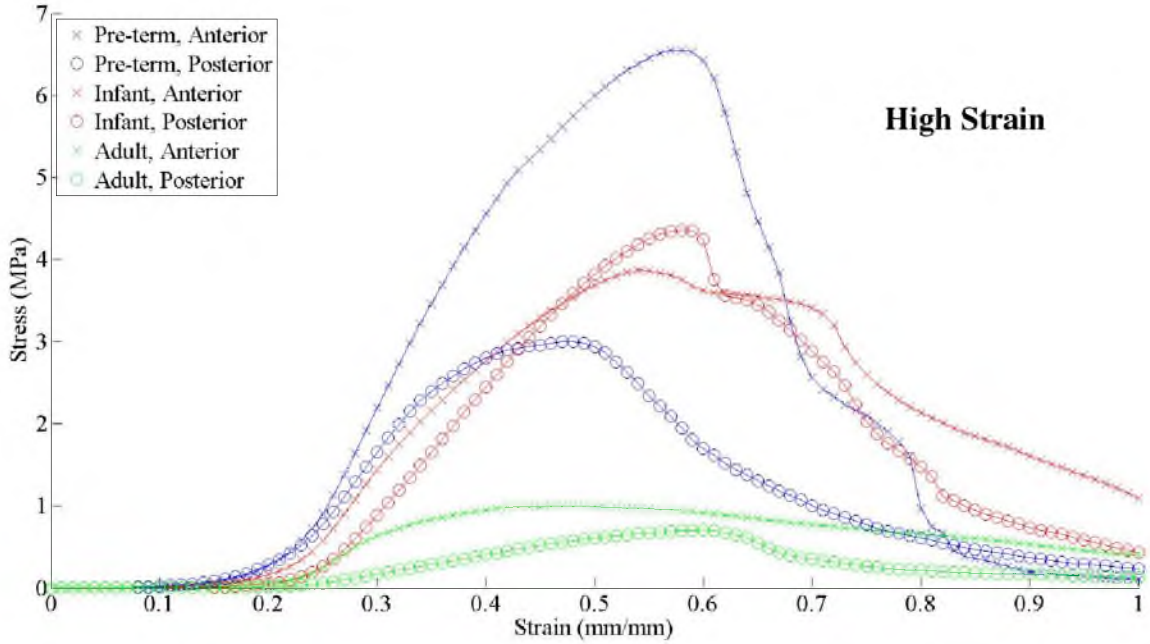

Figure 24: Average pull-to-failure response at high strain-rate across age and region.

1.4.2 Region

Regional material properties can be seen in Table 5 and Table 6.

1.4.2.1 Low strain-rate. The ε_{toe} of the preterm anterior sclera was longer than the preterm posterior sclera. The ε_{toe} of the infant and adult posterior sclera was significantly longer ($p<0.05$) than the anterior sclera (Figure 25). Generally, the anterior sclera trended towards a higher Young's modulus and ultimate stress than the posterior sclera for all age groups but no statistically significant differences were found (Figure 26, Figure 27). No significant differences were found for the ultimate stress or strain of the anterior and posterior sclera of all age groups (Figure 28).

Table 5: Average ± standard deviation of material properties for preterm, infant, and adult anterior and posterior sclera tested at low strain-rate. Similar symbols (*,†) in each row indicate groups that were significantly different than each other ($p<0.05$).

	Low Strain-rate					
	Preterm		*Infant*		*Adult*	
	Anterior	Posterior	Anterior	Posterior	Anterior	Posterior
ε_{toe}	0.25 ± 0.29	0.25 ± 0.04	0.13 ± 0.03 *	0.20 ± 0.06 *	0.06 ± 0.03 †	0.13 ± 0.06 †
E (MPa)	20.35 ± 20.71	17.22 ± 4.00	9.58 ± 4.75	9.35 ± 4.63	10.17 ± 12.52	2.49 ± 4.58
σ_{ult} (MPa)	5.70 ±5.62	4.62 ± 1.4	2.09 ± 0.61	2.69 ± 1.65	1.81 ± 3.11	0.72 ± 1.09
ε_{ult}	0.46 ± 0.11	0.57 ± 0.12	0.42 ± 0.07	0.48 ± 0.16	0.53 ± 0.33	0.49 ± 0.14

Table 6: Average ± standard deviation of stress relaxation constants for preterm, infant, and adult anterior and posterior sclera tested at high strain. Similar symbols (*) in each row indicate groups that were significantly different than each other ($p<0.05$).

	High Strain					
	Preterm		*Infant*		*Adult*	
	Anterior	Posterior	Anterior	Posterior	Anterior	Posterior
σ_i (MPa)	1.78 ± 1.37	1.39 ± 0.72	1.26 ± 0.65 *	0.61 ± 0.44 *	0.84 ± 0.61 *	0.14 ± 0.04 *
σ_1 (MPa)	0.45 ± 0.39	0.33 ± 0.18	0.27 ± 0.13 *	0.17 ± 0.11 *	0.13 ± 0.09 *	0.03 ± 0.01 *
σ_2 (MPa)	0.71 ± 0.50	0.54 ± 0.25	0.57 ± 0.32 *	0.27 ± 0.19 *	0.54 ± 0.44 *	0.07 ± 0.03 *
σ_e (MPa)	0.62 ± 0.49	0.52 ± 0.31	0.40 ± 0.23 *	0.18 ± 0.15 *	0.17 ± 0.11 *	0.03 ± 0.01 *
τ_1 (sec)	309.13 ± 118.71	243.93 ± 33.50	214.98 ± 29.51	237.64 ± 39.25	120.74 ± 90.65	144.43 ± 49.73
τ_2 (sec)	12.44 ± 4.45	10.60 ± 3.28	7.38 ± 2.85 *	11.56 ± 3.23 *	3.49 ± 3.54	6.09 ± 2.95

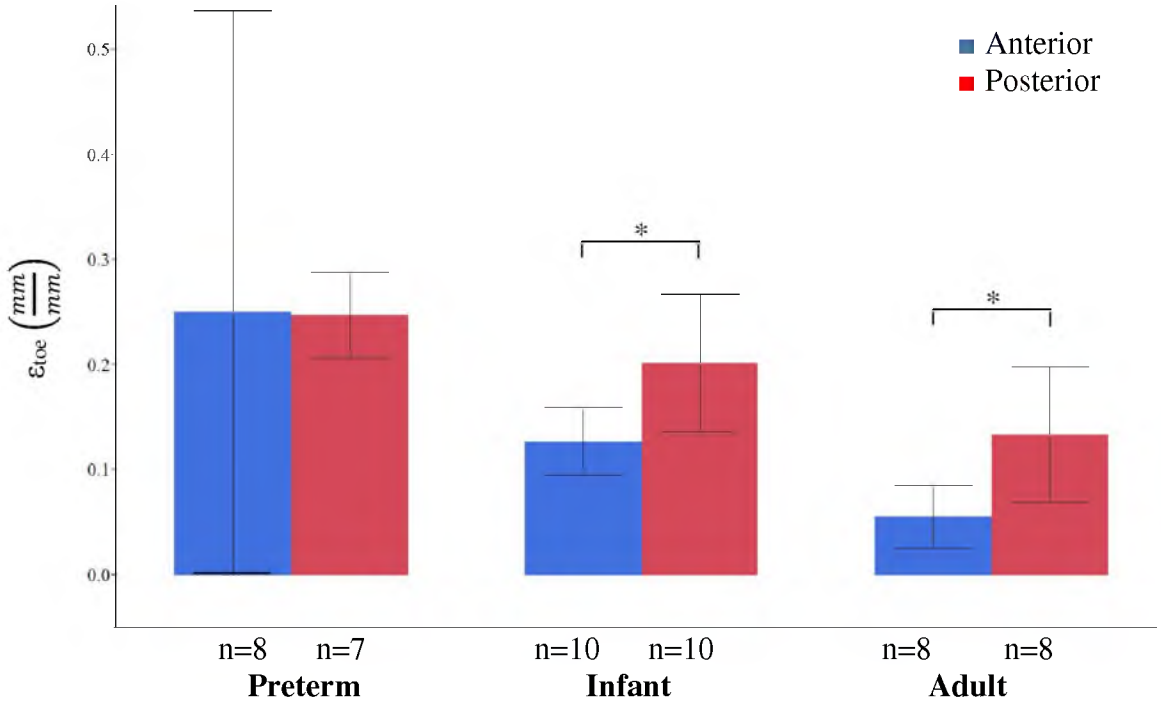

Figure 25: Average and standard deviation for toe region across age and region for sclera tested at low strain. * $p<0.05$

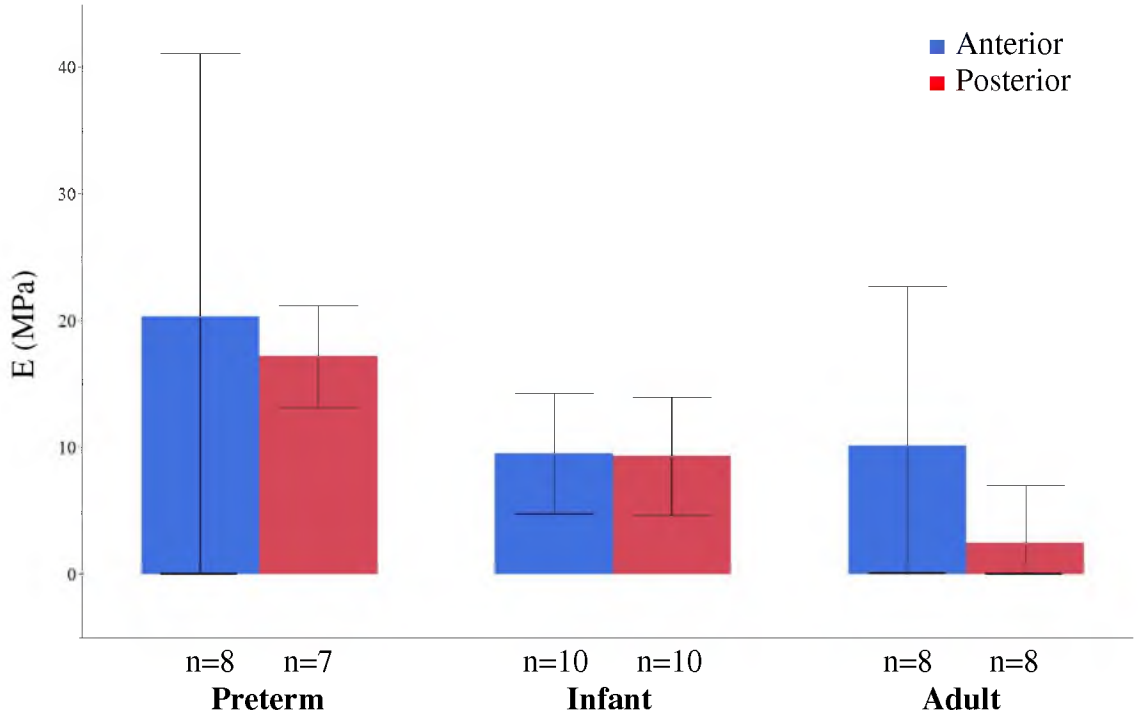

Figure 26: Average and standard deviation for Young's modulus across age and region for sclera tested at low strain.

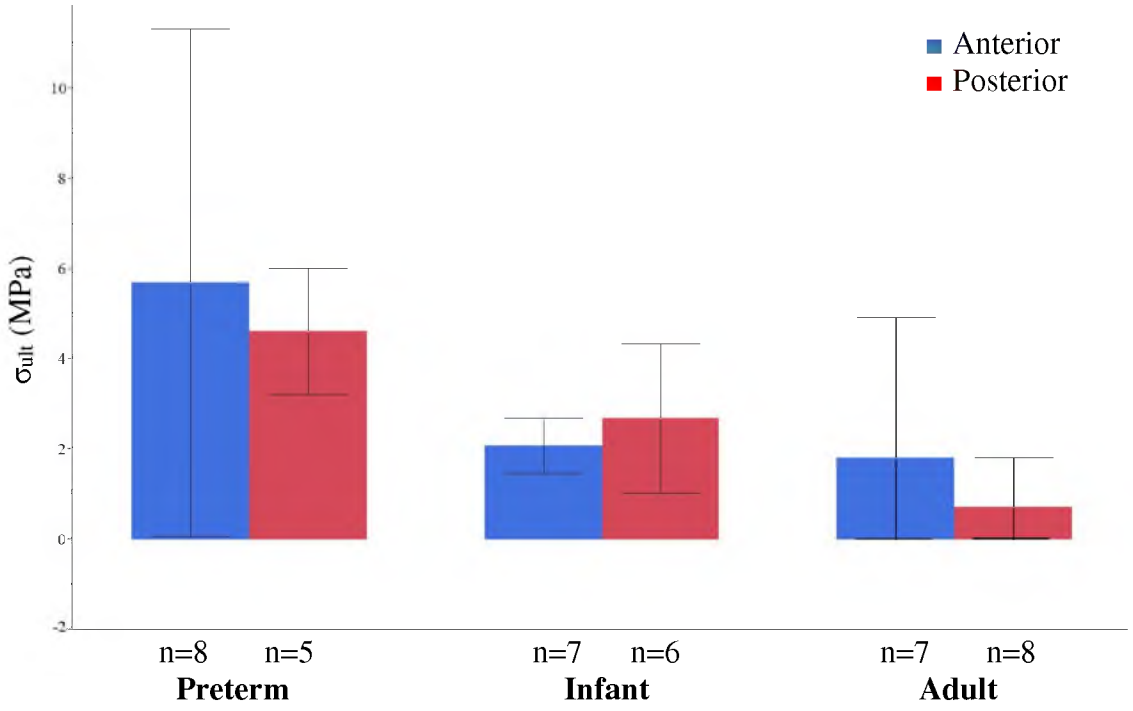

Figure 27: Average and standard deviation for ultimate stress across age and region for sclera tested at low strain.

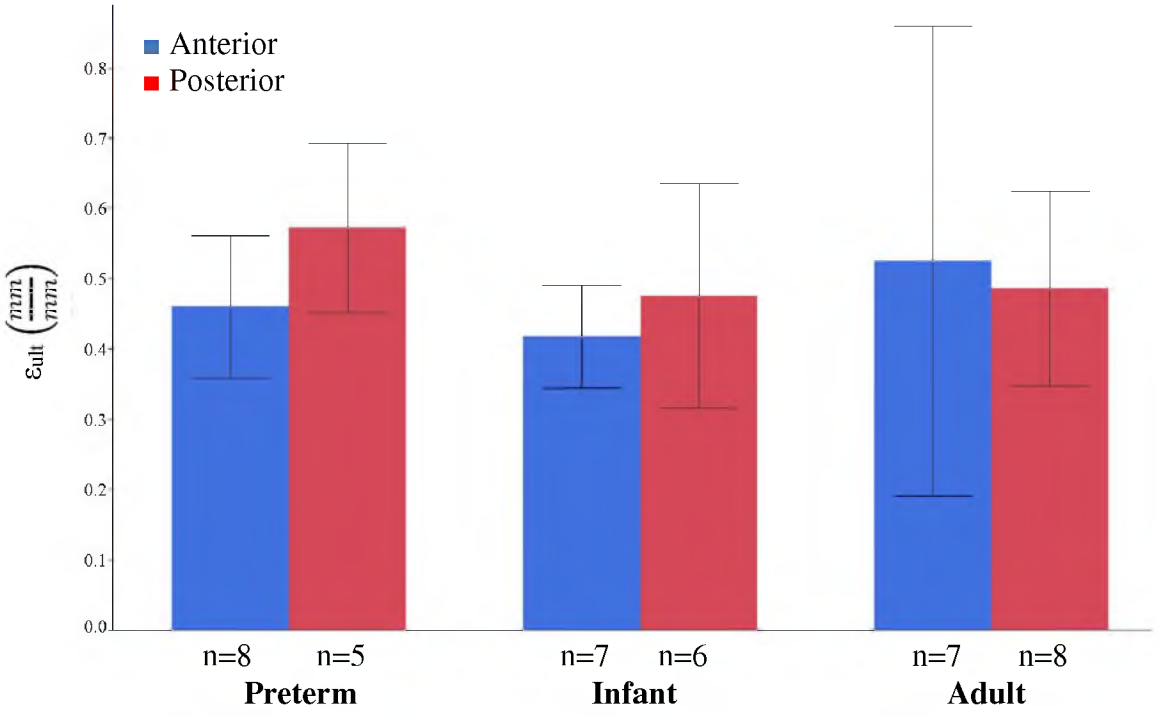

Figure 28: Average and standard deviation for ultimate strain across age and region for sclera tested at low strain.

1.4.2.2 High strain-rate. The pull-to-failure data measured at high strain-rate can be seen in Table 7. The preterm anterior sclera generally experienced higher stresses during relaxation than the preterm posterior sclera but no significant differences were found for any of the stress constants (σ_i, σ_1, σ_2, σ_e). All stress constants except σ_1 for the infant anterior sclera were significantly higher ($p<0.05$) than the infant posterior sclera. All stress constants for the adult anterior sclera were significantly higher ($p<0.05$) than the adult posterior sclera (Figure 29).

The decay time constants for the preterm anterior sclera were higher than the preterm posterior sclera but no significant differences were found (Figure 30). The decay time constants for the anterior sclera of infant and adult age groups were generally lower than the posterior sclera. The infant anterior sclera had a significantly shorter ($p<0.05$) long-term decay time constant than the infant posterior sclera (Figure 31).

No significant differences were found for the strain length of the toe region (ε_{toe}) and Young's modulus () of the anterior and posterior sclera for all age groups (Figure 32, Figure 33). Interestingly, the preterm and infant posterior sclera were stiffer than the anterior regions when tested at the high strain-rate, while the adult anterior sclera was stiffer than the posterior region. The ultimate stress and strain of both the infant and adult anterior sclera were lower than the posterior region. The ultimate stress of the infant anterior sclera was significantly lower ($p<0.05$) than the infant posterior sclera (Figure 34). The ultimate stress and strain of the preterm anterior sclera were higher than the preterm posterior sclera (Figure 35).

Table 7: Average ± standard deviation of material properties for preterm, infant, and adult anterior and posterior sclera tested at high strain. Similar symbols (*) in each row indicate groups that were significantly different than each other ($p<0.05$).

	High Strain-rate					
	Preterm		*Infant*		*Adult*	
	Anterior	Posterior	Anterior	Posterior	Anterior	Posterior
ε_{toe}	0.27 ± 0.09	0.23 ± 0.03	0.26 ± 0.06	0.29 ± 0.03	0.24 ± 0.01	0.26 ± 0.05
E (MPa)	20.62 ± 6.30	21.55 ± 9.42	18.00 ± 5.74	19.82 ± 7.02	10.86 ± 5.70	6.36 ± 7.89
σ_{ult} (MPa)	4.47 ± 1.60	4.16 ± 1.27	3.74 ± 1.20	5.32 ± 1.58	1.63 ± 1.01	1.68 ± 2.22
ε_{ult}	0.52 ± 0.10	0.45 ± 0.09	0.58 ± 0.13 *	0.59 ± 0.07 *	0.54 ± 0.15	0.62 ± 0.22

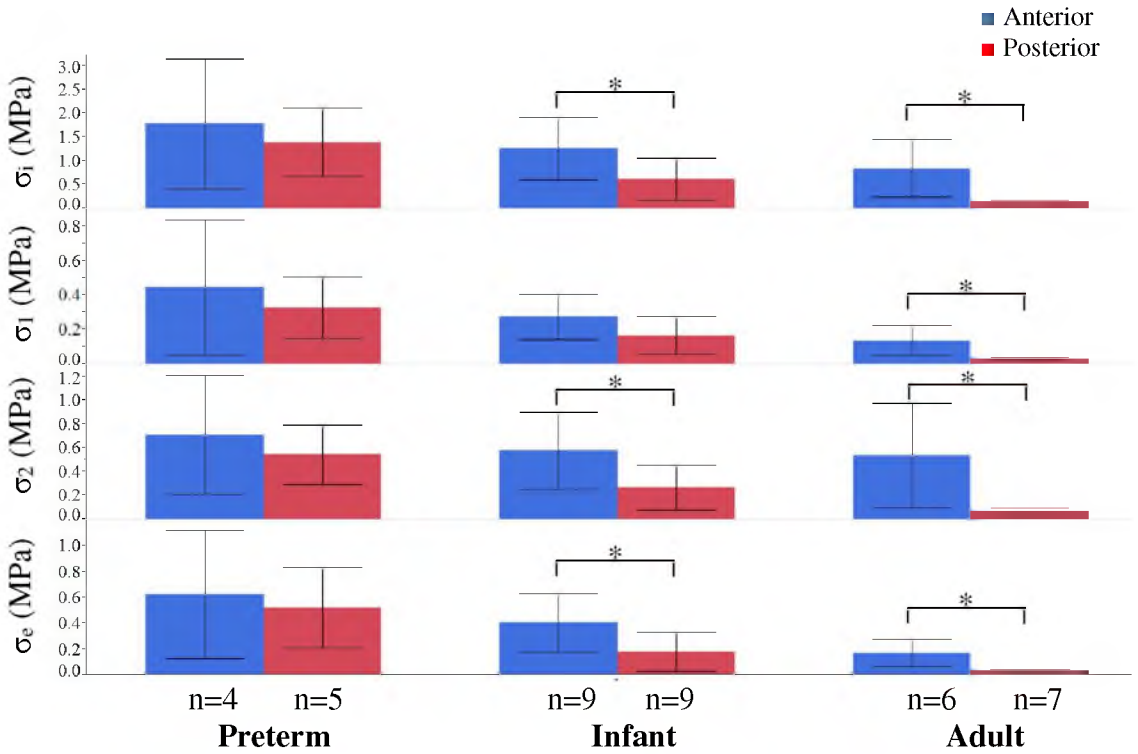

Figure 29: Average and standard deviation for stress constants across age and region for sclera tested at high strain. * $p<0.05$

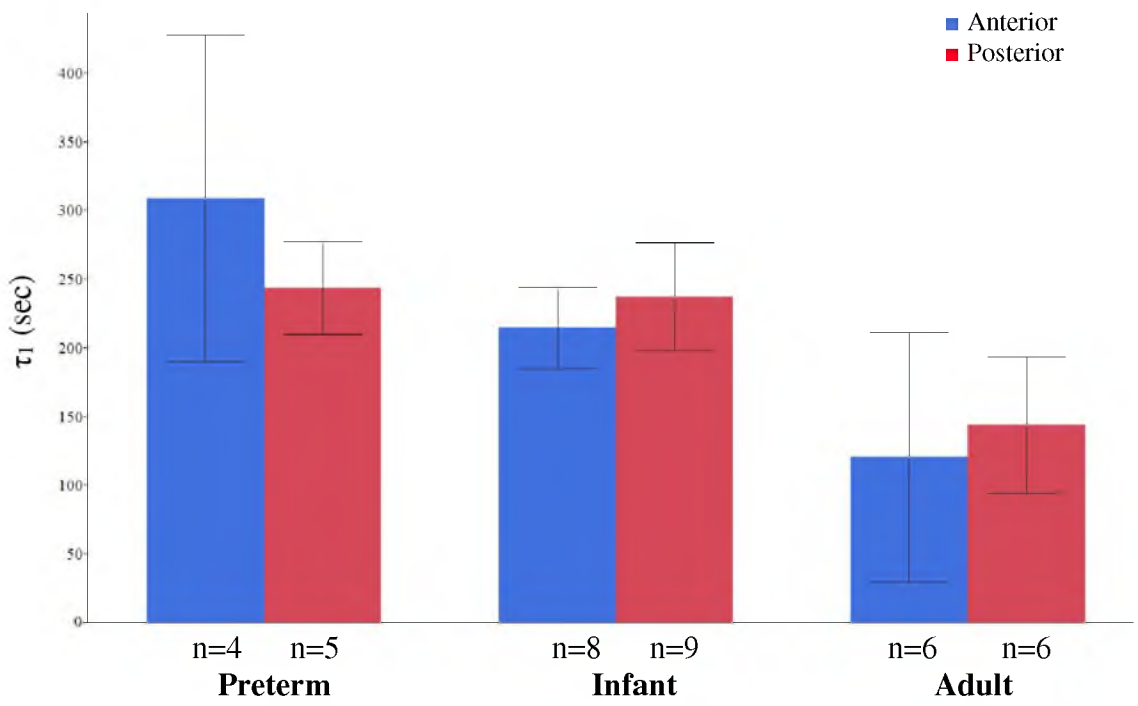

Figure 30: Average and standard deviation for immediate decay time across age and region for sclera tested at high strain.

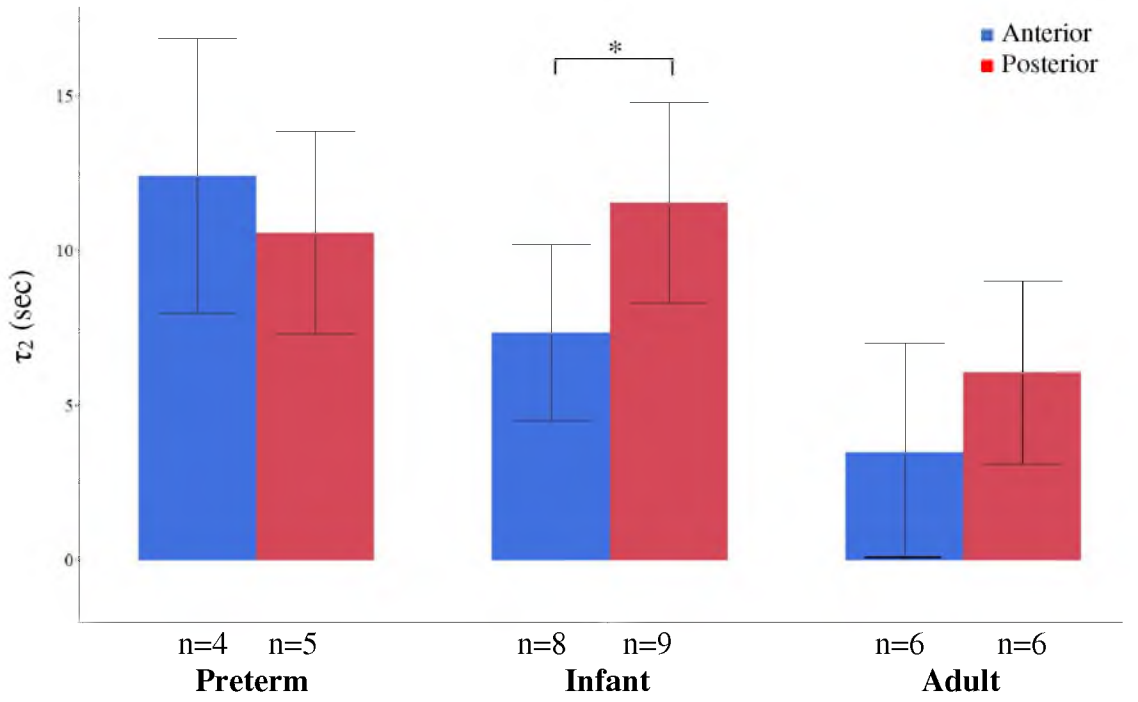

Figure 31: Average and standard deviation for long-term decay time across age and region for sclera tested at high strain. * $p<0.05$

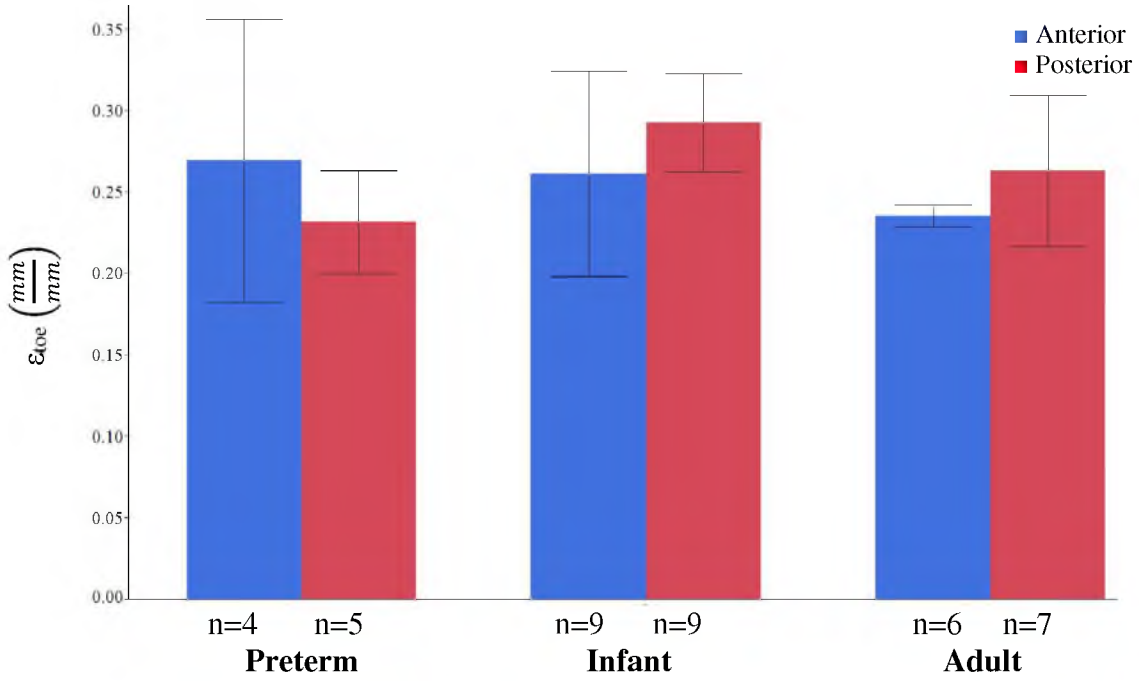

Figure 32: Average and standard deviation for toe region across age and region for sclera tested at high strain-rate. * $p<0.05$

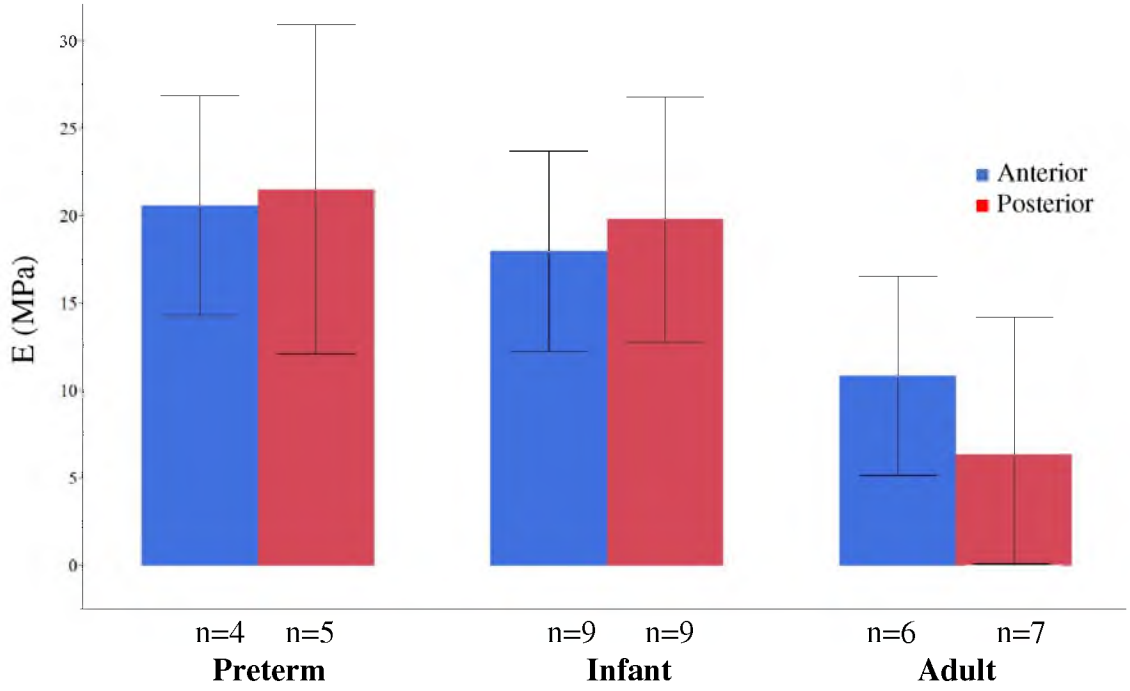

Figure 33: Average and standard deviation for Young's modulus across age and region for sclera tested at high strain-rate.

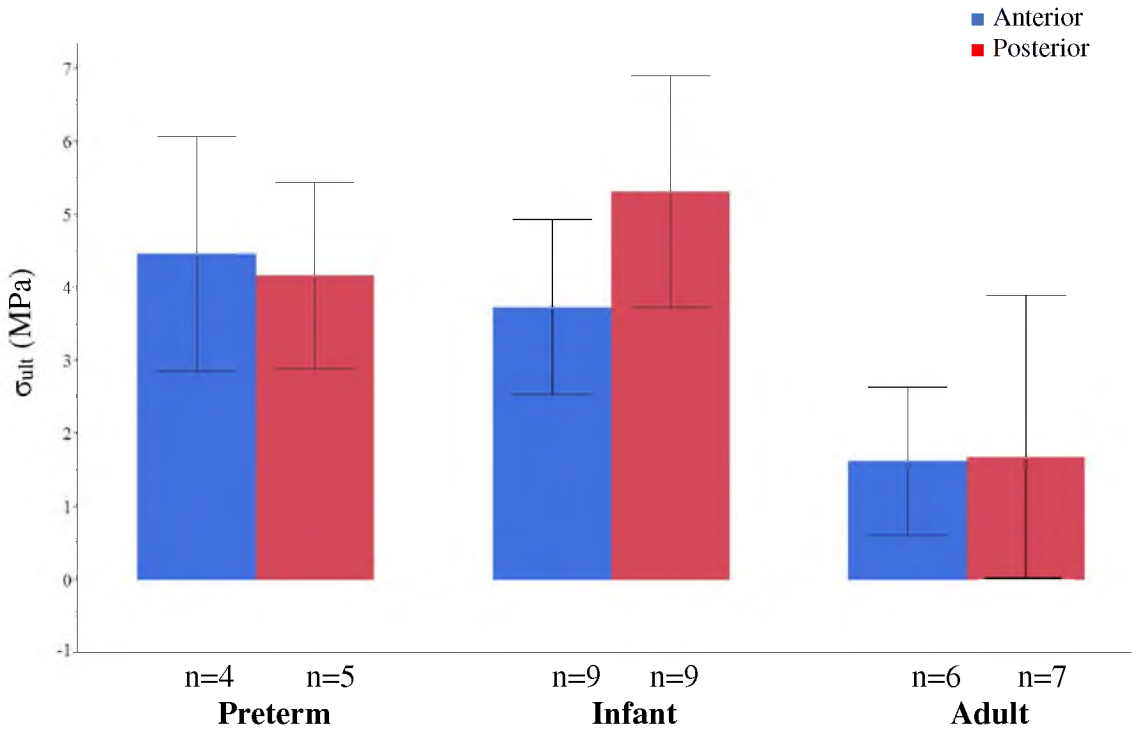

Figure 34: Average and standard deviation for ultimate stress across age and region for sclera tested at high strain. * $p<0.05$

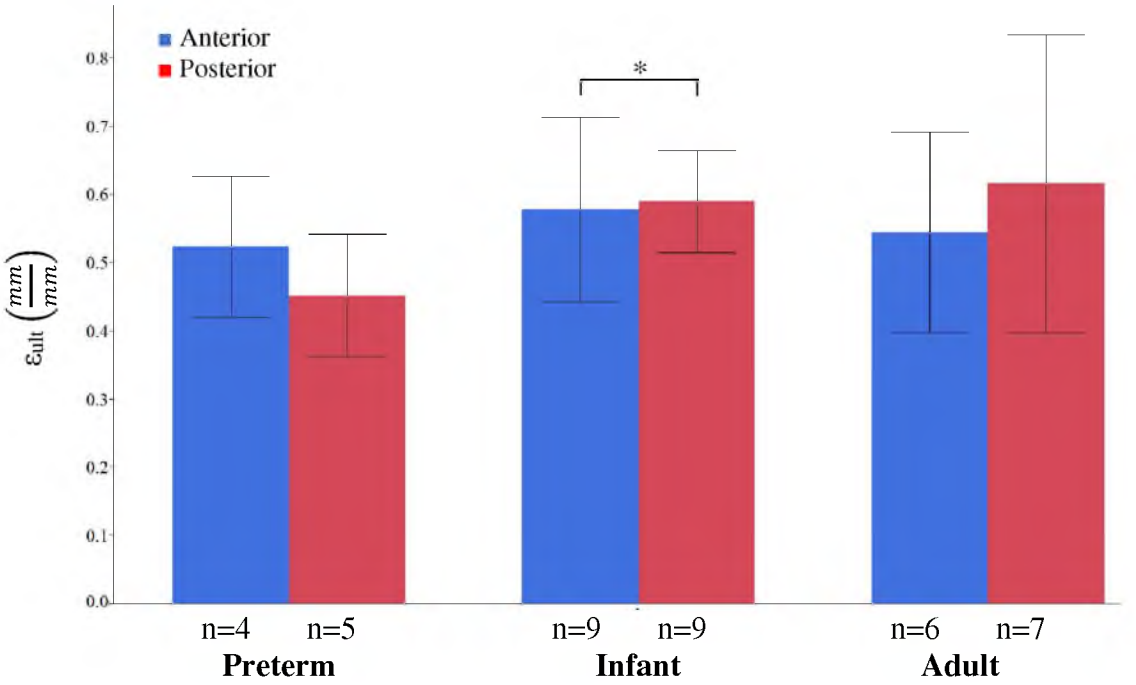

Figure 35: Average and standard deviation for ultimate strain across age and region for sclera tested at high strain.

1.4.3 Strain-rate

Sclera tested at high strain-rate generally had a greater Young's modulus and experienced higher stresses (Table 8).

1.4.3.1 Preterm. The preterm sclera tested at the high strain-rate had a greater Young's modulus than sclera tested at the low strain-rate but no significant differences were found. Interestingly, the preterm sclera tested at the low strain-rate experienced higher ultimate stress than the sclera tested at the high strain-rate but no significant differences were found. Preterm posterior sclera tested at the low strain-rate generally had a longer ε_{toe} and higher ultimate strain than posterior sclera tested at the high strain-rate. Conversely, the preterm anterior sclera tested at the low strain-rate had a shorter ε_{toe} and lower ultimate strain that anterior sclera tested at the high strain-rate (Figure 36).

1.4.3.2 Infant. In general, all material properties of infant sclera tested at the high strain-rate were higher than sclera tested at the low strain-rate. ε_{toe}, Young's modulus, ultimate stress, and ultimate strain for infant anterior sclera tested at high strain-rate were significantly higher than infant sclera tested at low strain-rate ($p<0.05$). The ε_{toe}, Young's modulus, and ultimate stress for infant posterior sclera tested at high strain-rate were significantly higher than infant sclera tested at low strain-rate ($p<0.05$) (Figure 37, Figure 38).

1.4.3.3 Adult. In general, all material properties of adult sclera tested at the high strain-rate were higher than sclera tested at the low strain-rate. ε_{toe} of the adult sclera tested at the high strain-rate was significantly longer ($p<0.05$) than the toe region of those tested at the low strain-rate (Figure 39). Adult sclera tested at the high strain-rate was stiffer than sclera tested at the low strain-rate but no significant differences were found (Figure 40).

Table 8: Average standard deviation of material properties for preterm, infant, and adult anterior and posterior sclera. Similar symbols (*,†) in each row indicate groups that were significantly different than each other ($p<0.05$).

	Preterm			
	High Strain-rate		**Low Strain-rate**	
	Anterior	Posterior	Anterior	Posterior
ε_{toe}	0.27 ± 0.09	0.23 ± 0.03	0.25 ± 0.29	0.25 ± 0.04
E (MPa)	20.62 ± 6.30	21.55 ± 9.42	20.35 ± 20.71	17.22 ± 4.00
σ_{ult} (MPa)	4.47 ± 1.60	4.16 ± 1.27	5.70 ±5.62	4.62 ± 1.4
ε_{ult}	0.52 ± 0.10	0.45 ± 0.09	0.46 ± 0.11	0.57 ± 0.12

	Infant			
	High Strain-rate		**Low Strain-rate**	
	Anterior	Posterior	Anterior	Posterior
ε_{toe}	0.26 ± 0.06 *	0.29 ± 0.03 †	0.13 ± 0.03 *	0.20 ± 0.06 †
E (MPa)	18.00 ± 5.74 *	19.82 ± 7.02 †	9.58 ± 4.75 *	9.35 ± 4.63 †
σ_{ult} (MPa)	3.74 ± 1.20 *	5.32 ± 1.58 †	2.09 ± 0.61 *	2.69 ± 1.65 †
ε_{ult}	0.58 ± 0.13 *	0.59 ± 0.07	0.42 ± 0.07 *	0.48 ± 0.16

	Adult			
	High Strain-rate		**Low Strain-rate**	
	Anterior	Posterior	Anterior	Posterior
ε_{toe}	0.24 ± 0.01 *	0.26 ± 0.05 †	0.06 ± 0.03 *	0.13 ± 0.06 †
E (MPa)	10.86 ± 5.70	6.36 ± 7.89	10.17 ± 12.52	2.49 ± 4.58
σ_{ult} (MPa)	1.63 ± 1.01	1.68 ± 2.22	1.81 ± 3.11	0.72 ± 1.09
ε_{ult}	0.54 ± 0.15	0.62 ± 0.22	0.53 ± 0.33	0.49 ± 0.14

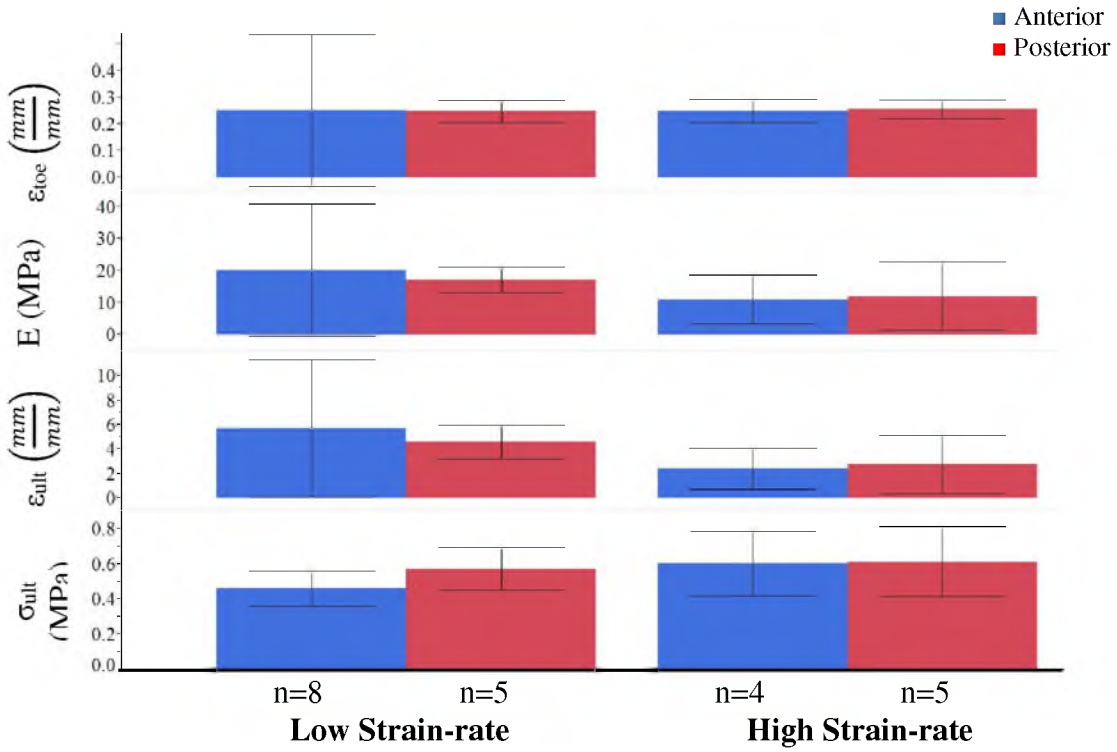

Figure 36: Average and standard deviation for material properties of preterm sclera across region and strain-rate.

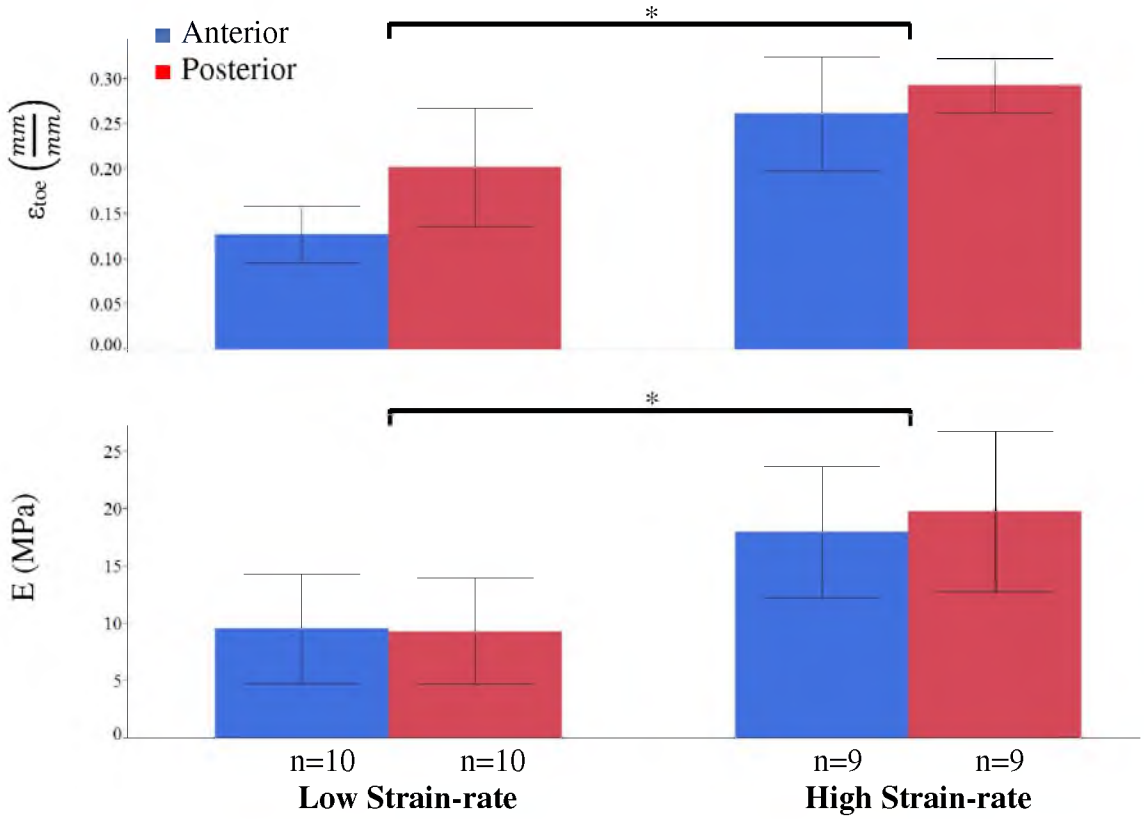

Figure 37: Average and standard deviation for toe region and Young's modulus for infant sclera across region and strain-rate. Black line indicating significant strain-rate effect between both anterior and posterior sclera. * $p<0.05$

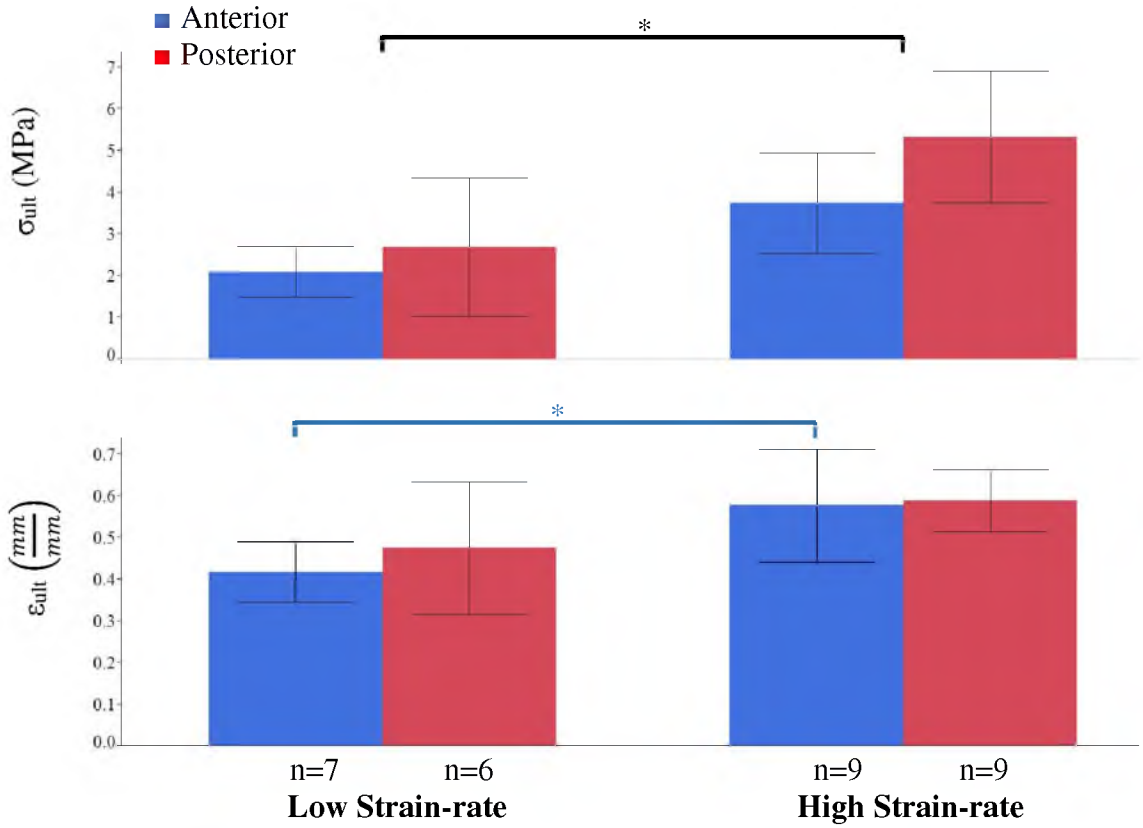

Figure 38: Average and standard deviation for ultimate stress and strain for infant sclera across region and strain-rate. Black line indicating significant strain-rate effect between both anterior and posterior sclera. Blue line indicating significant strain-rate effect in the anterior group only. * $p<0.05$

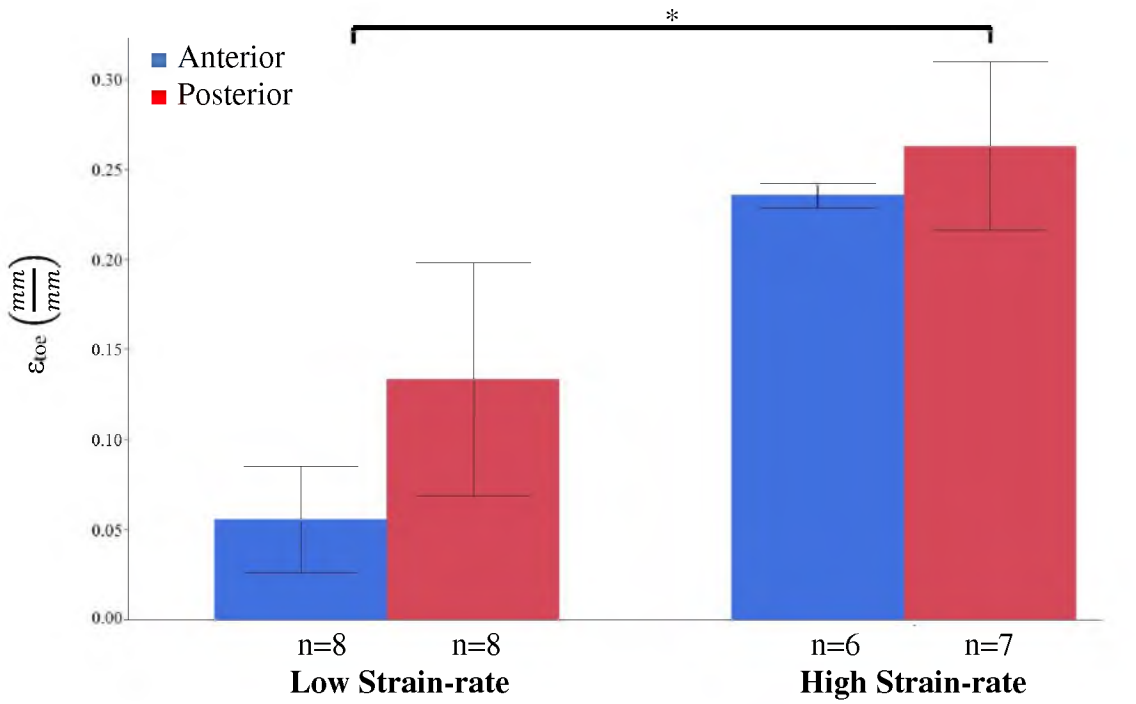

Figure 39: Average and standard deviation for toe region of adult sclera across region and strain-rate. Black line indicating significant strain-rate effect between anterior and posterior sclera. * $p<0.05$

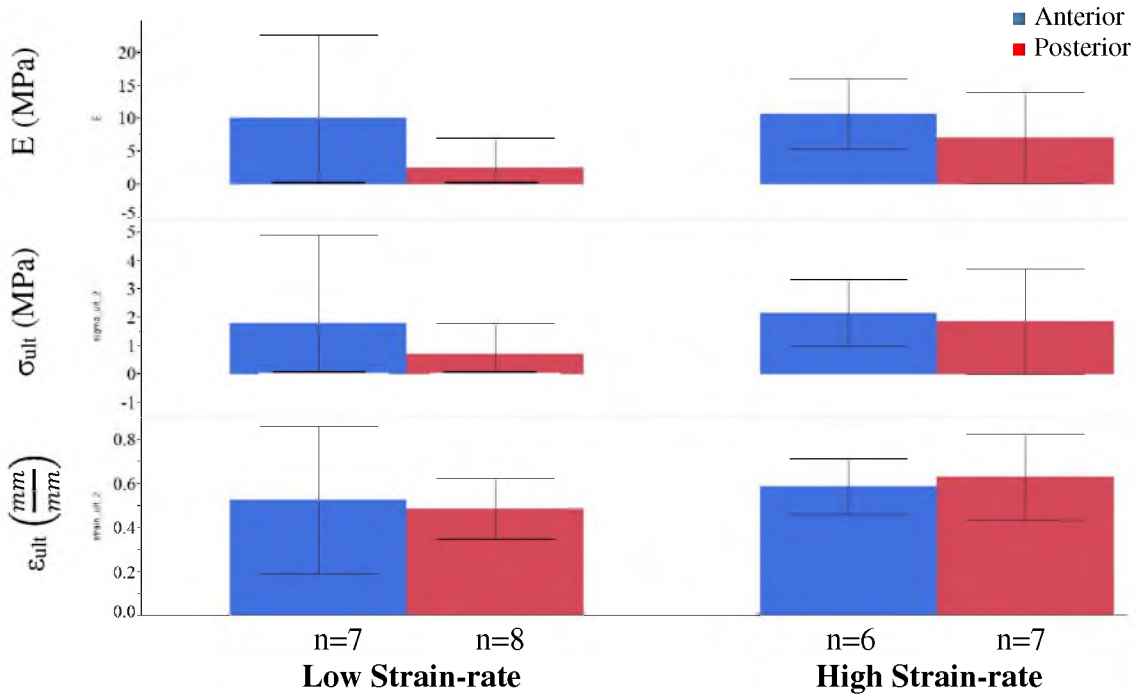

Figure 40: Average and standard deviation for ultimate strain of adult sclera across region and strain-rate.

1.5 Discussion

Overall, the younger aged sclera had a higher Young's modulus and ultimate stress than the adult sclera. The mechanical differences with age found herein have an interesting correlation to the extracellular matrix of the developing sclera. Particularly, there is a loss in collagen and GAGs in the aging sclera.[1] As aforementioned, these are the most influential constituents, acting as the load bearing structures and dampening mechanisms. This leads us to believe that the sclera should become less elastic, or stiffer with age. The sclera has been anecdotally reported to stiffen with age. Elastic modulus of the sclera from our study decreased with age. The discrepancy to this common perception is likely due to the structural rigidity of the sclera. Elastic modulus is the ratio of stress to strain and is independent of specimen. Structural rigidity is defined by the product of the Young's modulus and the moment of inertia. In our study, the scleral cross-sectional geometry can be simplified as a rectangle. Therefore, the moment of inertia is $\frac{(width)(thickness^3)}{12}$. Considering that the adult sclera thickness is 1.65 times larger than the infant, the adult anterior and posterior sclera have approximately 4.45 and 1.42 times greater structural rigidity than the infant sclera, respectively.

Furthermore, studies reporting age-related "stiffening" in the sclera incorporate older age ranges than those used in our study. Our infant age was modeled with 3-day to 6-week old lambs, where the youngest groups used in other studies were 4-5 years old humans,[6] 6-8 month old pigs,[30] or 1.5 year old monkeys.[15] These immature sclera models are outside the range of our infant group as the animal models correspond to toddlers, adolescents, and even adults. We believe our animal model more appropriately represents an infant and that there are biomechanical differences in the sclera that are being

overlooked between the reported younger populations and our youngest age. The species-related differences also must be considered when using an animal model to characterize sclera material properties. The human sclera grows in size rapidly during the first three years and is said to have decreased cellularity and undergo a densening of the extracellular matrix.[1] The sclera reaches maturity around 13-16 years[1] which raises concern about the mechanical changes happening up to this age. In future studies, supplementary histology should be conducted to parallel the similarities in the ovine and human sclera to bolster the age-related changes found in our study. The infant sclera is a biphasic material and perhaps the water content trapped at this young age significantly influences the stiff response seen in our results.

The stress-relaxation analysis shows that decay rate decreases with age with the preterm and infant groups exhibiting similar responses. As mentioned above, older sclera is more dehydrated making the tissue less viscous which was seen through the lower decay rates. No region-dependence was seen which can be attributed to an evenly dehydrated sclera throughout.

Generally, the anterior sclera was stiffer than the posterior sclera and had higher stress values. Our regional mechanical differences coincide with structural differences within the sclera as well as published data. There is no difference between the collagen content in the anterior and posterior sclera, but there is a substantial difference in the collagen arrangement.[1] The anterior sclera contains smaller, denser collagen bundles where the posterior sclera contains larger, looser collagen bundles having a "wide-angle weave".[1] This agrees with our finding that the toe region of the posterior sclera was generally longer and more extensible than the toe region of the anterior sclera. There were

fewer regional findings for the preterm sclera which may be explained by a premature growth phase of the sclera. In embryo, the sclera grows in an anterior to posterior fashion and both regions are developed by 11 weeks gestation. During the rest of gestation, the sclera continues to thicken and the extracellular matrix densens. Perhaps there are structural changes occurring in the sclera before birth that we are unable to detect. The results for preterm anterior sclera were very variable. This may be explained by some samples not purely being cut from the anterior region and partially including equatorial (mid) sclera. During the development of our testing protocols, scleral samples were taken from the equatorial region of preterm and infant eyes. To maximize the number of samples taken from each eye, only anterior and posterior specimens were collected. Data from these few equatorial specimens suggest that differences across anterior, equatorial, and posterior regions exist and the mid-scleral region should also be explored to further understand the mechanics of the younger eye.

In our study, the Young's modulus decreased with age, but was only significant in the posterior region. The preterm sclera had a higher Young's modulus than both infant and adult. The posterior sclera has a delayed growth as the anterior sclera is the first region to develop. This was seen in our significant differences only in the posterior sclera between the infant and preterm groups, while the difference between the infant and adult posterior sclera was minimal. A previous study incorporated low strain testing of human preterm, immature (4 - 6 years old) and adult sclera by subjecting specimens to a load-dependent tensile test. Weights were incrementally added to a lever arm and the stabilized displacement of the tissue was recorded. Results showed that human adult posterior sclera is more extensible than premature posterior sclera. This concurs with our findings and can

best be described by the relationship of stress and strain – more extensible, less stiff. Premature anterior sclera was not assessed in this work, but the results did show that adult anterior sclera was more stiff (less extensible) than the child anterior sclera. This trend does not correlate with our anterior sclera findings, but given the older age (4 - 6 years old), compared to adult there may be developmental changes. For example, as the sclera grows, one paper suggests the sclera is broken down and rebuilt. This would explain a stiffer infant eye, less stiff toddler eye, and stiff adult eye.

The Young's modulus in anterior sclera compared to posterior sclera was only noticeable at low rates. There was minimal significant differences at the high rate except that the adult sclera was generally different than the younger ages. At high rates, the regional differences are not seen. Similarly, at high rates, the differences between preterm and infant sclera are not seen.

Sclera tested at the higher strain-rate was generally stiffer and had higher stress values than sclera tested at the low strain-rate, which agrees with existing findings and shows that the ovine sclera is a viscoelastic material exhibiting rate-dependence under uniaxial tension. However, preterm sclera showed no significant strain-rate effects. This may be attributed to the incomplete growth of the tissue. Further analysis should focus on the developing constituents of sclera that may influence this behavior.

1.6 Conclusions

Scleral elastic modulus and ultimate stress were found to decrease with age, increase with strain-rate, and be greater in the anterior region. There is a wide spread of values reported for the material property data of sclera and our results are within the bounds

of published adult sclera mechanical properties. However, there is still a gap in the literature in the quantification of developmental and mechanical changes of the sclera across a broad age range. More pediatric ocular material property research is crucial. Previous experiments have been conducted to examine the scleral strain response in a few ages across a wide range of ages (premature, 4 - 6 year old, and adults)[6] but trends throughout development are still unclear. Our data are a start to characterizing the early developmental changes to sclera mechanics. These data will be used to identify an age-appropriate constitutive model for the sclera to be implemented into the first infant-specific eye FE model.

1.7 Acknowledgements

We would like to thank Dr. Kurt Albertine at the University of Utah for donating ovine ocular tissue. We would also like to thank the Knights Templar Eye Foundation for sponsoring this work.

1.8 References

1. Adler's Physiology of the Eye. 11th ed. St. Louis, Missouri: Mosby; 2003.
2. Brown, C.T., Vural, M., Johnson, M., Trinkaus-Randall, V. Age-related changes in scleral hydration and sulfated glycosaminoglycans. Mechanisms of Ageing and Development, 1994. 77(): p. 97-107.
3. Cirovic, S., Bhola, R.M., Howard, I.C., Lawford, P.V., Marr, J.E., Parsons, M.A., Computer modeling of the mechanism of optic nerve injury in blunt trauma. British Journal of Ophthalmology, 2006. 90(6): p. 778-783.Chen, K., Rowley, A.P., Weliand, J.D., Elastic properties of porcine ocular posterior soft tissues. Journal of Biomedical Materials Research, 2009. 93(2): p. 634-645.
4. Chen, K., Rowley, A.P., Weliand, J.D., Elastic properties of porcine ocular posterior soft tissues. Journal of Biomedical Materials Research, 2009. 93(2): p. 634-645.

5. Courdillier, B., Tian, J., Alexander, S., Myers, K.M., Quigley, H.A., Nguyen, T.D., Biomechanics of the human posterior sclera: age- and glaucoma-related changes measured using inflation testing. Investigative Ophthalmology & Visual Science, 2012. 53(4): p. 1714-1728.

6. Curtin, B.J., Physiopathologic Aspects of Scleral Stress-Strain. Tr. Am. Ophth. Soc., 1969. 67: p. 417-461.

7. Downs, J.C., Suh, J-K.f., Thomas, K.A., Belleza, A.J., Hart, R.T., Burgoyne, C.F., Viscoelastic material properties of the peripapillary sclera in normal and early-glaucoma monkey eyes. Investigative Ophthalmology & Visual Science, 2005. 46(2): p. 540-546.

8. Downs, J.C., Suh, J-K.F., Thomas, K.A., Belleza, A.J., Burgoyne, C.F., Hart, R.T., Viscoelastic characterization of peripapillary sclera: material properties by quadrant in rabbit and monkey eyes. Journal of Biomechanical Engineering, 2003. 125(1): p. 124-131.

9. Downs, J.C., Burgoyne, C.F., Thomas, K.A., Thompson, H.W., Hart, R.T. Effects of strain-rate on the mechanical properties of posterior rabbit sclera. in BMES/EMBS. 1999. Atlanta, GA.

10. Eilaghu, A., Flanagan, J.G., Tertinegg, I., Simmons, C.A., Biaxial mechanical testing of human sclera. Journal of Biomechanics, 2010. 43(9): p. 1696-1701.

11. Elsheikh, A., Geraghty, B., Alhasso, D., Knappett, J., Regional variation in the biomechanical properties of the human sclera. Experimental Eye Research, 2010. 90(5): p. 624-633.

12. Fazio, M.A., Grytz, R., Bruno, L., Girard, M.J.A., Gardiner, S., Girkin, C.A., Downs, J.C., Regional variations in mechanical strain in the posterior human sclera. Investigative Ophthalmology & Visual Science, 2012. 53(9): p. 5326-5333.

13. Fazio, M.A., Grytz, R., Morris, J.S., Bruno, L., Girkin, C.A., Downs, J.C. Age-related changes in the non-linear mechanical strain response of human peripapillary sclera. in 2013 ASME Summer Bioengineering Conference. 2013. Sunriver, OR.

14. Girard, M., Suh, J-K., Bottlang, M., Burgoyne, C.F., Downs, J.C., Biomechanical changes in the sclera of monkey eyes exposed to chronic IOP elevations. Investigative Ophthalmology & Visual Science, 2011. 52(8): p. 5656-5668.

15. Girard, M., Suh, J.-K.F., Hart, R.T., Bottlang, M., Burgoyne, C.F., Downs, J.C., Scleral biomechanics in the aging monkey eye. Investigative Ophthalmology & Visual Science, 2009. 50(11): p. 5226-5237.

16. Girard, M.J.A., Downs, J.C., Burgoyne, C.F., Downs, J.C., Suh, J.K., Peripapillary and posterior scleral mechanics-part I: development of an anisotropic hyperelastic constitutive model. Journal of Biomechanical Engineering, 2009. 131(5): p. 051011.

17. Hans, S.A., Bawab, S.Y., Woodhouse, M.L., A finite element infant eye model to investigate retinal forces in shaken baby syndrome. Graefe's Archives for Clinical and Experimental Ophthalmology, 2009. 247(4): p. 561-571.

18. Kim, W., Argento, A., Rozsa, F.W., Mallett, K., Constitutive behavior of ocular tissues over a range of strain-rates. Journal of Biomechanical Engineering, 2012. 134(6): p. 061002.

19. Krag, S., Olsen, T., Andreassen, T. Biomechanical characteristics of the human anterior lens capsule in relation to age. Investigative Ophthalmology & Visual Science, 1997. 38(2): p.357-363.

20. Moran, P.R. (2012) Characterization of the vitreoretinal interface and vitreous in the porcine eye as it changes with age (Master's thesis). Retrieved from http://content.lib.utah.edu/cdm/ref/collection/etd3/id/1932

21. Myers, K.M., Courdillier, B., Boyce, B.L., Nguyen, T.D., The inflation response of the posterior bovine sclera. Acta Biomaterialia, 2010. 6(11): p. 4327-4335.

22. Nagase, S.Y., M., Tanaka, R., Yasui, T., Miura, M., Iwasaki, T., Goto, H., Yasuno, Y. (2013) Anisotropic Alteration of Scleral Birefringence to Uniaxial Mechanical Strain. PLoS ONE 8(3): e58716. doi:10.1371/journal.pone.0058716

23. Palko, J.R., Pan, X., Liu, J., Dynamic testing of regional viscoelastic behavior of canine sclera. Experimental Eye Research, 2011. 93(6): p. 825-832.

24. Palko, J.R., Iwabe, S., Pan, X., Agarwal, G., Komaromy, A.M., Liu, J., Biomechanical properties and correlation with collagen solubility profile in the posterior sclera of canine eyes with an ADAMTS10 mutation. Investigative Ophthalmology & Visual Science, 2013. 54(4): p. 2685-2695.

25. Pallikaris, I.G., Kymionis, G.D., Harilaos, S.G., Kounis, G.A., Tsilimbaris, M.K., Ocular rigidity in living humans. Investigative Ophthalmology & Visual Science, 2005. 46(2): p. 409-414.

26. Rangarajan, N., Kamalakkhannan, S., Hasija, V., Shams, T., Jenny, C., Serbanescu, I., Ho, J., Rusinek, M., Levin, A., Finite element model of ocular injury in abusive head trauma. Journal of the American Association for Pediatric Ophthalmology and Stribismus, 2009. 13(4): p. 364-369.

27. Rudra, R.P., A curve-fitting program to stress relaxation data. Canadian Agricultural Engineering, 1987. 29(2): p. 209-211.

28. Schultz, D.S., Lotz, J.C., Lee, S.M., Trinidad, M.L., Stewart, J.M., Structural factors that mediate scleral stiffness. Investigative Ophthalmology & Visual Science, 2008. 49(10): p. 4232-4236.

29. Siegwart, J.T., Norton, T.T., Regulation of the mechanical properties of tree shrew

sclera by the visual environment. Vision Research, 1998. 39(2): p. 387-407.

30. Stewart, J.M., Schultz, D.S., Lee, O., Trinidad, M.L. Exogenous collagen cross-linking reduces sclera permeability: modeling the effects of age-related cross-link accumulation. Investigative Ophthalmology & Visual Science, 2009. 50(1): p. 352-357.

CHAPTER 2

CHARACTERIZATION OF AGE AND STRAIN-RATE RATE DEPENDENT MATERIAL PROPERTIES OF OVINE RETINA

2.1 Abstract

Retinal hemorrhages (RH) are prominent findings in abusive head trauma; however, injury mechanisms of RH are unclear. Finite element modeling may be useful in understanding the mechanical response of the retina yet current computational models of the pediatric eye do not incorporate age appropriate material properties. There is a paucity of infant eye material property data and as yet there are no published data characterizing the age-dependent material properties of retina. To quantify the effect of age on the mechanical response of retina, we tested tissue from immature and mature ovine eyes. Two strain-dependent uniaxial tensile tests were implemented to assess the mechanical response to different loading conditions. Differences were statistically tested by comparing the material properties (ε_{toe}, E, σ_{ult}, ε_{ult}) across age and strain-rate. Mature retina had higher Young's modulus and ultimate stress than immature retina but no statistically significant differences were found between immature and mature retinal material properties. Retina tested at the high strain-rate had a greater Young's modulus and higher ultimate stress compared to retina tested at the low strain-rate. However, no statistically significant rate

effects were found for the material properties of immature and mature retina. Although age did not have a significant effect on the mechanical properties of retina, the strain-rate dependence suggests that retina is sensitive to different loading conditions and may provide useful insight into understanding injury mechanisms of RH.

2.2 Introduction

Finite element (FE) analysis can be used as a tool to investigate the mechanical response of the infant eye to trauma and assist in the prediction of ocular injuries from accidental or abusive head trauma. However, current FE models of the pediatric eye are based on adult material properties with little or no consideration for mechanical changes during maturation.[9,12] To date, there are no published data characterizing the age-dependent material properties of retina. Our studies indicate that there are developmental changes in the vitreous and sclera, which suggests that changes in other ocular tissues should be considered.[12] The retina is the light sensitive, fibrous inner layer of the eye which connects to the optic nerve and delivers visual information to the brain. The retina is a multilayered structure, and is delicate and vulnerable to deformation.

Traditional tensile testing[3,4,5,14,15,16] and atomic force microscopy (AFM)[7,8] have been used to characterize the mechanical response of adult retina. From these studies, adult retina has been reported to be rate-dependent[14], inhomogeneous, and anisotropic. Retinal samples containing vasculature were stiffer than specimens containing no vasculature.[4] Retina containing a vein in the axial direction was found to be stiffer and exhibit greater stresses than retina containing a vein in the circumferential direction.[4]

All of the aforementioned studies were performed on adult retina. It is unknown if

characteristics of immature retina are similar to adult retina. Furthermore, it is unclear if there are significant mechanical changes occurring during early development. Therefore, in this study, we characterized the age and strain-rate dependent material properties of immature ovine retina. Immature (n=12) and mature (n=13) ovine retina were tested according to a uniaxial tensile test protocol to measure the mechanical response to tensile ramp to failure. Retina was tested according to either a low or high strain-rate test. These data will be used to identify an age-appropriate constitutive model for retina to implement in a FE model of the infant eye.

2.3. Materials and Methods

2.3.1. Tissue sample preparation

Immature (0-6 weeks) and mature (≥ 4 years) sheep eyes were obtained from non-ocular studies being conducted at the University of Utah. Whole eyes were collected immediately upon death and stored in phosphate buffered saline (PBS) at ~2°C. All ocular tissues were tested within 6 hours postmortem. Prior to testing, enucleated eyes were transferred to a petri dish containing PBS. Eyes were kept in PBS throughout dissection to prevent the ocular tissues from drying out. The extraocular muscles and soft tissues were removed from the eye and discarded. The optic nerve was severed at the optic nerve scleral junction. Each eye was bisected sagittally into nasal and temporal halves (Figure 41a). The vitreous was removed from each half by gently pulling with tweezers while squirting PBS between the vitreous and retina. The retina was isolated using the same technique by squirting PBS between the retina and choroid allowing the retina to detach and fall into the petri dish of PBS. The hemisections of retina were carefully cut using a

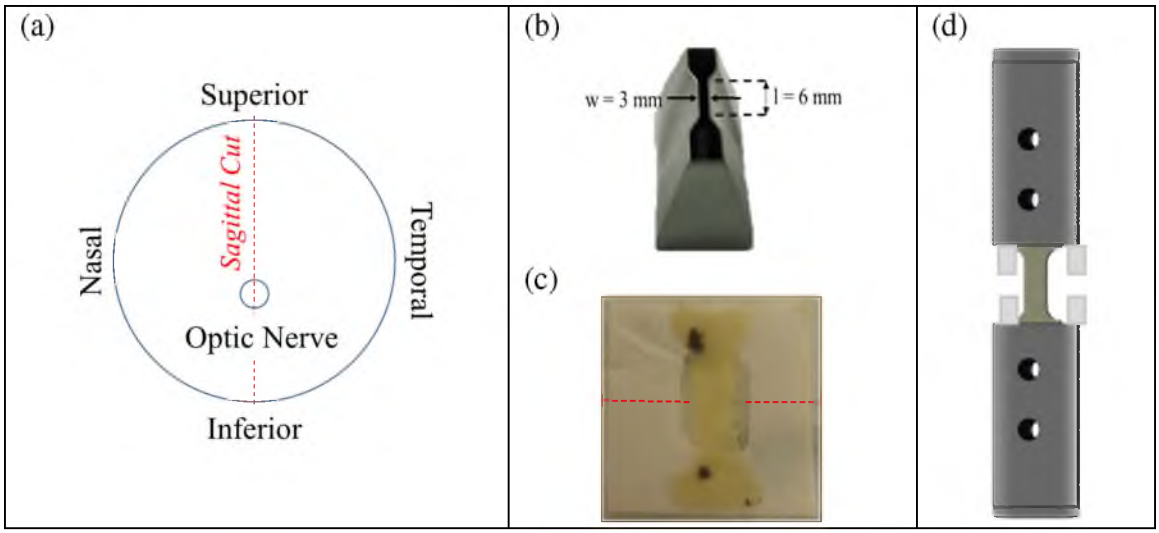

Figure 41: Ocular dissection procedure. (a) The red dashed line indicates the dissection cut on an eye globe. (b) A dog bone cutting die was used to cut samples. (c) A paper frame was used to support the retinal samples to transfer into grips. (d) Each specimen and support frame was aligned in custom grips. The frame was cut prior to testing.

custom made, dog-bone cutting die (Figure 41b). Each retinal sample was shifted onto a glass slide for support as it was lifted out of the PBS. Excessive water surrounding the sample was absorbed with a tissue so retina would not slip off the glass. The glass slide was turned on its side and tissue thickness was measured with an optical microscope at 1x magnification (SZX16, Olympus, Center Valley, PA). A minimum of three measurements was taken for each tissue, at the center and ends of the gage length. A precut paper frame was placed on the exposed surface of the retina (Figure 41c). The paper and retina were peeled away by lifting a corner of the paper as the glass offers minimal adhesion to the retina. The paper support frame and retina were placed in custom, screw-driven grips (Figure 41d). Once the retina was properly aligned in the clamps, the two sides of the paper support frame were cut (dotted red line in Figure 41c). Width (3 mm) and gage length (6 mm) were determined by the dog-bone shape. The material test system (5943, Instron, Norwood, MA) was equipped with a 500 gram load cell (LSB210, Futek, Irvine, CA).

2.3.2. Mechanical testing

All specimens were subjected to uniaxial tension according to one of two protocols (Figure 42). A low strain test protocol was implemented to characterize the mechanical response of ocular tissues during physiological increased intraocular pressure.[16] A high strain protocol was implemented to characterize the mechanical response of ocular tissues during high rate trauma.[6] All tests were performed in a water bath filled with PBS at room temperature.

2.3.2.1 Low strain-rate. Each tissue was subjected to ten cycles of preconditioning from 0 to 1% strain at a strain-rate of 0.01 s^{-1}. Specimens were allowed to recover for 60 s and then subjected to a tensile ramp to failure at 0.01 s^{-1}.

2.3.2.2 High strain-rate. Each tissue was subjected to ten cycles of preconditioning from 0 to 5% strain at a strain-rate of 0.05 s^{-1}. Specimens were allowed to recover for 60 s and then subjected to a tensile ramp to failure at 0.1 s^{-1}.

The raw load and displacement data were sampled at 10 Hz and extracted to calculate engineering stress and strain. A custom Matlab (Mathworks, Natick, MA) code was implemented for retinal analysis and plotting and can be seen in Appendices A and C. Stress was calculated by dividing the current force by the reference cross-sectional area. Strain was calculated by dividing displacement by the original gage length. Each tissue was preloaded to approximately 0.001 N to remove any slack in the tissue sample. The strain length of the toe region (ε_{toe}), elastic modulus (E), ultimate stress (σ_{ult}), and ultimate strain (ε_{ult}) were extracted from each pull-to-failure test.

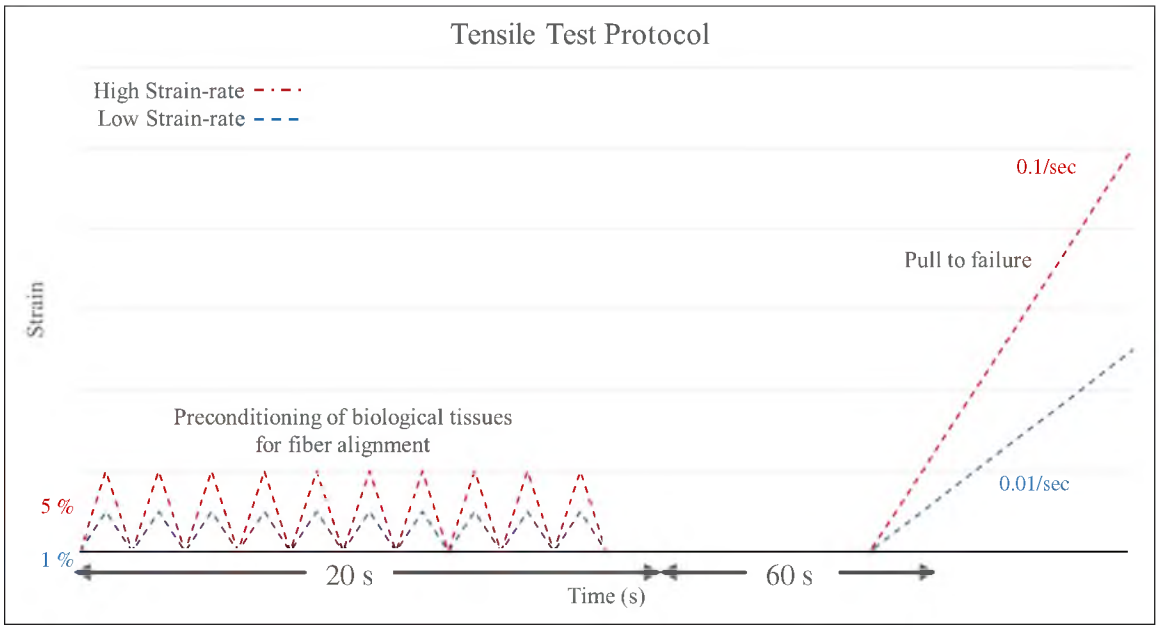

Figure 42: The strain-dependent uniaxial tensile test protocol consisted of preconditioning, a recovery phase, and pull-to-failure.

2.3.3. Statistical analysis

Age and strain-rate were analyzed independently in this study. A Student's t-test with a p-value of 0.05 was used to determine if age or strain-rate significantly affected the material properties (ε_{toe}, E, σ_{ult}, ε_{ult}). The retinal data can be seen in Appendix D.

2.4. Results

2.4.1 Age

The immature and mature retinal samples had roughly the same thickness (Table 9). Average and standard deviations for retinal material properties can be seen in Table 10. No significant age difference was found for retinal thickness (Figure 43). At both high and low rate, the mature retina had higher Young's modulus an ultimate stress. No statistical significance with age was found for the material properties at the high and low strain-rates (Figure 44-45).

Table 9: Average ± standard deviations thickness of immature and mature retina

	Immature	**Mature**
Thickness (mm)	0.16 ± 0.03	0.18 ± 0.03

Table 10: Average ± standard deviations of the material properties for immature and mature retina tested at the high and low strain-rates.

	Immature		**Mature**	
	Low Strain-rate (n=8)	*High Strain-rate (n=9)*	*Low Strain-rate (n=8)*	*High Strain-rate (n=8)*
$\varepsilon_{toe}\left(\frac{mm}{mm}\right)$	0.1698 ± 0.2482	0.181 ± 0.149	0.2446 ± 0.2747	0.1477 ± 0.1649
E (MPa)	0.0082 ± 0.0139	0.009 ± 0.011	0.0178 ± 0.0226	0.0211 ± 0.02
σ_{ult} (MPa)	0.0030 ± 0.0014	0.0076 ± 0.0113	0.0113 ± 0.0130	0.0261 ± 0.024
$\varepsilon_{ult}\left(\frac{mm}{mm}\right)$	1.0898 ± 0.6253	1.0366 ± 0.4033	1.0294 ± 0.3356	1.76 ± 1.06

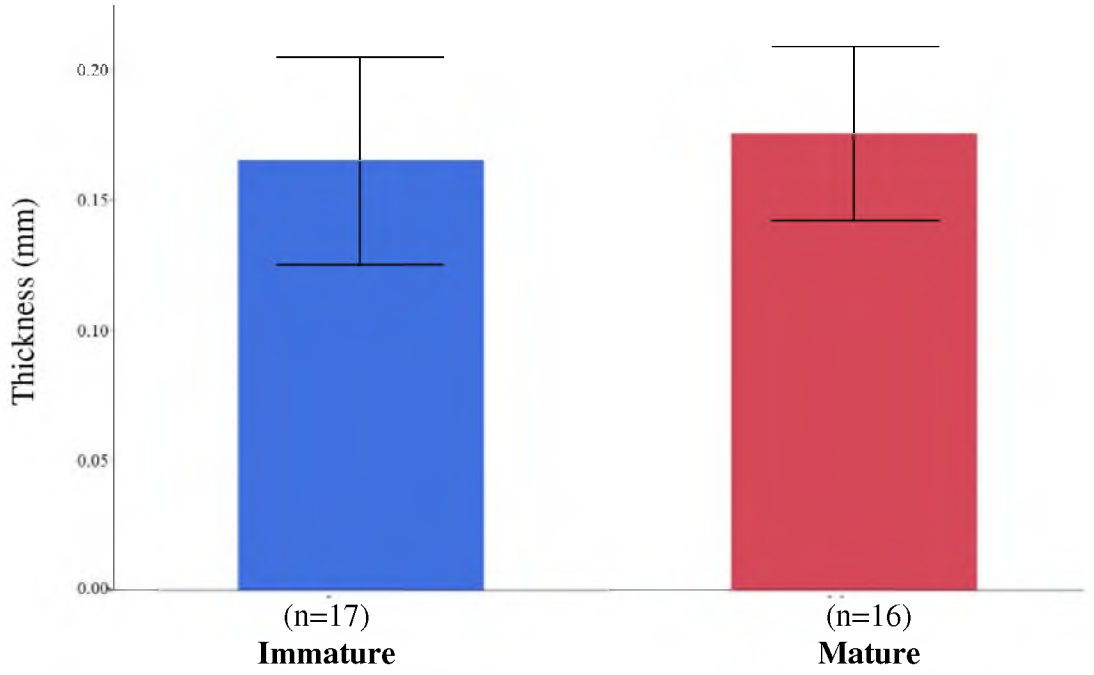

Figure 43: Average and standard deviation for immature and mature retinal thickness.

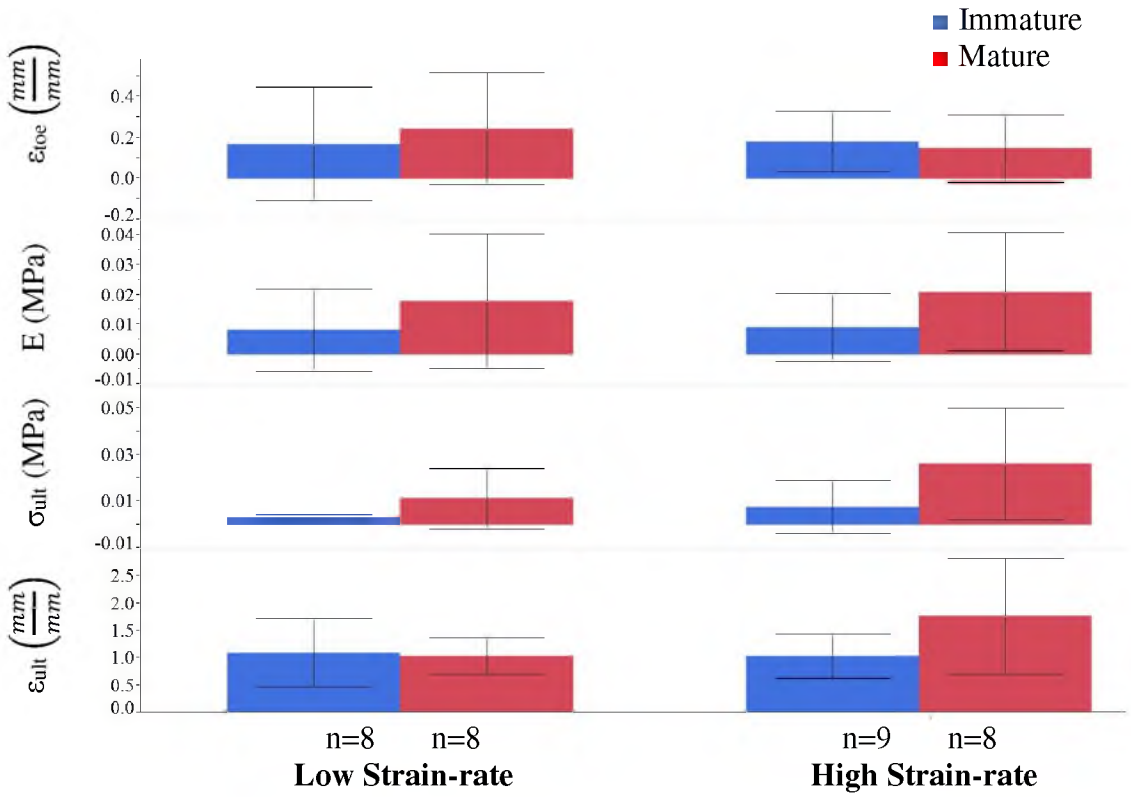

Figure 44: Average and standard deviation for retinal material properties across age and strain-rate.

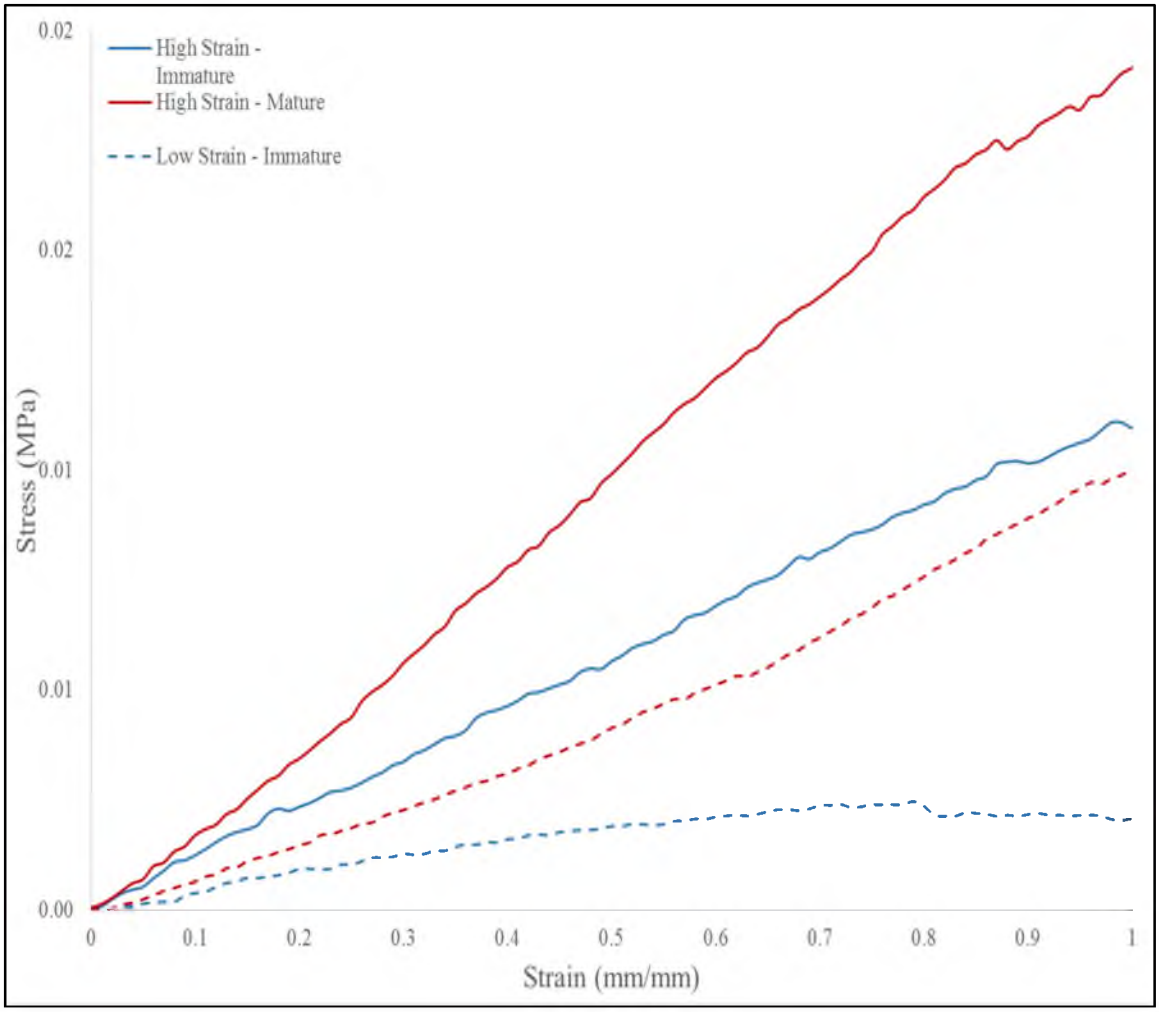

Figure 45: Pull-to-failure response of all included trials at low and high strain-rate across age and region.

2.4.2 Strain-rate

The strain length of the toe region, Young's modulus, and ultimate stress of immature retina increased at high rate. The ultimate strain of immature retina was lower at the high rate. For the mature retina, the Young's modulus, ultimate stress, and ultimate strain increased at high rate. The ε_{toe} of mature retina decreased when tested at the high strain-rate. No statistically significance strain-rate effect was found for immature and mature retina (Figure 46).

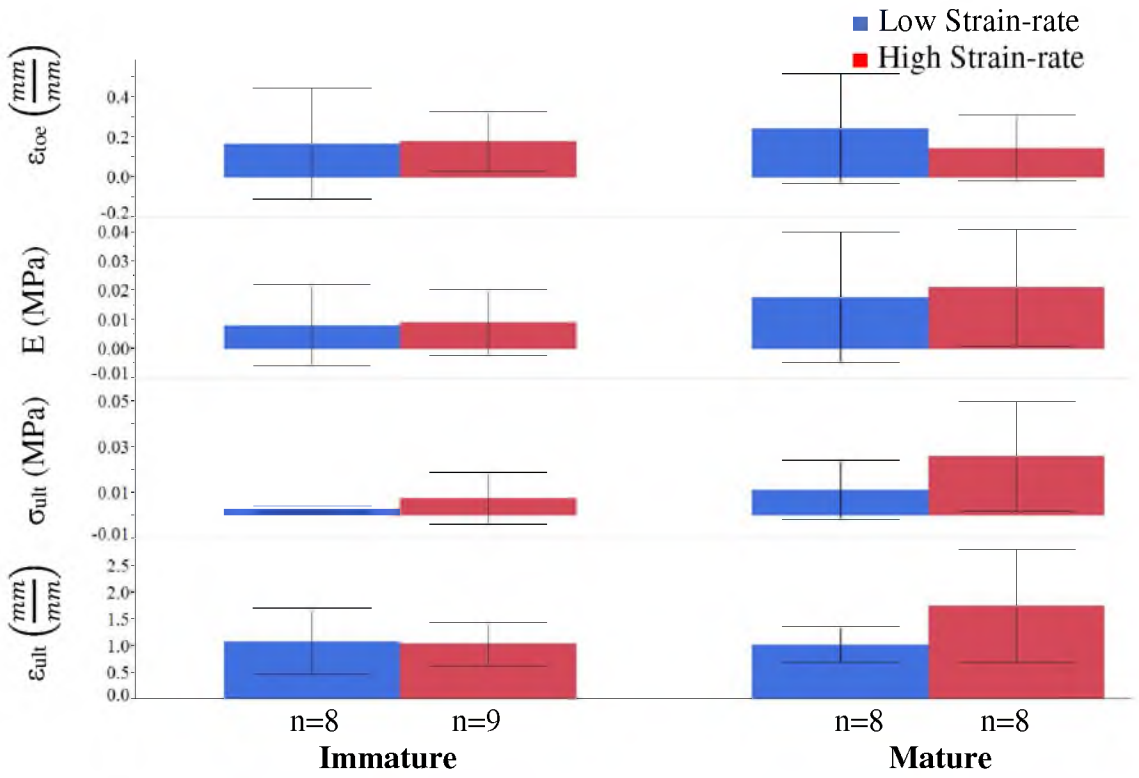

Figure 46: Average and standard deviation for retinal material properties across age and strain-rate.

2.5 Discussion

Retinal hemorrhages are thought to be key indicators of pediatric abusive head trauma. It is important to incorporate an age-appropriate constitutive model into finite element models of the infant eye when investigating mechanical influences on the retina. In this study, we sought to characterize the age-dependent material properties of ovine retina. The retina proved to be an extremely difficult tissue to handle and test mechanically. A number of samples were lost due to tearing or simply being damaged during preparation and handling. Future techniques to measure the biomechanics of the retina in-vitro would be helpful. We found the elastic modulus of retina to be about three orders of magnitude less than our scleral findings. This mechanical comparison stresses the importance of the

scleral structure to protect the inner ocular components, specifically preventing deformation of the retina.

We found the Young's modulus of all retina to be between 8-26 kPa when tested at low and high strain-rates. Our findings fall within the range of values from previous adult retina studies. Typical tensile testing resulted in Young's moduli of approximately 2-110 kPa.[3,4,5,14,15,16] Atomic force microscopy resulted in Young's moduli of 0.94-3.6 kPa.[7,8] Our findings agree with existing literature that the retina stiffens with increased strain-rate. The retina is a viscoelastic material and indeed experiences higher stresses when stretched at high strain-rates. This trend was seen previously as the Young's modulus of retina was reported to be 100 and 110 kPa at low and high rate, respectively.[14] The average moduli in this study were smaller; however, a couple of the retinal samples had Young's moduli greater than 50 kPa. The variation may be attributed to discrepancies in vasculature between specimens.

In this study, we were able to capture the retinal vasculature in several of the specimens by imaging the tissue with our microscope. Retinal samples either contained vasculature perpendicular or parallel to the direction of the load, or no visible vessel. However, the samples sizes within each age group and strain-rate were not large enough to include vasculature directionality as a variable. Anecdotal comparisons indicate that retina containing vasculature in the direction of the applied force (parallel) at low strain-rate is stiffer than retina containing vasculature perpendicular to the direction of the applied force. Future mechanical testing of the retina should compare tissue samples with different compositions and orientations of vasculature. Histology in these specimens would also be useful to better understand the extracellular matrix of ovine retinal specimens and its

contribution to the mechanical response.

We did not find any significant age effect on the material properties of retina. The retina is a well-organized, multilayered lining of the eye which does not change drastically from birth to adulthood. The retinal layer is made up photoreceptor cells and accessory components designed specifically for vision. These do not offer any mechanical support; therefore, we would not expect to see a significant change in the material response between the infant and adult retina.

2.6 Conclusion

The material properties of the retina were not significantly different between the immature and mature age groups. Anatomically, this may support that structurally and functionally, the retina should not change drastically with age unless there is a specific vision-related disease or damage occurring in an elderly eye. In accordance with the literature, the retina is a strain-rate dependent material and becomes stiffer with increased strain-rate. This was also seen for the sclera and may shed light on injury mechanisms of retinal hemorrhages. These data will be implemented as the material definitions into an age-appropriate FE model of the infant eye, and thereby increasing the accuracy of computational models investigating retinal stress and strain.

2.7 Acknowledgements

We would like to thank Dr. Kurt Albertine at the University of Utah for donating ovine ocular tissue. We would also like to thank the Knights Templar Eye Foundation for sponsoring this work.

2.8 References

1. Alamouti, B., Funk, J., Retinal thickness decreases with age: an OCT study. British Journal of Ophthalmology, 2003. 87(7): p. 899-901.

2. Bottega, W.J., Bishay, P.L., On the mechanics of a detaching retina. Mathematical Medicine and Biology, 2013. 30(4): p. 287-310.

3. Chen, K., Rowley, A.P., Weliand, J.D., Elastic properties of porcine ocular posterior soft tissues. Journal of Biomedical Materials Research, 2009. 93(2): p. 634-645.

4. Chen, K., Weiland, J.D., Anisotropic and inhomogeneous mechanical characteristics of the retina. Journal of Biomechanics, 2010. 43(7): p. 1417-1421.

5. Chen, K., Weiland, J.D., Mechanical characteristics of the porcine retina in low temperatures. Retina, 2012. 32(4): p. 844-847.

6. Chen, K., Weiland, J.D., Discovery of retinal elastin and its possible role in age-related macular degeneration. Annals of Biomedical Engineering, 2013. 42(3): p. 678-684.

7. Franze, K., Francke, M., Gunter, K., Christ, A.F., Korber, N., Reichenbach, A., Guck, J., Spatial mapping of the mechanical properties of the living retina using scanning force microscopy. Soft Matter, 2011. 7(7): p. 3147-3154.

8. Grant, C.A., Twigg, P.C., Savage, M.D., Woon, W.H., Wilson, M, Estimating the mechanical properties of retinal tissue using contact angle measurements of a spreading droplet. Langmuir, 2013. 29(16): p. 5080-5084.

9. Hans, S.A., Bawab, S.Y., Woodhouse, M.L., A finite element infant eye model to investigate retinal forces in shaken baby sundrome. Graefe's Archives for Clinical and Experimental Ophthalmology, 2009. 247(4): p. 561-571.

10. Jerdan, J.A., Glaser, B.M., Retinal microvessel extracellular matrix: an immunofluorescent study. Investigative Ophthalmology & Visual Science, 1986. 27(2): p. 194-203.

11. Jones, I.L., Warner, M., Steven, J.D., Mathematical modelling of the elastic properties of retina: a determination of Young's modulus. Eye, 1992. 6(Pt 6): p. 556-559.

12. Moran, P.R. (2012) Characterization of the vitreoretinal interface and vitreous in the porcine eye as it changes with age (Master's thesis). Retrieved from http://content.lib.utah.edu/cdm/ref/collection/etd3/id/1932

13. Rangarajan, N., Kamalakkhannan, S., Hasija, V., Shams, T., Jenny, C., Serbanescu, I., Ho, J., Rusinek, M., Levin, A., Finite element model of ocular injury in abusive head trauma. Journal of the American Association for Pediatric Ophthalmology and Stribismus, 2009. 13(4): p. 364-369.

14. Wollensak, G., Spoerl, E., Biomechanical Characteristics of retina. Retina, 2004. 24(6): p. 967-970.

15. Wollensak, G., Spoerl, E., Grosse, G., Wirbelauer, C., Biomechanical significance of the human internal limiting lamina. Retina, 2006. 26(8): p. 965-968.

16. Wu, W., Peter, W.H., Hammer, M.E., Basic mechanical properties of retina in simple elongation. Journal of Biomechanical Engineering, 1987. 109(1): p. 65-67.

CHAPTER 3

CHARACTERIZING THE EFFECT OF POSTMORTEM TIME AND STORAGE CONDITION ON MECHANICAL PROPERTIES OF IMMATURE AND MATURE OVINE SCLERA AND RETINA

3.1 Abstract

Material property testing of soft biological tissues is ideally conducted just after death to reflect the most physiologic response for that species. However, human ocular tissues may only be available 24-72 hours postmortem. To date, there are no known studies evaluating the effect of postmortem time (PMT) on pediatric ocular tissues. Furthermore, it is unclear what storage parameters are suitable, if any, during shipping and transportation. To determine a viable time period for material testing, we characterized the effect of PMT on the mechanical response of immature and mature ovine sclera. To determine a shipping strategy for material testing, we characterized the effect of storage condition on the mechanical response of immature and mature ovine sclera and retina. Scleral samples were tested in uniaxial tension up to 24 hours postmortem, and differences were assessed among fresh, frozen/thawed, and fixed sclera and retina. A significant negative correlation with PMT was found for stress relaxation constants, Young's modulus, and ultimate stress for the immature sclera, with the primary change occurring after 10

hours postmortem. PMT had no significant effect on the material properties of mature sclera. In the storage condition analysis, fixed immature and mature sclera and retina were significantly stiffer than fresh tissue and had higher ultimate stresses. Freezing then thawing only had a significant effect on the ultimate stress of immature posterior sclera and ultimate strain of retina. These data suggest that immature sclera can be mechanically tested up to 10 hours postmortem and freezing sclera or retina may be a viable shipping technique for pediatric ocular tissues. Mature ovine sclera can be stored in phosphate buffered saline for up to at least 24 hours postmortem.

3.2 Introduction

There is a paucity of pediatric eye material property data in the literature as obtaining human donor eyes in this age range is difficult. In order to obtain a sufficient number of specimens for testing, eye banks across the country will need to be utilized. Material property testing of any soft biological tissues is ideally conducted just after death to reflect the most physiologic mechanical response for that species. However, pediatric donor eyes may only be available 24-72 hours postmortem, and will likely need to be shipped across the country. The effect of postmortem time (PMT) on the material properties of mature rabbit sclera has been previously measured and suggests that it can be stored up to 72 hours in phosphate buffered saline (PBS).[2] To date, there are no known studies evaluating the effect of PMT on pediatric ocular tissues. Furthermore, it is unclear what storage parameters are suitable, if any, during shipping and transportation. Fixation and freezing are two storage methodologies that have not been explored for sclera and retina. Fixation has only been investigated for the cornea, which becomes stiffer at higher

concentrations of glutaraldehyde fixation.[3] To determine viable shipping and storage strategies for pediatric ocular tissues, we characterized the effect of PMT and storage condition on the mechanical response of mature and immature ovine sclera. Due to the limited availability of retinal samples, only PMT was assessed for sclera over a broad range of testing time frames. These data will provide guidance for the requirements of collecting and accurately measuring the material properties of human sclera and retina.

3.3 Materials and Methods

3.3.1 Tissue collection and storage

Whole eyes were collected from newborn lambs and adult sheep immediately upon death and stored according to the desired storage condition (Table 11 and Table 12). Whole eyes for PMT evaluation were stored in a 2°C refrigerator in containers of PBS and tested up to ~24 hours postmortem. Frozen/thawed whole eyes were collected within an hour postmortem, placed in PBS, and stored in a -23°C freezer immediately. The frozen samples were kept in the freezer 24 hours then and allowed to thaw at room temperature for approximately 3 hours before testing. Fixed eyes were also collected within an hour postmortem, but stored in a 1%-formaldehyde/1.25%-glutaraldehyde mixture for a minimum of 72 hours.

Table 11: Retinal sample sizes by storage condition (low strain-rate).

		Immature	Mature
Storage Condition (low strain)	Fresh	n=8	n=8
	Frozen	n=3	n=2
	Fixed	n=11	n=5

Table 12: Scleral sample sizes by postmortem time (high strain-rate) and storage condition (low strain-rate).

		Immature		Mature	
		Anterior	Posterior	Anterior	Posterior
PMT (fresh, high strain)	0-6 hrs	n=13	n=14	n=6	n=7
	6-12 hrs	n=6	n=5	n=N/A	n=N/A
	12-24 hrs	n=11	n=10	n=7	n=6
	> 24 hrs	n=5	n=5	n=5	n=5
Storage Condition (low strain)	Fresh	n=11	n=11	n=5	n=5
	Frozen	n=8	n=8	n=4	n=4
	Fixed	n=8	n=9	n=6	n=6

3.3.2 Tissue dissection

On the day of testing, enucleated eyes were transferred to a petri dish containing PBS. Eyes were kept in PBS throughout dissection to prevent the ocular tissues from drying out. The extraocular muscles and soft tissues were trimmed from the eye and discarded, and the optic nerve was severed at the optic nerve scleral junction. Each eye was bisected sagittally into nasal and temporal halves (Figure 47a,c). The vitreous was removed from each half by gently pulling with tweezers while squirting PBS between the vitreous and retina. The retina was isolated by squirting PBS between the retina and choroid allowing the retina to detach and fall into the petri dish of PBS. The hemisections of retina were carefully cut using a dog-bone cutting die (Figure 47b). Each retinal sample was shifted onto a glass slide for support as it was lifted out of the PBS. Any excessive water surrounding the sample was absorbed with a tissue so that the retina would not slip

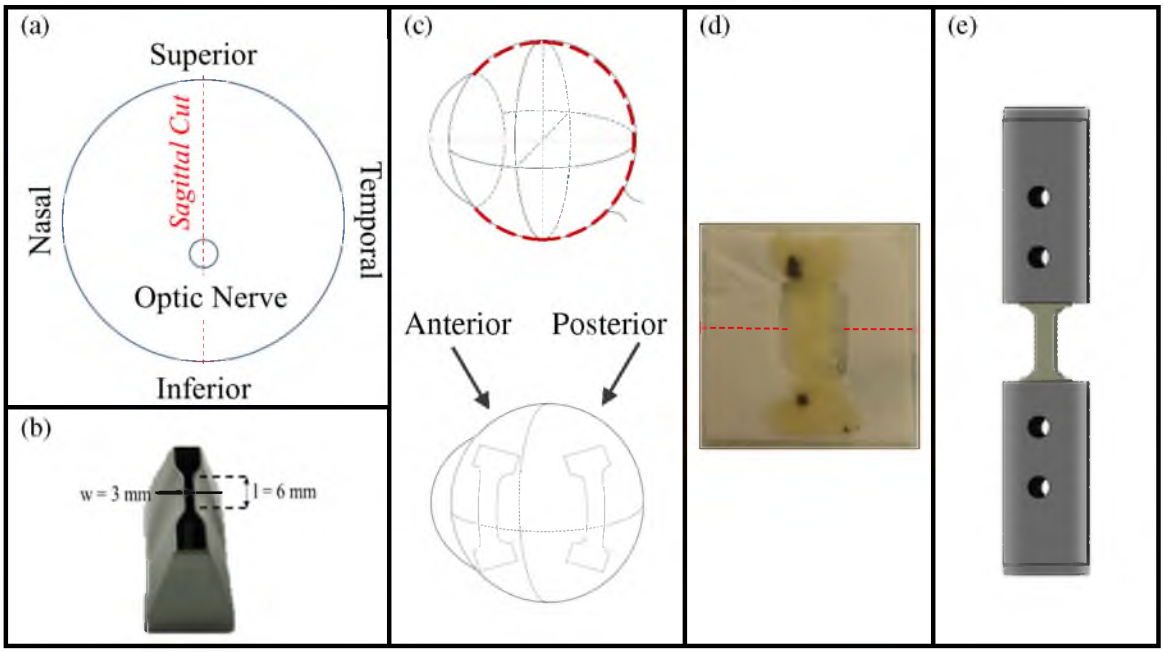

Figure 47: Ocular dissection procedure. (a) The red dashed line indicates the direction of dissection cut on an eye globe. (b) A custom dog bone cutting die was used to cut scleral samples. (c) The eye is bisected sagittally leaving nasal and temporal halves from which scleral and retinal samples were taken from anterior and posterior regions. (d)A paper frame was used to support the retinal samples during transfer into grips. (e) Each tissue sample was aligned in custom screw-driven grips.

off the glass slide. The glass slide was turned on its side and tissue thickness was measured with an optical microscope at 1x magnification (SZX16, Olympus, Center Valley, PA). Thickness was measured at the center and ends of the gage length. A precut paper support frame was placed on the exposed surface of the retina (Figure 47d) and both were slid away from the slide by lifting a corner of the paper. The paper support frame and retina were placed in custom made, screw-driven clamps (Figure 47e). Once the retina was properly aligned in the clamps, the two sides of the paper frame were cut (dotted red line in Figure 47d). Width (3 mm) and gage length (6 mm) were determined by the dog-bone shape. The material test system (Model 5943, Instron, Norwood, MA) was equipped with a 500 gram load cell (LSB210, Futek, Irvine, CA).

Sclera was isolated by removing the choroid with tweezers. The resulting hemisections of sclera were placed on a cutting board and press-cut with the dog-bone cutting die. Anterior and posterior scleral samples were cut from each of the ocular halves (Figure 47c). Tissue thickness was measured using the optical microscope at 1x magnification and the average of three measurements were taken from the center and each end of the gage length. Width and gage length were determined by the dog-bone shape of the tissue sample. Each scleral sample was aligned in the clamps and measured with a 1 kN (Instron, Norwood, MA) or 500 gram load cell for high and low strain tests, respectively.

3.3.3 Mechanical testing

Uniaxial stress relaxation and pull-to-failure tests in tension were performed on fresh sclera at low strain-rates (0.01 s^{-1}, Figure 48). To determine the rate dependence of PMT, a high strain-rate protocol was also performed on sclera (0.1 s^{-1}). Due to limited retinal specimens and constraints of the lower limit accuracy of the load cell, only low strain-rate pull-to-failure tests were performed on retina (Figure 49). All tests were performed in an environmental bath filled with phosphate buffered saline at room temperature.

3.3.3.1 PMT study - Sclera. Each tissue was subjected to ten cycles of preconditioning from 0 to 5% strain at a strain-rate of 0.05 s^{-1}. Specimens were allowed to recover for 60 s and then a stress relaxation test was performed by applying 25% strain and holding for 900 s. The tissue was allowed to recover for 60 s, and then subjected to a tensile ramp to failure at 0.1 s^{-1}.

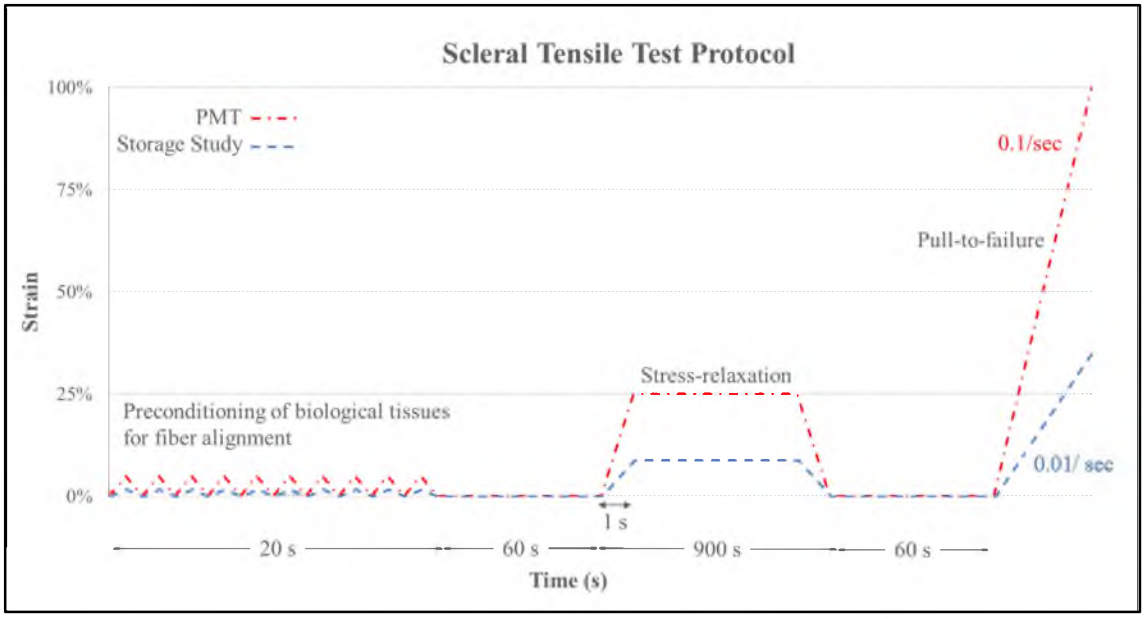

Figure 48: The strain-dependent uniaxial tensile test protocol for the PMT and storage studies of sclera consisted of preconditioning, stress relaxation, and pull-to-failure at either a high or low strain level.

3.3.3.2 Storage study - Sclera. Each tissue was subjected to ten cycles of preconditioning from 0 to 1% strain at a strain-rate of 0.01 s^{-1}. Specimens were allowed to recover for 60 s and then a stress relaxation test was performed by applying 1% strain and holding for 900 s. The tissue was allowed to recover for 60 s, and then subjected to a tensile ramp to failure at 0.01 s^{-1}.

3.3.3.3 Storage study - Retina. Each tissue was subjected to ten cycles of preconditioning from 0 to 1% strain at a strain-rate of 0.01 s^{-1}. Specimens were allowed to recover for 60 s and then subjected to a tensile ramp to failure at 0.01 s^{-1}. The retina load response during stress relaxation tests was very low and was strongly influenced by low-frequency noise. This prohibited us from performing stress relaxation tests on retinal samples.

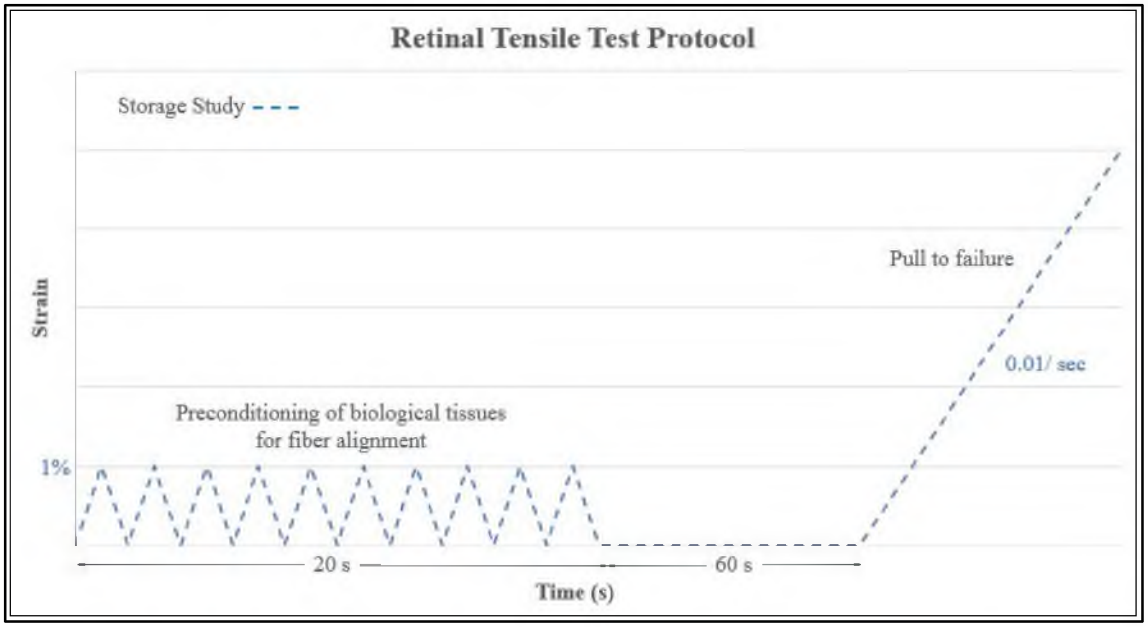

Figure 49: The strain-dependent uniaxial tensile test protocol for retinal samples consisted of preconditioning and pull-to-failure at a low strain level.

The raw load and displacement data were sampled at 10 Hz and extracted to calculate engineering stress and strain. Stress relaxation data for each scleral specimen were fit to a two-term generalized Maxwell model [Eq.1].[4] A least-squares curve-fitting technique was used to solve for equilibrium stress (σ_e), intermediate stress (σ_1, σ_2), and the decay (τ_1, τ_2) constants. Instantaneous stress (σ_i) was defined as the sum of the equilibrium and intermediate stress constants [Eq.2]. The strain length of the toe region (ε_{toe}), elastic modulus (E), ultimate stress (σ_{ult}), and ultimate strain (ε_{ult}) were extracted from the scleral and retinal pull-to-failure tests. Preliminary results repeatedly showed a good fit to the experimental data using this viscoelastic material model.

$$\sigma(t) = \sigma_e + \sum_{i=1}^{2} \sigma_i e^{-\frac{t}{\tau_i}} \quad (1)$$

$$\sigma_i = \sigma_e + \sigma_1 + \sigma_2 \quad (2)$$

3.3.4 Statistical analysis

A normal bivariate correlation analysis was performed to evaluate significant postmortem time changes in the stress relaxation constants (σ_i, σ_e, σ_1, σ_2, τ_1, τ_2) and material properties (σ_{ult}, ε_{ult}, E, ε_{toe}) of anterior and posterior scleral samples. A Pearson correlation coefficient was computed to identify significant correlation with PMT (ρ=0.95). A one-way analysis of variance (ANOVA) was used to determine if storage condition significantly affected the relaxation constants of sclera and material properties of sclera and retina. A Dunnett's test with a p-value of 0.05 was used to identify significant differences between fresh tissue and frozen/thawed and fixed tissue. Age and region were analyzed independently for both the PMT and storage condition study. The scleral and retinal data can be seen in Appendix D.

3.4 Results

The results from the correlation analyses were depicted using either diagonal or straight lines. The diagonal lines do not represent the fit lines, but rather representing significant correlation. Similarly, the straight lines signify no significant correlation.

3.4.1 PMT – Immature sclera

A slightly negative correlation with PMT was seen for the immediate and long-term decay constants for immature sclera, but this negative correlation was not significant (Figure 50). A significant negative correlation with PMT was found for the instantaneous

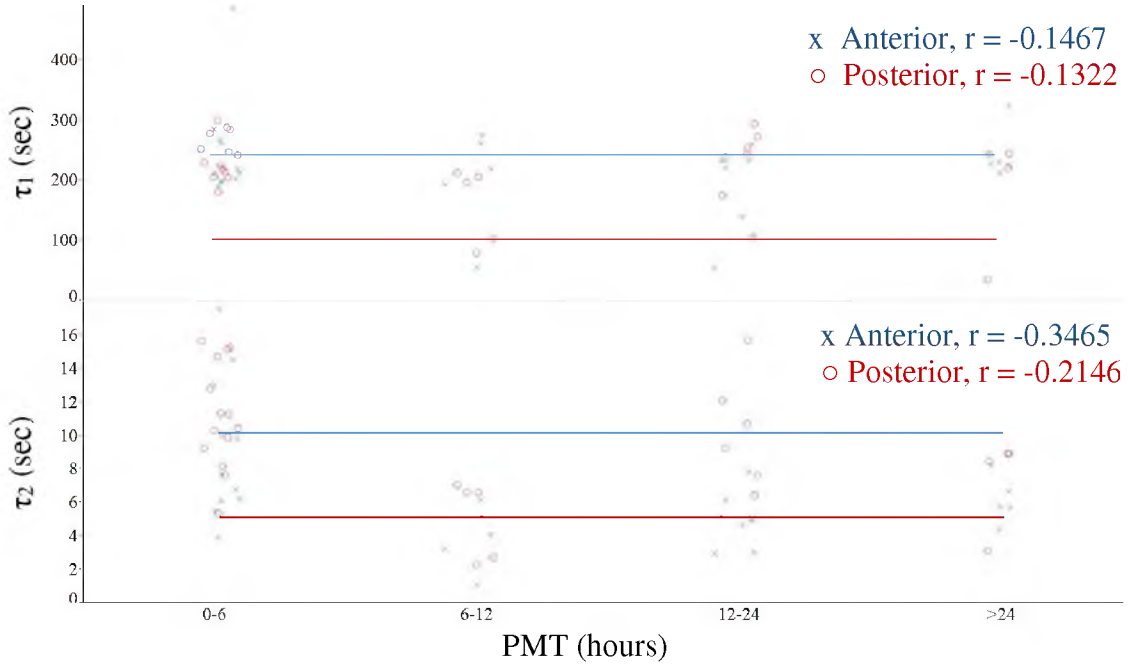

Figure 50: Statistical correlation (red and blue lines) found no significant effect of PMT on the decay time constants for immature anterior and posterior sclera.

stress (σ_i), intermediate stress constants (σ_1, σ_2), and equilibrium stress (σ_e) of the immature anterior and posterior sclera (Figure 51, Figure 52). No changes with PMT were seen for the ε_{toe} of the immature sclera (Figure 53), but a significant negative correlation with PMT was found for the Young's modulus (E) (Figure 54). A significant negative correlation with PMT was found for the ultimate stress (σ_{ult}) of the immature anterior and posterior sclera (Figure 55), but there was no correlation of ultimate strain with PMT (Figure 56).

3.4.2 PMT – Mature sclera

Unlike immature sclera, no significant correlation with PMT was found for any of the stress relaxation constants or material properties of the mature anterior and posterior sclera (Figure 57-Figure 63).

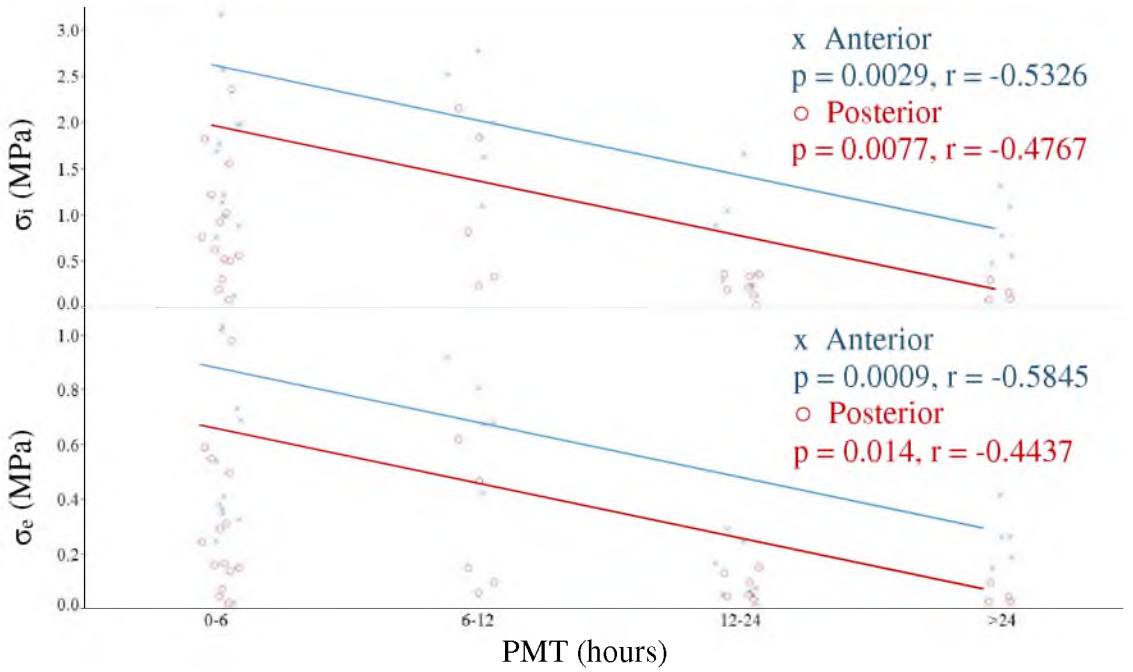

Figure 51: Statistical correlation (red and blue lines) found significant effect of PMT on the instantaneous and equilibrium stress for immature anterior and posterior sclera.

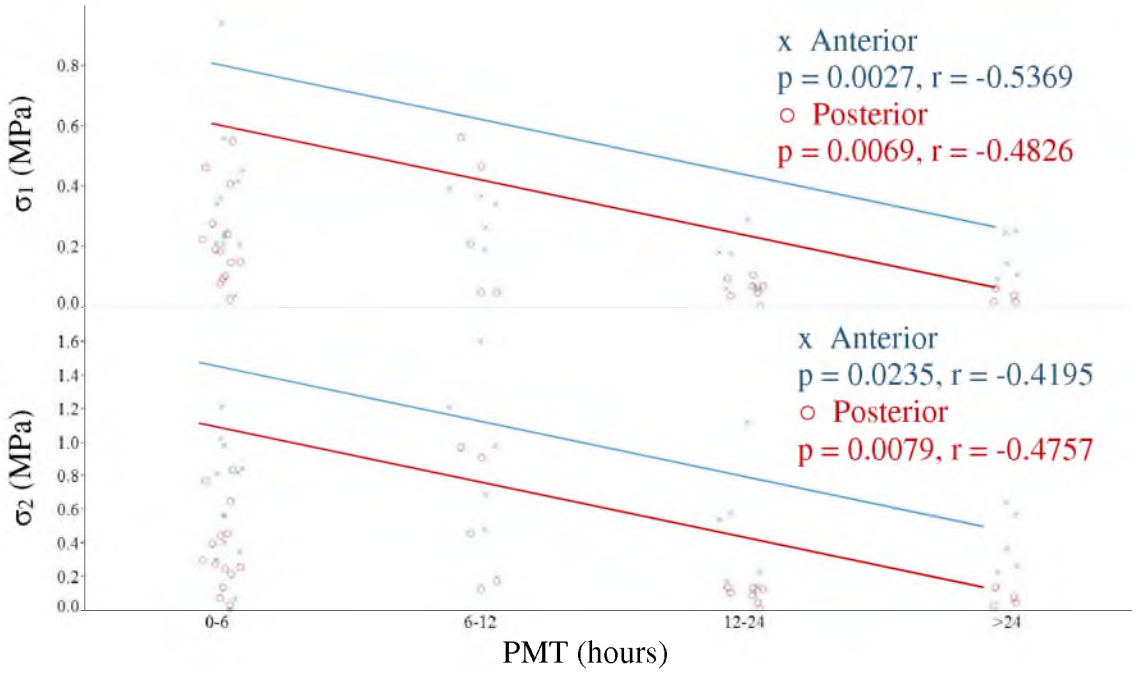

Figure 52: Statistical correlation (red and blue lines) found significant effect of PMT on the intermediate stresses for immature anterior and posterior sclera.

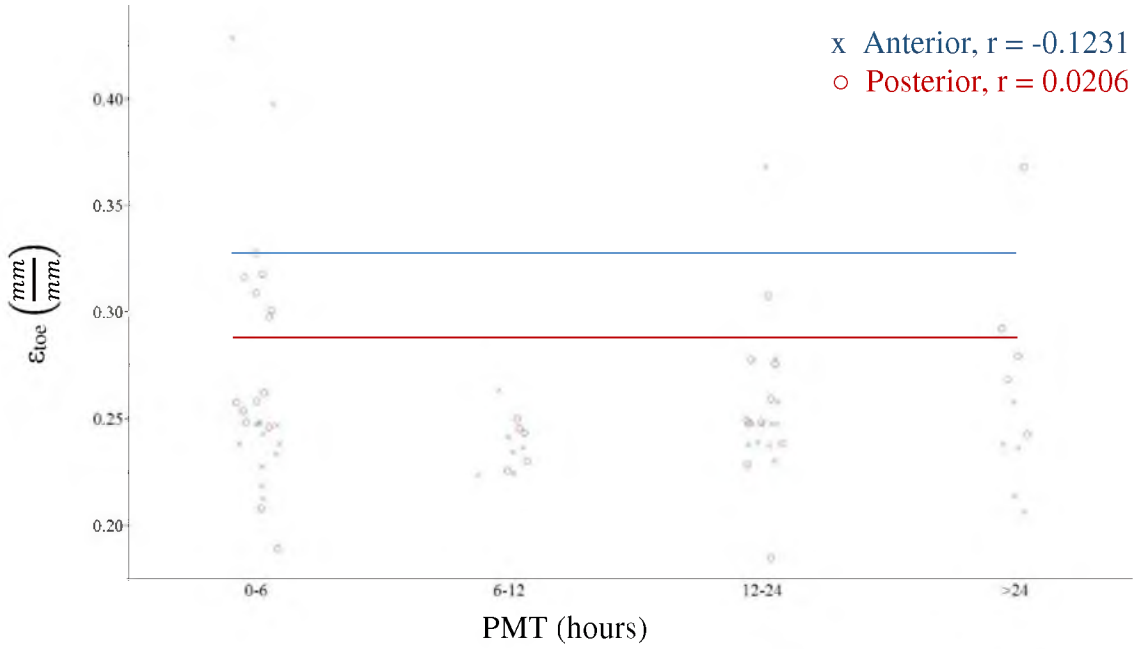

Figure 53: Statistical correlation (red and blue lines) found no significant effect of PMT on the strain length of the toe region for immature anterior and posterior sclera.

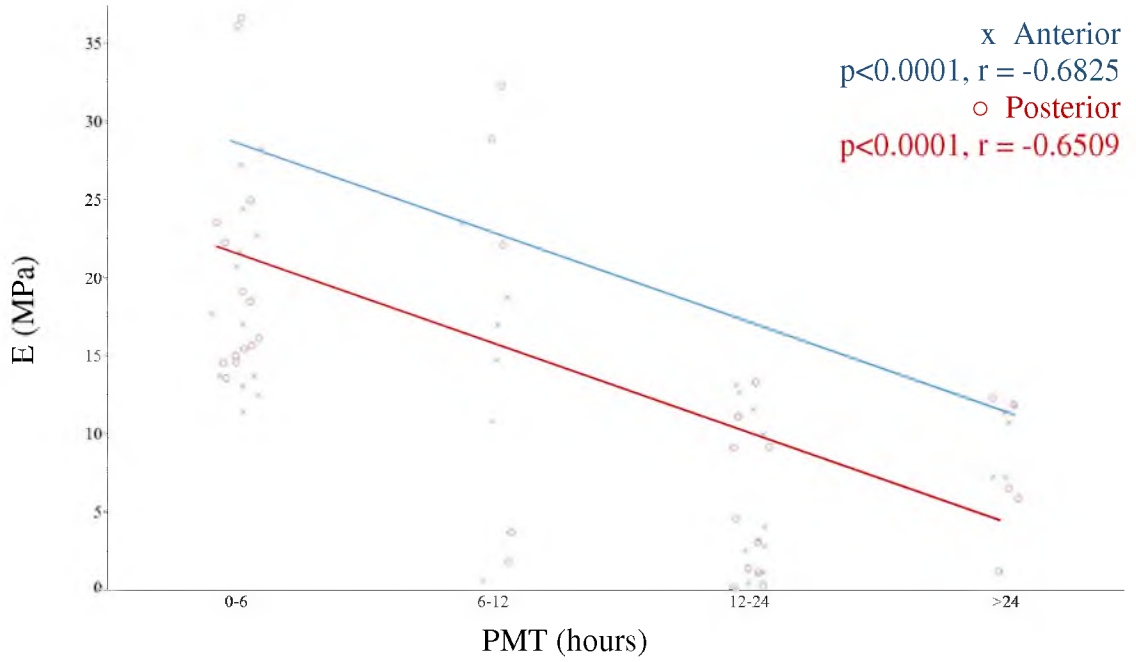

Figure 54: Statistical correlation (red and blue lines) found significant effect of PMT on the Young's modulus for immature anterior and posterior sclera.

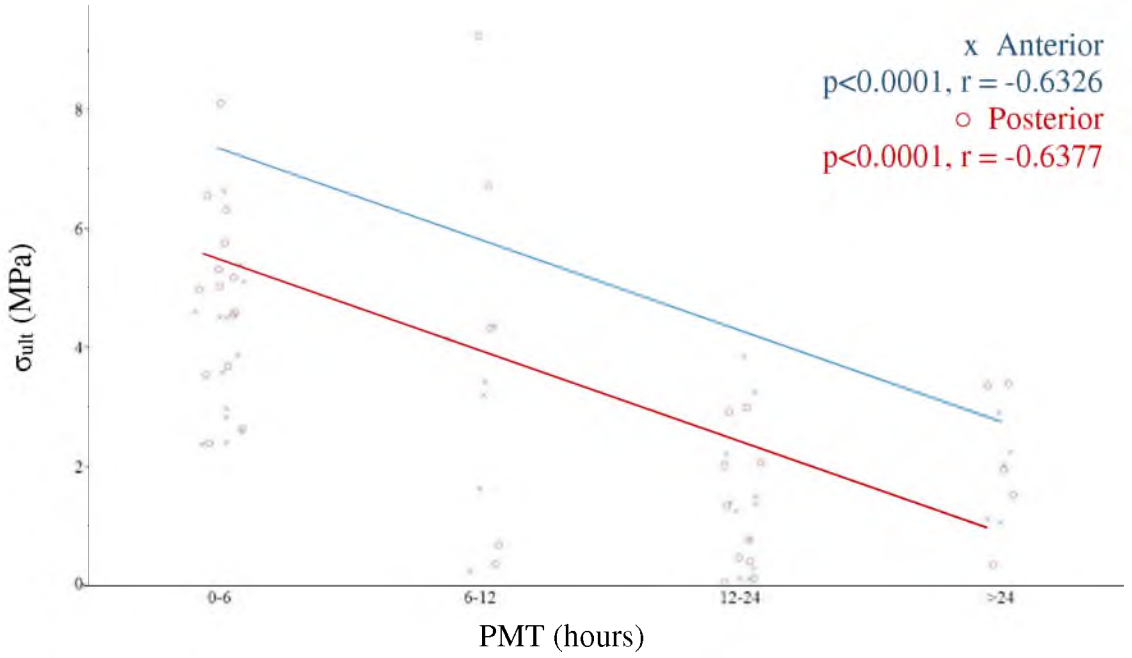

Figure 55: Statistical correlation (red and blue lines) found significant effect of PMT on the ultimate stress for immature anterior and posterior sclera.

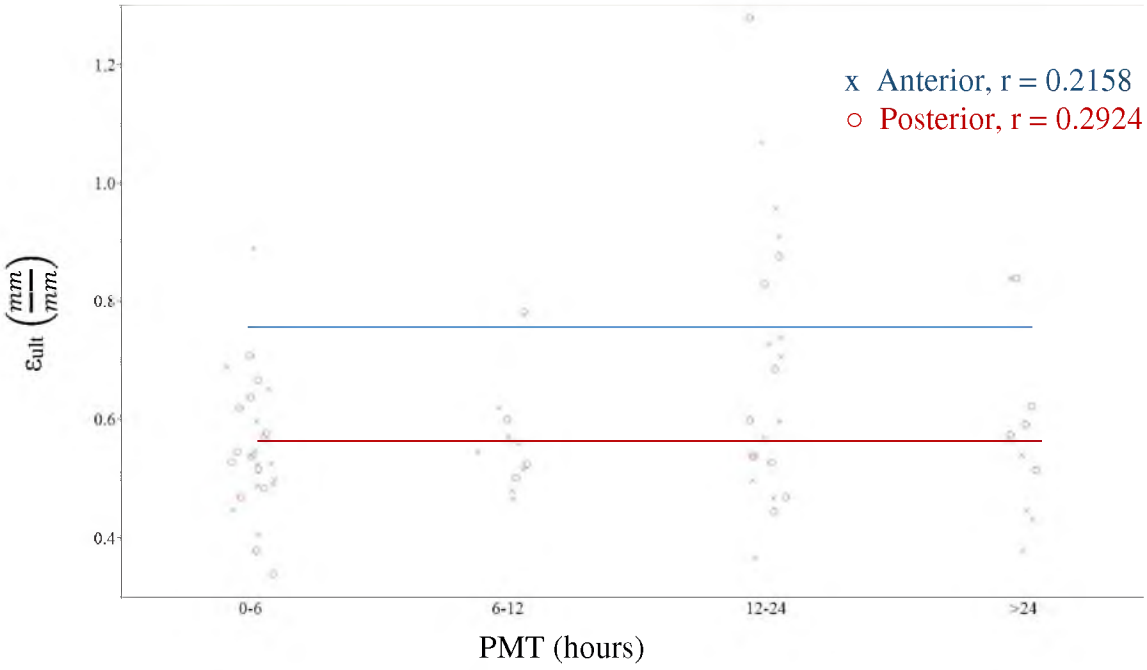

Figure 56: Statistical correlation (red and blue lines) found no significant effect of PMT on the ultimate strain for immature anterior and posterior sclera.

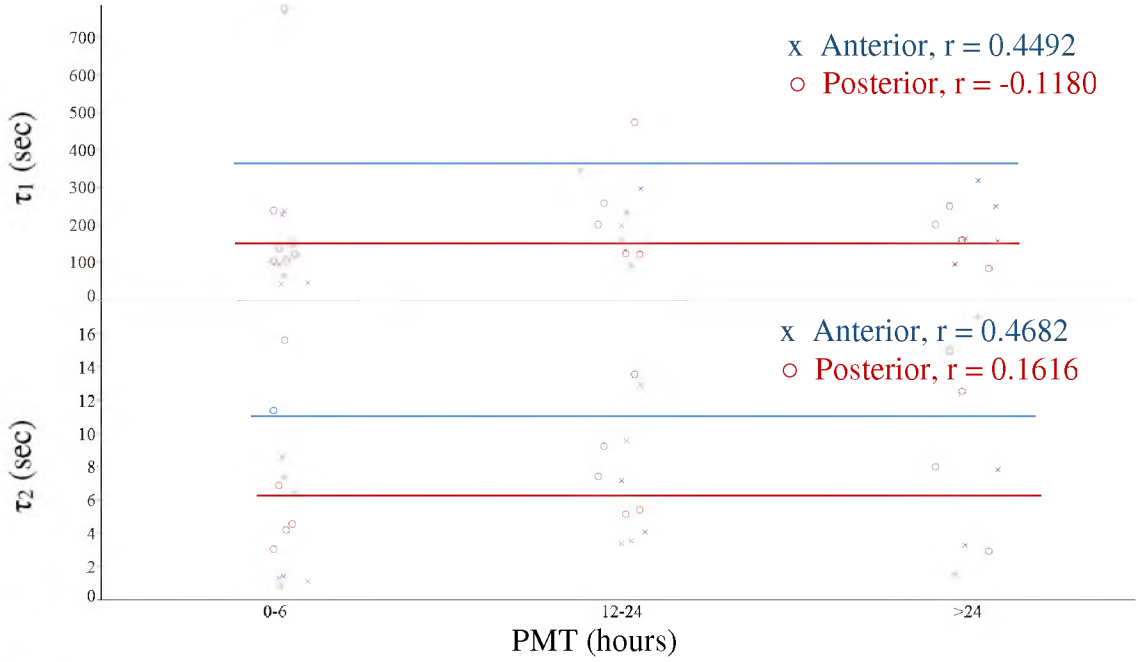

Figure 57: Statistical correlation (red and blue lines) found no significant effect of PMT on the decay time constants for mature anterior and posterior sclera.

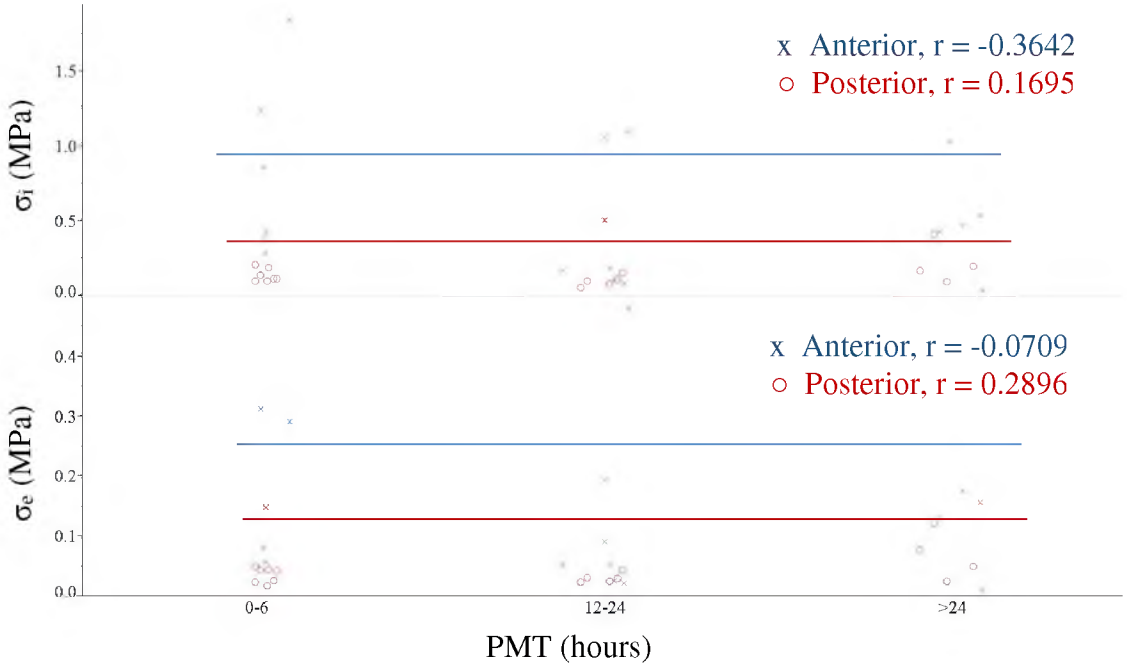

Figure 58: Statistical correlation (red and blue lines) found no significant effect of PMT on the instantaneous and equilibrium stress for mature anterior and posterior sclera.

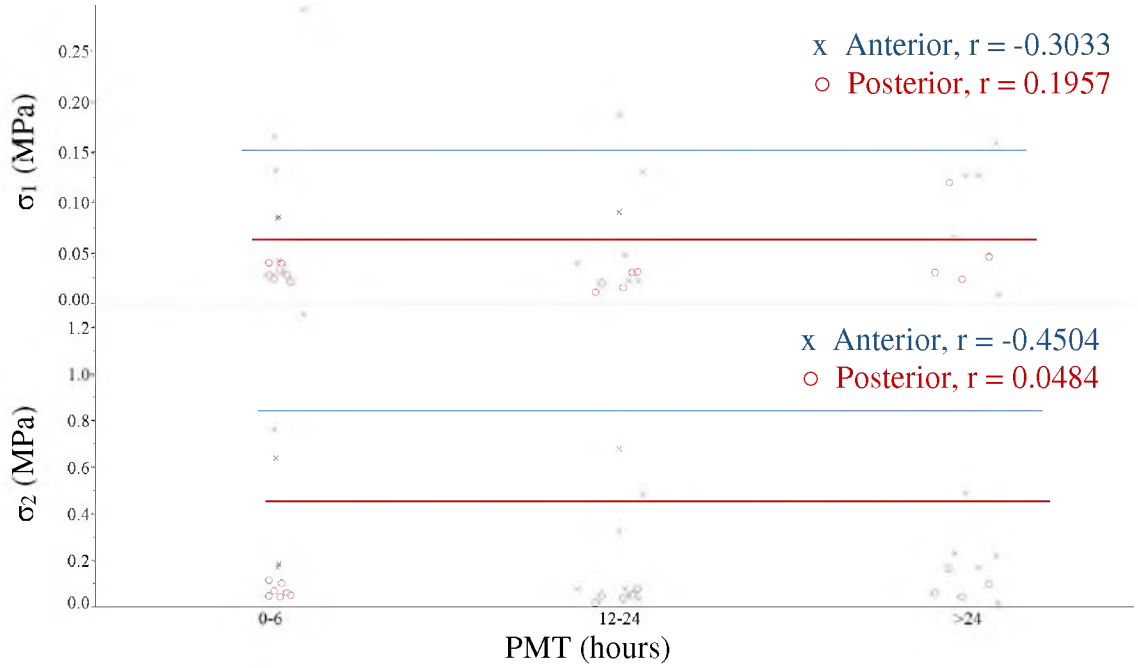

Figure 59: Statistical correlation (red and blue lines) found no significant effect of PMT on the intermediate stresses for mature anterior and posterior sclera.

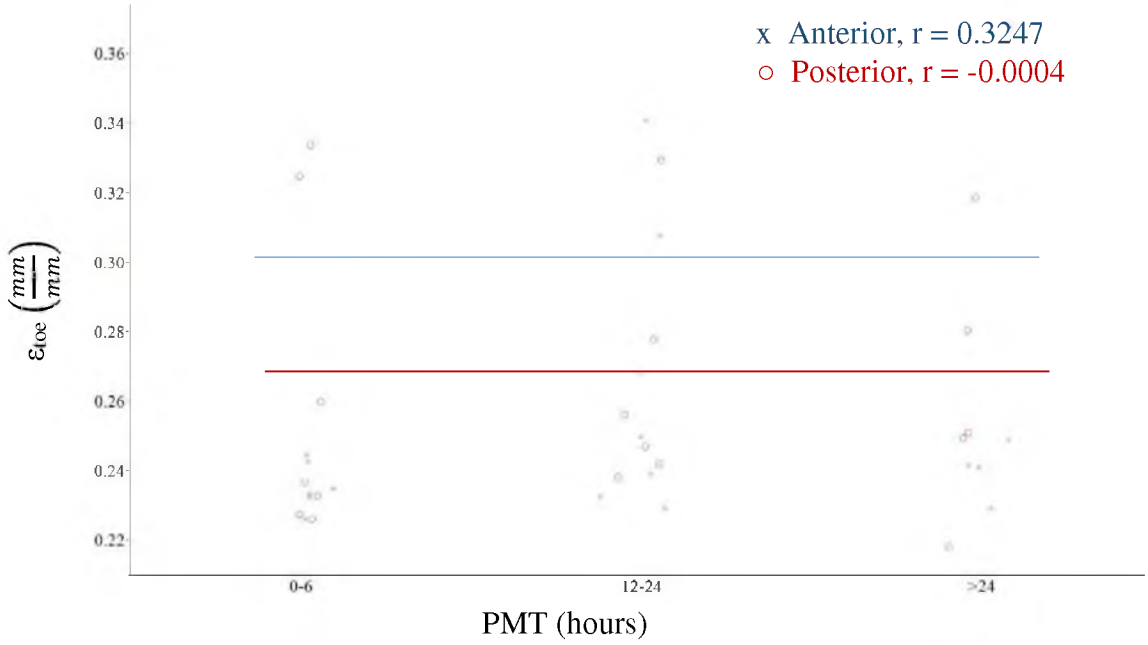

Figure 60: Statistical correlation (red and blue lines) found no significant effect of PMT on the strain length of the toe region for mature anterior and posterior sclera.

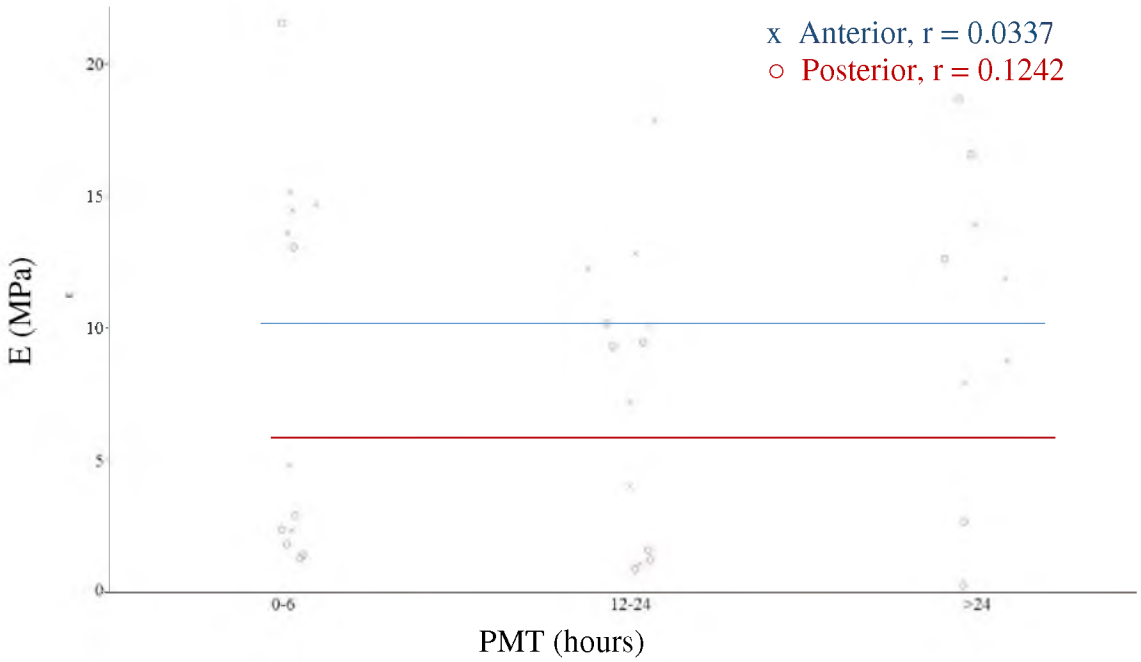

Figure 61: Statistical correlation (red and blue lines) found no significant effect of PMT on the Young's modulus for mature anterior and posterior sclera.

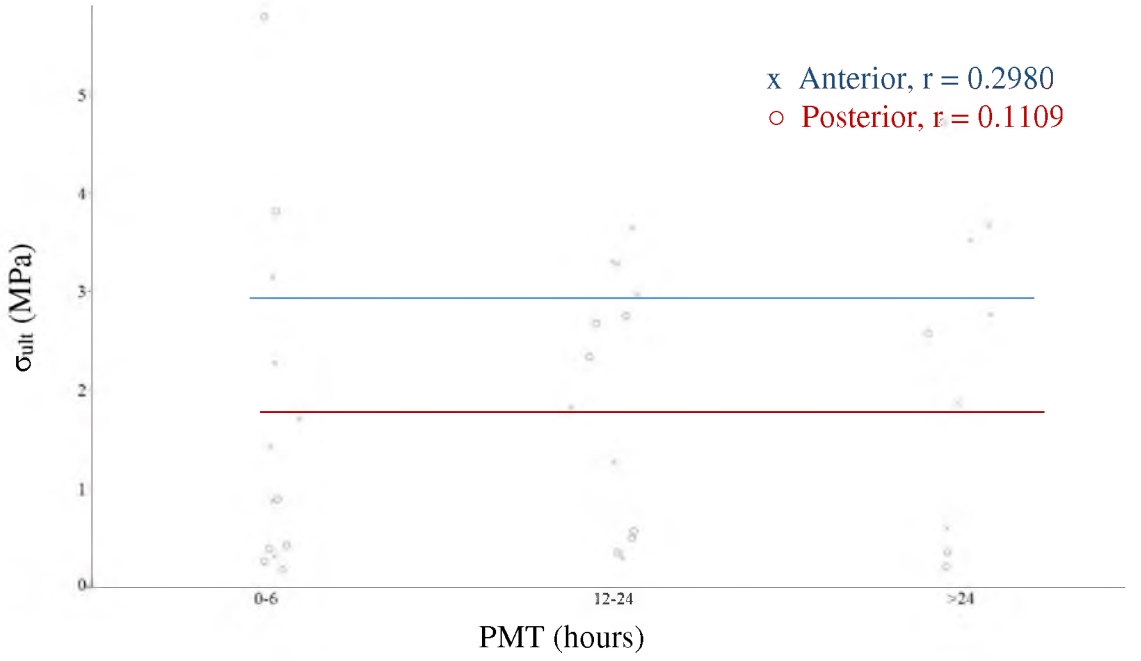

Figure 62: Statistical correlation (red and blue lines) found no significant effect of PMT on the ultimate stress for mature anterior and posterior sclera.

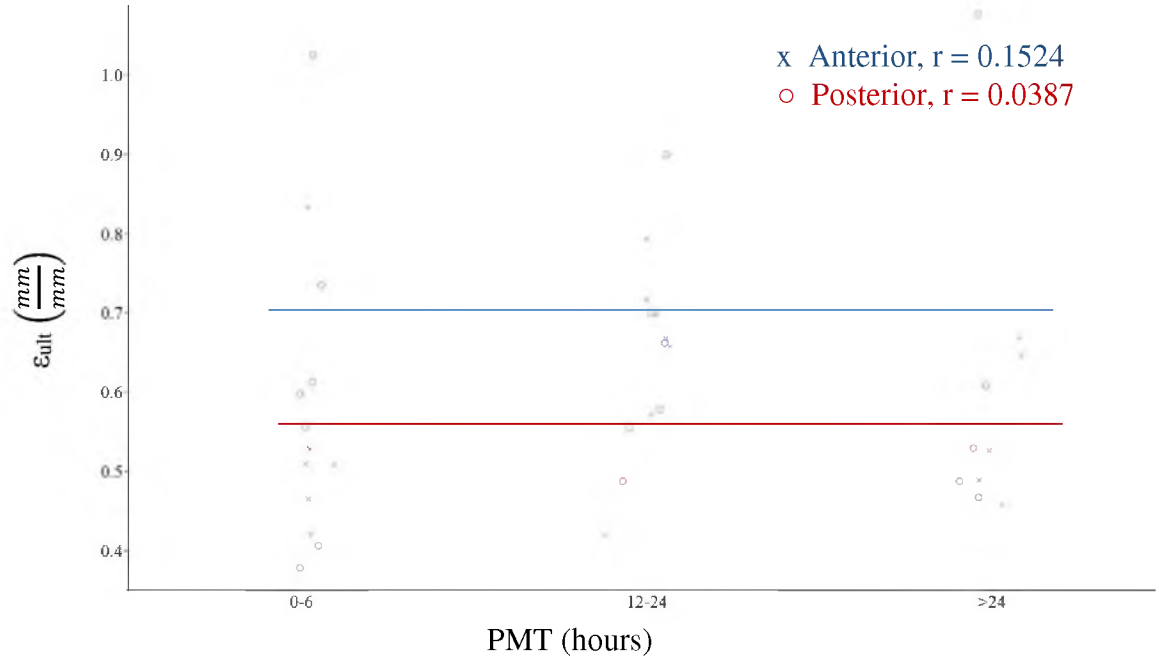

Figure 63: Statistical correlation (red and blue lines) found no significant effect of PMT on the ultimate strain for mature anterior and posterior sclera.

3.4.3 Storage condition – Immature sclera

Fixation of immature sclera significantly stiffened the tissue and increased the ultimate stress of the anterior and posterior sclera ($p<0.05$). The toe region of fixed immature posterior sclera was significantly shorter than fresh (<6 hours) immature posterior sclera ($p<0.05$). Freezing then thawing significantly decreased the ultimate stress of immature posterior sclera ($p<0.05$). Average and standard deviations of the immature scleral material properties for each storage condition can be found in Table 13.

Figure 64 illustrates all immature scleral trials subjected to tensile ramp to failure for this study. The measured force from several scleral tests exceeded the upper limits of the load cell before failure. These specimens are removed in Figure 65. Average pull-to-failure responses for the immature scleral samples in Figure 65 are shown in Figure 66.

Table 13: Average +/- standard deviation for immature scleral material properties. Fresh sclera was tested within 6 hours postmortem. * p<0.05

	Immature Sclera			
	Anterior			
	ε_{toe} (mm/mm)	E (MPa)	σ_{ult} (MPa)	ε_{ult} (mm/mm)
Fresh	0.14 ± 0.04	12.22 ± 5.29	3.18 ± 1.61	0.43 ± 0.10
Frozen	0.11 ± 0.06	6.23 ± 2.67	1.85 ± 0.73	0.54 ± 0.16
Fixed	0.10 ± 0.03	38.85 ± 12.28 *	7.88 ± 4.63 *	0.26 ± 0.09
	Posterior			
	ε_{toe} (mm/mm)	E (MPa)	σ_{ult} (MPa)	ε_{ult} (mm/mm)
Fresh	0.22 ± 0.05	12.99 ± 6.63	3.48 ± 2.27	0.49 ± 0.17
Frozen	0.25 ± 0.07	4.76 ± 3.98	0.40 ± 0.14 *	0.58 ± 0.16
Fixed	0.09 ± 0.02	31.95 ± 12.12 *	13.88 ± 0.32 *	0.32 ± 0.02

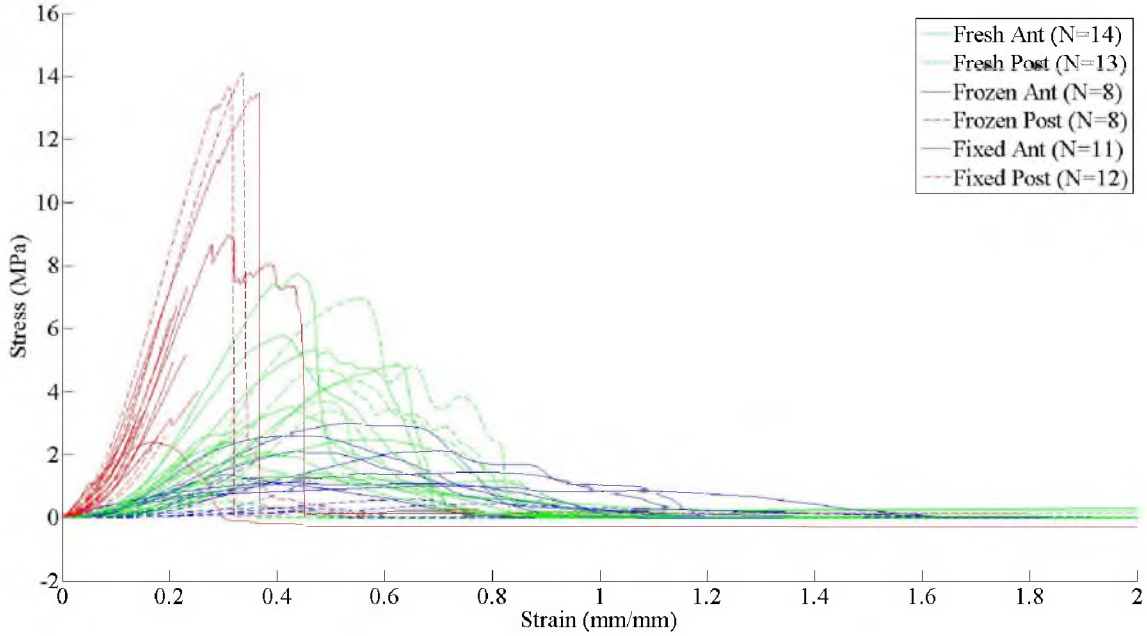

Figure 64: All pull-to-failure responses for immature anterior and posterior sclera by storage condition.

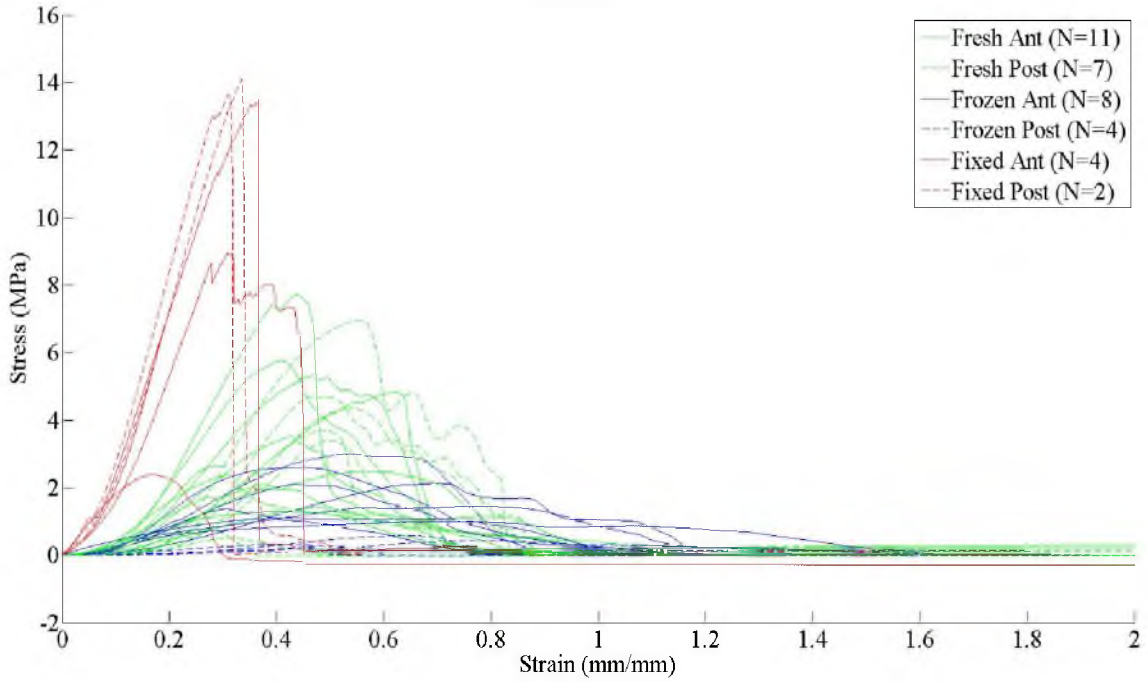

Figure 65: Pull-to-failure responses for immature anterior and posterior sclera that reached tissue failure before the upper limit of the load cell. Legend on graph indicates samples sizes for storage condition.

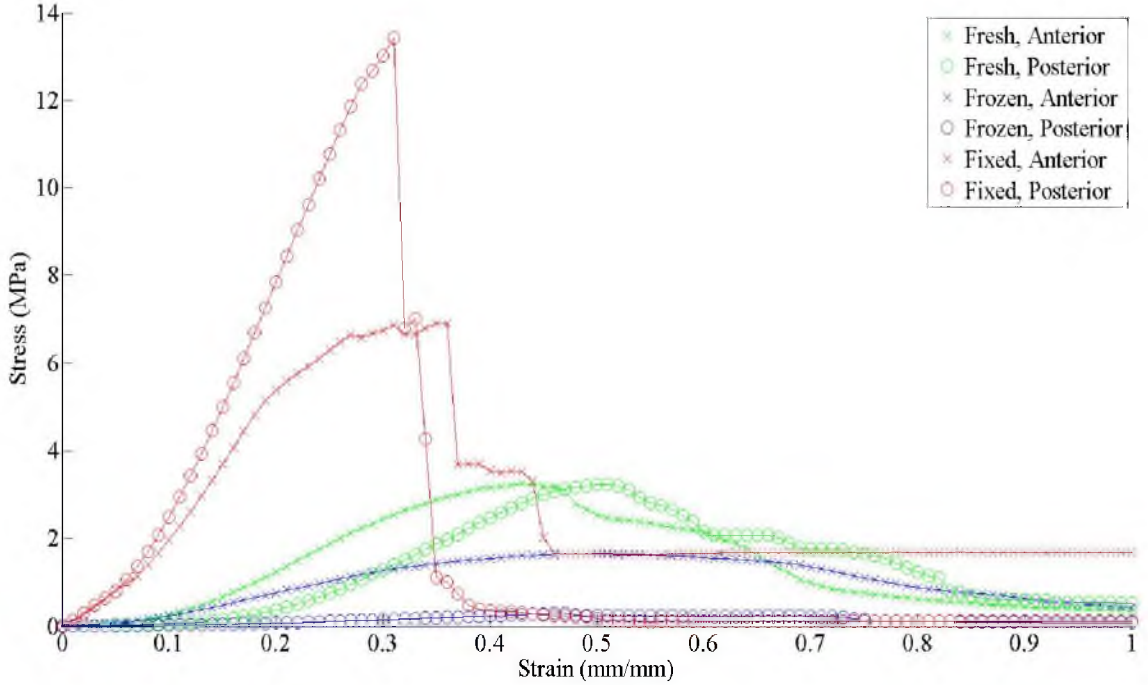

Figure 66: Averaged pull-to-failure response for the immature anterior and posterior sclera that failed.

3.4.4 Storage condition – Mature sclera

Similar to immature sclera, fixation of mature sclera significantly stiffened the tissue and increased the ultimate stress of the anterior and posterior sclera ($p<0.05$). ε_{toe} of fixed mature posterior sclera was significantly shorter than fresh mature posterior sclera ($p<0.05$). Freezing then thawing had no significant effect on the material properties of mature sclera ($p<0.05$). Average and standard deviations of the immature scleral material properties for each storage condition can be found in Table 14. Figure 67 illustrates all mature scleral trials subjected to tensile ramp to failure for this study. Scleral samples that reached the maximum limit of the load cell before failure were removed in Figure 68. Average pull-to-failure responses for the mature scleral samples in Figure 68 are shown in Figure 69. Significant storage condition effects for the immature and mature sclera can be seen in Figure 70-Figure 72.

Table 14: Average +/- standard deviation for mature scleral material properties. Fresh tissue was tested within 6 hours postmortem. * $p<0.05$

	Mature Sclera			
	Anterior			
	ε_{toe} (mm/mm)	E (MPa)	σ_{ult} (MPa)	ε_{ult} (mm/mm)
Fresh	0.06 ± 0.03	10.17 ± 12.52	1.81 ± 3.11	0.53 ± 0.33
Frozen	0.07 ± 0.01	16.95 ± 11.75	1.74 ± 0.77	0.55 ± 0.03
Fixed	0.06 ± 0.02	34.56 ± 11.71 *	9.69 ± 4.21 *	0.27 ± 0.03
	Posterior			
	ε_{toe} (mm/mm)	E (MPa)	σ_{ult} (MPa)	ε_{ult} (mm/mm)
Fresh	0.13 ± 0.06	2.49 ± 4.58	0.72 ± 1.09	0.49 ± 0.14
Frozen	0.14 ± 0.03	0.99 ± 0.27	0.27 ± 0.05	0.41 ± 0.09
Fixed	0.07 ± 0.03 *	13.16 ± 4.65 *	7.23 ± 1.48 *	0.28 ± 0.09

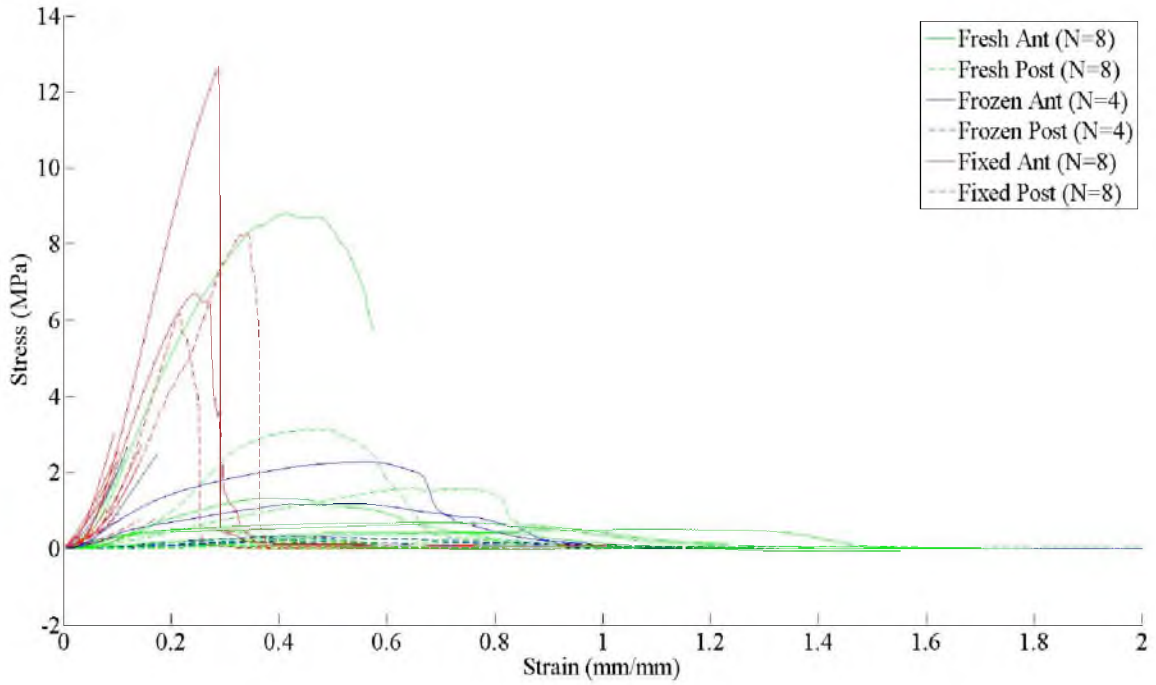

Figure 67: All pull-to-failure responses for mature anterior and posterior sclera by storage condition.

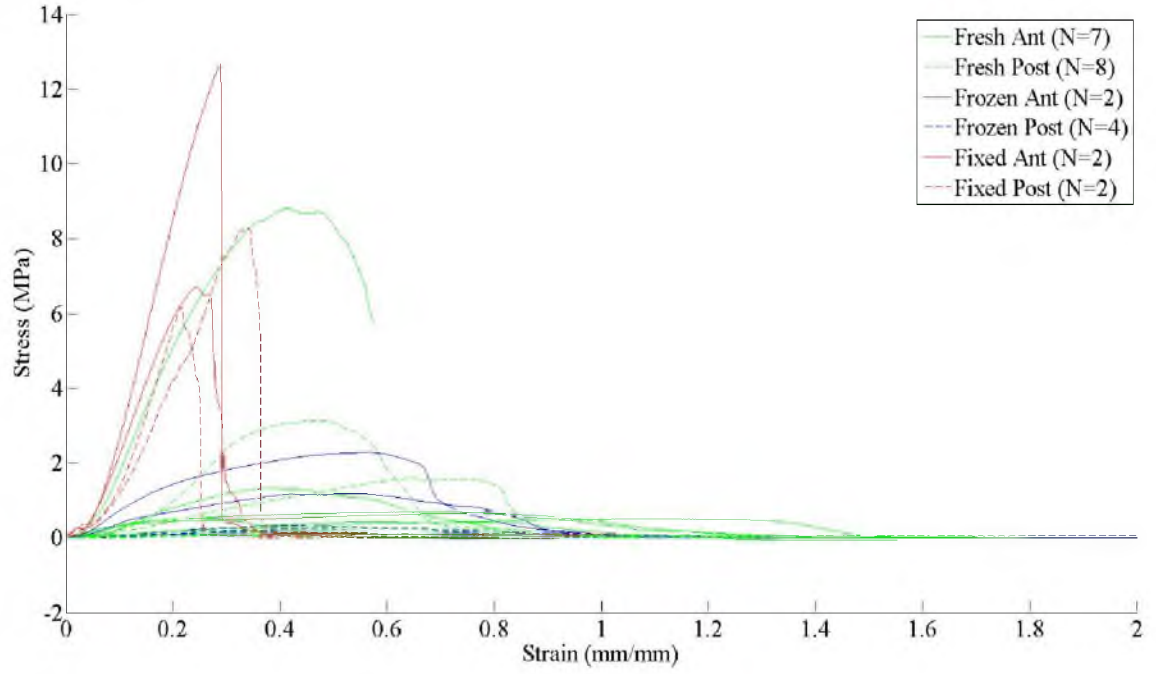

Figure 68: Pull-to-failure responses for mature anterior and posterior sclera that reached tissue failure before the limits of the load cell were reached. Legend on graph indicates samples sizes for storage condition.

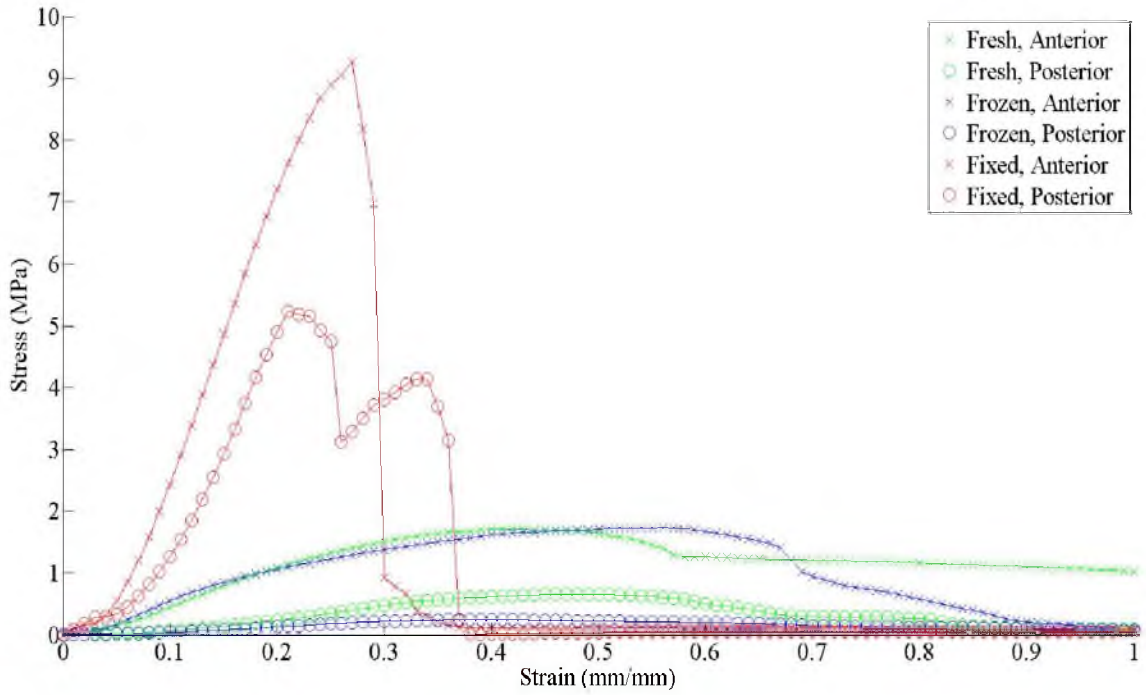

Figure 69: Averaged pull-to-failure response for the mature anterior and posterior sclera that failed. Dip in fixed posterior average is due to offset failure strains in the two specimens averaged.

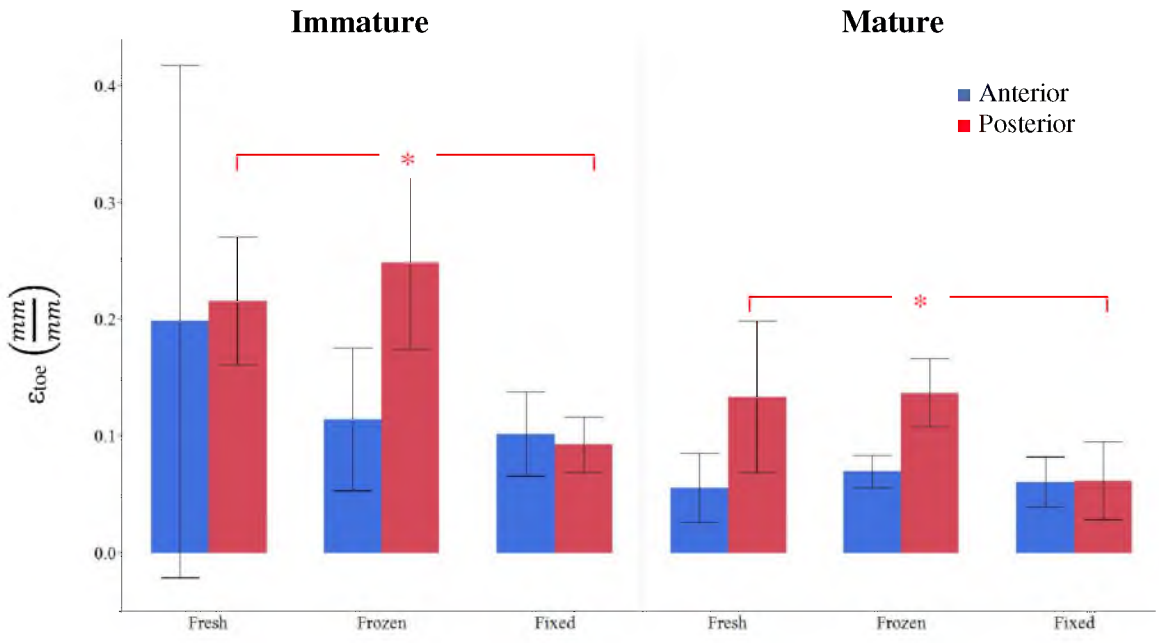

Figure 70: Average and standard deviation for ε_{toe} and Young's modulus across storage condition for immature and mature anterior and posterior sclera.

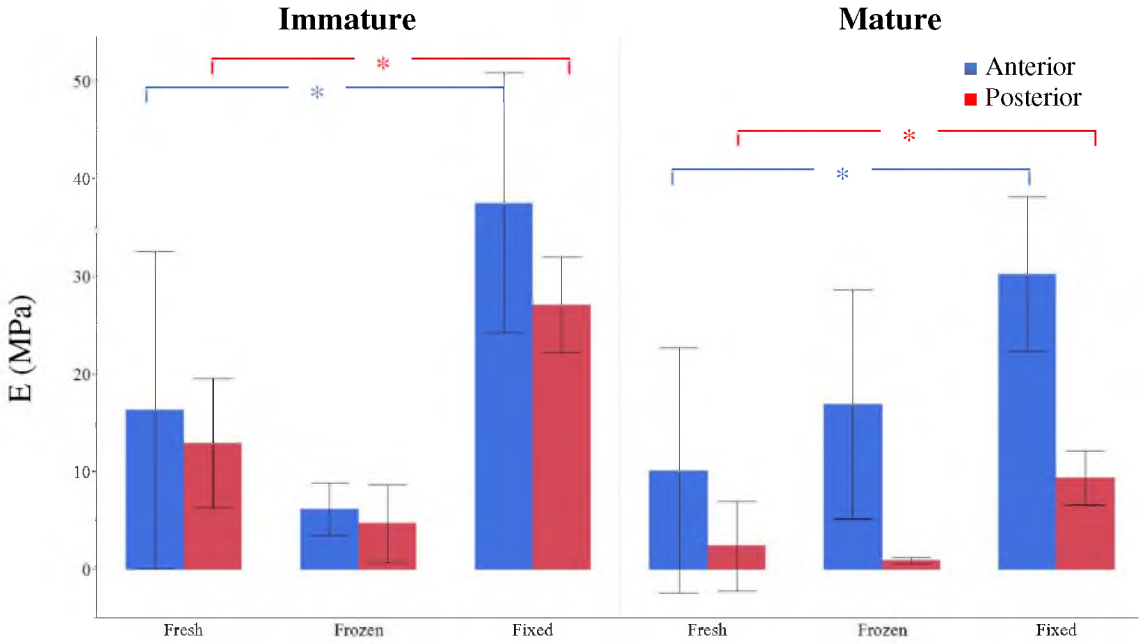

Figure 71: Average and standard deviation for ε_{toe} and Young's modulus across storage condition for immature and mature anterior and posterior sclera.

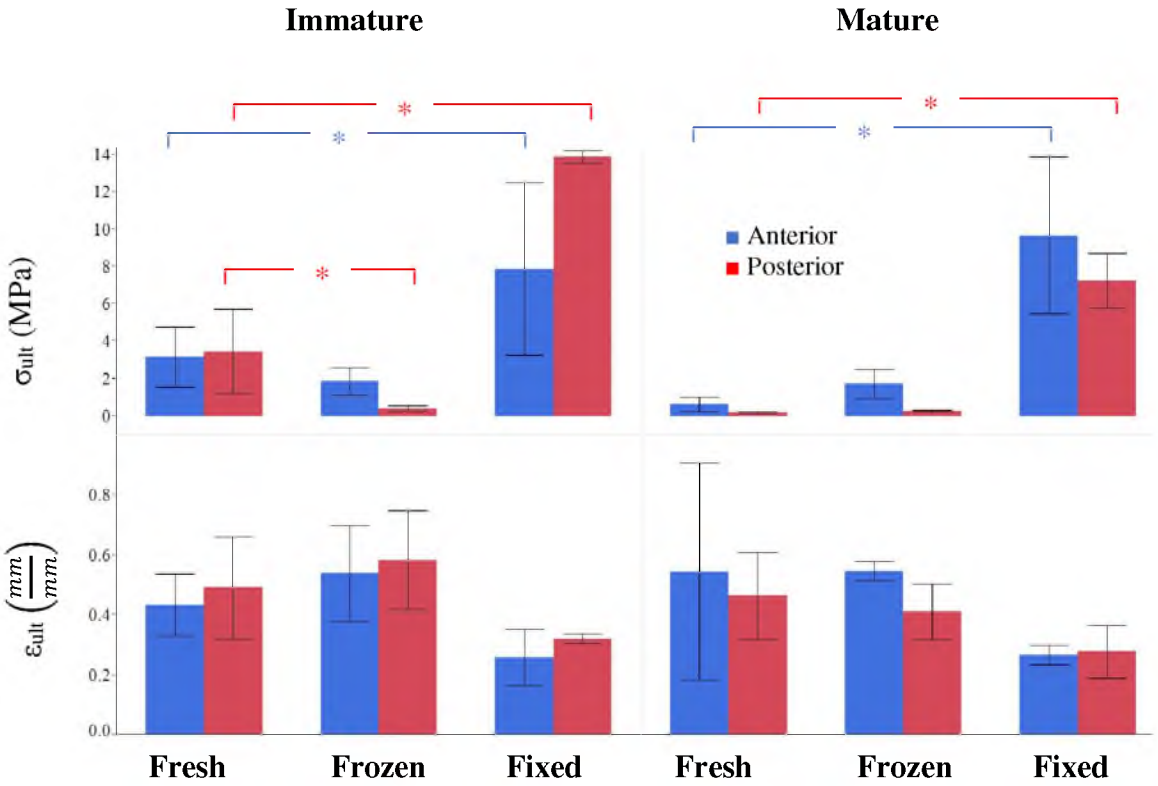

Figure 72: Average and standard deviation for ultimate stress and strain across storage condition for immature and mature anterior and posterior sclera.

3.4.5 Storage condition – Retina

Fixation of immature and mature retina significantly stiffened the tissue ($p<0.05$), increased the ultimate stress ($p<0.05$), and decreased the ultimate strain ($p<0.05$). Freezing then thawing immature and mature retina significantly increased the ultimate strain ($p<0.05$). Average and standard deviations for the immature and mature retinal material properties can be seen in Table 15 and Table 16. Significant storage condition effects for the immature and mature retina can be seen in Figure 73-Figure 76.

Table 15: Average +/- standard deviation for immature retinal material properties. Fresh retina tested within 6 hours. * $p<0.05$

	Immature Retina			
	ε_{toe} (mm/mm)	E (MPa)	σ_{ult} (MPa)	ε_{ult} (mm/mm)
Fresh (n=8)	0.170 ± 0.278	0.008 ± 0.014	0.003 ± 0.001	1.090 ± 0.625
Frozen (n=3)	0.224 ± 0.211	0.001 ± 0.0002	0.002 ± 0.0006	2.238 ± 0.510 *
Fixed (n=11)	0.141 ± 0.038	0.034 ± 0.028 *	0.014 ± 0.013 *	0.518 ± 0.196 *

Table 16: Average +/- standard deviation for mature retinal material properties. Fresh retina tested within 6 hours. *$p<0.05$

	Mature Retina			
	ε_{toe} (mm/mm)	E (MPa)	σ_{ult} (MPa)	ε_{ult} (mm/mm)
Fresh (n=8)	0.245 . 0.275	0.018 ± 0.023	0.011 ± 0.013	1.029 ± 0.336
Frozen (n=2)	0.522 ± 0.600	0.0017 ± 0.0007	0.002 ± 0.002	1.719 ± 0.578 *
Fixed (n=5)	0.180 ± 0.050	0.097 ± 0.048 *	0.047 ± 0.016 *	0.581 ± 0.043 *

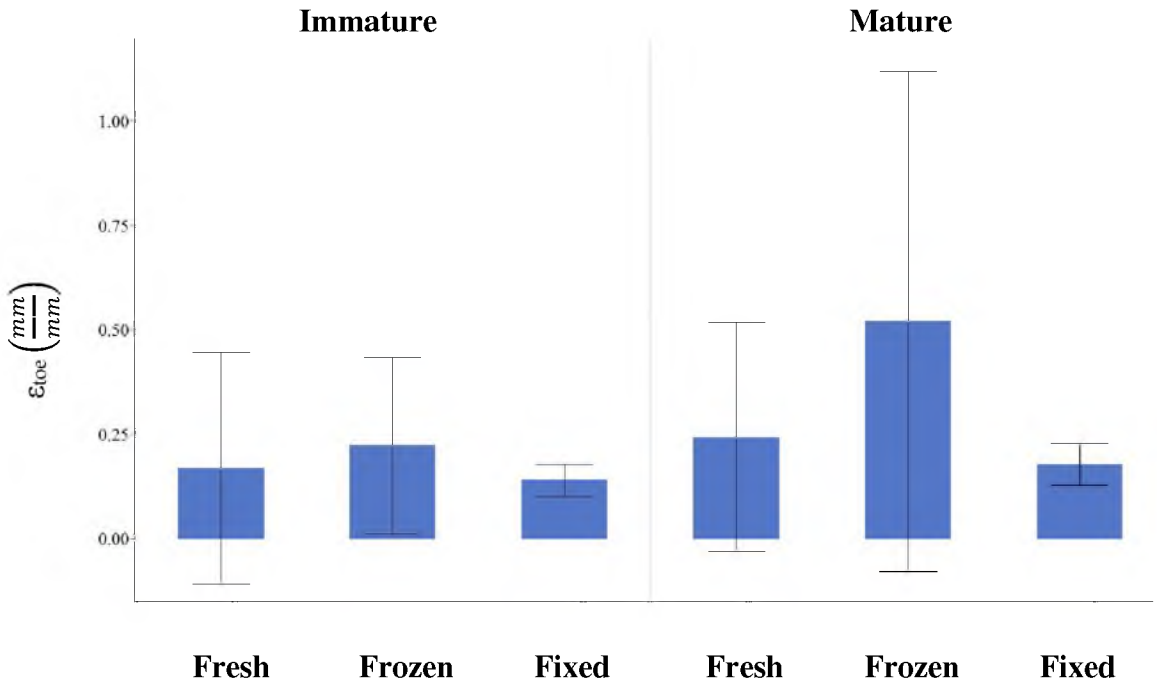

Figure 73: Average and standard deviation for ε_{toe} across storage condition for immature and mature retina.

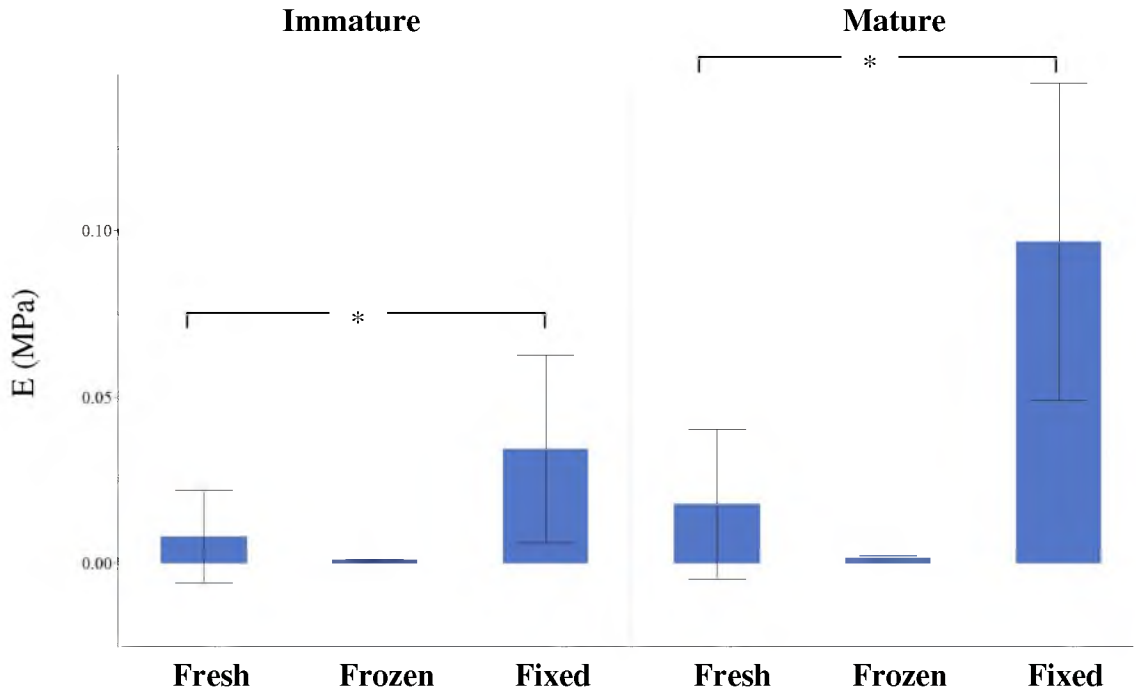

Figure 74: Average and standard deviation for Young's modulus across storage condition for immature and mature retina. * $p<0.05$

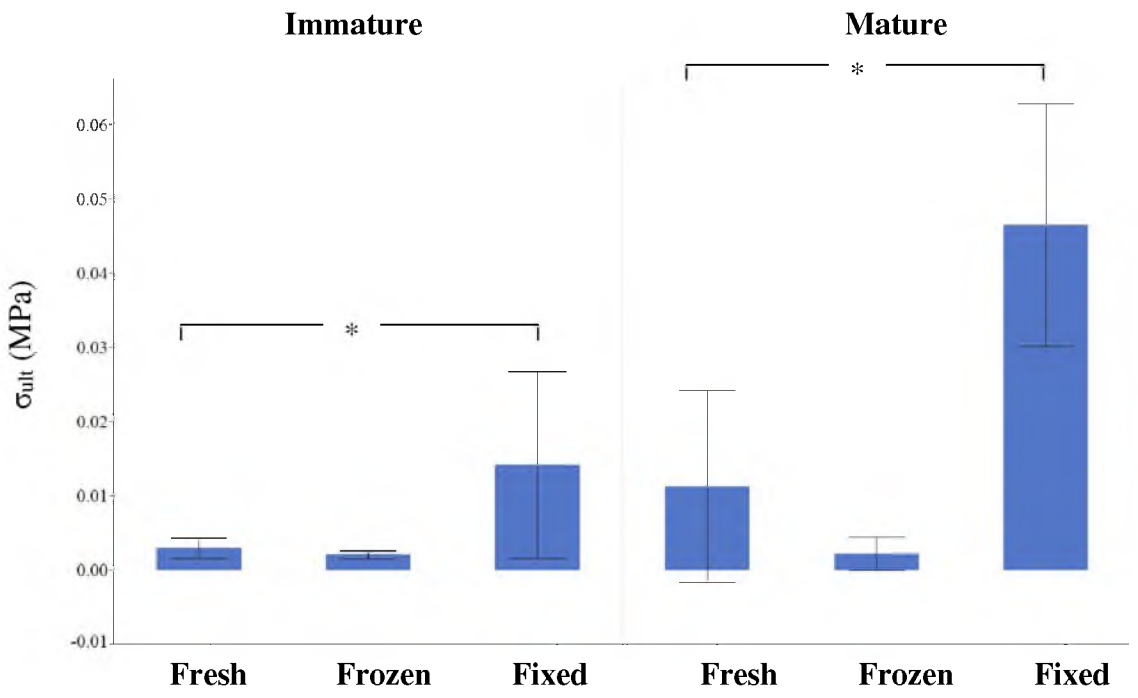

Figure 75: Average and standard deviation for ultimate stress across storage condition for immature and mature retina. * p<0.05

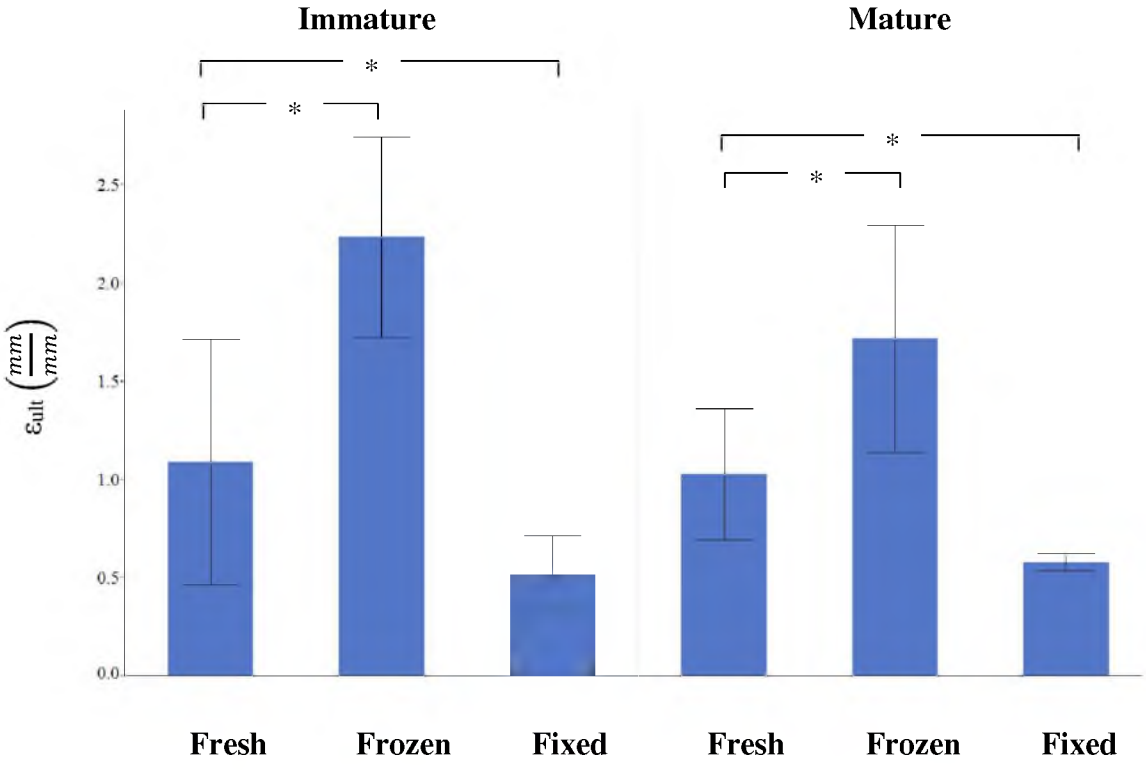

Figure 76: Average and standard deviation for ultimate strain across storage condition for immature and mature retina. * p<0.05

3.5 Discussion

No significant correlation with PMT was found for the mature scleral material properties. This agrees with the published data reporting no significant effect on the material properties of adult rabbit sclera up to 72 hours postmortem. Our results suggest that adult ovine sclera can be stored up to at least 24 hours postmortem in PBS without compromising the mechanical characteristics. Expanding our time frame may prove that adult ovine sclera can be stored for longer than 24 hours. The infant sclera, however, changes considerably up to 24 hours postmortem. Specifically, negative correlations with PMT were found for Young's modulus, suggesting the infant sclera becomes less stiff over time. This finding was not specific to the anterior or posterior region. There is likely a structural difference between the mature and immature sclera which alters the mechanical response after death, ocular enucleation, or tissue dissection. During tissue preparation the immature sclera was observably softer and seemed less 'inflated' than mature sclera. The infant sclera is still developing and it is possible that without the support of intraocular pressure or nutrient supply the tissue fails to maintain its integrity. Or, the age-related effect may be attributed to a time-dependent loss in water in the immature sclera after enucleation. The mature sclera is more dehydrated than immature sclera[1] and may not be as mechanically influenced over time. The change in mechanical properties of immature sclera with PMT was not linear. The more significant changes in mechanical properties occurred after 10 hours PMT (Figures 42-43,45-46). This suggests that the immature sclera will maintain its integrity up to at least 10 hours postmortem. Notably, no specimens were tested between 10 and 20 hours postmortem, so the PMT testing window may be longer.

Both immature and mature sclera and retina became stiffer after fixation which

agrees with the literature showing increases in stiffness in fixed adult rabbit eyes. There is said to be significant collagen cross-linking with fixation which infers that this preservation method is not a suitable means to maintain the mechanical strength of ocular tissues. Freezing then thawing only significantly effected σ_{ult} of immature sclera and retina, and suggests that freezing may be a viable shipping technique for pediatric ocular tissues. Future studies looking at freeze time and thawing temperature and time may be beneficial for minimizing storage effects even more.

3.6 Conclusions

Pediatric ocular tissues are limited and there are little data characterizing the mechanical response of the infant eye. Our results suggest that while mature sclera can be stored up to at least 24 hours postmortem, the immature sclera may only maintain its integrity up to 10 hours postmortem. We also found that freezing and thawing sclera and retina does not significantly affect most mechanical properties and may be a viable means of storing and shipping. The findings from our PMT and storage condition studies provide useful guidelines for a feasible testing time frames and shipping modes for material testing of pediatric ocular tissues.

3.7 Acknowledgements

We would like to thank Dr. Kurt Albertine at the University of Utah for donating ovine ocular tissue. We would also like to thank the Knights Templar Eye Foundation for sponsoring this work.

3.8 References

1. Adler's Physiology of the Eye. 11th ed. St. Louis, Missouri: Mosby; 2003.

2. Girard, M.J.A., Suh, J.-K.F., Hart, R.T., Burgoyne, C.F., Downs, J.C., Effects of storage time on the mechanical properties of rabbit peripapillary sclera after enucleation. Current Eye Research, 2007. 32(5): p. 465-470.

3. Liu, J., He, X., Corneal stiffness affects IOP elevation during rapid volume change in the eye. Investigative Ophthalmology & Visual Science, 2009. 50(5): p. 2224-2229.

4. Rudra, R.P., A curve-fitting program to stress relaxation data. Canadian Agricultural Engineering, 1987. 29(2): p. 209-211.

CHAPTER 4

MATERIAL MODEL IDENTIFICATION AND VERIFICATION

4.1 Abstract

Current FE models of the infant eye are based on adult material properties and do not account for developmental changes of ocular tissues. Experimental data collected from mechanical tests conducted in our lab were used to identify constitutive models for the immature sclera, retina, and vitreous. The material models were included in a FE model of the infant eye and validated against experimental ocular inflation tests using digital image correlation (DIC) to calculate strain on the anterior and posterior scleral surfaces of an immature eye. Most strains from the FE analysis were within the range of values from the DIC analysis. Maximum principal strain in the simulation had the most accurate correlation with both anterior and posterior regions of the experimental data. The close prediction values support the appropriateness of the material models for implementation into a finite element model of the immature eye.

4.2 Introduction

A paucity of pediatric eye material property data has drastically limited the utility of FE modeling such that the current models rely heavily on material properties of the adult eye.[3,8] As yet, there are no published data thoroughly characterizing the age-dependent

mechanical differences in human ocular tissues from a broad age range. Our studies indicate that there are developmental changes in the aging ovine sclera, retina, and vitreous from preterm, infant, and adult equivalent ages. The well-defined mechanical data were used to identify material models which need to be implemented to create an accurate FE model. Age-appropriate constitutive models were identified using the infant data from Chapters 1 and 2. To verify the selection and fit of these models, ocular inflation tests of an immature ovine eye were conducted and scleral strain results were compared to FE simulations of the experiments. Once verified, the material models will be used in the development of a pediatric FE model in Chapter 5.

4.3 Materials and Methods

4.3.1 Inflation device design

A custom ocular device was designed to prescribe a set pressure to a sectioned immature ovine eye while measuring resulting strains using DIC. The device consisted of a lower mounting fixture that housed the eye and ports for pressurization, and an upper cap that sealed the perimeter of the eye and prevented leaking. Eye pressurization was created by a volume controlled syringe pump (NE-1000 Single Syringe Pump, New Era Pump Systems, Inc., Farmingdale, NY) attached to the inflow valve of the mounting fixture. An extrusion on the mounting fixture sat inside the sectioned eye and ensured a watertight seal with the upper cap. An outlet with an inline ball valve was also included in the mounting fixture for drainage. A port on the side of the mounting fixture was used to insert a pressure transducer catheter (FISO LS 0.9F, Harvard Apparatus). Soft clay was pressed around the pressure transducer at the port to ensure a watertight seal (Figure 77).

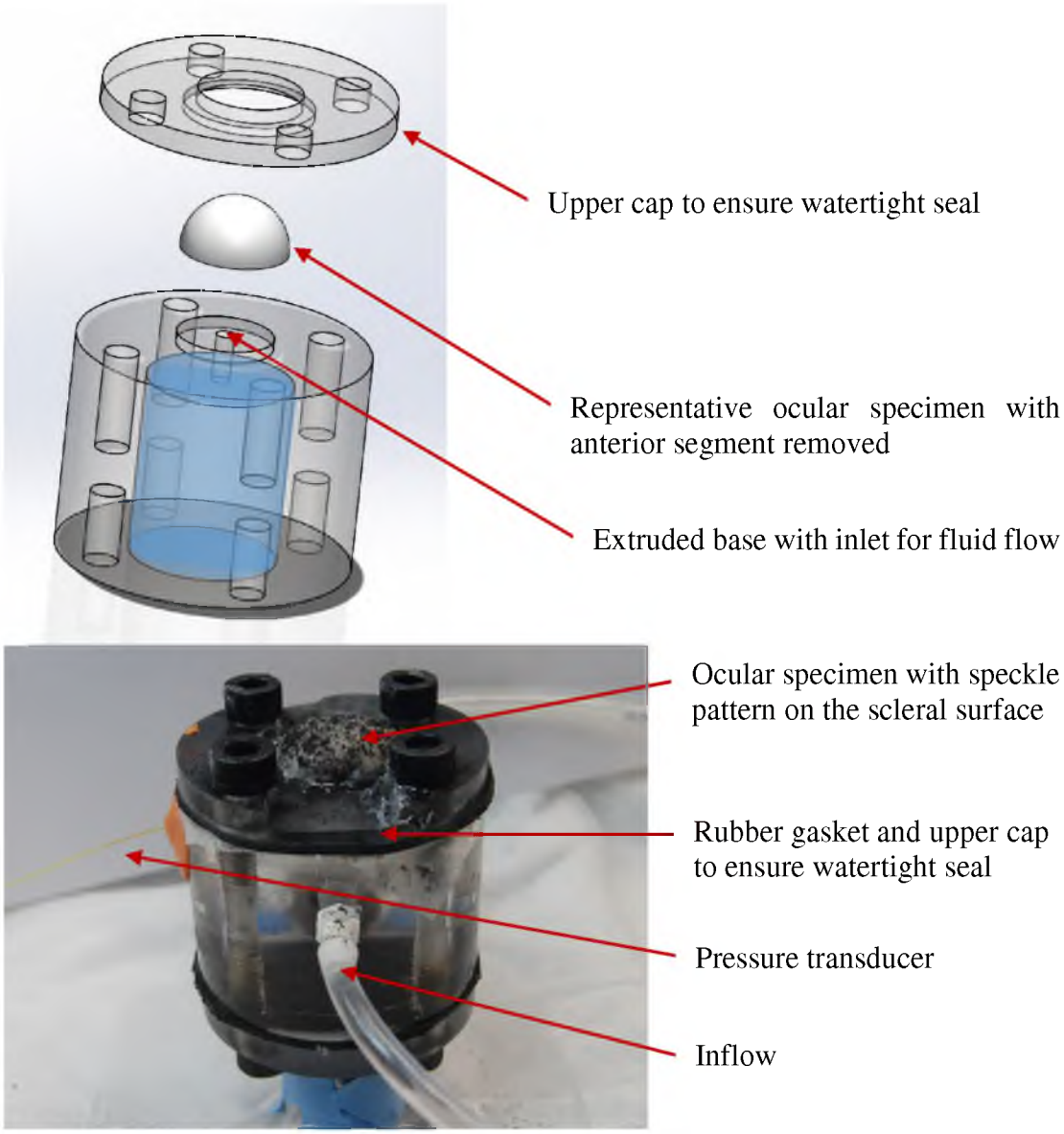

Figure 77: Three-dimensional schematic of our experimental inflation test setup. The inlet and outlet ports are not shown here.

4.3.2 Ocular specimen preparation and inflation

Due to scheduling challenges, a fresh ocular specimen was not available on the day we had access to three-dimensional digital image correlation. Subsequently, we tested a single frozen/thawed immature ovine eye for this analysis. In Chapter 3, only σ_{ult} was significantly different between fresh and frozen/thawed immature sclera and retina. Therefore, it was assumed the frozen/thawed eye would behave similarly to a fresh eye. Following thawing, the extraocular muscles and soft tissues were removed from the eye and discarded, and the optic nerve was severed at the optic nerve scleral junction. A scalpel was used to cut around the limbus and remove the anterior portion of the eye. The sectioned eye contained the sclera, choroid, retina, and vitreous. A paraffin film was stretched over the top of the chamber, and holes were made in the film for fluid flow and screw connections. The addition of the film allowed for quick removal of the ocular specimen and ensured the sanitation of the device. The sectioned eye was placed on the film and around the extrusion. An O-ring was positioned around the eye and cyanoacrylate was applied such that the perimeter of the sclera was glued and fixed at the base. A rubber gasket was situated around the eye, and the upper cap was screwed on top for a watertight seal. A speckle pattern was marked on the sclera by sifting graphite powder over the exposed scleral surface through a fine, perforated mesh.

An initial baseline pressure (< 2 mmHg) was applied with the syringe pump to inflate the eye enough to prevent the tissue from collapsing. While continuously measuring intraocular pressure (IOP), the eye was filled with 1mL of PBS at a rate of 10 mL/min. This resulted in the eye being inflated to a pressure of 30 mmHg at a rate of 11.7 mmHg/s. The sampling rate for IOP was 125 Hz.

4.3.3 Three-dimensional digital image correlation

The 3D deformation of the speckles was recorded using digital image correlation (VicSnap, Correlated Solutions, Inc., Columbia, SC). The cameras were calibrated by imaging custom calibration blocks marked with a specific speckle pattern to define the three-dimensional space used in the inflation test. The inflation device was positioned approximately 1 foot in front of two cameras (Pt. Grey Research GRAS-20SM/C, Schneider Kreuznach 35 mm lens, f8; VicSnap, Correlated Solutions, Inc., Columbia, SC) which recorded the inflation event at a rate of 4 frames per second (Figure 78).

The graphite powder speckle coordinates were mapped during the inflation test to measure the speckle displacements. Resulting images collected were analyzed using Vic3D (Correlated Solutions, Inc., Columbia, SC) to compute the scleral surface Lagrangian strains consisting of the major principal strain, strain in the x-direction, and strain in the y-direction.

An area of interest (AOI) was selected from the final frame of the captured ocular inflation video (Figure 79). The quality of the resulting strain map relied heavily on the quality and granularity of the applied speckle pattern. A subset of 39 and step size of 1 were specified within the AOI toolset to optimize the resolution. Inspection points were selected from the anterior and posterior regions of the sclera and the Lagrangian strains were computed at each video frame. The digital image correlation software uses algorithms to determine in-plane Lagrangian strain by calculating the strain tensors based on the separation in the grid f datapoints over time.

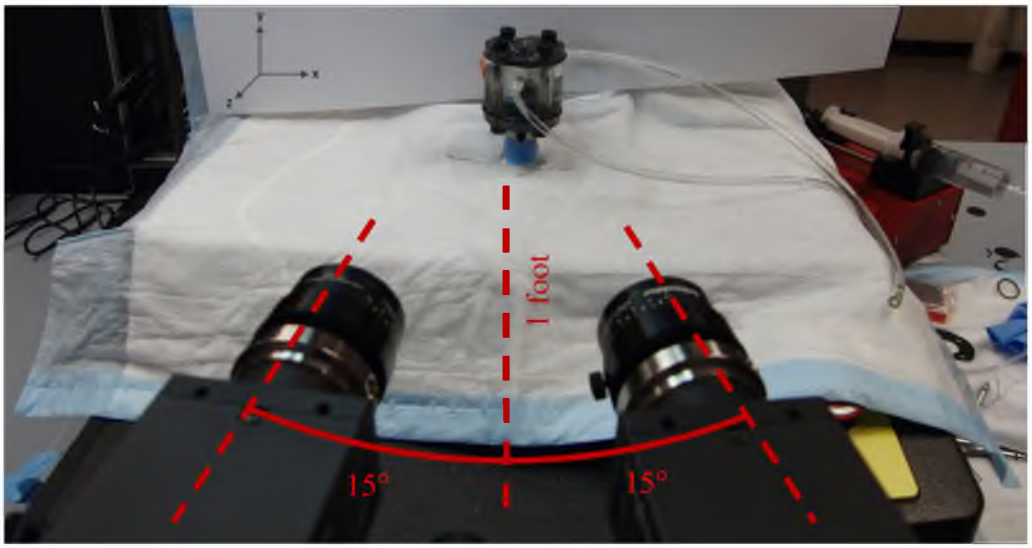

Figure 78: The ocular inflation device was positioned approximately 1 foot in front of two cameras which were situated ~15° from the central axis.

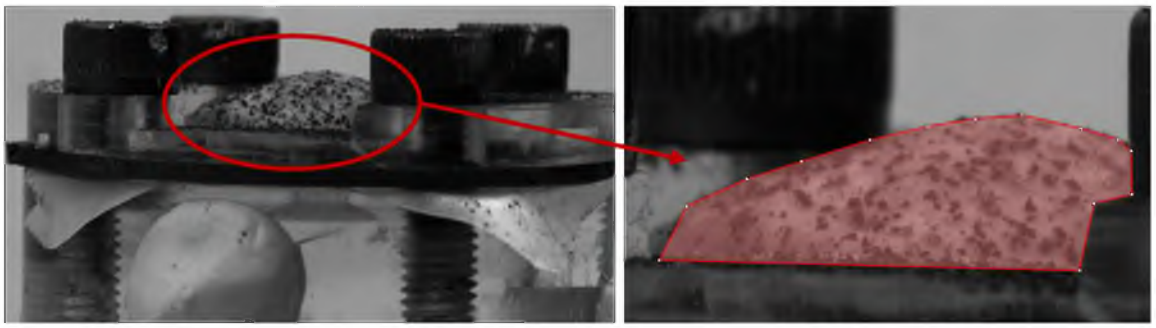

Figure 79: Typical DIC image and a representative area of interest for analysis.

4.3.4 FE model

4.3.4.1 Geometry and meshing. A computational model of the immature ovine eye was generated to simulate the experimental ocular inflation tests. Sclera, choroid, retina, and vitreous were generated using 3D CAD software (SolidWorks, Dassault Systemes, Waltham, MA) with dimensions that matched approximated ex vivo measurements made in our lab (Figure 80a). The geometry was imported into ABAQUS (Dassault Systemes, Waltham, MA) for meshing and analysis. Hexahedral linear elements with reduced

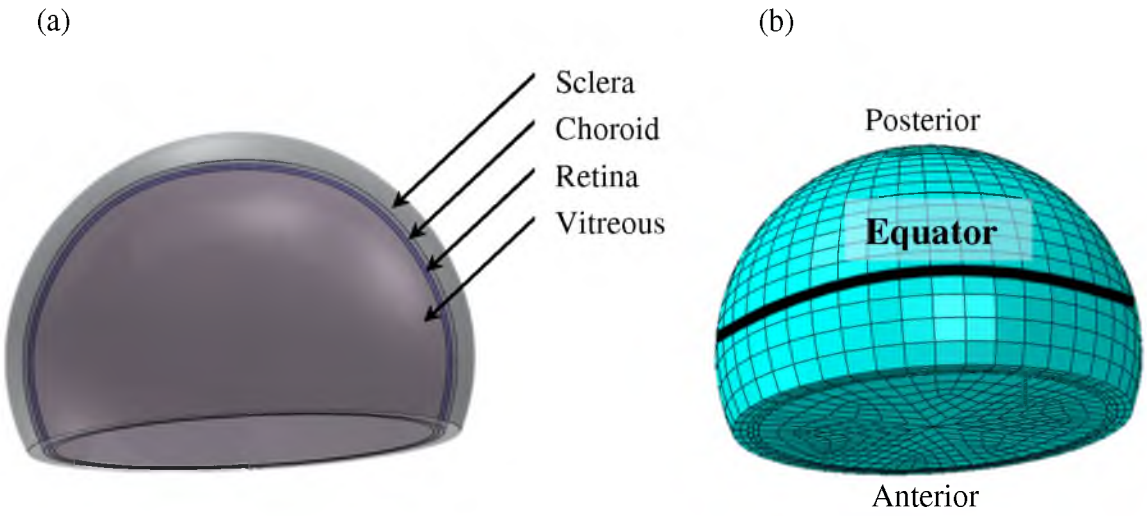

Figure 80: A three-dimensional geometry was generated and meshed using finite element analysis software. (a) The three-dimensional geometry of the eye was created to include the sclera, choroid, retina, and vitreous. (b) The 3D geometry was imported into Abaqus and the tissue layers were meshed.

integration and hourglass control were used to mesh all ocular components in the model (Figure 80b).

A convergence study was performed on sclera to determine the best mesh density for the ocular tissues and can be seen in Appendix E. The Lagrangian strains were output for the anterior and posterior sclera and the average of the top 5% of the maximum values were plotted for each mesh density (Figure 81). The final model contained a seed size of 0.6 and contained a total of 22,879 nodes and 16,768 elements. The scleral-choroid and vitreoretinal boundaries were connected by a tied contact parameter. An approximated friction contact parameter (ρ=0.9) was defined for the choroid-retina boundary. The contact parameters were qualitatively determined based on the observed relative adhesion between the tissue layers during dissection.

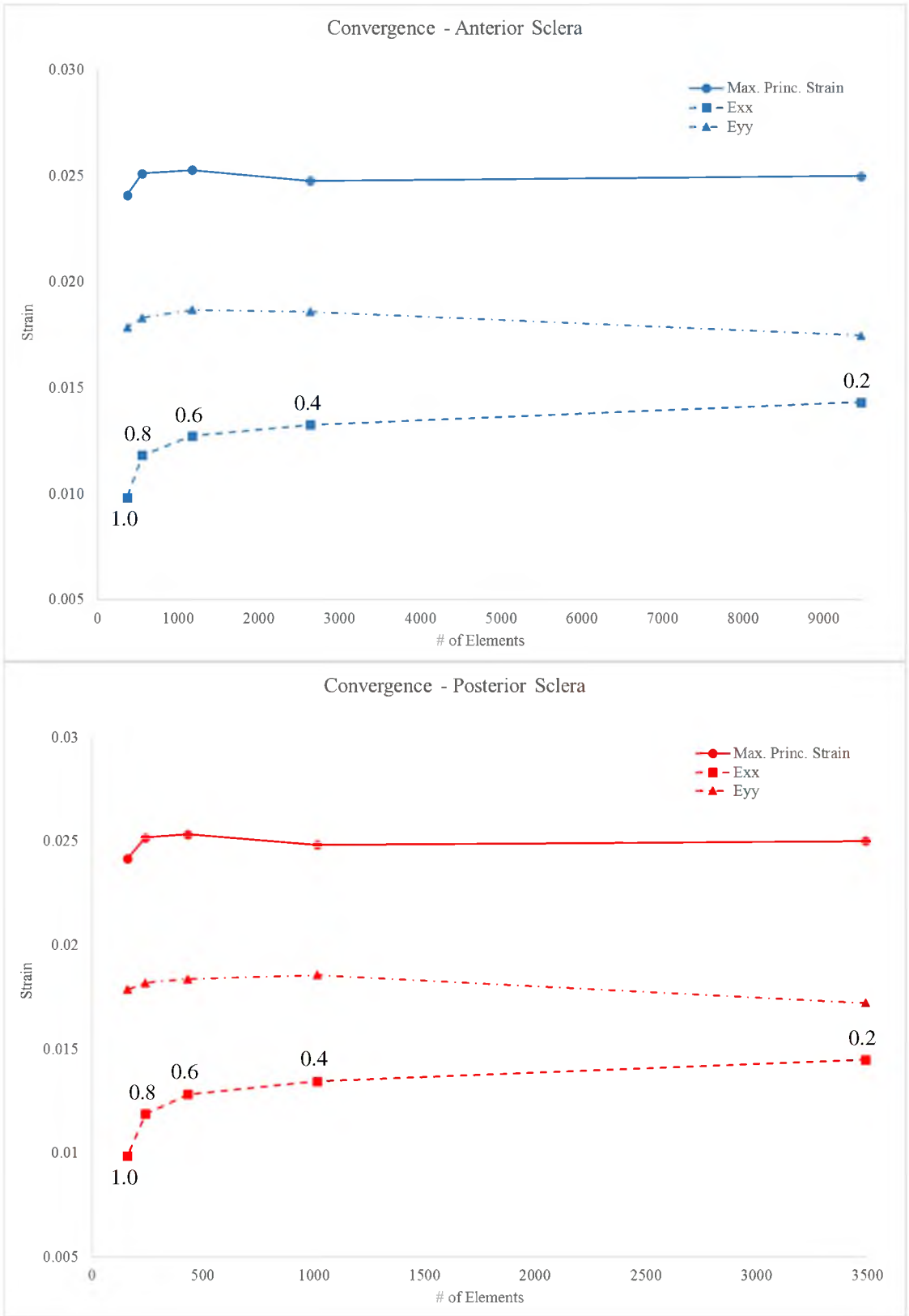

Figure 81: A convergence study was conducted for the anterior and posterior sclera. The mesh density was varied by changing the global seed size from 1.0 to 0.2.

4.3.4.2 Material definition. The choroid was modeled as linear, elastic, and isotropic. The material data included for the choroid were based on published data from adult human.[3] Based on the stress-strain curves collected in Chapters 1 and 2, the sclera was modeled as a linear, hyperelastic, viscoelastic, isotropic material, and the retina was modeled as a linear, elastic, isotropic material. Although the retina is regarded as an anisotropic material, we did not characterize this mechanically and assumed isotropy for this analysis. The values included in the FE model can be seen in Table 17.

The average scleral stress relaxation curves reported in Chapter 1 were selected as the representative viscoelastic response for the anterior and posterior sclera in the inflation tests. The anterior region of the sclera was defined as all elements between the equator and cut surface of the eye. The posterior region was all remaining elements of the sclera. The time-dependent elastic modulus, E(t), was calculated as the stress/strain ratio from the averaged relaxation response for the sclera [Eq.2]. This was then used to estimate the shear modulus, G(t), defined as a function of the elastic modulus and Poisson's ratio (ν) [Eq.3].

The time-dependent shear modulus for the anterior and posterior sclera was normalized by the normal shear modulus and implemented into ABAQUS. The resulting viscoelastic material models generated from ABAQUS are shown in Figure 82. To determine an appropriate hyperelastic model, the stress-strain responses from the pull-to-failure data were averaged for both the anterior and posterior sclera and implemented into ABAQUS. The built-in material evaluator was used to fit the stress-strain responses to multiple strain energy functions. A 3rd-order Ogden model was determined to be the best fit for both the anterior and posterior sclera (Figure 83). The Ogden model is defined by an isotropic strain energy formulation based on the deviatoric principal stretches (λ_i) and

Table 17: The material properties for each ocular component were determined from mechanical tests performed in our lab or published data.

Ocular Componenet	Element Type	Material Parameters	Poisson's Ratio	E (MPa)	Density (kg/mm^3)	Thickness (mm)
Anterior Sclera	Hex, Solid	Isotropic, Hyperelastic, Linear, Viscoelastic	0.49	---	1.24E-06	0.451
Posterior Sclera [3]	Hex, Solid	Isotropic, Hyperelastic, Linear, Viscoelastic	0.49	---	1.24E-06	1.066
Choroid	Hex, Solid	Isotropic, Linear	0.49	0.0968	1.00E-06	0.186
Retina	Hex, Solid	Isotropic, Hyperelastic, Linear	0.49	0.0305	1.00E-06	0.186
Vitreous	Hex, Solid	Isotropic, Linear, Viscoelastic	0.49	1.84E-03	1.20E-06	N/A

shear modulus which are defined by a function of α_i [Eq.4]. Incompressibility was assumed for this model.

Previously in our lab, ovine immature vitreous was subjected to shear creep testing. The resulting vitreous strain-time responses were averaged and used as a representative viscoelastic response for vitreous. The time-dependent shear modulus, G(t), was calculated from the averaged creep response for the vitreous. Shear compliance, J(t), was computed as the inverse of the shear modulus. The shear compliance was normalized by the initial shear compliance and implemented into ABAQUS for the vitreous viscoelastic definition (Figure 84). The data input to fit the material models within ABAQUS can be seen in Appendix E.

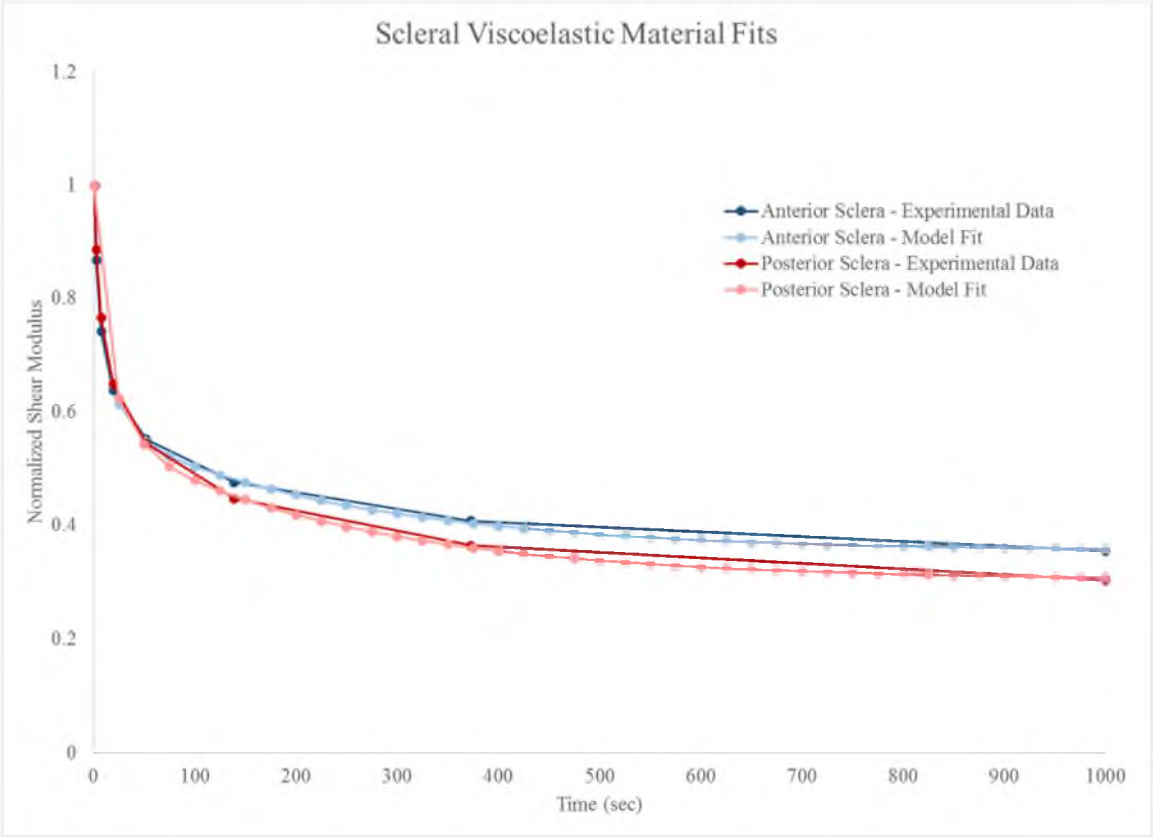

Figure 82: The normalized relaxation responses for the anterior and posterior sclera were fit with a viscoelastic model in ABAQUS.

$$E(t) = \frac{\sigma(t)}{\epsilon(t)} \qquad \text{Eq. 2}$$

$$G(t) = \frac{E(t)}{2(1+\nu)} \qquad \text{Eq. 3}$$

$$u = \sum_{i=1}^{N} \frac{2\mu_i}{{\alpha_i}^2}\left({\lambda_1}^{-\alpha_i} + {\lambda_2}^{-\alpha_i} + {\lambda_3}^{-\alpha_i} - 3\right) \qquad \text{Eq. 4}$$

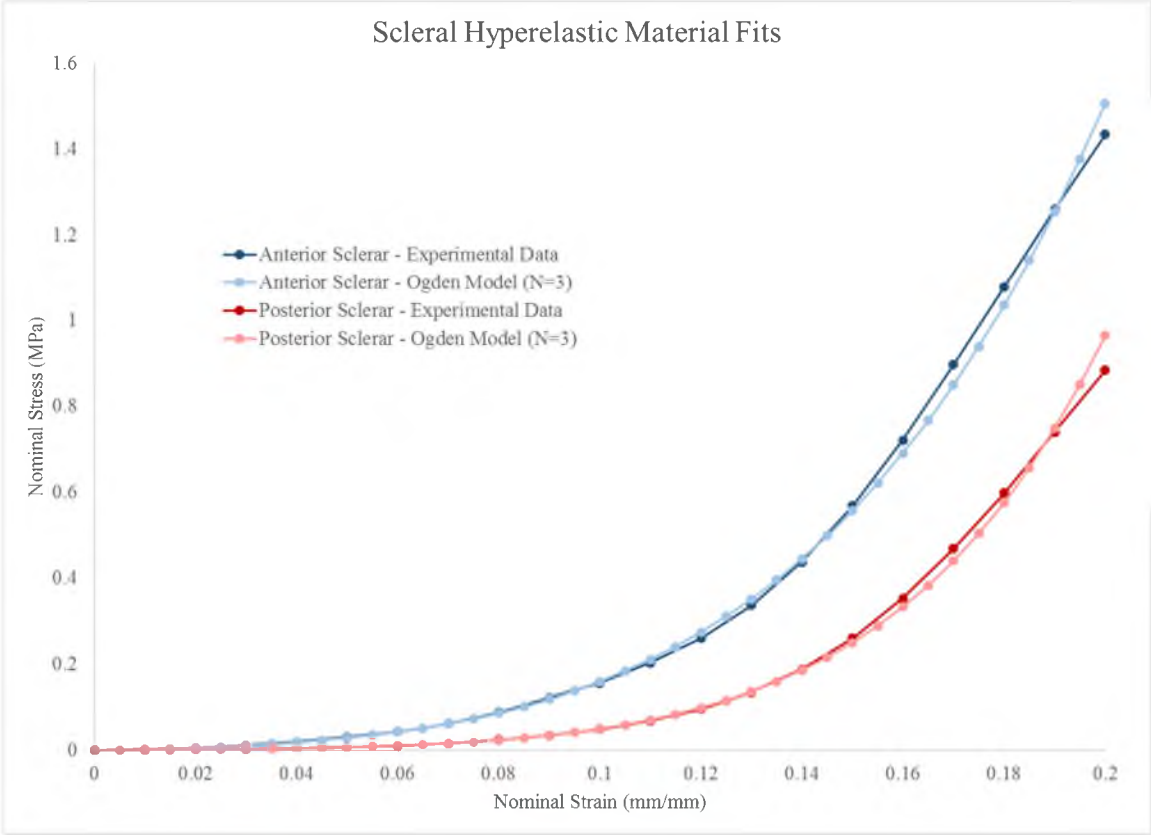

Figure 83: A 3rd-order Ogden model was identified as an appropriate strain energy function for the anterior and posterior sclera using the ABAQUS material evaluator.

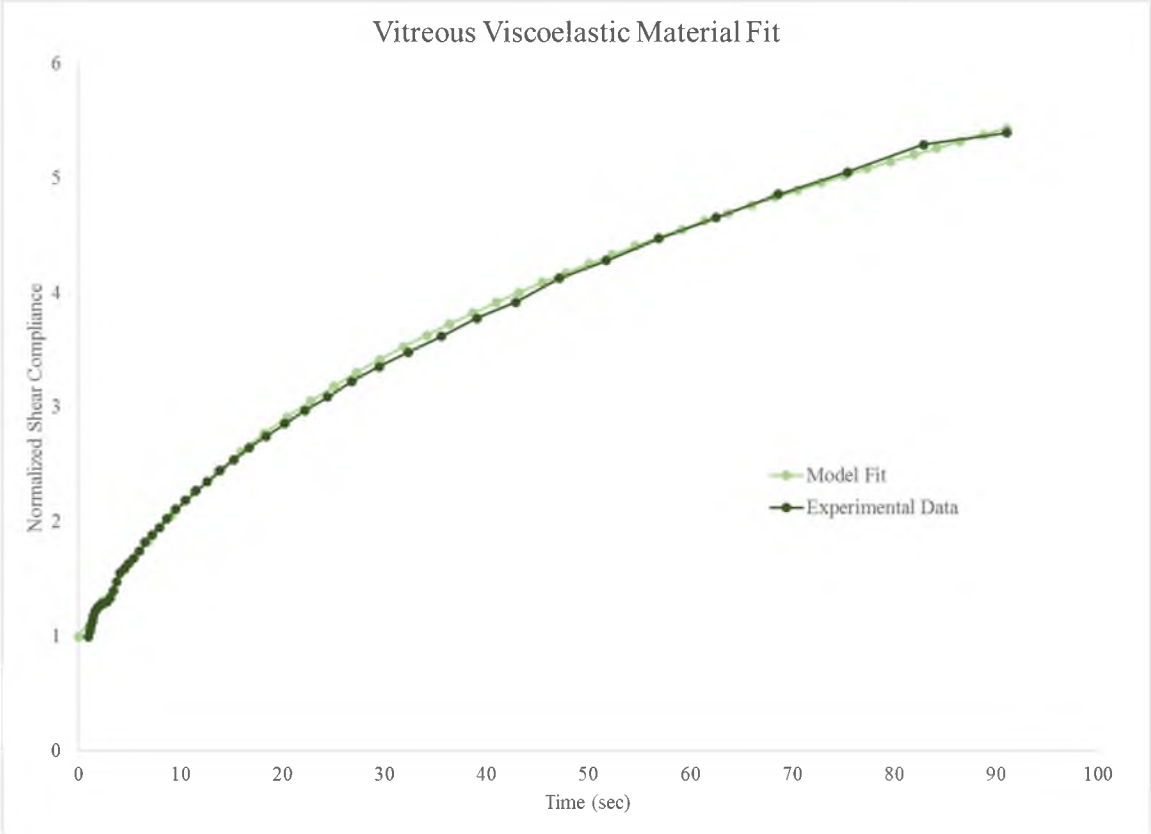

Figure 84: The normalized creep response for the vitreous was fit with a viscoelastic model in ABAQUS.

4.3.4.3 Boundary conditions. A fixed constraint was prescribed to the lower perimeter of the scleral layer such that there was no linear and no rotational degrees of freedom ($u_1=u_2=u_3=\theta_1=\theta_2=\theta_3=0$) (Figure 85a). A pressure-dependent function was prescribed and applied to bottom surface of the ocular model (Figure 85b). The pressure function was extracted from the experimental inflation test data described in the section 4.3.2 above. The maximum principal strain, strain in the x-direction, and strain in the y-direction of the anterior and posterior regions of the sclera were output from the model for comparison with the Lagrangian strains from the experimental inflation tests.

Strip sections of sclera were selected from the anterior and posterior regions which were representative of the area of interest selected in the DIC analysis. Maximum principal

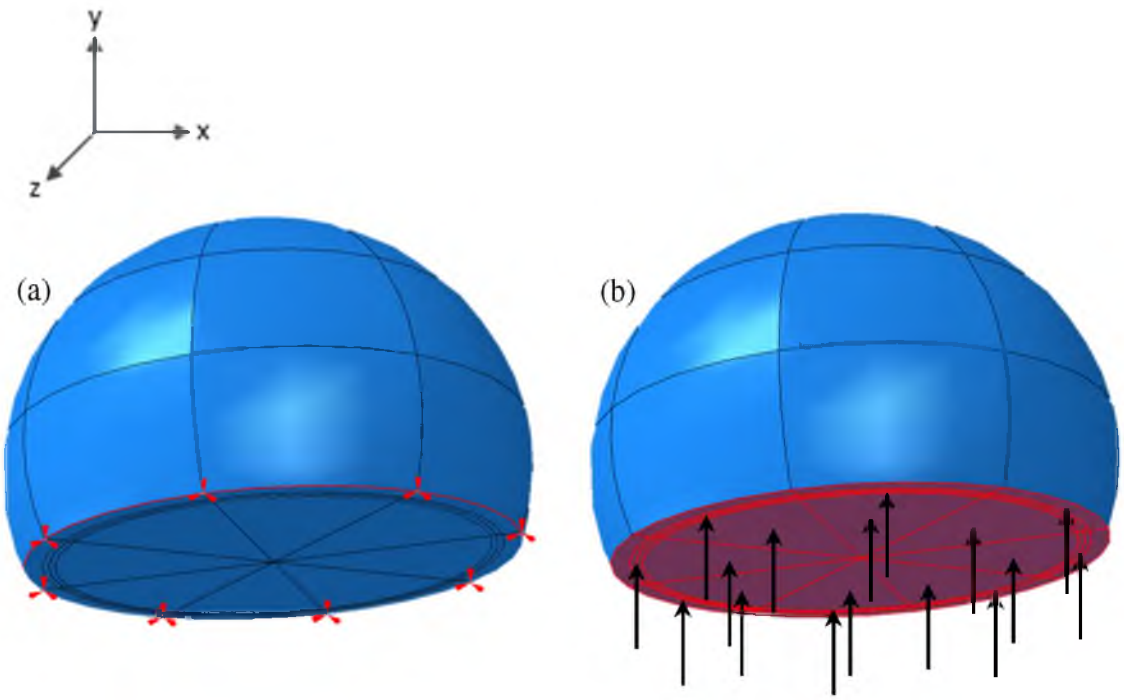

Figure 85: The boundary conditions prescribed in the FE model were (a) a pinned constraint around the lower perimeter of the sclera and (b) a uniformly distributed pressure applied to the bottom surface of the eye.

strain, E_{xx} and E_{yy} were averaged across all elements in the strip at every time point in the simulation.

4.4 Results

4.4.1 Digital image correlation

In general, the posterior sclera was more extensible than the anterior sclera. Three-dimensional plots of the maximum principal strains, and the Lagrangian strain in the x and y directions in the selected areas at full inflation (30 mmHg) can be seen in Figure 86 - Figure 88. The average ± standard deviation of the inspection points for the maximum principal strain of the anterior and posterior sclera at full inflation was 0.0089±0.007 and 0.0299±0.007, respectively (Figure 89). The average ± standard deviation of the inspection

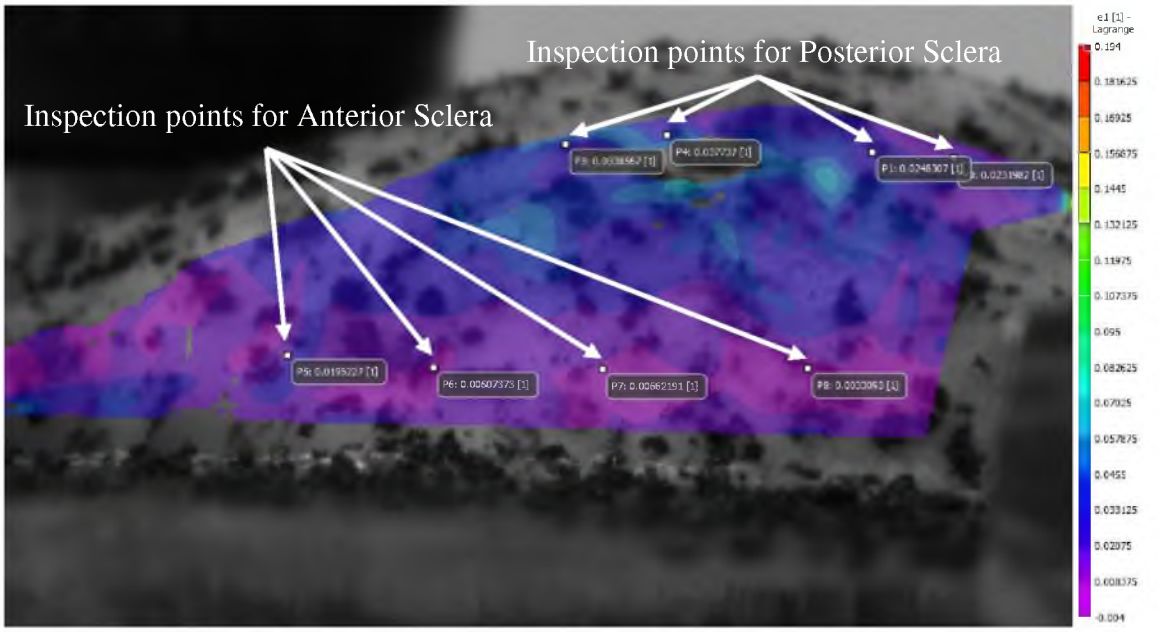

Figure 86: The maximum principal strain across the area of interest (AOI) was computed for the sclera at full inflation. Four inspection points were selected from the anterior (P5, P6, P7, P8) and posterior (P0, P1, P2, P3, P4) sclera.

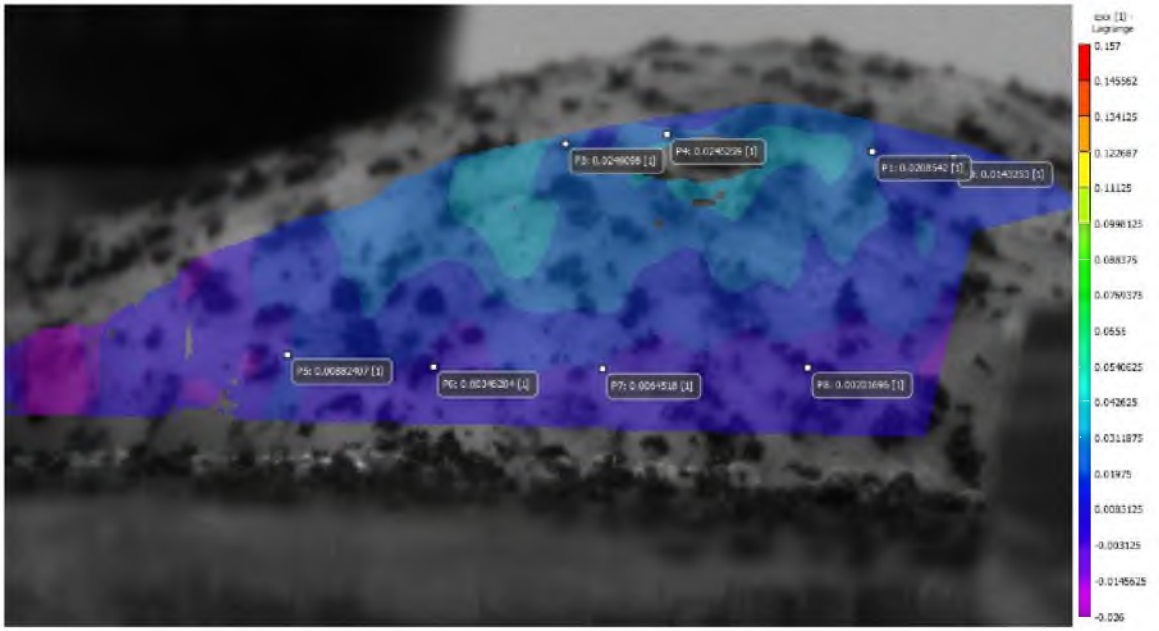

Figure 87: The strain in the x-direction across the area of interest was computed for the sclera at full inflation.

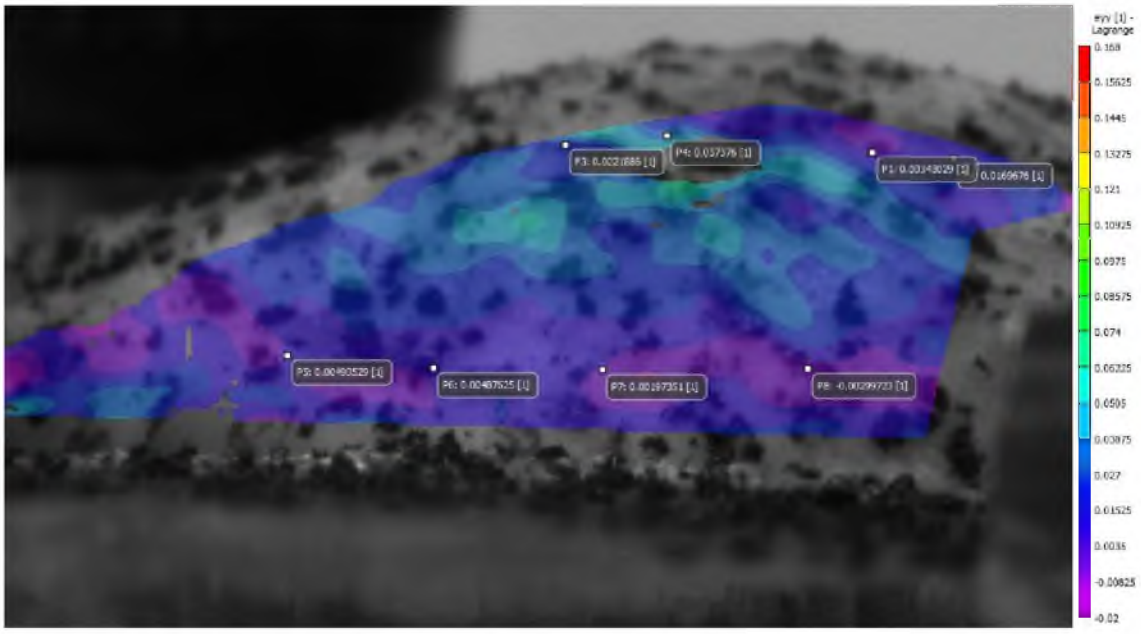

Figure 88: The strain in the y-direction across the area of interest was computed for the sclera at full inflation.

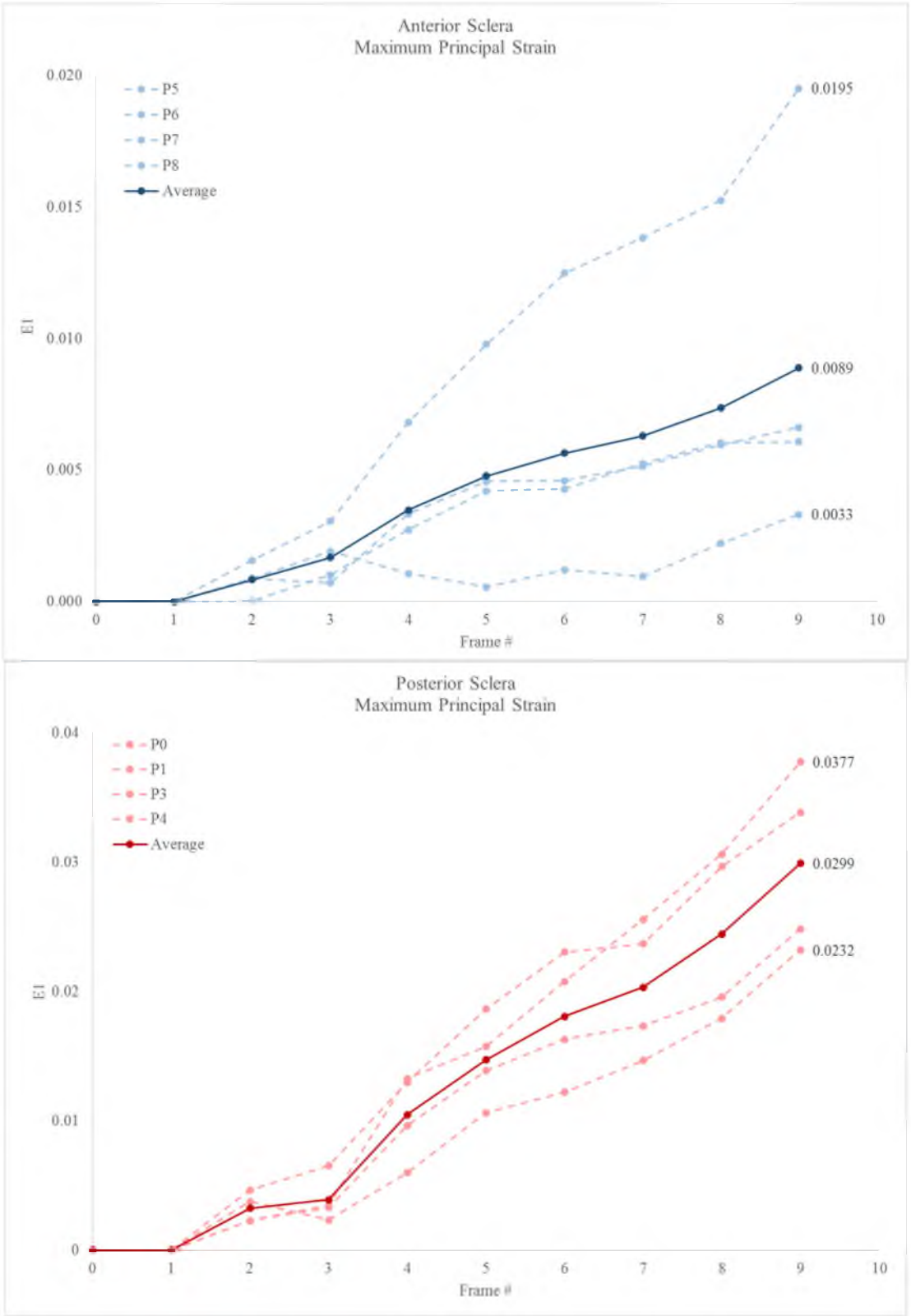

Figure 89: The maximum principal strain for the four inspection points in each region (anterior/posterior) was computed for all frames of the inflation video. Theses strains were then averaged (dark lines).

points for the strain in the x-direction of the anterior and posterior sclera at full inflation was 0.0052±0.003 and 0.0211±0.005, respectively (Figure 90). The average ± standard deviation of the inspection points for the strain in the y-direction of the anterior and posterior sclera at full inflation was 0.0022±0.004 and 0.0200±0.014, respectively (Figure 91). A negative value is indicative of compressive strain and may be explained by the eye not being inflated enough before the inflation test was applied.

4.4.2 Finite element model

Similar to the DIC analysis, posterior sclera was more extensible than the anterior sclera for maximum principal strain and strain in the x-direction, but the anterior sclera was more extensible in the y-direction at full inflation. The average maximum principal strains of the anterior and posterior sclera at full inflation were 0.0128 and 0.0255, respectively. The average strains in the x-direction of the anterior and posterior sclera at full inflation were 0.0046 and 0.0116, respectively. The average strains in the y-direction of the anterior and posterior sclera at full inflation were 0.012 and 0.0097, respectively. Contour maps of the scleral surface strains at full inflation are shown in Figure 92 and Figure 93. The resulting strains for the anterior and posterior sclera from the FE analysis are provided with the peak and average values from the DIC analysis in Table 18.

4.4.2.1 Maximum principal strain. The maximum principal strain at full inflation for the anterior sclera from the FE analysis was within the range of values from the DIC analysis (Figure 94). The FE maximum principal strain for the anterior sclera at full inflation was 1.44 times larger than the average maximum principal strain at full inflation from DIC. The maximum principal strain at full inflation for the posterior sclera from the

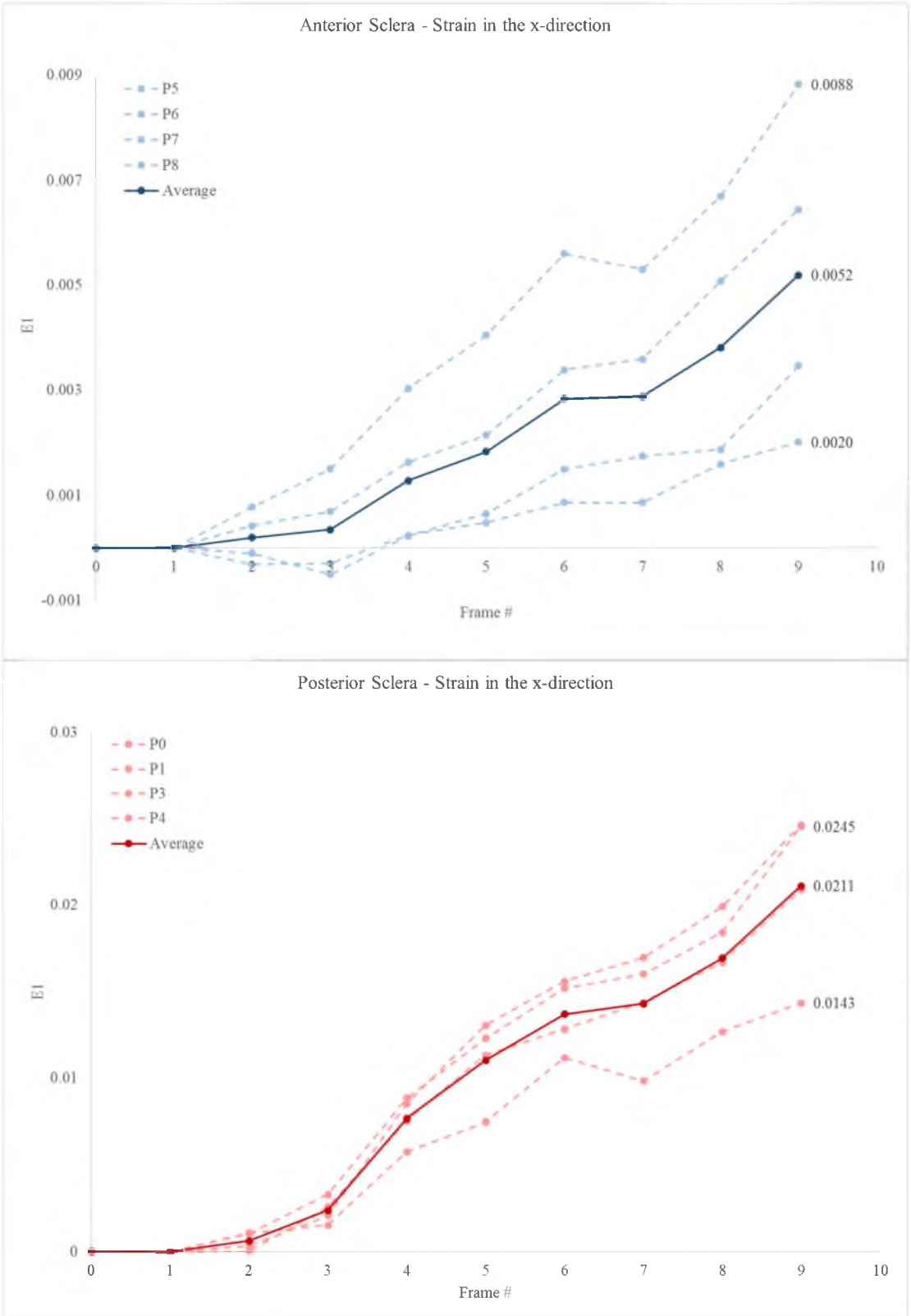

Figure 90: The strain in the x-direction for the anterior and posterior inspection points was computed for all frames of the inflation video. These strains were then averaged (dark lines).

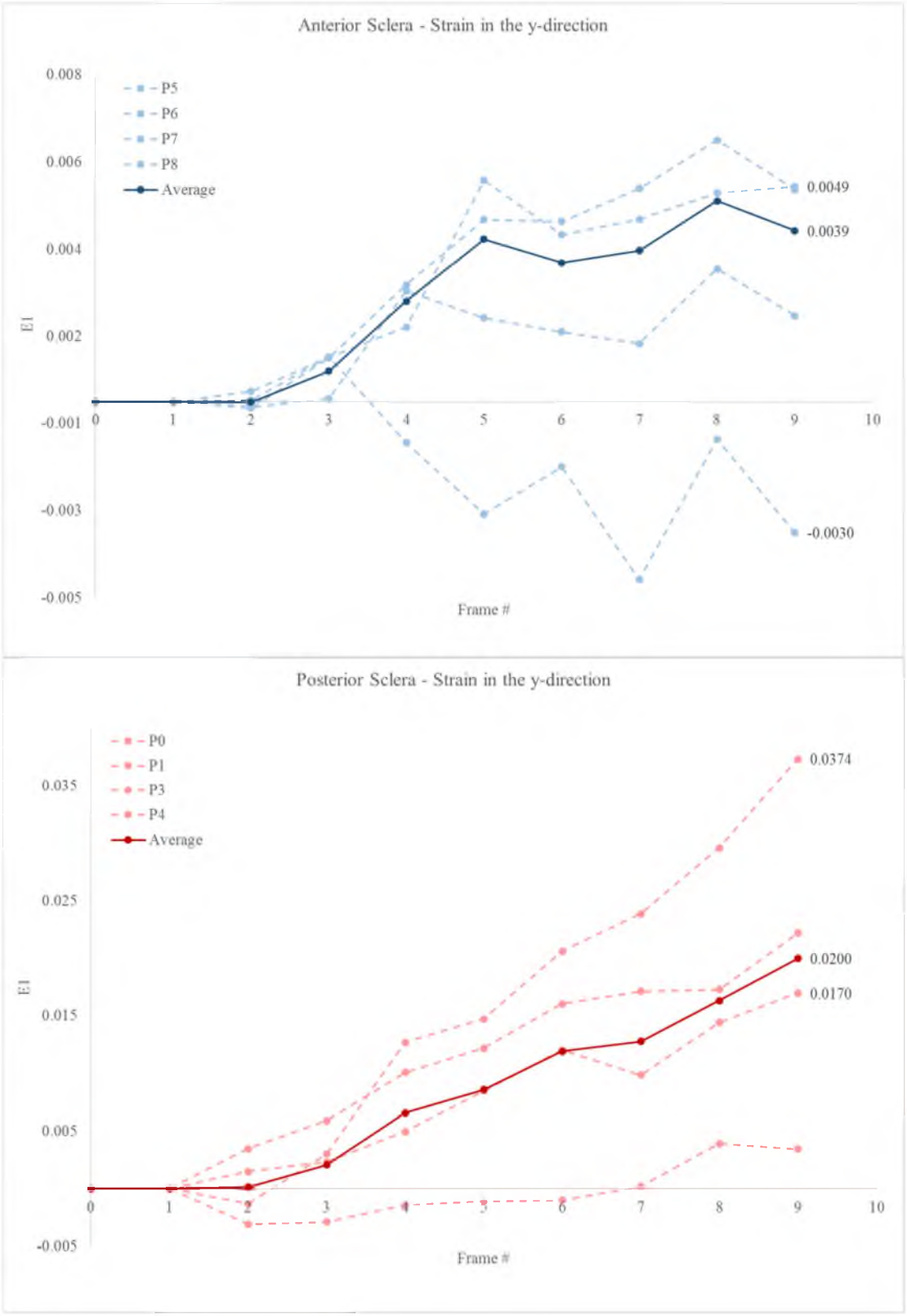

Figure 91: The strain in the y-direction for the anterior and posterior inspection points was computed for all frames of the inflation video. These strains were then averaged (dark lines). The lower irregular anterior dataset was not included in the average.

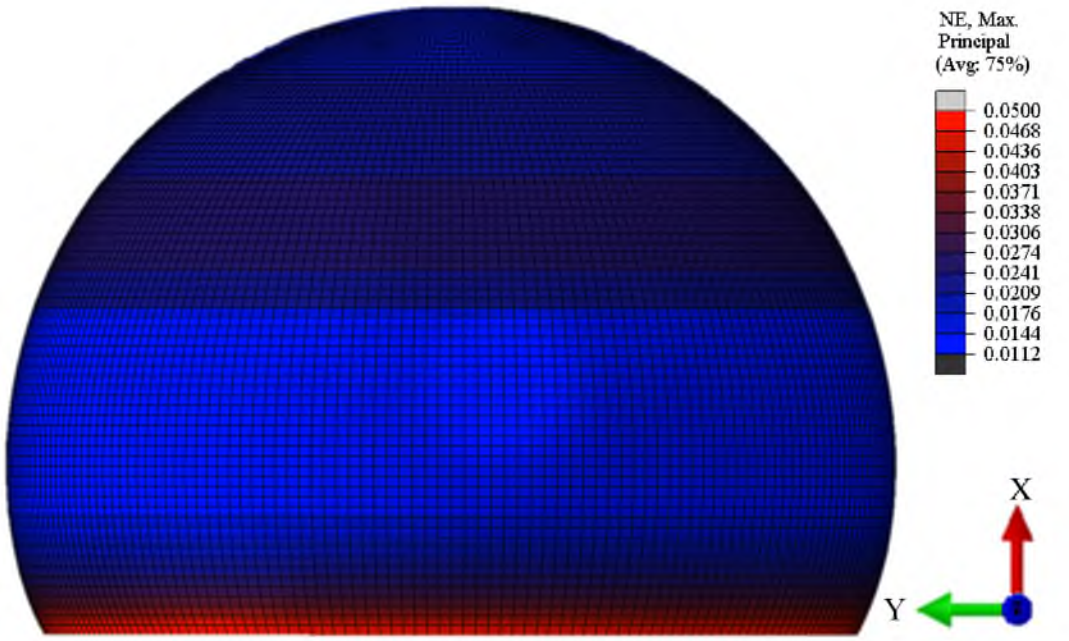

Figure 92: A three-dimensional contour plot of the resulting maximum principal strain was generated for the ocular model at full inflation.

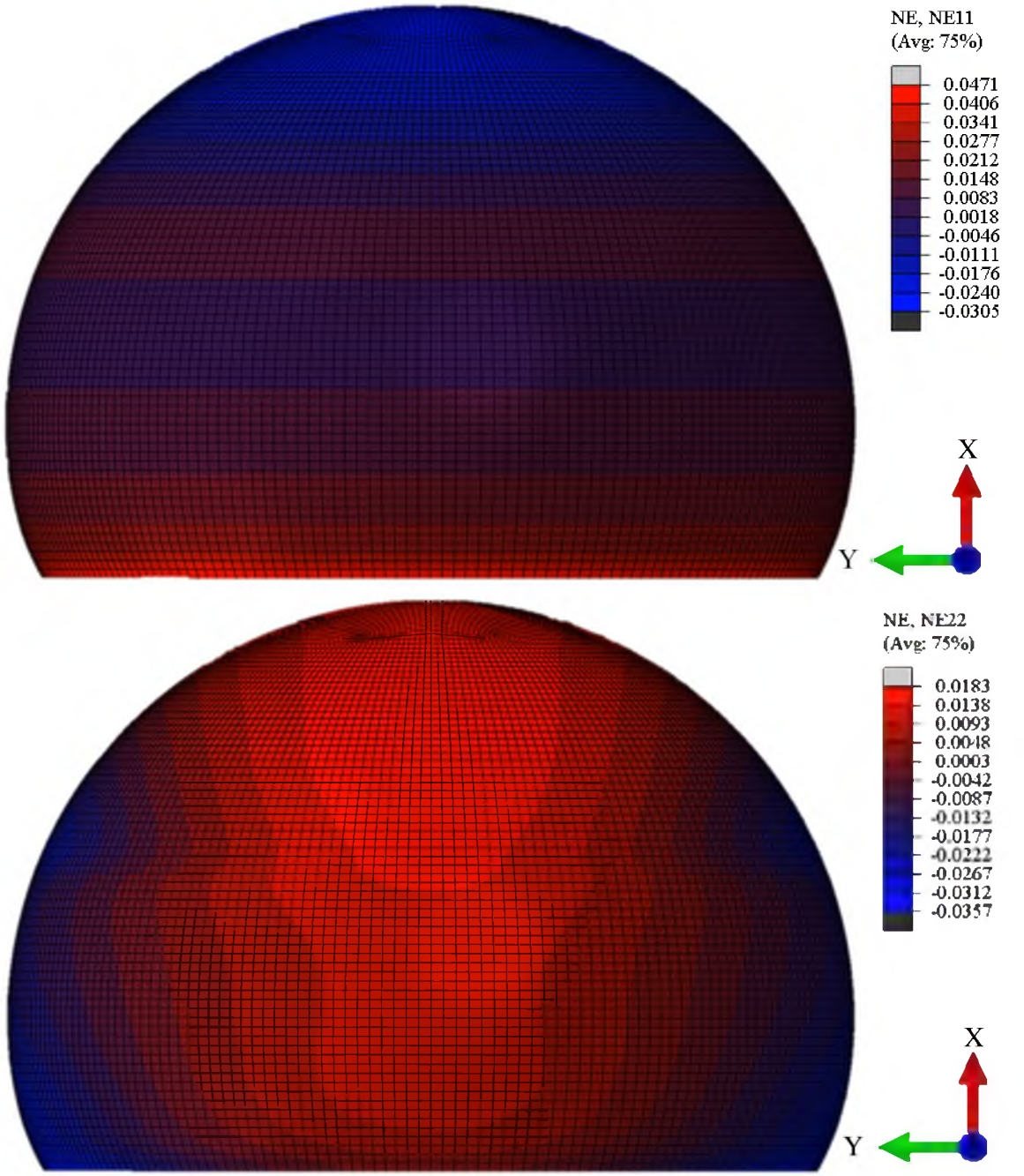

Figure 93: Three-dimensional contour plots of the resulting strain in the x-direction (top) and strain in the y-direction (bottom) were generated for the ocular model at full inflation.

Table 18: The average Lagrangian strains at full inflation from the DIC and FE analyses.

	Anterior Sclera			Posterior Sclera		
	Max	Exx	Eyy	Max	Exx	Eyy
DIC	0.00888	0.00519	0.0039	0.0299	0.02108	0.0246
FE	0.01283	0.0046	0.01205	0.02548	0.01159	0.00972

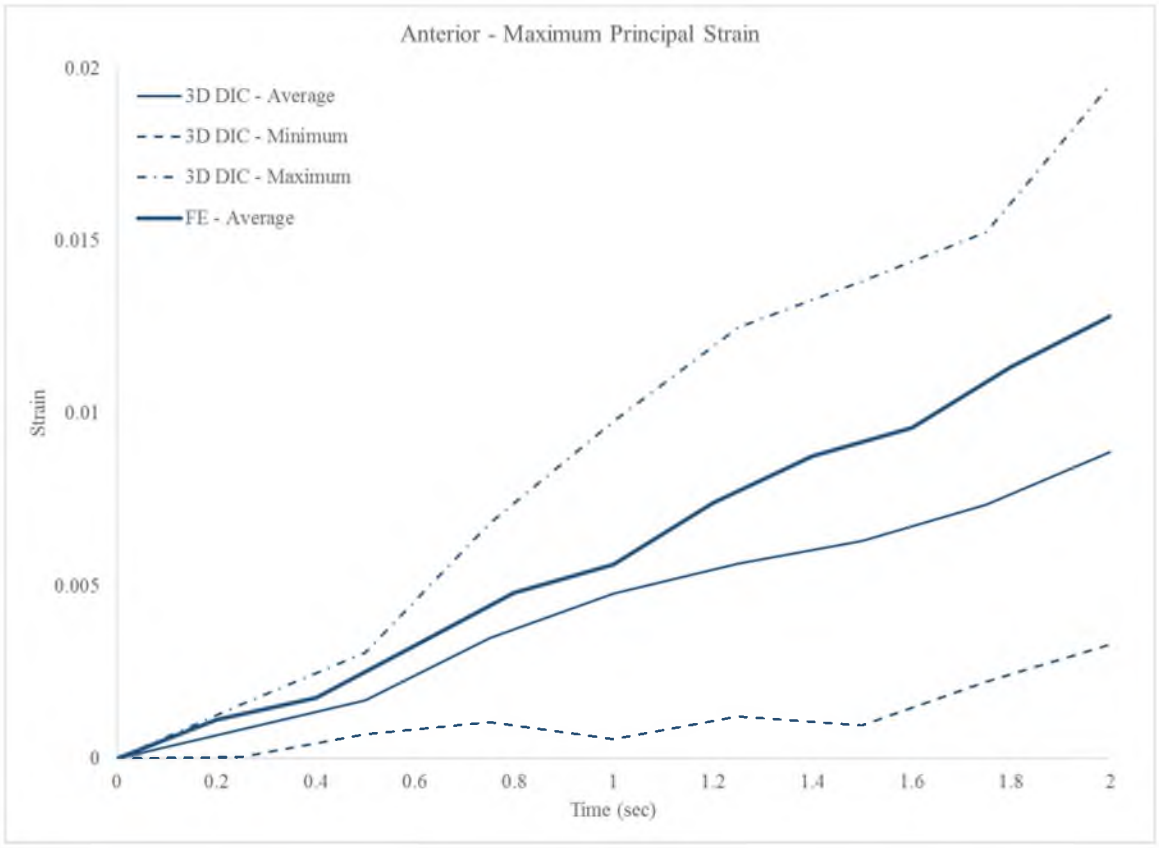

Figure 94: From the DIC analysis, the maximum, minimum, and average maximum principal strains for the anterior sclera were plotted across time. The corresponding average maximum principal strains from the FE analysis were compared to the range of values from DIC.

FE analysis was also within the range of values from the DIC analysis (Figure 95). The FE maximum principal strain for the posterior sclera at full inflation was 0.85 times smaller than the average maximum principal strain at full inflation from DIC. Regression lines were generated for the strains at each pressure increment from the FE analysis with respect to the results from the DIC analysis. The regression line for the maximum principal strain of the anterior and posterior sclera had R^2 values of 0.98 and 0.97, respectively (Figure 96).

4.4.2.2 Strain in the x-direction. The strain in the x-direction at full inflation for the anterior sclera from the FE analysis was within the range of values from the DIC analysis (Figure 97). The FE strain in the x-direction for the anterior sclera at full inflation was

0.89 times smaller than the average maximum principal strain at full inflation from DIC. The strain in the x-direction at full inflation for the posterior sclera from the FE analysis was less than the minimum value from the DIC analysis (Figure 98). The FE strain in the x-direction for the posterior sclera at full inflation was 0.55 times smaller than the average maximum principal strain at full inflation from DIC. The regression line for the strain in the x-direction of the anterior and posterior sclera had R^2 values of 0.90 and 0.97, respectively (Figure 99).

4.4.2.3 Strain in the y-direction. The strain in the y-direction at full inflation for the anterior sclera from the FE analysis was greater than the maximum value from the DIC analysis (Figure 100). The FE strain in the y-direction for the anterior sclera at full inflation was 5.48 times larger than the average maximum principal strain at full inflation from DIC. The strain in the y-direction at full inflation for the posterior sclera from the FE analysis was within the range of values form the DIC analysis (Figure 101). The FE strain in the y-direction for the posterior sclera at full inflation was 0.49 times smaller than the average maximum principal strain at full inflation from DIC. The regression line for strain in the y-direction of the anterior and posterior sclera had R^2 values of 0.74 and 0.92, respectively (Figure 102).

4.5 Discussion

Overall, the posterior sclera was more extensible than the anterior sclera in both the physical inflation tests and FE simulations. This correlates well with our material property data that showed the anterior sclera was stiffer than the posterior sclera in the immature ovine eye. This may have been attributed to the set boundary conditions, yet the result is

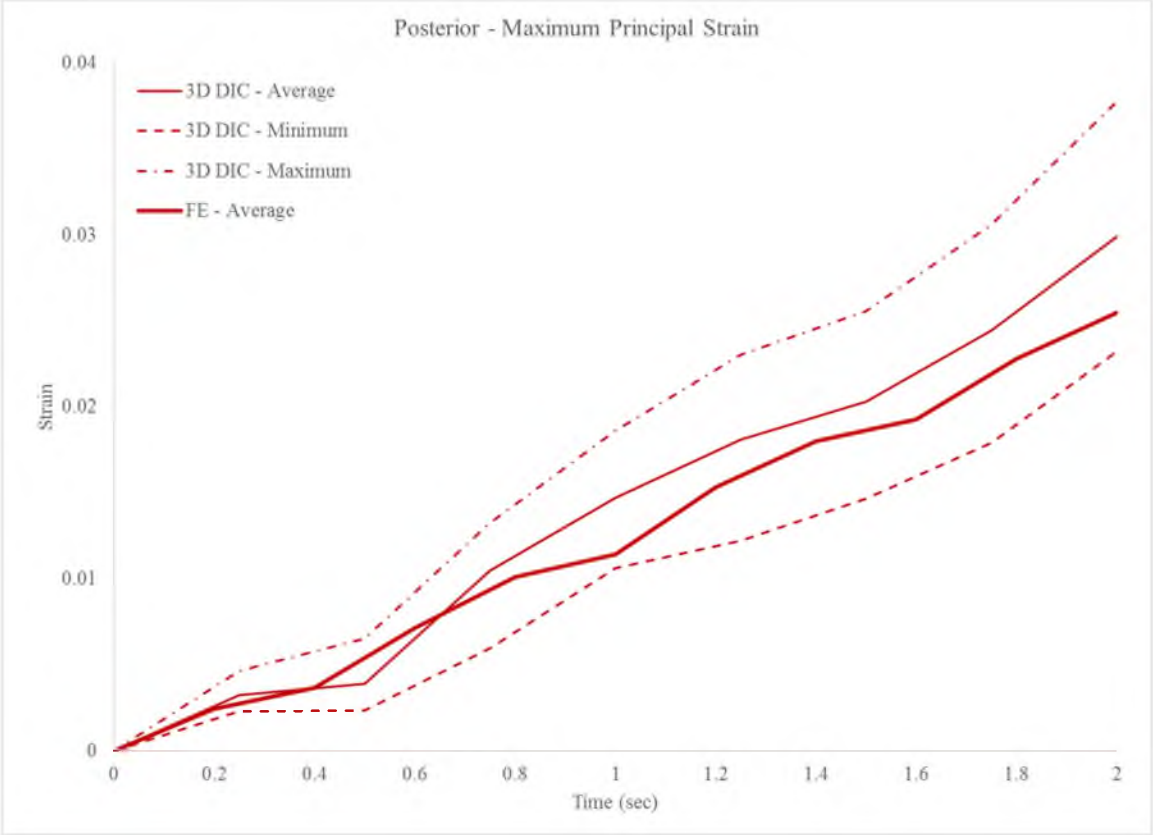

Figure 95: From the DIC analysis, the maximum, minimum, and average maximum principal strains for the posterior sclera were plotted across time. The corresponding average maximum principal strains from the FE analysis were compared to the range of values from DIC.

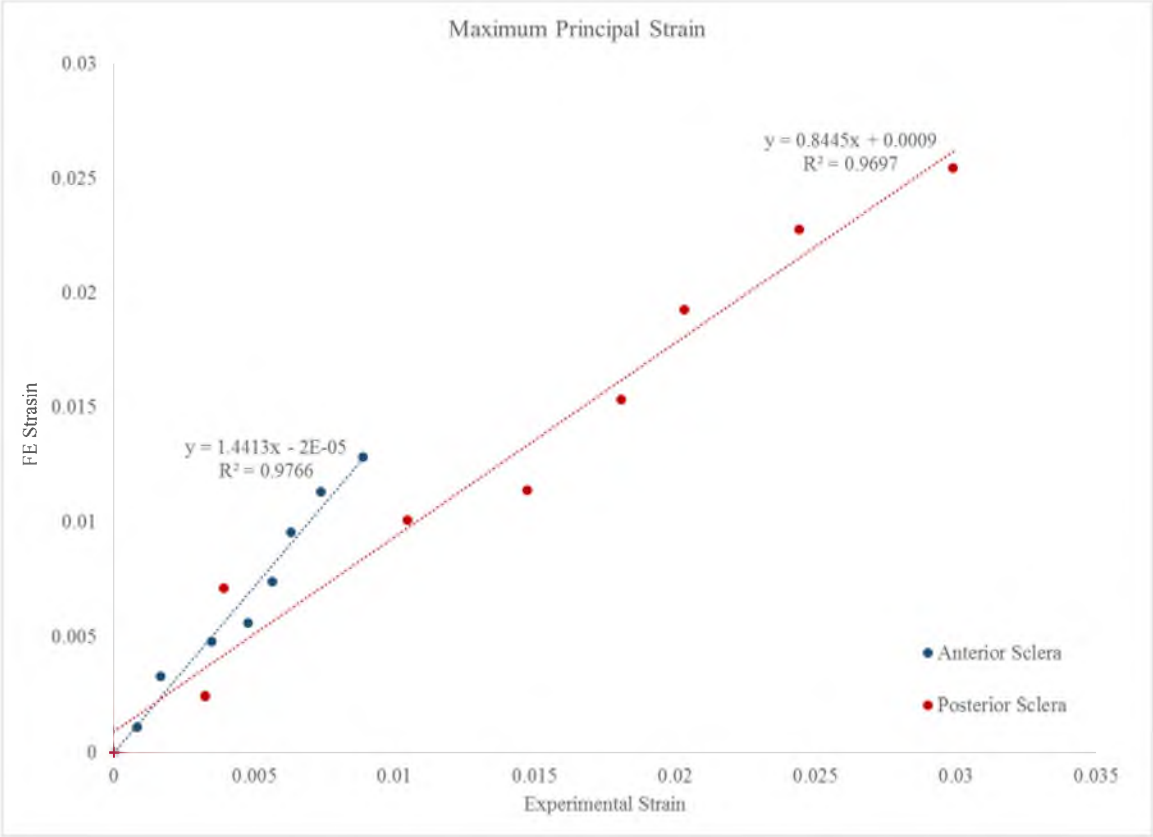

Figure 96: Regression lines for the maximum principal strain of the anterior (blue) and posterior (red) sclera.

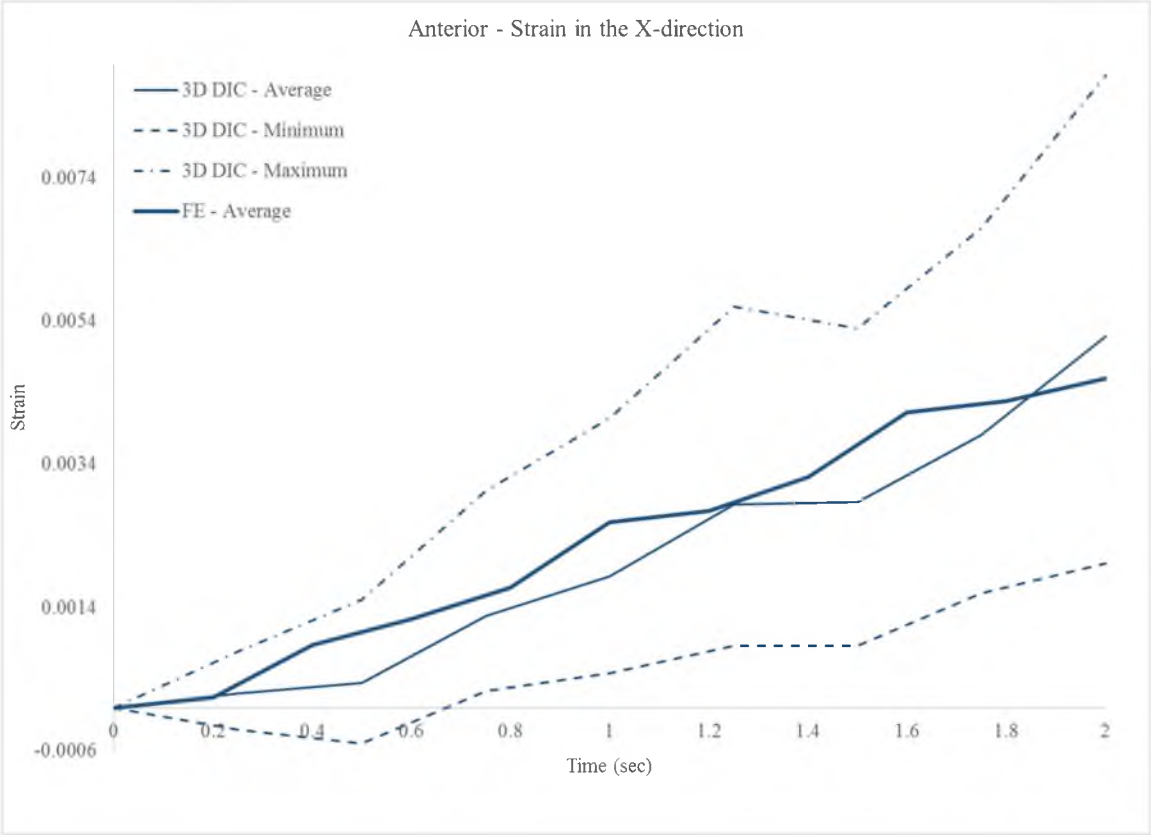

Figure 97: From the DIC analysis, the maximum, minimum, and average strains in the x-direction for the anterior sclera were plotted across time. The corresponding average strains in the x-direction from the analysis were compared to the range of values from DIC.

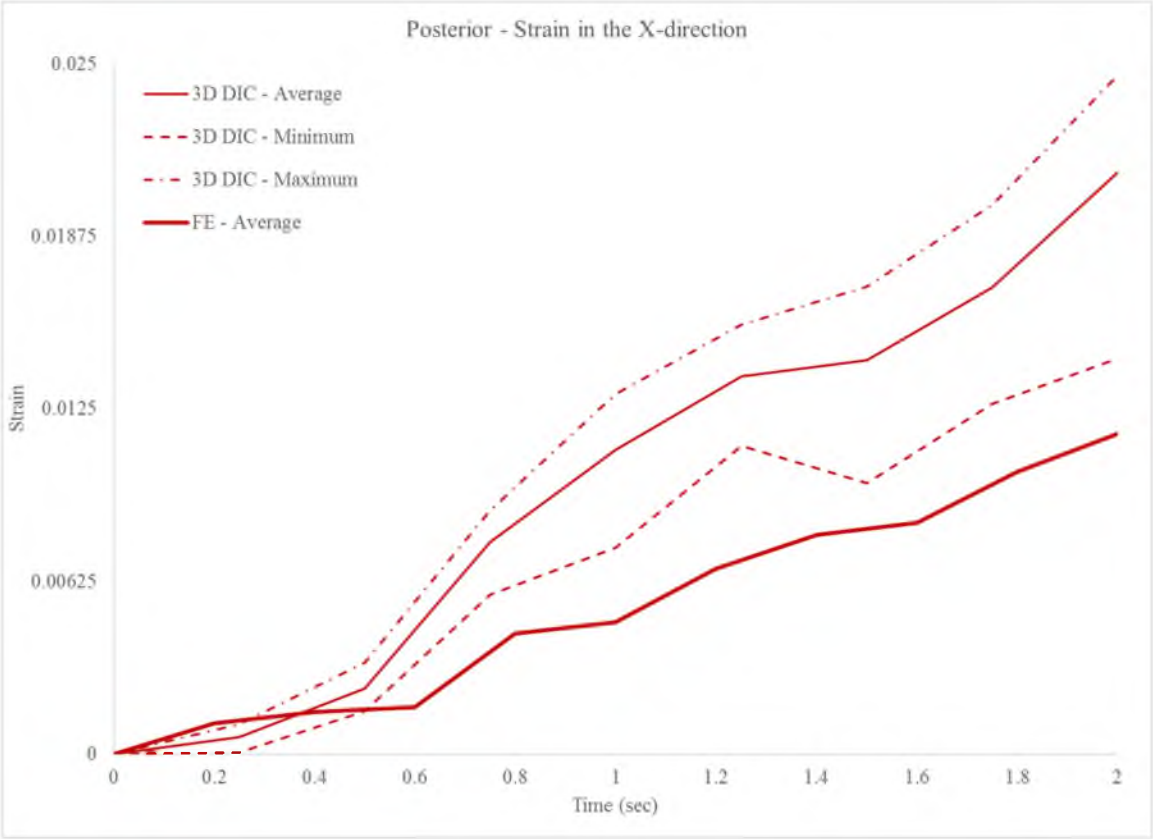

Figure 98: From the DIC analysis, the maximum, minimum, and average strains in the x-direction for the posterior sclera were plotted across time. The corresponding average strains in the x-direction from the FE analysis were compared to the range of values from DIC.

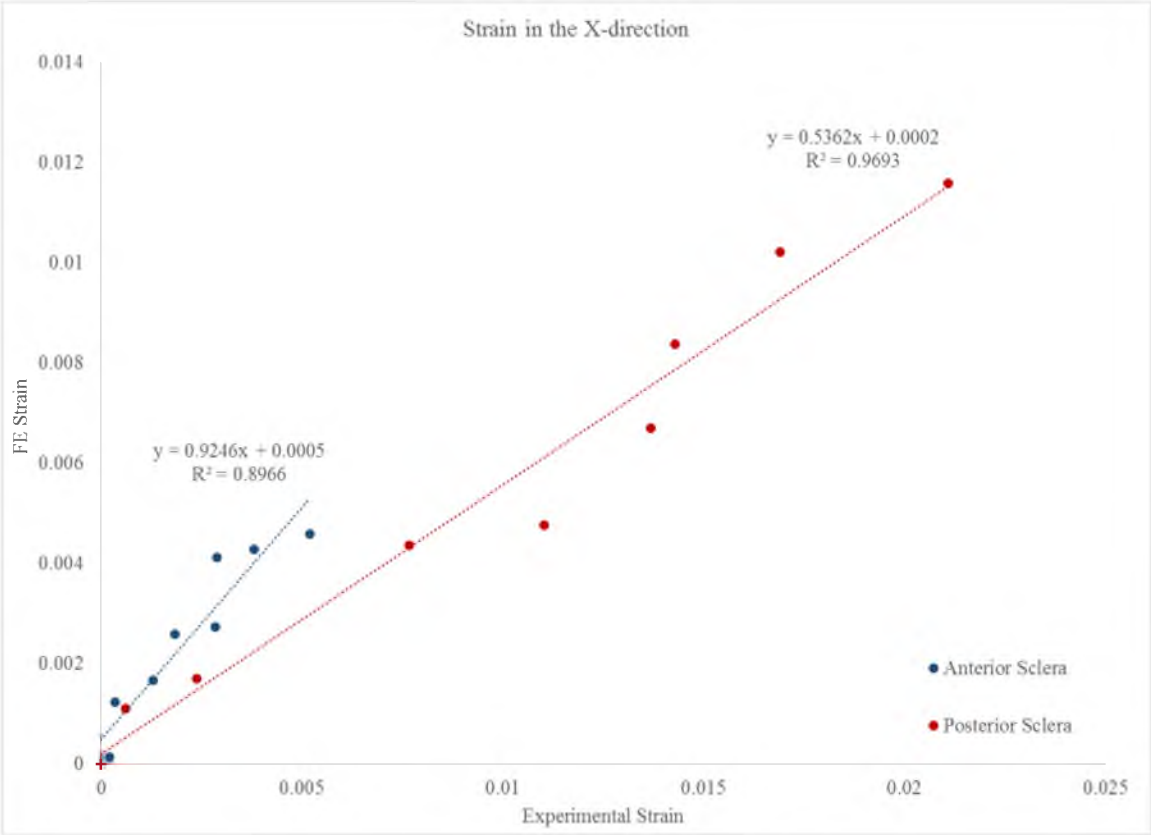

Figure 99: Regression lines for the strain in the x-direction of the anterior (blue) and posterior (red) sclera.

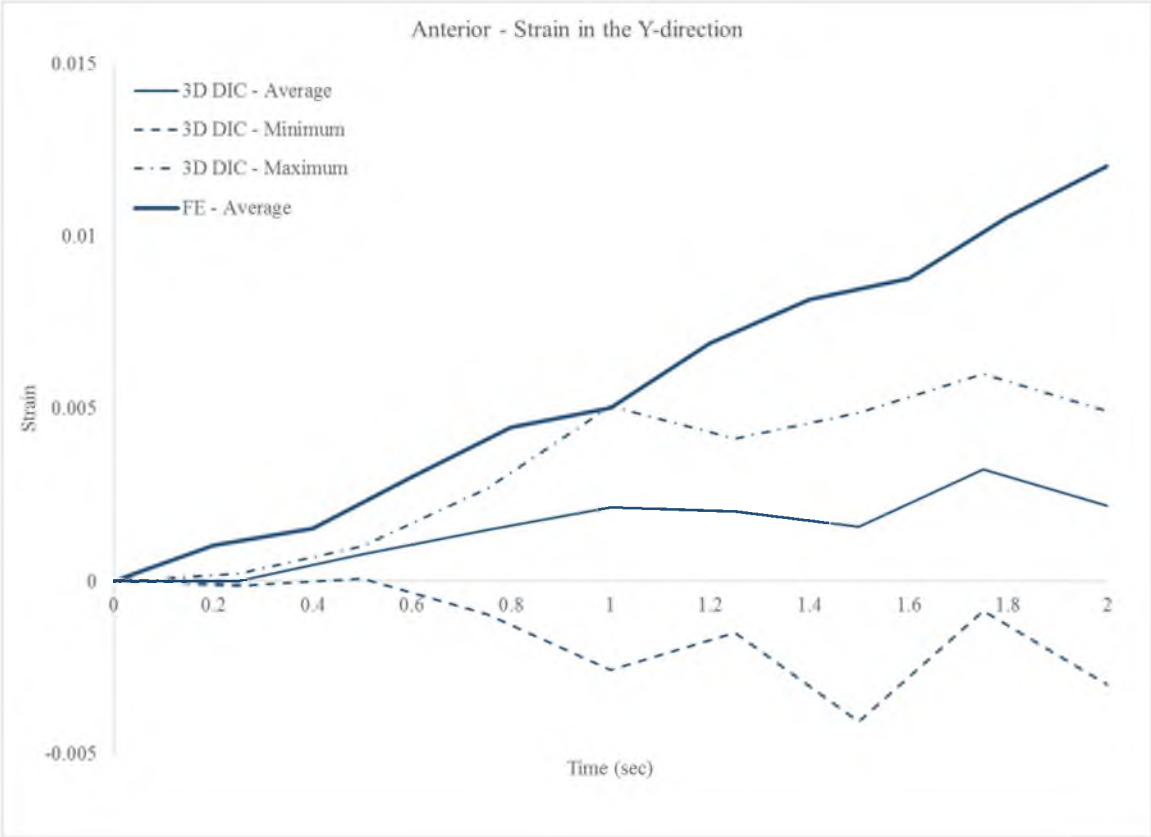

Figure 100: From the DIC analysis, the maximum, minimum, and average strains in the y-direction for the anterior sclera were plotted across time. The corresponding average strains in the x-direction from the FE analysis were compared to the range of values from DIC.

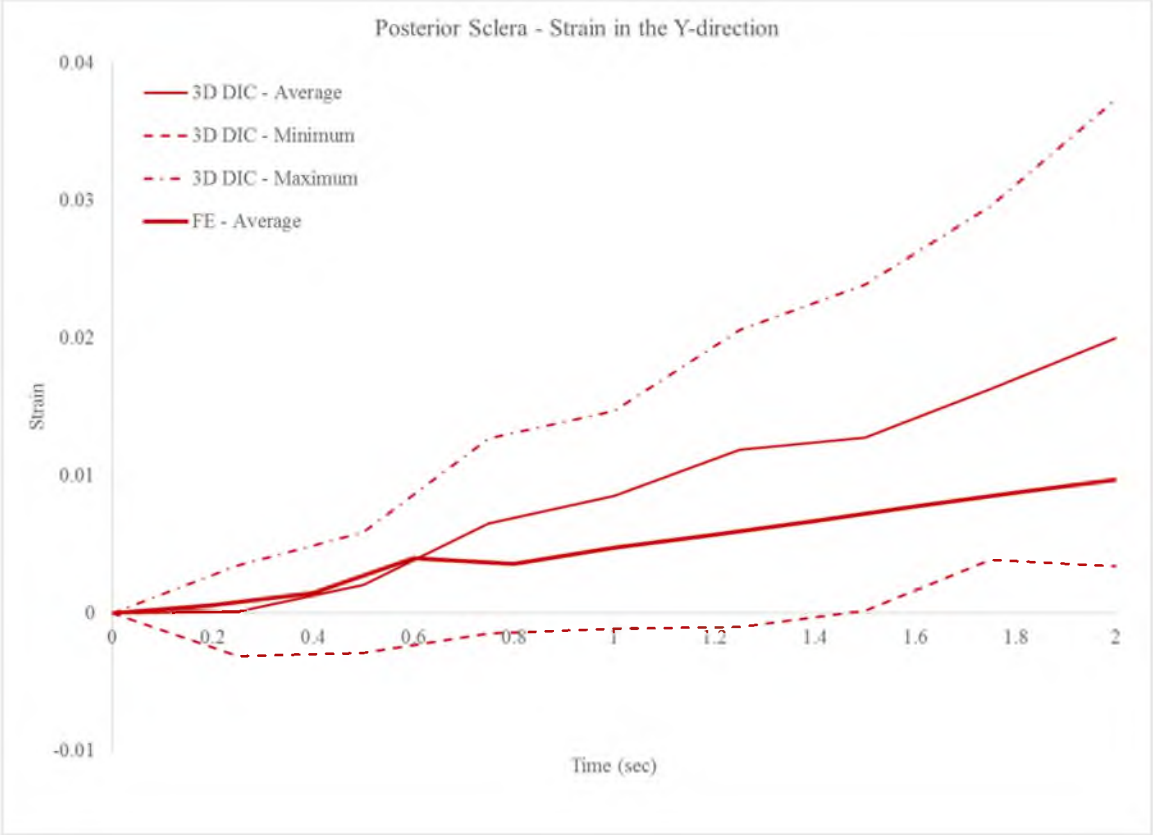

Figure 101: From the DIC analysis, the maximum, minimum, and average strains in the x-direction for the posterior sclera were plotted across time. The corresponding average strains in the y-direction from the FE analysis were compared to the range of values from DIC.

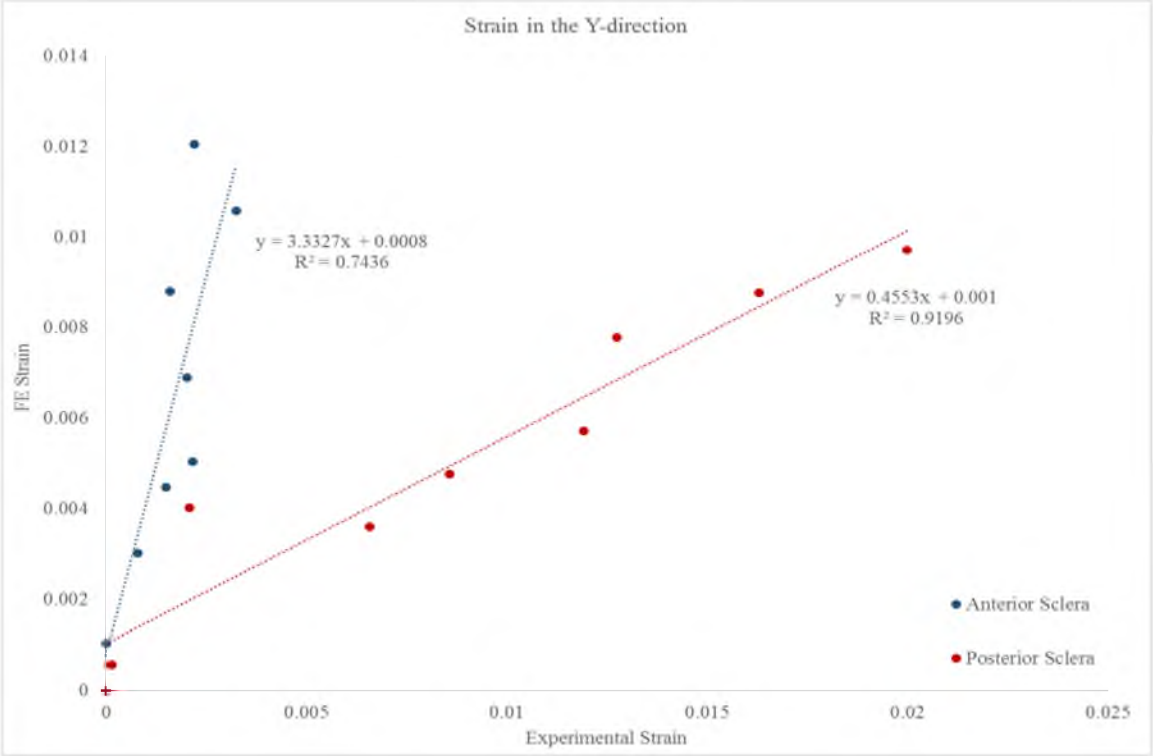

Figure 102: Regression lines for the strain in the y-direction of the anterior (blue) and posterior (red) sclera.

expected in the FE model as the material models enforced the mechanical response.

While the use of a frozen/thawed eye for the DIC analysis is a limitation, we previously found that freezing/thawing only significantly affected the ultimate stress of sclera. Although not significantly different, frozen then thawed anterior and posterior immature sclera trended to be slightly less stiff than fresh sclera suggesting the DIC studies may overestimate strain. This may explain the larger E_{xx} and E_{yy} from the DIC posterior measurements. Anterior E_{yy} from the DIC analysis may have had artificially low strains because a region at the bottom of the eye was restricted by the glue, where in simulations only a line is restricted.

Overall, the FE model proved to be a reliable means for predicting scleral surface strains. All coefficients of determination from the linear regression models were at least

0.9 with the exception for the strain in the y-direction of the anterior sclera and in the x-direction for the posterior sclera. Only the strain in the y-direction for the anterior sclera and strain in the x-direction for the posterior sclera from the FE analysis was outside the bounds of the results from DIC. Maximum principal strain in the FE model, however, was excellently correlated with the experimental data. This verifies that the constitutive equations have been implemented correctly and that the model is valuable in predicting scleral surface strains.

4.6 Conclusions

The FE simulation data correlated well with the experimental results. Maximum principal strain was the best correlated between the experimental and simulation results. From these data, the material models for the immature eye appear to be well defined and can be implement into an age-appropriate pediatric eye FE model to investigate retinal stress and strain.

4.7 Acknowledgements

We would like to thank Jeff Kessler and Dr. Dan Adams for providing the digital image correlation system as well as assisting with the experimental inflation tests. We would also like to thank the Knights Templar Eye Foundation for sponsoring this work.

4.8 References

1. Boyce, B.L., Grazier, J.M., Jones, R.E., Nguyen, T.D., Full-field deformation of bovine cornea under constrained inflation conditions. Biomaterials, 2008. 29(28): p. 3896-3904.

2. Courdillier, B., Tian, J., Alexander, S., Myers, K.M., Quigley, H.A., Nguyen, T.D., Biomechanics of the human posterior sclera: age- and glaucoma-related changes measured using inflation testing. Investigative Ophthalmology & Visual Science, 2012. 53(4): p. 1714-1728.

3. Hans, S.A., Bawab, S.Y., Woodhouse, M.L., A finite element infant eye model to investigate retinal forces in shaken baby syndrome. Graefe's Archives for Clinical and Experimental Ophthalmology, 2009. 247(4): p. 561-571.

4. Levin, A.V., Retinal Hemorrhage in Abusive Head Trauma. Pediatrics, 2010. 126(5): p. 961-970.

5. Maguire, S.W., Watts, P.O., Shaw, A.D., Holden, S., Taylor, R.H., Watkins, W.J., Mann, M.K., Tempest, V., Kemp, A.M., Retinal haemorrhages and related findings in abusive and non-abusive head trauma: a systemic review. Eye, 2012. 27(1): p. 28-36.

6. Moran, P.R. (2012) Characterization of the vitreoretinal interface and vitreous in the porcine eye as it changes with age (Master's thesis). Retrieved from http://content.lib.utah.edu/cdm/ref/collection/etd3/id/1932

7. Myers, K.M., Courdillier, B., Boyce, B.L., Nguyen, T.D., The inflation response of the posterior bovine sclera. Acta Biomaterialia, 2010. 6(11): p. 4327-4335.

8. Rangarajan, N., Kamalakkhannan, S., Hasija, V., Shams, T., Jenny, C., Serbanescu, I., Ho, J., Rusinek, M., Levin, A., Finite element model of ocular injury in abusive head trauma. Journal of the American Association for Pediatric Ophthalmology and Stribismus, 2009. 13(4): p. 364-369.

CHAPTER 5

WHOLE EYE MODEL

5.1 Abstract

Finite element (FE) analysis will be invaluable in understanding injury mechanisms and thresholds of retinal hemorrhages (RH). However, current finite element models of the pediatric eye rely heavily on adult material properties. We have now characterized the age-dependent mechanical differences in retina, sclera, and vitreous, and can implement the age-appropriate properties into a FE model of the infant eye designed to investigate mechanics of RH. One theoretical cause of RH is the traction between the vitreous and retina during rapid head acceleration. If this theory were correct, adhesion at the vitreoretinal (VR) interface would significantly influence predictions of RH. To determine the sensitivity of retinal stress and strain to VR adhesion, the interaction parameters between the retina and vitreous were varied and changes in retinal stress and strain quantified. The equatorial retina experienced the greatest stresses and strains in all simulations. Varying the interaction parameters had minimal effect on the regional stress and strain of the retina. Simulating a single head rotation versus multiple cyclic head rotations resulted in an increase in stress and strain with each rotation. Interestingly, the posterior retina experienced greater stress than anterior retina after one cycle while the anterior retina underwent larger strain after one cycle. Caution should be made while

interpreting these data as regional VR adhesion is unknown, but the data highlight the importance of VR adhesion in predictions of RH.

5.2 Introduction

Abusive head trauma (AHT) is a leading cause of death and disability in children in the United States. Retinal hemorrhages (RH) have been reported in 78-85%[5, 6] of AHT cases, and are one of the constellation of injuries assessed in AHT. RH have also been reported in 0-20%[6] of accidental trauma, and the injury mechanisms are not fully understood. This leads to some uncertainty as to whether RH were caused by abusive or accidental head trauma in the absence of other signs of abuse. A better understanding of the mechanism of RH may help distinguish abusive versus accidental traumatic RH. One hypothesized cause of RH is the traction between the vitreous and retina during rapid head acceleration during shaking. Quantitatively, there are stronger attachment points at different regions of the vitreoretinal (VR) interface. Specifically, there may be stronger adhesion in the vitreous base, the periphery where the retina meets the anterior chamber of the eye. Computational models may provide insight on injury mechanisms of RH through assessing magnitudes and distributions of retinal stress and strain under different loading conditions. To date, two finite element (FE) models exist of the pediatric eye. Hans et al. generated a pediatric eye model comparing the retinal force experienced from shaking to that of an impact pulse. They conclude that shaking alone is capable of causing retinal stresses high enough for RH, but injury thresholds for RH do not currently exist.[4] The other FE model by Ranganrajan et al. had a simplified ocular geometry and was used to evaluate the influence of the vitreous and extraocular fat on retinal stress and stress

distribution. The prescribed angular acceleration was similar to shaking. They concluded that vitreous properties have a significant influence on the retina, and that peak stresses occurred in the posterior retina where RH is commonly located.[9] In both of these studies, ocular structures were represented with adult material properties and the potential for mechanical changes in the developing eye was neglected.

We have previously characterized the age-dependent mechanical changes in the ovine sclera, retina, and vitreous through tensile and dynamic shear testing. The immature sclera constitutive model has been validated by comparing scleral regional predicted surface strains from a FE model to experimental scleral strains from ocular inflation tests. The objective of this study was to assess the mechanical influence of VR adhesion on the magnitude and distribution of retinal stress and strain through the use of an infant shaking FE model. The model will enhance our understanding of the theoretical model of VR traction and retinal detachment as a key cause of RH.

5.3 Materials and Methods

5.3.1 Geometry and meshing

A whole eye FE model was generated to include the sclera, choroid, retina, vitreous, lens, and a combined anterior ocular chamber which was simplified as the cornea. To generate the three-dimensional geometry of the eye, an ocular cross-section was generated using ex vivo measurements made in our lab, and then revolved about the x-axis (anterior-posterior axis) (Figure 103) using 3D CAD software (SolidWorks, Dassault Systemes, Waltham, MA) The 3D eye volume was imported into ABAQUS (Dassault Systemes, Waltham, MA) for meshing and analysis. Hexahedral, linear elements with reduced

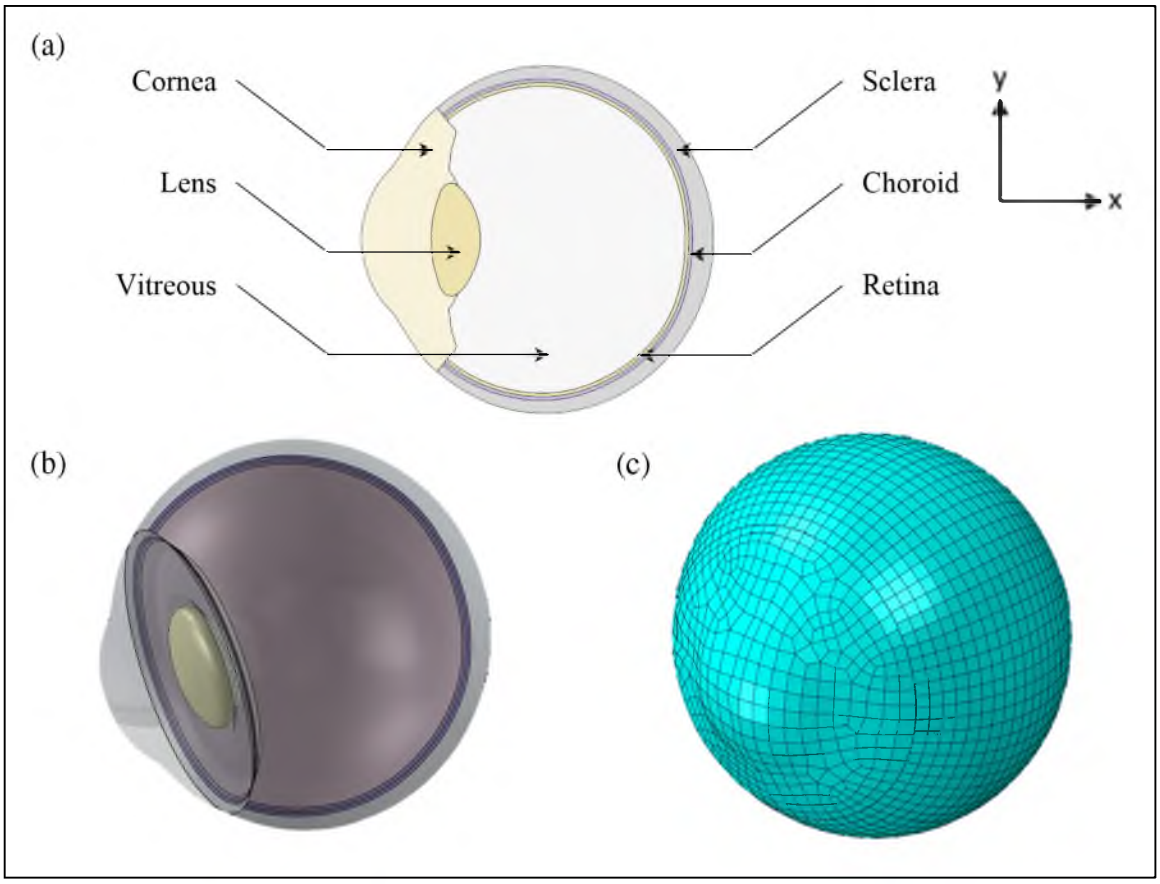

Figure 103: A three-dimensional model of the eye was generated and imported into finite element analysis software to be meshed. (a) A cross section of the eye was drawn using CAD software and revolved about the x-axis to generate the three-dimensional geometry of the ocular structures included in the model. (b) The 3D geometry included the cornea, lens, vitreous, sclera choroid, and retina. (c) The 3D model was imported into ABAQUS and meshed.

integration and hourglass control were used to mesh the sclera, choroid, cornea, and lens. Tetrahedral quadratic elements were used to mesh the retina and vitreous. A convergence study on each structure was performed to determine an appropriate mesh and the final model contained a total of 115,836 nodes and 78,111 elements (Figure 103c). Data from the convergence study is reported in Appendix E.

5.3.2 Material definition

The choroid, cornea, and lens were modeled as linear, elastic, and isotropic using material constants reported in the literature (Table 19). Previously, infant sheep sclera and retina were subjected to strain-dependent uniaxial tension and the load response to stress-relaxation for sclera and pull-to-failure for sclera and retina were collected. Retina stress-strain curves exhibited an initial linear elastic region up to approximately 50% strain followed by plastic deformation. Retinal strain in simulations was thought to be lower than 50%, so the retina was modeled as linear elastic with an elastic modulus of 0.0305 MPa and Poisson's ratio of 0.49. The sclera exhibited hyperelastic and viscoelastic characteristics and a 3rd-order Ogden model was determined to be the best fit for both the anterior and posterior sclera (Chapter 4). Vitreous was modeled as linear isotropic and viscoelastic. Shear creep tests were used to define the viscoelastic response of vitreous. The data input to fit the material models within ABAQUS can be seen in Appendix E.

Table 19: The material properties for each ocular component were determined from mechanical tests performed in our lab or based on published data.

Ocular Componenet	Element Type	Material Parameters	Poisson's Ratio	E (MPa)	Density (kg/mm^3)	Thickness (mm)
Anterior Sclera	Hex, Solid	Isotropic, Hyperelastic, Linear, Viscoelastic	0.49	---	1.24E-06	0.451
Posterior Sclera	Hex, Solid	Isotropic, Hyperelastic, Linear, Viscoelastic	0.49	---	1.24E-06	1.066
Retina	Hex, Solid	Isotropic, Linear	0.49	0.0305	1.00E-06	0.186
Vitreous	Hex, Solid	Isotropic, Linear, Viscoelastic	0.49	0.00184	1.20E-06	N/A
Choroid [4]	Hex, Solid	Isotropic, Linear	0.49	0.0968	1.00E-06	0.186
Cornea [4]	Hex, Solid	Isotropic, Linear	0.42	124	1.40E-06	N/A
Lens [4]	Hex, Solid	Isotropic, Linear	0.49	6.89E+00	1.08E-06	N/A

5.3.3 Boundary conditions

A center of rotation (COR) was approximated based on a moment arm incorporated in previous infant eye FE simulations of shaking (Figure 104).[4] The distance was approximately 45 mm from the center of the eye to the COR. This is an averaged length based on measurements of the skull base to the T-1 vertebra in infants and thought to be an appropriate moment arm in shaking simulations.[3] The eye was prescribed a very basic rotation about the COR to investigate the eye's response during a flexion-extension head rotation. The angular velocity of the rotation was 57°/sec. A single cycle was used to compare VR interaction parameters. Multiple shaking cycles were also simulated to assess the influence of repeated head rotations. A multiple shaking cycle consisted of three single cycles (Figure 105). The prescribed angular velocity was also based on previous simulations using data obtained from surrogate shaking studies previously conducted.[4]

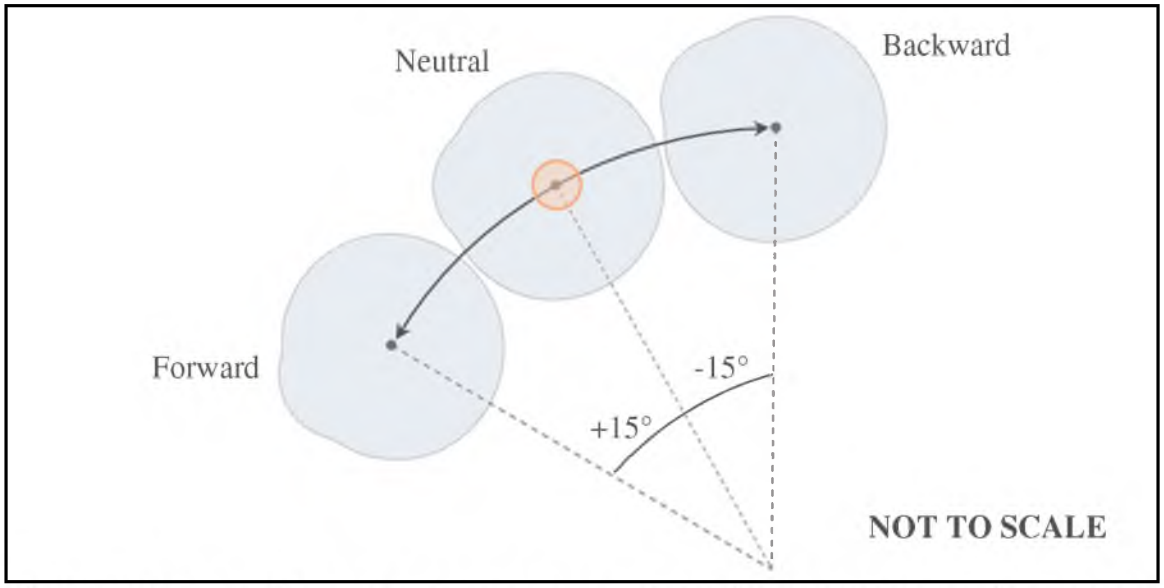

Figure 104: A simplified shaking event was simulating by prescribing a cyclic rotational displacement to the eye about a center of rotation.

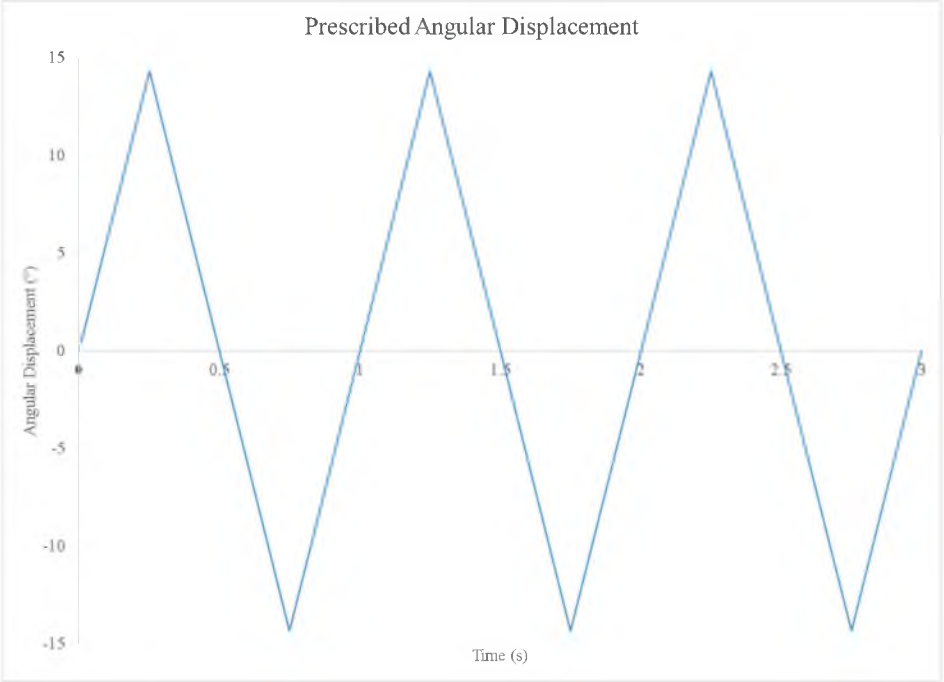

Figure 105: The cyclic rotation was defined by an angular displacement amplitude.

5.3.4 Interaction parameters

The base model incorporated a tied interaction between all ocular layers. The interaction parameter assigned between the retina and vitreous was varied in order to assess the effect of VR adhesion on retinal stress and strain. The iterations of the VR interaction were: (1) completely tied VR layer, (2) tied posterior and anterior VR boundaries with low friction (μ=0.1) at the equatorial VR layer, (3) tied posterior and anterior VR boundaries with high friction (μ=0.9) at the equatorial VR layer, and (4) high friction (μ=0.9) at the posterior and anterior VR layers with low friction (μ=0.1) at the equatorial VR layer.

The retina was subdivided into anterior, equatorial, and posterior sections for the analysis of regional stress and strain (Figure 106). The Lagrangian maximum principal strain and von Mises stress for all elements of the three regions was averaged at each time point for all model variations.

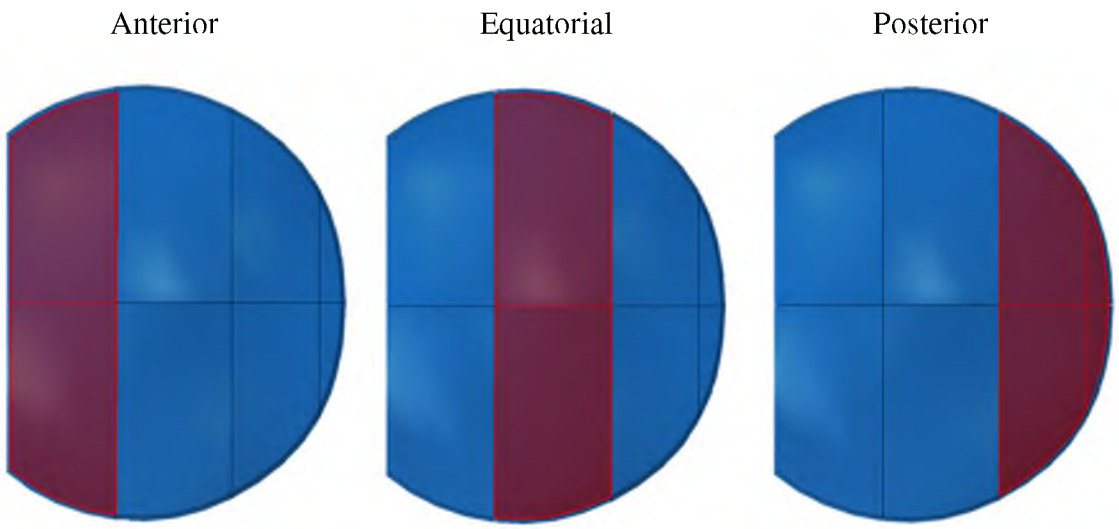

Figure 106: The retina was subdivided into anterior, equatorial, and posterior regions.

5.4 Results

5.4.1 Interaction effects

The first apparent spike in Figure 107 (t=0.25 s) represents the eye at full forward position and the second spike represents full backward position (t=0.75 s). The equatorial retina experienced the greatest stresses and strains in the single shake cycle simulations. The complete VR tie consistently produced the greatest stress and strain. However, varying the interaction parameter had little effect on the magnitude or distribution of stresses and strains experienced by all retinal regions. During the initial forward motion, the anterior retina experienced comparable stress and strain to the equatorial retina. During backward motion, the posterior retina experienced slightly higher stress than the anterior retina. Interestingly, the anterior retina experienced greater strain than the posterior retina during backward motion (Figure 107).

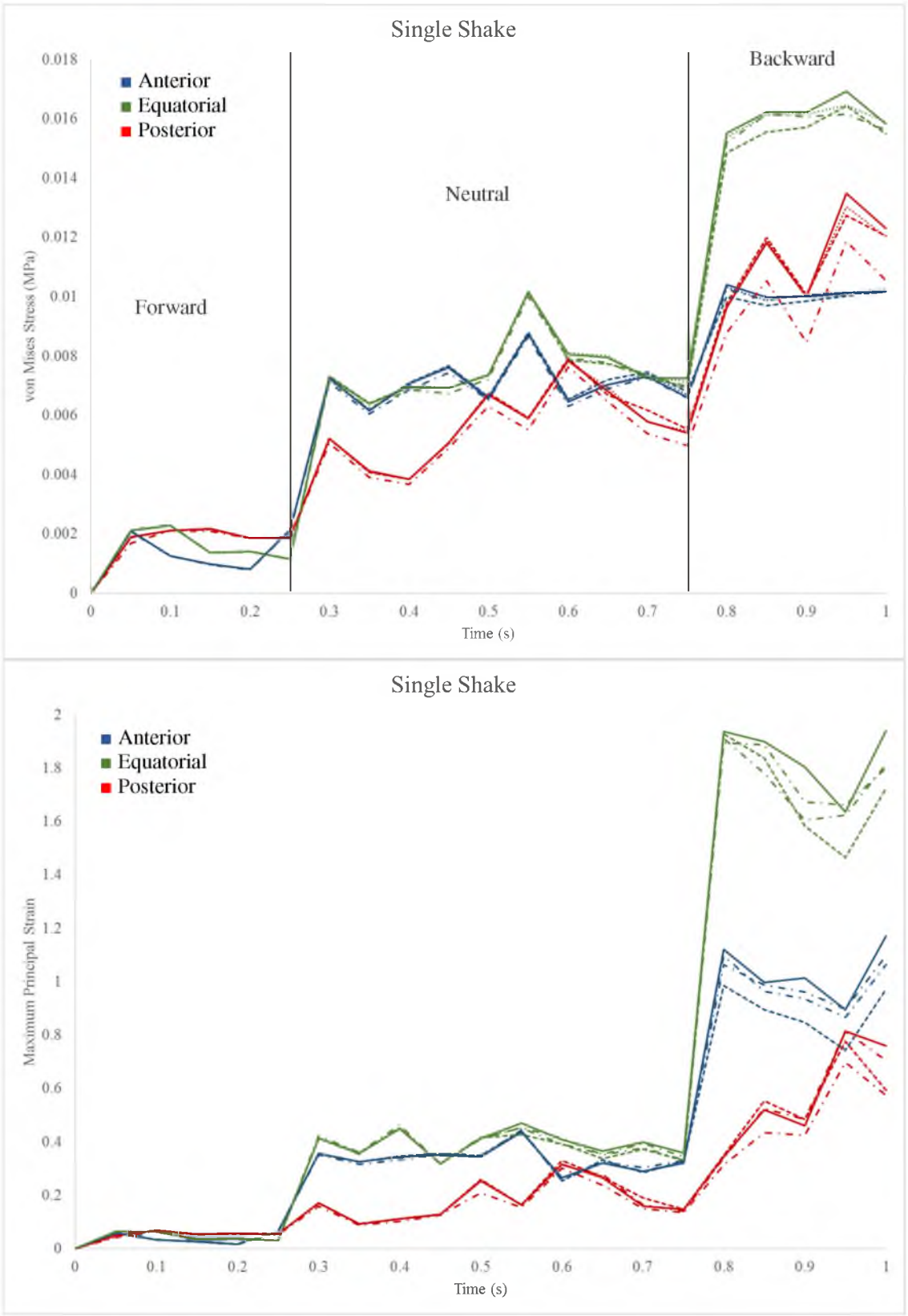

Figure 107: Average von Mises stress (top) and maximum principal strain (bottom) for the retinal regions for a single cycle of shaking.

5.4.2 Multiple shaking cycles

The difference in linestyle in Figure 107 represents the different vitreoretinal interactions implemented in the simulations. Because there was little variation between the interactions, only one VR interaction parameter was assessed for the multiple shaking cycles. The retinal stress and strain increased with the addition of rotation cycles. This may be attributed to the reverberation due to the nature of the prescribed rotation. Or, there may be a viscoelastic response from the retina that we have not yet mechanically characterized. As with the single shake, the equatorial retina experienced the greatest stresses and strains and this continued throughout all three cycles. The posterior retina also continued to have greater stress than the anterior retina during backward motion, and the anterior retina still experienced slightly higher strains than the posterior retina during backward motion (Figure 108).

5.5 Discussion

In general, the equatorial retina experienced the greatest von Mises stress and highest maximum principal strain. The anterior retina experienced slightly larger strain than the posterior retina during backward motion and with additional shake cycles. This is interesting when considering the strong attachment at the vitreous base, the most anterior VR periphery. Studies have also shown greater collagen content in this region of the VR interface.[7] The complete VR tie produced greater stresses and strains, but varying this interaction parameter minimally influenced the material response of the retina. True adhesion mechanics of the VR interface is unclear so caution should be made while interpreting this data. Different VR adhesion parameters should be explored in the future.

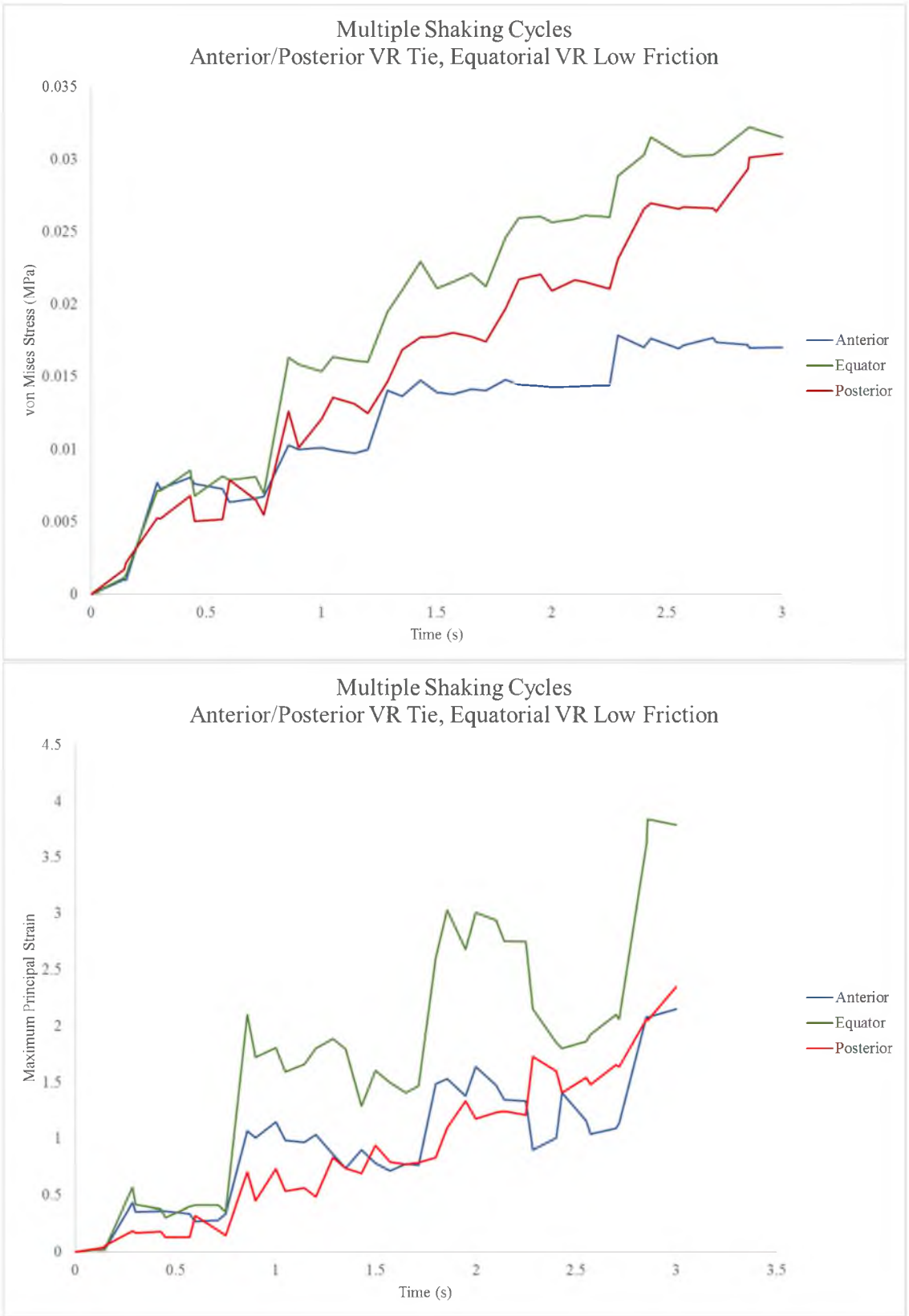

Figure 108: Average von Mises stress (top) and maximum principal strain (bottom) for the retinal regions for three cycles of shaking.

The inclusion of spring elements to connect the vitreous and retina may better simulate the presence and mechanics of collagen at the VR interface.

Rangarajan et al. assessed the von Mises stress during shaking for select retinal elements and showed maximum von Mises stresses of approximately 0.012 MPa and 0.003 MPa when using a viscoelastic solid or Newtonian fluid vitreous material model, respectively.[9] The peak von Mises stress for the anterior, equatorial, and posterior retina in our multishake simulation was, 0.017 MPa, 0.031 MPa, and 0.030 MPa, respectively. Although this is not a direct regional comparison, our findings were similar to those reported previously. As mentioned earlier, this group set out to examine the influence of vitreous and fat on retinal stress. After simulating a 5 Hz back and forth rotation of the eye, they found the vitreous to greatly affect the von Mises stress as the cycles increased. Modeling the vitreous as a viscoelastic solid material with a low bulk modulus resulted in a slight increase in retinal stress with repeated cycles, but this stress reached a steady state after 0.9 s. Representing the vitreous as a viscoelastic solid with a high bulk modulus did not increase stress with each cycle. Using a Newtonian fluid, however, to represent the vitreous did substantially increase stress with each cycle. Our results, simulating a 3 Hz rotation and utilizing only a solid viscoelastic material model for vitreous, showed a similar increasing stress trend with time. Interestingly, the bulk modulus in our vitreous material definition was approximately 0.03 which was roughly an order of ten lower than the minimum value used by Rangarajan et al. Our vitreous constitutive model was obtained through mechanical testing which we believe to accurately portray the mechanical influence on ocular kinematics. In the future, we would like to enhance the mesh of the vitreous and include the use of Eulerian elements to assess the difference in the

representative material mesh for vitreous.

Our current whole eye model is the first model to incorporate age appropriate properties. There are several limitations which will continue to be addressed in future models. These include incorporating an anatomically appropriate optic nerve head, the junction through which the retina transmits visual messages to the brain through the optic nerve. This is an extensively studied area of ocular computational modeling which we will research and develop age appropriate mechanical interactions at this location. We will also include more ocular tissues, such as the extraocular fat and muscles, to depict more accurate mechanics of the eye during a kinematic event.

The variation of VR interaction parameters in this study was a preliminary approach at understanding the changes in retinal stress and strain with simple changes at the VR interface. A study is currently underway in our lab to measure the peel force between retina and vitreous which will be an important contribution to defining VR adhesion in our model. Another study which will be conducted in our lab is the assessment of the collagen content and orientation at the VR interface. This will further add to our knowledge of the interaction between the retina and vitreous in an infant eye. This will also help us understand where there is a stronger presence in the infant VR interface which may complement our high stress and strain findings in the equatorial retina.

5.6 Conclusions

The current whole eye model assessed the retinal mechanics for simple loading conditions depicting shaking. We found VR interaction parameters to have minimal effect on retinal stress and strain. VR adhesion has yet to be mechanically characterized and the

inclusion of measured data will add to the utility of VR adhesion in predictions of RH. Importantly, our results may not be in the range of true retinal stresses and strains experienced with the inclusion of mechanically defined VR adhesion. We plan to simulate different traumatic scenarios, such as falls and blunt trauma. This will be beneficial in our understanding of differences in mechanisms of injury from accidental and abusive head trauma. Our ovine infant eye FE model is the first to incorporate age-dependent mechanical properties. This will serve as a base model for future refinement and investigations of pediatric ocular mechanics.

5.7 Acknowledgements

We would like to thank the Knights Templar Eye Foundation for sponsoring this work.

5.8 References

1. Boyce, B.L., Grazier, J.M., Jones, R.E., Nguyen, T.D., Full-field deformation of bovine cornea under constrained inflation conditions. Biomaterials, 2008. 29(28): p. 3896-3904.

2. Courdillier, B., Tian, J., Alexander, S., Myers, K.M., Quigley, H.A., Nguyen, T.D., Biomechanics of the human posterior sclera: age- and glaucoma-related changes measured using inflation testing. Investigative Ophthalmology & Visual Science, 2012. 53(4): p. 1714-1728.

3. Duhaime, A.C., Gennarelli, T.A., Thibault, L.E., Bruce, D.A., Margulies, S.S., Wiser, R. The shaken baby sundrome. A clinical, pathological, and biomechanical study. Journal of Neurosurgery, 1987. 66(3): p. 409-415.

4. Hans, S.A., Bawab, S.Y., Woodhouse, M.L., A finite element infant eye model to investigate retinal forces in shaken baby syndrome. Graefe's Archives for Clinical and Experimental Ophthalmology, 2009. 247(4): p. 561-571.

5. Levin, A.V., Retinal Hemorrhage in Abusive Head Trauma. Pediatrics, 2010. 126(5): p. 961-970.

6. Maguire, S.W., Watts, P.O., Shaw, A.D., Holden, S., Taylor, R.H., Watkins, W.J., Mann, M.K., Tempest, V., Kemp, A.M., Retinal haemorrhages and related findings in abusive and non-abusive head trauma: a systemic review. Eye, 2012. 27(1): p. 28-36.

7. Moran, P.R. (2012) Characterization of the vitreoretinal interface and vitreous in the porcine eye as it changes with age (Master's thesis). Retrieved from http://content.lib.utah.edu/cdm/ref/collection/etd3/id/1932

8. Myers, K.M., Courdillier, B., Boyce, B.L., Nguyen, T.D., The inflation response of the posterior bovine sclera. Acta Biomaterialia, 2010. 6(11): p. 4327-4335.

9. Rangarajan, N., Kamalakkhannan, S., Hasija, V., Shams, T., Jenny, C., Serbanescu, I., Ho, J., Rusinek, M., Levin, A., Finite element model of ocular injury in abusive head trauma. Journal of the American Association for Pediatric Ophthalmology and Stribismus, 2009. 13(4): p. 364-369.

CONCLUSIONS AND FUTURE WORK

The goal of this dissertation was to characterize the developmental changes in the mechanical properties of ocular tissues to implement age-appropriate constitutive models in a finite element (FE) model of the infant eye. To achieve this goal, we characterized the age- and rate-dependent material properties of the ovine sclera and retina. In preparation to collect human pediatric ocular specimens, a viable postmortem time frame and storage method was determined. The age-appropriate mechanical data were then used to identify appropriate constitutive models. To validate the FE model and constitutive relationship, scleral surface strains from ocular inflation were simulated and measured experimentally. Finally, all material data were incorporated into a whole eye finite element model to assess the changes in retinal stress and strain by varying the interaction parameter at the vitreoretinal interface.

Summary of Key Findings

Sclera material properties

Fresh, ovine sclera from preterm, infant, and adult human-equivalent ages were tested in uniaxial tension according to two strain-rate dependent protocols. The results show that younger aged sclera generally had greater Young's moduli than the adult sclera. The sclera is said to stiffen with age; however, we believe the reported anecdotal age-related stiffening can be attributed to an increase in structural rigidity with age. Regional

assessment shows that the anterior sclera was stiffer than the posterior sclera, which agrees with existing literature and the structural makeup of the regional sclera. Additionally, sclera tested at high strain-rates generally had higher material properties (E, σ_{ult}) from the pull-to-failure tests. The regional and strain-rate results from our study agree with the literature findings in adult sclera.

Retina material properties

Fresh, ovine retina from preterm, infant, and adult equivalent ages were tested in uniaxial tension according to two strain-dependent protocols. There was no significant age effect on retina, suggesting the retinal structure does not change with age. Retina tested at high strain-rates was significantly stiffer than retina tested at low strain-rates. These data suggest that the retina is sensitive to rate change and must be recognized when simulating traumatic scenarios.

Effect of postmortem time and storage condition

The effect of postmortem time and storage condition was assessed on the material properties of sclera and retina. Mature sclera can be stored up to 24 hours postmortem with no significant influence on the mechanical properties. Immature sclera, however, significantly softens after 10 hours postmortem. Fixation of sclera and retina significantly stiffened the tissue and confirms that this is not a suitable technique to preserve the mechanical integrity of ocular tissues. Freezing then thawing retina and sclera had minimal effect on their mechanical properties. These data suggest that freezing may be a viable shipping method for pediatric ocular specimens.

Eye inflation FE validation

The mechanical property data of retina and sclera were used to create a finite element model of the immature eye to simulate ocular inflation. The posterior sclera was found to be more extensible than the anterior sclera which agrees with existing literature and the mechanical inflation test findings. The FE inflation model successfully predicted scleral surface maximum principal strain. A majority of the direction specific FE strains were within the range of values from the experimental DIC analysis and linear regression models showed strong relationships between the model and experimental strains.

Whole eye model

All mechanical property data were integrated to create a FE model of the whole pediatric eye to simulate a shaking event. The sensitivity of retinal stress and strain to modifications in vitreoretinal (VR) adhesion was assessed in a single shake cycle simulation. A completely tied VR interaction parameter consistently produced the largest retinal stress and strain. However, varying the VR interaction only minimally affected the results. One interaction was implemented into a simulation representing repetitive head rotations. Stress and strain increased with the addition of shaking cycles. The posterior retina experienced greater stress than anterior retina during backward motion and subsequent shaking cycles. Future mechanical data characterizing VR adhesion implemented in the FE model will advance our understanding of mechanisms of RH.

Limitations and Future Work

The greatest limitation in this work was not gaining access to human specimens. As mentioned earlier, pediatric ocular tissues are difficult to obtain. We remain on multiple waitlists to receive pediatric ocular specimens and plan to mechanically characterize any tissue that becomes available. Until that time, we will continue to fully characterize the material properties of pediatric ocular tissues from other species.

We originally planned to test the mechanical properties of the optic nerve which proved to be more problematic than expected. The optic nerve has a tubular core covered by an external sheath. Clamping the optic nerve without breaking it was challenging, and the outer sheath pulled off of the core during a tensile test. A new clamp design or a different material test may enhance measurements of the optic nerve. We collected a limited amount of data which were not included in this work but will be implemented when we add this component to future FE models.

The retina was also a challenging tissue as it is a delicate membrane and difficult to dissect and handle. We would like to conduct additional retinal tests to increase our sample size which will also allow for assessing anisotropic material properties of the immature retina. We have initiated this study by capturing the vessel composition and orientation using an optical microscope. Furthermore, it would be useful to incorporate a micro-scale measurement of the retina, such as the atomic force microscopy (AFM), to compare to our retinal results. We assumed a Poisson's ratio for the sclera and retina. In the future, we could utilize digital image correlation to track out-of-plane deformations of our tissue. It would also be interesting to record tissue deformation under a microscope to visualize retinal vasculature and scleral fiber orientation during tensile testing.

We encountered drift noise during stress-relaxation testing at a low strain level which was not reported in this work. Enhanced signal conditioning and processing should be explored to avoid this in the future.

Our current whole eye FE model is a simplified ocular anatomy. We hope to incorporate more ocular tissues such as extraocular fat and muscle for a more complete model. Basic interaction parameters were assumed between the retina and vitreous in this FE model. Experimental studies are currently underway in our lab to test the peel force between the retina and vitreous, which can then be utilized to define vitreoretinal adhesion. Furthermore, we will be imaging the collagen density and direction at the vitreoretinal interface to include in the computational model. In the future, we would like to simulate various shaking scenarios as well as different traumatic events to analyze the retinal stress and strain from a range of kinematic loading scenarios. One long-term goal of this work would be to incorporate our infant eye model into an overall head model in conjunction with previous and current skull and brain models.

APPENDIX A

MATLAB CODE FOR LOADING DATA

```
% LOAD DATA

%%% Columns 1:6
%%% [time(s) load(N) RawData(Mpa) Extension(mm) Strain(%) Strain(mm/mm)]

%%% Row 1, Column 7
%%% thickness or diameter(mm)

%%% Row 2, Column 7
%%% Age - Pre 11; Infant 12; Mature 13; 14 Adolescent

%%% Row 3, Column 7
%%% Region - Ant 21; Post 22; ? 23; Para 24; Perp 25; None 26; NA 27

%%% Row 4, Column 7
%%% Condition - Fresh 31; Frozen 32; Fixed 33

%%% Row 5, Column 7
%%% Condition - Sclera 41; Retina 42; OpN 43

%%% Row 6, Column 7
%%% Strain - Hi 51; Lo 52

%% RUN THIS EVERY TIME!!

close all; clear; clc
load RawData.mat


% %% Loaded in 11/12/13
% RawData{1} = xlsread('Ovine Sclera Relaxation.xlsx', '3-4-13', 'A17:F11493');
% RawData{1}(1:6,7) = [.674;11;23;31;41;51];
% RawData{2} = xlsread('Ovine Sclera Relaxation.xlsx', '3-4-13', 'J17:O13881');
% RawData{2}(1:6,7) =[.6389;11;23;31;41;51];
% RawData{3} = xlsread('Ovine Sclera Relaxation.xlsx', '3-4-13', 'S17:X12767');
% RawData{3}(1:6,7) =[.8543;11;23;31;41;51];
% RawData{4} = xlsread('Ovine Sclera Relaxation.xlsx', '3-4-13', 'AB17:AG12714');
% RawData{4}(1:6,7) =[.8158;11;23;31;41;51];
%
% RawData{5} = xlsread('Ovine Sclera Relaxation.xlsx', '3-5-13', 'A17:F12778');
% RawData{5}(1:6,7) =[.858;11;23;31;41;51];
% RawData{6} = xlsread('Ovine Sclera Relaxation.xlsx', '3-5-13', 'J17:O12640');
% RawData{6}(1:6,7) =[.7028;11;23;31;41;51];
% RawData{7} = xlsread('Ovine Sclera Relaxation.xlsx', '3-5-13', 'S17:X12573');
% RawData{7}(1:6,7) =[.9136;11;23;31;41;51];
% RawData{8} = xlsread('Ovine Sclera Relaxation.xlsx', '3-5-13', 'AB17:AG13017');
```

```
% RawData{8}(1:6,7) =[1.0997;11;23;31;41;51];
%
% RawData{9} = xlsread('Ovine Sclera Relaxation.xlsx', '3-20-13', 'A17:F10605');
% RawData{9}(1:6,7) =[.7532;11;23;31;41;51];
% RawData{10} = xlsread('Ovine Sclera Relaxation.xlsx', '3-20-13', 'J17:O10598');
% RawData{10}(1:6,7) =[1.0715;11;23;31;41;51];
% RawData{11} = xlsread('Ovine Sclera Relaxation.xlsx', '3-20-13', 'S17:X10598');
% RawData{11}(1:6,7) =[.6129;11;23;31;41;51];
% RawData{12} = xlsread('Ovine Sclera Relaxation.xlsx', '3-20-13', 'AB17:AG10598');
% RawData{12}(1:6,7) =[.4762;11;23;31;41;51];
%
% RawData{13} = xlsread('Ovine Sclera Relaxation.xlsx', '4-4-13', 'A17:F10599');
% RawData{13}(1:6,7) =[.4839;11;23;31;41;51];
% RawData{14} = xlsread('Ovine Sclera Relaxation.xlsx', '4-4-13', 'J17:O10601');
% RawData{14}(1:6,7) =[.9008;11;23;31;41;51];
%
% RawData{15} = xlsread('Ovine Sclera Relaxation.xlsx', '4-15-13', 'A17:F10598');
% RawData{15}(1:6,7) =[.56;11;23;31;41;51];
% RawData{16} = xlsread('Ovine Sclera Relaxation.xlsx', '4-15-13', 'J17:O10612');
% RawData{16}(1:6,7) =[.6845;11;23;31;41;51];
% RawData{17} = xlsread('Ovine Sclera Relaxation.xlsx', '4-15-13', 'S17:X10604');
% RawData{17}(1:6,7) =[.5881;11;23;31;41;51];
% RawData{18} = xlsread('Ovine Sclera Relaxation.xlsx', '4-15-13', 'AB17:AG10617');
% RawData{18}(1:6,7) =[.6903;11;23;31;41;51];
%
% RawData{19} = xlsread('Ovine Sclera Relaxation.xlsx', '4-17-13', 'A17:F10598');
% RawData{19}(1:6,7) =[.6785;12;23;31;41;51];
% RawData{20} = xlsread('Ovine Sclera Relaxation.xlsx', '4-17-13', 'J17:O10617');
% RawData{20} = xlsread('Scleral Retests Compared to Originals.xlsx', '4-17-13 (20)',
'A10:F135');
% RawData{20}(1:6,7) =[.9606;12;23;31;41;51];
%
% RawData{21} = xlsread('Ovine Sclera Relaxation.xlsx', '4-18-13', 'A17:F10617');
% RawData{21}(1:6,7) =[.3452;12;21;31;41;51];
% RawData{22} = xlsread('Ovine Sclera Relaxation.xlsx', '4-18-13', 'J17:O10617');
% RawData{22}(1:6,7) =[1.2727;12;22;31;41;51];
% RawData{23} = xlsread('Ovine Sclera Relaxation.xlsx', '4-18-13', 'S17:X10601');
% RawData{23} = xlsread('Scleral Retests Compared to Originals.xlsx', '4-18-13 (23)',
'A10:F40');
% RawData{23}(1:6,7) =[.7652;12;22;31;41;51];
% RawData{24} = xlsread('Ovine Sclera Relaxation.xlsx', '4-18-13', 'AB17:AG10598');
% RawData{24}(1:6,7) =[.4954;12;21;31;41;51];
% RawData{25} = xlsread('Ovine Sclera Relaxation.xlsx', '4-18-13', 'AK17:AP10617');
% RawData{25}(1:6,7) =[1.018;12;22;31;41;51];
% RawData{26} = xlsread('Ovine Sclera Relaxation.xlsx', '4-18-13', 'AT17:AY10617');
% RawData{26}(1:6,7) =[.7533;12;21;31;41;51];
```

```
%
% RawData{27} = xlsread('Ovine Sclera Relaxation.xlsx', '5-6-13', 'A17:F10598');
% RawData{27}(1:6,7) =[.754;11;22;31;41;51];
% RawData{28} = xlsread('Ovine Sclera Relaxation.xlsx', '5-6-13', 'J17:O10617');
% RawData{28}(1:6,7) =[.3998;11;21;31;41;51];
% RawData{29} = xlsread('Ovine Sclera Relaxation.xlsx', '5-6-13', 'S17:X10604');
% RawData{29}(1:6,7) =[.3366;11;21;31;41;51];
% RawData{30} = xlsread('Ovine Sclera Relaxation.xlsx', '5-6-13', 'AB17:AG10598');
% RawData{30}(1:6,7) =[.5218;11;22;31;41;51];
%
% RawData{31} = xlsread('Ovine Sclera Relaxation.xlsx', '5-9-13', 'A17:F11926');
% RawData{31}(1:6,7) =[.4945;11;22;31;41;51];
% RawData{32} = xlsread('Ovine Sclera Relaxation.xlsx', '5-9-13', 'J17:O11258');
% RawData{32}(1:6,7) =[.3437;11;21;31;41;51];
% RawData{33} = xlsread('Ovine Sclera Relaxation.xlsx', '5-9-13', 'S17:X11780');
% RawData{33}(1:6,7) =[.3782;11;21;31;41;51];
% RawData{34} = xlsread('Ovine Sclera Relaxation.xlsx', '5-9-13', 'AB17:AG11204');
% RawData{34} = xlsread('Scleral Retests Compared to Originals.xlsx', '5-9-13 (34)',
'A10:F148');
% RawData{34}(1:6,7) =[.7071;11;22;31;41;51];
% RawData{35} = xlsread('Ovine Sclera Relaxation.xlsx', '5-9-13', 'AK17:AP12275');
% RawData{35}(1:6,7) =[.733;11;22;31;41;51];
% RawData{36} = xlsread('Ovine Sclera Relaxation.xlsx', '5-9-13', 'AT17:AY11152');
% RawData{36}(1:6,7) =[.3774;11;21;31;41;51];
% RawData{37} = xlsread('Ovine Sclera Relaxation.xlsx', '5-9-13', 'BC17:BH12544');
% RawData{37}(1:6,7) =[.588;11;22;31;41;51];
% RawData{38} = xlsread('Ovine Sclera Relaxation.xlsx', '5-9-13', 'BL17:BQ11484');
% RawData{38}(1:6,7) =[.3437;11;21;31;41;51];
%
% RawData{39} = xlsread('Ovine Sclera Relaxation.xlsx', '5-10-13', 'A17:F11999');
% RawData{39}(1:6,7) =[.9631;13;21;31;41;51];
% RawData{40} = xlsread('Ovine Sclera Relaxation.xlsx', '5-10-13', 'J17:O11033');
% RawData{40} = xlsread('Scleral Retests Compared to Originals.xlsx', '5-10-13 (40)',
'A10:F162');
% RawData{40}(1:6,7) =[1.9569;13;22;31;41;51];
% RawData{41} = xlsread('Ovine Sclera Relaxation.xlsx', '5-10-13', 'S17:X12056');
% RawData{41}(1:6,7) =[.6677;13;21;31;41;51];
% RawData{42} = xlsread('Ovine Sclera Relaxation.xlsx', '5-10-13', 'AB17:AG10876');
% RawData{42}(1:6,7) =[1.7867;13;22;31;41;51];
%
% RawData{43} = xlsread('Ovine Sclera Relaxation.xlsx', '5-13-13', 'A17:F10882');
% RawData{43}(1:6,7) =[1.5264;13;22;31;41;51];
% RawData{44} = xlsread('Ovine Sclera Relaxation.xlsx', '5-13-13', 'J17:O10996');
% RawData{44}(1:6,7) =[1.0018;13;21;31;41;51];
% RawData{45} = xlsread('Ovine Sclera Relaxation.xlsx', '5-13-13', 'S17:X11576');
% RawData{45}(1:6,7) =[.7118;13;21;31;41;51];
```

```
% RawData{46} = xlsread('Ovine Sclera Relaxation.xlsx', '5-13-13', 'AB17:AG10912');
% RawData{46}(1:6,7) =[2.3137;13;22;31;41;51];
% RawData{47} = xlsread('Ovine Sclera Relaxation.xlsx', '5-13-13', 'AK17:AP10814');
% RawData{47}(1:6,7) =[2.165;13;22;31;41;51];
%
% RawData{48} = xlsread('Ovine Sclera Relaxation.xlsx', '5-14-13', 'A17:F12917');
% RawData{48}(1:6,7) =[1.2139;12;22;31;41;51];
% RawData{49} = xlsread('Ovine Sclera Relaxation.xlsx', '5-14-13', 'J17:O11498');
% RawData{49}(1:6,7) =[.733;12;21;31;41;51];
% RawData{50} = xlsread('Ovine Sclera Relaxation.xlsx', '5-14-13', 'S17:X11693');
% RawData{50}(1:6,7) =[.7338;12;21;31;41;51];
% RawData{51} = xlsread('Ovine Sclera Relaxation.xlsx', '5-14-13', 'AB17:AG12426');
% RawData{51} = xlsread('Scleral Retests Compared to Originals.xlsx', '5-14-13 (51)',
'A10:F101');
% RawData{51}(1:6,7) =[1.47;12;22;31;41;51];
%
% RawData{52} = xlsread('Ovine Sclera Relaxation.xlsx', '5-15-13', 'A17:F13602');
% RawData{52}(1:6,7) =[1.2535;12;22;31;41;51];
% RawData{53} = xlsread('Ovine Sclera Relaxation.xlsx', '5-15-13', 'J17:O11573');
% RawData{53}(1:6,7) =[.4206;12;21;31;41;51];
% RawData{54} = xlsread('Ovine Sclera Relaxation.xlsx', '5-15-13', 'S17:X13446');
% RawData{54}(1:6,7) =[1.1603;12;22;31;41;51];
% RawData{55} = xlsread('Ovine Sclera Relaxation.xlsx', '5-15-13', 'AB17:AG11808');
% RawData{55}(1:6,7) =[.4413;12;21;31;41;51];
%
% RawData{56} = xlsread('Ovine Sclera Relaxation.xlsx', '5-16-13', 'A17:F11845');
% RawData{56}(1:6,7) =[.9259;11;22;31;41;51];
% RawData{57} = xlsread('Ovine Sclera Relaxation.xlsx', '5-16-13', 'J17:O10990');
% RawData{57}(1:6,7) =[.3725;11;21;31;41;51];
% RawData{58} = xlsread('Ovine Sclera Relaxation.xlsx', '5-16-13', 'S17:X11236');
% RawData{58}(1:6,7) =[.4243;11;21;31;41;51];
% RawData{59} = xlsread('Ovine Sclera Relaxation.xlsx', '5-16-13', 'AB17:AG12441');
% RawData{59}(1:6,7) =[.8452;11;22;31;41;51];
% RawData{60} = xlsread('Ovine Sclera Relaxation.xlsx', '5-16-13', 'AK17:AP12395');
% RawData{60}(1:6,7) =[1.0184;11;22;31;41;51];
% RawData{61} = xlsread('Ovine Sclera Relaxation.xlsx', '5-16-13', 'AT17:AY11067');
% RawData{61}(1:6,7) =[.311;11;21;31;41;51];
% RawData{62} = xlsread('Ovine Sclera Relaxation.xlsx', '5-16-13', 'BC17:BH12033');
% RawData{62}(1:6,7) =[.999;11;22;31;41;51];
% RawData{63} = xlsread('Ovine Sclera Relaxation.xlsx', '5-16-13', 'BL17:BQ11284');
% RawData{63}(1:6,7) =[.4022;11;21;31;41;51];
% RawData{64} = xlsread('Ovine Sclera Relaxation.xlsx', '5-16-13', 'BU17:BZ10854');
% RawData{64}(1:6,7) =[2.2898 ;13;22;31;41;51];
% RawData{65} = xlsread('Ovine Sclera Relaxation.xlsx', '5-16-13', 'CD17:CI11552');
% RawData{65}(1:6,7) =[0.9052 ;13;21;31;41;51];
% RawData{66} = xlsread('Ovine Sclera Relaxation.xlsx', '5-16-13', 'CM17:CR10918');
```

```
% RawData{66}(1:6,7) =[1.1092 ;13;21;31;41;51];
% RawData{67} = xlsread('Ovine Sclera Relaxation.xlsx', '5-16-13', 'CV17:DB10812');
% RawData{67}(1:6,7) =[2.2641 ;13;22;31;41;51];
%
% RawData{68} = xlsread('Ovine Sclera Relaxation.xlsx', '5-17-13', 'A17:F12436');
% RawData{68}(1:6,7) =[1.0754;11;22;31;41;51];
% RawData{69} = xlsread('Ovine Sclera Relaxation.xlsx', '5-17-13', 'J17:O11263');
% RawData{69}(1:6,7) =[.4596;11;21;31;41;51];
% RawData{70} = xlsread('Ovine Sclera Relaxation.xlsx', '5-17-13', 'S17:X11502');
% RawData{70}(1:6,7) =[1.0008;11;22;31;41;51];
% RawData{71} = xlsread('Ovine Sclera Relaxation.xlsx', '5-17-13', 'AB17:AG11169');
% RawData{71}(1:6,7) =[.3441;11;21;31;41;51];
% RawData{72} = xlsread('Ovine Sclera Relaxation.xlsx', '5-17-13', 'AK17:AP11640');
% RawData{72}(1:6,7) =[.9182;11;22;31;41;51];
% RawData{73} = xlsread('Ovine Sclera Relaxation.xlsx', '5-17-13', 'AT17:AY10881');
% RawData{73}(1:6,7) =[.3436;11;21;31;41;51];
% RawData{74} = xlsread('Ovine Sclera Relaxation.xlsx', '5-17-13', 'BC17:BH12113');
% RawData{74}(1:6,7) =[1.141;11;22;31;41;51];
% RawData{75} = xlsread('Ovine Sclera Relaxation.xlsx', '5-17-13', 'BL17:BQ11155');
% RawData{75}(1:6,7) =[.4018;11;21;31;41;51];
%
% RawData{76} = xlsread('Ovine Sclera Relaxation.xlsx', '5-18-13', 'A17:F11411');
% RawData{76}(1:6,7) =[0.6112;11;22;31;41;51];
% RawData{77} = xlsread('Ovine Sclera Relaxation.xlsx', '5-18-13', 'J17:O10987');
% RawData{77}(1:6,7) =[.216;11;21;31;41;51];
% RawData{78} = xlsread('Ovine Sclera Relaxation.xlsx', '5-18-13', 'S17:X11903');
% RawData{78}(1:6,7) =[1.0703;11;22;31;41;51];
% RawData{79} = xlsread('Ovine Sclera Relaxation.xlsx', '5-18-13', 'AB17:AG11418');
% RawData{79}(1:6,7) =[.3685;11;21;31;41;51];
% RawData{80} = xlsread('Ovine Sclera Relaxation.xlsx', '5-18-13', 'AK17:AP11026');
% RawData{80}(1:6,7) =[1.6485;13;22;31;41;51];
% RawData{81} = xlsread('Ovine Sclera Relaxation.xlsx', '5-18-13', 'AT17:AY11320');
% RawData{81}(1:6,7) =[.8015;13;21;31;41;51];
% RawData{82} = xlsread('Ovine Sclera Relaxation.xlsx', '5-18-13', 'BC17:BH10927');
% RawData{82}(1:6,7) =[1.0058;13;21;31;41;51];
% RawData{83} = xlsread('Ovine Sclera Relaxation.xlsx', '5-18-13', 'BL17:BQ10864');
% RawData{83}(1:6,7) =[1.7947;13;22;31;41;51];
%
% RawData{84} = xlsread('Ovine Sclera Relaxation.xlsx', '5-21-13', 'A17:F10685');
% RawData{84}(1:6,7) =[0.9483;11;22;31;41;51];
% RawData{85} = xlsread('Ovine Sclera Relaxation.xlsx', '5-21-13', 'J17:O10658');
% RawData{85}(1:6,7) =[.3723;11;21;31;41;51];
% RawData{86} = xlsread('Ovine Sclera Relaxation.xlsx', '5-21-13', 'S17:X10712');
% RawData{86}(1:6,7) =[.3815;11;21;31;41;51];
% RawData{87} = xlsread('Ovine Sclera Relaxation.xlsx', '5-21-13', 'AB17:AG10656');
% RawData{87}(1:6,7) =[1.1386;11;22;31;41;51];
```

```
% RawData{88} = xlsread('Ovine Sclera Relaxation.xlsx', '5-21-13', 'AK17:AP10731');
% RawData{88}(1:6,7) =[1.364;13;21;31;41;51];
% RawData{89} = xlsread('Ovine Sclera Relaxation.xlsx', '5-21-13', 'AT17:AY10776');
% RawData{89}(1:6,7) =[2.1396;13;22;31;41;51];
% RawData{90} = xlsread('Ovine Sclera Relaxation.xlsx', '5-21-13', 'BC17:BH10782');
% RawData{90}(1:6,7) =[1.9211;13;22;31;41;51];
% RawData{91} = xlsread('Ovine Sclera Relaxation.xlsx', '5-21-13', 'BL17:BQ10771');
% RawData{91}(1:6,7) =[1.277;13;21;31;41;51];
%
% RawData{92} = xlsread('Ovine Sclera Relaxation.xlsx', '5-22-13', 'A17:F11052');
% RawData{92}(1:6,7) =[.9295;13;21;31;41;51];
% RawData{93} = xlsread('Ovine Sclera Relaxation.xlsx', '5-22-13', 'J17:O11218');
% RawData{93}(1:6,7) =[2.941;13;22;31;41;51];
% RawData{94} = xlsread('Ovine Sclera Relaxation.xlsx', '5-22-13', 'S17:X11698');
% RawData{94}(1:6,7) =[1.0936;13;21;31;41;51];
% RawData{95} = xlsread('Ovine Sclera Relaxation.xlsx', '5-22-13', 'AB17:AG11462');
% RawData{95}(1:6,7) =[2.1362;13;22;31;41;51];
%
% RawData{96} = xlsread('Ovine Sclera Relaxation.xlsx', '6-4-13', 'A17:F11017');
% RawData{96}(1:6,7) =[1.0666;11;22;31;41;51];
% RawData{97} = xlsread('Ovine Sclera Relaxation.xlsx', '6-4-13', 'J17:O11015');
% RawData{97}(1:6,7) =[.7044;11;21;31;41;51];
% RawData{98} = xlsread('Ovine Sclera Relaxation.xlsx', '6-4-13', 'S17:X11002');
% RawData{98}(1:6,7) =[.9612;11;22;31;41;51];
% RawData{99} = xlsread('Ovine Sclera Relaxation.xlsx', '6-4-13', 'AB17:AG11017');
% RawData{99}(1:6,7) =[0.3796;11;21;31;41;51];
% RawData{100} = xlsread('Ovine Sclera Relaxation.xlsx', '6-4-13', 'AK17:AP10998');
% RawData{100}(1:6,7) =[2.3274;13;22;31;41;51];
% RawData{101} = xlsread('Ovine Sclera Relaxation.xlsx', '6-4-13', 'AT17:AY10999');
% RawData{101}(1:6,7) =[.7112;13;21;31;41;51];
% RawData{102} = xlsread('Ovine Sclera Relaxation.xlsx', '6-4-13', 'BC17:BH11017');
% RawData{102}(1:6,7) =[1.4954;13;22;31;41;51];
% RawData{103} = xlsread('Ovine Sclera Relaxation.xlsx', '6-4-13', 'BL17:BQ10906');
% RawData{103}(1:6,7) =[.9785;13;21;31;41;51];
%
% RawData{104} = xlsread('Ovine Sclera Relaxation.xlsx', '6-15-13', 'A17:F11047');
% RawData{104}(1:6,7) =[.80814;13;21;31;41;51];
% RawData{105} = xlsread('Ovine Sclera Relaxation.xlsx', '6-15-13', 'J17:O10841');
% RawData{105}(1:6,7) =[2.5011;13;22;31;41;51];
% RawData{106} = xlsread('Ovine Sclera Relaxation.xlsx', '6-15-13', 'S17:X10935');
% RawData{106}(1:6,7) =[.6685;13;21;31;41;51];
%
% RawData{107} = xlsread('Ovine Sclera Relaxation.xlsx', '6-25-13', 'A17:F10732');
% RawData{107}(1:6,7) =[.81605;11;22;31;41;51];
% RawData{108} = xlsread('Ovine Sclera Relaxation.xlsx', '6-25-13', 'J17:O11047');
% RawData{108}(1:6,7) =[.3316;11;21;31;41;51];
```

```
% RawData{109} = xlsread('Ovine Sclera Relaxation.xlsx', '6-25-13', 'S17:X10693');
% RawData{109}(1:6,7) =[.4661;11;21;31;41;51];
% RawData{110} = xlsread('Ovine Sclera Relaxation.xlsx', '6-25-13', 'AB17:AG10769');
% RawData{110}(1:6,7) =[1.0627;11;22;31;41;51];
% RawData{111} = xlsread('Ovine Sclera Relaxation.xlsx', '6-25-13', 'AK17:AP10749');
% RawData{111}(1:6,7) =[0.3576;11;21;31;41;51];
% RawData{112} = xlsread('Ovine Sclera Relaxation.xlsx', '6-25-13', 'AT17:AY10871');
% RawData{112}(1:6,7) =[1.0512;11;22;31;41;51];
% RawData{113} = xlsread('Ovine Sclera Relaxation.xlsx', '6-25-13', 'BC17:BH11065');
% RawData{113}(1:6,7) =[.4282;11;21;31;41;51];
% RawData{114} = xlsread('Ovine Sclera Relaxation.xlsx', '6-25-13', 'BL17:BQ10755');
% RawData{114}(1:6,7) =[1.1975;12;22;31;41;51];
% RawData{115} = xlsread('Ovine Sclera Relaxation.xlsx', '6-25-13', 'BU17:BZ10859');
% RawData{115}(1:6,7) =[0.3763 ;12;21;31;41;51];
% RawData{116} = xlsread('Ovine Sclera Relaxation.xlsx', '6-25-13', 'CD17:CI10746');
% RawData{116}(1:6,7) =[1.2533 ;12;22;31;41;51];
% RawData{117} = xlsread('Ovine Sclera Relaxation.xlsx', '6-25-13', 'CM17:CR10790');
% RawData{117}(1:6,7) =[.4047 ;12;21;31;41;51];
%
% %%% Started using pneumatic, submersible grips
% RawData{118} = xlsread('Ovine Sclera Relaxation.xlsx', '7-20-13', 'A17:F10622');
% RawData{118} = xlsread('Scleral Retests Compared to Originals.xlsx', '7-20-13 (118)',
'A10:F216');
% RawData{118}(1:6,7) =[1.7943;12;22;31;41;51];
% RawData{119} = xlsread('Ovine Sclera Relaxation.xlsx', '7-20-13', 'J17:O10627');
% RawData{119}(1:6,7) =[0.4282;12;21;31;41;51];
% RawData{120} = xlsread('Ovine Sclera Relaxation.xlsx', '7-20-13', 'S17:X10966');
% RawData{120}(1:6,7) =[1.8312;12;22;31;41;51];
% RawData{121} = xlsread('Ovine Sclera Relaxation.xlsx', '7-20-13', 'AB17:AG11065');
% RawData{121}(1:6,7) =[0.3614;12;21;31;41;51];
%
% %%% Back to old grips
% RawData{122} = xlsread('Ovine Sclera Relaxation.xlsx', '7-26-13', 'A17:F11065');
% RawData{122}(1:6,7) =[1.4942;14;22;31;41;51];
% RawData{123} = xlsread('Ovine Sclera Relaxation.xlsx', '7-26-13', 'J17:O10788');
% RawData{123}(1:6,7) =[0.4478;14;21;31;41;51];
% RawData{124} = xlsread('Ovine Sclera Relaxation.xlsx', '7-26-13', 'S17:X10819');
% RawData{124}(1:6,7) =[1.1884;14;22;31;41;51];
% RawData{125} = xlsread('Ovine Sclera Relaxation.xlsx', '7-26-13', 'AB17:AG10705');
% RawData{125}(1:6,7) =[0.5379;14;21;31;41;51];
%
% %%% Retina and optic nerve data from earlier
% RawData{126} = xlsread('High_Retina.OpN.xlsx', '5-18-13', 'A17:F10738');
% RawData{126}(1:6,7) =[0.1356;11;24;31;42;51];
% RawData{127} = xlsread('High_Retina.OpN.xlsx', '5-18-13', 'J17:O10999');
% RawData{127}(1:6,7) =[0.1523;11;26;31;42;51];
```

```
% RawData{128} = xlsread('High_Retina.OpN.xlsx', '5-18-13', 'S17:X11012');
% RawData{128}(1:6,7) =[1.1182;13;24;31;42;51];
% RawData{129} = xlsread('High_Retina.OpN.xlsx', '5-18-13', 'AB17:AG10897');
% RawData{129}(1:6,7) =[0.1512;13;24;31;42;51];
%
% %%% Switching to low strain (mainly) testing
% RawData{130} = xlsread('High_Retina.OpN.xlsx', '5-20-13', 'A17:F10651');
% RawData{130}(1:6,7) =[0.1241;11;24;31;42;51];
% RawData{131} = xlsread('High_Retina.OpN.xlsx', '5-20-13', 'J17:O10665');
% RawData{131}(1:6,7) =[0.0878;11;24;31;42;51];
% RawData{132} = xlsread('High_Retina.OpN.xlsx', '5-20-13', 'S17:X10774');
% RawData{132}(1:6,7) =[0.1485;13;24;31;42;51];
% RawData{133} = xlsread('High_Retina.OpN.xlsx', '5-20-13', 'AB17:AG10662');
% RawData{133}(1:6,7) =[0.2093;13;26;31;42;51];
%
% RawData{134} = xlsread('High_Retina.OpN.xlsx', '5-22-13', 'A17:F10897');
% RawData{134}(1:6,7) =[0.1525;13;26;31;42;51];
%
% RawData{135} = xlsread('High_Retina.OpN.xlsx', '6-25-13', 'A17:F10704');
% RawData{135}(1:7,7) =[2.6587;12;27;31;43;51;6];
% RawData{136} = xlsread('High_Retina.OpN.xlsx', '6-25-13', 'J17:O10742');
% RawData{136}(1:7,7) =[2.5495;12;27;31;43;51;3];
%
% RawData{137} = xlsread('High_Retina.OpN.xlsx', '7-20-13', 'A17:F10711');
%  RawData{137}(1:7,7) =[1.7943;12;27;31;43;51;6];
%
% RawData{138} = xlsread('Fresh Ovine_JMS_2.xlsx', '08-22-13', 'A17:F12660');
% RawData{138}(1:6,7) =[0.1991;13;25;31;42;52];
% RawData{139} = xlsread('Fresh Ovine_JMS_2.xlsx', '08-22-13', 'J17:O12710');
% RawData{139}(1:6,7) =[0.7685;13;21;31;41;52];
% RawData{140} = xlsread('Fresh Ovine_JMS_2.xlsx', '08-22-13', 'S17:X12128');
% RawData{140}(1:6,7) =[2.1424;13;22;31;41;52];
% RawData{141} = xlsread('Fresh Ovine_JMS_2.xlsx', '08-22-13', 'AB17:AG10905');
% RawData{141}(1:6,7) =[0.7417;13;21;31;41;52];
%
% RawData{142} = xlsread('Fresh Ovine_JMS_2.xlsx', '08-27-13', 'A17:F11487');
% RawData{142}(1:6,7) =[2.1435;13;22;31;41;52];
% RawData{143} = xlsread('Fresh Ovine_JMS_2.xlsx', '08-27-13', 'J17:O10780');
% RawData{143}(1:6,7) =[0.4238;11;21;31;41;52];
% RawData{144} = xlsread('Fresh Ovine_JMS_2.xlsx', '08-27-13', 'S17:X11486');
% RawData{144}(1:6,7) =[0.7015;11;22;31;41;52];
% RawData{145} = xlsread('Fresh Ovine_JMS_2.xlsx', '08-27-13', 'AB17:AG11094');
% RawData{145} = xlsread('Scleral Retests Compared to Originals.xlsx', '8-27-13 (145)',
'A10:F305');
% RawData{145}(1:6,7) =[0.2952;11;21;31;41;52];
%
```

```
% RawData{146} = xlsread('Fresh Ovine_JMS_2.xlsx', '09-04-13', 'A17:F6181');
% RawData{146}(1:6,7) =[0.1715;13;25;31;42;52];
% RawData{147} = xlsread('Fresh Ovine_JMS_2.xlsx', '09-04-13', 'J17:O8475');
% RawData{147}(1:6,7) =[0.2079;13;25;31;42;52];
% RawData{148} = xlsread('Fresh Ovine_JMS_2.xlsx', '09-04-13', 'S17:X2579');
% RawData{148}(1:6,7) =[0.2156;13;24;31;42;52];
% RawData{149} = xlsread('Fresh Ovine_JMS_2.xlsx', '09-04-13', 'AB17:AG6143');
% RawData{149}(1:6,7) =[0.1884;11;25;31;42;52];
%
% RawData{150} = xlsread('Fresh Ovine_JMS_2.xlsx', '09-05-13', 'A17:F1914');
% RawData{150}(1:6,7) =[0.4815;11;21;31;41;52];
% RawData{151} = xlsread('Fresh Ovine_JMS_2.xlsx', '09-05-13', 'J17:O2009');
% RawData{151}(1:6,7) =[0.9215;11;22;31;41;52];
% RawData{152} = xlsread('Fresh Ovine_JMS_2.xlsx', '09-05-13', 'S17:X1873');
% RawData{152}(1:6,7) =[0.7213;11;22;31;41;52];
% RawData{153} = xlsread('Fresh Ovine_JMS_2.xlsx', '09-05-13', 'AB17:AG1871');
% RawData{153}(1:6,7) =[0.5426;11;21;31;41;52];
%
% RawData{154} = xlsread('Fresh Ovine_JMS_2.xlsx', '09-12-13', 'A17:F5755');
% RawData{154}(1:6,7) =[0.204;13;24;31;42;52];
% RawData{155} = xlsread('Fresh Ovine_JMS_2.xlsx', '09-12-13', 'J17:O7390');
% RawData{155}(1:6,7) =[0.211;13;25;31;42;52];
%
% RawData{156} = xlsread('Fresh Ovine_JMS_2.xlsx', '10-02-13', 'A17:F11803');
% RawData{156}(1:6,7) =[0.1538;12;24;31;42;52];
% RawData{157} = xlsread('Fresh Ovine_JMS_2.xlsx', '10-02-13', 'J17:O11539');
% RawData{157}(1:6,7) =[0.1864;12;25;31;42;52];
% RawData{158} = xlsread('Fresh Ovine_JMS_2.xlsx', '10-02-13', 'S17:X10955');
% RawData{158}(1:6,7) =[0.7965;12;21;31;41;52];
% RawData{159} = xlsread('Fresh Ovine_JMS_2.xlsx', '10-02-13', 'AB17:AG10899');
% RawData{159}(1:6,7) =[1.9689;12;22;31;41;52];
% RawData{160} = xlsread('Fresh Ovine_JMS_2.xlsx', '10-02-13', 'AK17:AP10920');
% RawData{160}(1:6,7) =[0.8195;12;21;31;41;52];
% RawData{161} = xlsread('Fresh Ovine_JMS_2.xlsx', '10-02-13', 'AT17:AY14550');
% RawData{161}(1:6,7) =[1.8812;12;22;31;41;52];
%
% RawData{162} = xlsread('Fresh Ovine_JMS_2.xlsx', '10-10-13', 'A17:F4487');
% RawData{162}(1:6,7) =[0.2203;12;25;31;42;52];
% RawData{163} = xlsread('Fresh Ovine_JMS_2.xlsx', '10-10-13', 'J17:O7508');
% RawData{163}(1:6,7) =[0.1487;12;25;31;42;52];
% RawData{164} = xlsread('Fresh Ovine_JMS_2.xlsx', '10-10-13', 'S17:X10983');
% RawData{164}(1:6,7) =[1.0557;12;22;31;41;52];
% RawData{165} = xlsread('Fresh Ovine_JMS_2.xlsx', '10-10-13', 'AB17:AG10955');
% RawData{165}(1:6,7) =[0.5911;12;21;31;41;52];
% RawData{166} = xlsread('Fresh Ovine_JMS_2.xlsx', '10-10-13', 'AK17:AP10932');
% RawData{166}(1:6,7) =[0.6782;12;21;31;41;52];
```

```
% RawData{167} = xlsread('Fresh Ovine_JMS_2.xlsx', '10-10-13', 'AT17:AY10969');
% RawData{167}(1:6,7) =[0.9705;12;22;31;41;52];
%
% RawData{168} = xlsread('Fresh Ovine_JMS_2.xlsx', '10-11-13', 'A17:F9394');
% RawData{168}(1:6,7) =[0.2141;12;25;31;42;52];
% RawData{169} = xlsread('Fresh Ovine_JMS_2.xlsx', '10-11-13', 'J17:O4460');
% RawData{169}(1:6,7) =[0.1993;12;24;31;42;52];
% RawData{170} = xlsread('Fresh Ovine_JMS_2.xlsx', '10-11-13', 'S17:X11890');
% RawData{170}(1:6,7) =[0.5473;12;21;31;41;52];
% RawData{171} = xlsread('Fresh Ovine_JMS_2.xlsx', '10-11-13', 'AB17:AG14429');
% RawData{171}(1:6,7) =[1.4254;12;22;31;41;52];
% RawData{172} = xlsread('Fresh Ovine_JMS_2.xlsx', '10-11-13', 'AK17:AP12368');
% RawData{172}(1:6,7) =[0.3862;12;21;31;41;52];
% RawData{173} = xlsread('Fresh Ovine_JMS_2.xlsx', '10-11-13', 'AT17:AY11003');
% RawData{173}(1:6,7) =[1.526;12;22;31;41;52];
%
% RawData{174} = xlsread('Fresh Ovine_JMS_2.xlsx', '10-17-13', 'A17:F12041');
% RawData{174}(1:6,7) =[0.6236;12;21;32;41;52];
% RawData{175} = xlsread('Fresh Ovine_JMS_2.xlsx', '10-17-13', 'J17:O11011');
% RawData{175}(1:6,7) =[0.9193;12;22;32;41;52];
% RawData{176} = xlsread('Fresh Ovine_JMS_2.xlsx', '10-17-13', 'S17:X11669');
% RawData{176}(1:6,7) =[0.7703;12;21;32;41;52];
% RawData{177} = xlsread('Fresh Ovine_JMS_2.xlsx', '10-17-13', 'AB17:AG11105');
% RawData{177}(1:6,7) =[1.3212;12;22;32;41;52];
%
% RawData{178} = xlsread('Fresh Ovine_JMS_2.xlsx', '10-30-13', 'A17:F2686');
% RawData{178}(1:6,7) =[0.225;11;25;33;42;52];
%
% RawData{179} = xlsread('Fresh Ovine_JMS_2.xlsx', '10-31-13', 'A17:F10912');
% RawData{179}(1:6,7) =[0.54;12;22;33;41;52];
% RawData{180} = xlsread('Fresh Ovine_JMS_2.xlsx', '10-31-13', 'J17:O10926');
% RawData{180}(1:6,7) =[0.3371;12;21;33;41;52];
% RawData{181} = xlsread('Fresh Ovine_JMS_2.xlsx', '10-31-13', 'S17:X10934');
% RawData{181}(1:6,7) =[0.2396;12;21;33;41;52];
% RawData{182} = xlsread('Fresh Ovine_JMS_2.xlsx', '10-31-13', 'AB17:AG10908');
% RawData{182}(1:6,7) =[0.5281;12;22;33;41;52];
% RawData{183} = xlsread('Fresh Ovine_JMS_2.xlsx', '10-31-13', 'AK17:AP10920');
% RawData{183}(1:6,7) =[0.7347;12;22;33;41;52];
% RawData{184} = xlsread('Fresh Ovine_JMS_2.xlsx', '10-31-13', 'AT17:AY20649');
% RawData{184}(1:6,7) =[0.3003;12;21;33;41;52];
% RawData{185} = xlsread('Fresh Ovine_JMS_2.xlsx', '10-31-13', 'BC17:BH10931');
% RawData{185}(1:6,7) =[0.7131;12;22;33;41;52];
% RawData{186} = xlsread('Fresh Ovine_JMS_2.xlsx', '10-31-13', 'BL17:BQ2699');
% RawData{186}(1:6,7) =[00.00;12;23;33;42;52];
% RawData{187} = xlsread('Fresh Ovine_JMS_2.xlsx', '10-31-13', 'BU17:BZ3195');
% RawData{187}(1:6,7) =[00.00;12;23;33;42;52];
```

```
% RawData{188} = xlsread('Fresh Ovine_JMS_2.xlsx', '10-31-13', 'CD17:CI3631');
% RawData{188}(1:6,7) =[00.00;12;23;33;42;52];
%
% RawData{189} = xlsread('Fresh Ovine_JMS_2.xlsx', '11-05-13_Lo', 'A17:F12382');
% RawData{189}(1:6,7) =[0.7929;13;21;31;41;52];
% RawData{190} = xlsread('Fresh Ovine_JMS_2.xlsx', '11-05-13_Lo', 'J17:O12063');
% RawData{190}(1:6,7) =[2.8413;13;22;31;41;52];
% RawData{191} = xlsread('Fresh Ovine_JMS_2.xlsx', '11-05-13_Lo', 'S17:X12516');
% RawData{191}(1:6,7) =[0.8528;13;21;31;41;52];
% RawData{192} = xlsread('Fresh Ovine_JMS_2.xlsx', '11-05-13_Lo',
'AB17:AG12344');
% RawData{192}(1:6,7) =[2.3421;13;22;31;41;52];
%
% RawData{193} = xlsread('Fresh Ovine_JMS_2.xlsx', '11-05-13_Hi', 'A17:F10977');
% RawData{193}(1:6,7) =[0.7209;13;21;31;41;51];
% RawData{194} = xlsread('Fresh Ovine_JMS_2.xlsx', '11-05-13_Hi', 'J17:O10978');
% RawData{194}(1:6,7) =[2.6904;13;22;31;41;51];
% RawData{195} = xlsread('Fresh Ovine_JMS_2.xlsx', '11-05-13_Hi', 'S17:X12026');
% RawData{195}(1:6,7) =[0.831;13;21;31;41;51];
% RawData{196} = xlsread('Fresh Ovine_JMS_2.xlsx', '11-05-13_Hi',
'AB17:AG11737');
% RawData{196}(1:6,7) =[2.5946;13;22;31;41;51];
%
% RawData{197} = xlsread('Fresh Ovine_JMS_2.xlsx', '11-07-13', 'A17:F2098');
% RawData{197}(1:6,7) =[0.2407;11;25;33;42;52];
% RawData{198} = xlsread('Fresh Ovine_JMS_2.xlsx', '11-07-13', 'J17:O8379');
% RawData{198}(1:6,7) =[0.2184;11;26;33;42;52];
% RawData{199} = xlsread('Fresh Ovine_JMS_2.xlsx', '11-07-13', 'S17:X4367');
% RawData{199}(1:6,7) =[0.203;11;26;33;42;52];
% RawData{200} = xlsread('Fresh Ovine_JMS_2.xlsx', '11-07-13', 'AB17:AG3526');
% RawData{200}(1:6,7) =[0.1314;11;24;33;42;52];
% RawData{201} = xlsread('Fresh Ovine_JMS_2.xlsx', '11-07-13', 'AK17:AP4536');
% RawData{201}(1:6,7) =[0.2227;11;25;33;42;52];
% RawData{202} = xlsread('Fresh Ovine_JMS_2.xlsx', '11-07-13', 'AT17:AY10926');
% RawData{202}(1:6,7) =[0.2592;11;21;33;41;52];
% RawData{203} = xlsread('Fresh Ovine_JMS_2.xlsx', '11-07-13', 'BC17:BH10905');
% RawData{203}(1:6,7) =[0.5283;11;22;33;41;52];
% RawData{204} = xlsread('Fresh Ovine_JMS_2.xlsx', '11-07-13', 'BL17:BQ10922');
% RawData{204}(1:6,7) =[0.2612;11;21;33;41;52];
% RawData{205} = xlsread('Fresh Ovine_JMS_2.xlsx', '11-07-13', 'BU17:BZ10968');
% RawData{205}(1:6,7) =[0.6802;11;22;33;41;52];
% RawData{206} = xlsread('Fresh Ovine_JMS_2.xlsx', '11-07-13', 'CD17:CI10921');
% RawData{206}(1:6,7) =[0.2783;11;21;33;41;52];
% RawData{207} = xlsread('Fresh Ovine_JMS_2.xlsx', '11-07-13', 'CL17:CR10925');
% RawData{207}(1:6,7) =[0.6762;11;22;33;41;52];
% RawData{208} = xlsread('Fresh Ovine_JMS_2.xlsx', '11-07-13', 'CV17:DA10908');
```

```
% RawData{208}(1:6,7) =[0.3319;11;21;33;41;52];
% RawData{209} = xlsread('Fresh Ovine_JMS_2.xlsx', '11-07-13', 'DE17:DJ10931');
% RawData{209}(1:6,7) =[0.6645;11;22;33;41;52];
%
% RawData{210} = xlsread('Fresh Ovine_JMS_2.xlsx', '11-08-13', 'A17:F10055');
% RawData{210}(1:6,7) =[0.2566;12;26;32;42;52];
% RawData{211} = xlsread('Fresh Ovine_JMS_2.xlsx', '11-08-13', 'J17:O9886');
% RawData{211}(1:6,7) =[0.2163;12;26;32;42;52];
% RawData{212} = xlsread('Fresh Ovine_JMS_2.xlsx', '11-08-13', 'S17:X8089');
% RawData{212}(1:6,7) =[0.1589;12;26;32;41;52];
% RawData{213} = xlsread('Fresh Ovine_JMS_2.xlsx', '11-08-13', 'AB17:AG20488');
% RawData{213}(1:6,7) =[0.4359;12;21;32;41;52];
% RawData{214} = xlsread('Fresh Ovine_JMS_2.xlsx', '11-08-13', 'AK17:AP10988');
% RawData{214}(1:6,7) =[1.3482;12;22;32;41;52];
% RawData{215} = xlsread('Fresh Ovine_JMS_2.xlsx', '11-08-13', 'AT17:AY11938');
% RawData{215}(1:6,7) =[0.4426;12;21;32;41;52];
% RawData{216} = xlsread('Fresh Ovine_JMS_2.xlsx', '11-08-13', 'BC17:BH11036');
% RawData{216}(1:6,7) =[1.2898;12;22;32;41;52];
%
% %% Loaded in 11/13/13
%
```

```
%
% RawData{217} = xlsread('Fresh Ovine_JMS_2.xlsx', '11-13-13', 'A17:F5806');
% RawData{217}(1:6,7) =[0.2141;13;24;33;42;52];
% RawData{218} = xlsread('Fresh Ovine_JMS_2.xlsx', '11-13-13', 'J17:O8442');
% RawData{218}(1:6,7) =[0.2398;13;24;3;42;52];
% RawData{219} = xlsread('Fresh Ovine_JMS_2.xlsx', '11-13-13', 'S17:X3250');
% RawData{219}(1:6,7) =[0.1225;13;26;33;42;52];
% RawData{220} = xlsread('Fresh Ovine_JMS_2.xlsx', '11-13-13', 'AB17:AG3086');
% RawData{220}(1:6,7) =[0.1966;13;26;33;42;52];
% RawData{221} = xlsread('Fresh Ovine_JMS_2.xlsx', '11-13-13', 'AK17:AP3755');
% RawData{221}(1:6,7) =[0.1642;13;26;33;42;52];
%
% RawData{222} = xlsread('Fresh Ovine_JMS_2.xlsx', '11-13-13', 'AT17:AY11345');
% RawData{222}(1:6,7) =[1.8588;13;22;33;41;52];
% RawData{223} = xlsread('Fresh Ovine_JMS_2.xlsx', '11-13-13', 'BC17:BH10923');
% RawData{223}(1:6,7) =[0.7825;13;21;33;41;52];
% RawData{224} = xlsread('Fresh Ovine_JMS_2.xlsx', '11-13-13', 'BL17:BQ11167');
% RawData{224}(1:6,7) =[1.5507;13;22;33;41;52];
% RawData{225} = xlsread('Fresh Ovine_JMS_2.xlsx', '11-13-13', 'BU17:BZ10933');
% RawData{225}(1:6,7) =[0.6431;13;21;33;41;52];
% RawData{226} = xlsread('Fresh Ovine_JMS_2.xlsx', '11-13-13', 'CD17:CI11912');
% RawData{226}(1:6,7) =[3.6693;13;27;33;43;52];
%
% %% Loaded in 12/18/13
%
% RawData{227} = xlsread('Fresh Ovine_JMS_2.xlsx', '12-12-13', 'A17:F12224');
```

```
% RawData{227}(1:6,7) =[0.49;12;21;32;41;52];
% RawData{228} = xlsread('Fresh Ovine_JMS_2.xlsx', '12-12-13', 'J17:O11201');
% RawData{228} = xlsread('Scleral Retests Compared to Originals.xlsx', '12-12-13
(228)', 'A10:F3246');
% RawData{228}(1:6,7) =[2.2681;12;22;32;41;52];
% RawData{229} = xlsread('Fresh Ovine_JMS_2.xlsx', '12-12-13', 'S17:X11840');
% RawData{229}(1:6,7) =[0.6521;12;21;32;41;52];
% RawData{230} = xlsread('Fresh Ovine_JMS_2.xlsx', '12-12-13', 'AB17:AG11660');
% RawData{230}(1:6,7) =[2.2515;12;22;32;41;52];
% RawData{231} = xlsread('Fresh Ovine_JMS_2.xlsx', '12-12-13', 'AK17:AP12180');
% RawData{231}(1:6,7) =[0.5472;12;21;32;41;52];
% RawData{232} = xlsread('Fresh Ovine_JMS_2.xlsx', '12-12-13', 'AT17:AY12572');
% RawData{232}(1:6,7) =[2.3884;12;22;32;41;52];
% RawData{233} = xlsread('Fresh Ovine_JMS_2.xlsx', '12-12-13', 'BC17:BH12209');
% RawData{233}(1:6,7) =[0.8541;12;21;32;41;52];
% RawData{234} = xlsread('Fresh Ovine_JMS_2.xlsx', '12-12-13', 'BL17:BQ12532');
% RawData{234} = xlsread('Scleral Retests Compared to Originals.xlsx', '12-12-13
(234)', 'A10:F3352');
% RawData{234}(1:6,7) =[2.5043;12;22;32;41;52];
%
% %% Loaded in 12/20/13
%
% RawData{235} = xlsread('Fresh Ovine_JMS_2.xlsx', '12-19-13', 'A17:F2627');
% RawData{235}(1:6,7) =[0.2744;12;25;33;42;52];
% RawData{236} = xlsread('Fresh Ovine_JMS_2.xlsx', '12-19-13', 'J17:O1675');
% RawData{236}(1:6,7) =[0.2366;12;25;33;42;52];
% RawData{237} = xlsread('Fresh Ovine_JMS_2.xlsx', '12-19-13', 'S17:X11148');
% RawData{237}(1:6,7) =[0.6332;12;21;33;41;52];
% RawData{238} = xlsread('Fresh Ovine_JMS_2.xlsx', '12-19-13', 'AB17:AG11149');
% RawData{238}(1:6,7) =[0.8787;12;22;33;41;52];
% RawData{239} = xlsread('Fresh Ovine_JMS_2.xlsx', '12-19-13', 'AK17:AP10956');
% RawData{239}(1:6,7) =[0.4373;12;21;33;41;52];
% RawData{240} = xlsread('Fresh Ovine_JMS_2.xlsx', '12-19-13', 'AT17:AY10951');
% RawData{240}(1:6,7) =[0.9664;12;22;33;41;52];
%
% %% Loaded in 01/08/14
%
% RawData{241} = xlsread('Fresh Ovine_JMS_2.xlsx', '01-06-14', 'A17:F8421');
% RawData{241}(1:6,7) =[0.1513;13;24;31;42;52];
% RawData{242} = xlsread('Fresh Ovine_JMS_2.xlsx', '01-06-14', 'J17:O7471');
% RawData{242}(1:6,7) =[0.1451;13;25;31;42;52];
% RawData{243} = xlsread('Fresh Ovine_JMS_2.xlsx', '01-06-14', 'S17:X12120');
% RawData{243}(1:6,7) =[1.4295;13;21;31;41;52];
% RawData{244} = xlsread('Fresh Ovine_JMS_2.xlsx', '01-06-14', 'AB17:AG11657');
% RawData{244}(1:6,7) =[2.0204;13;22;31;41;52];
% RawData{245} = xlsread('Fresh Ovine_JMS_2.xlsx', '01-06-14', 'AK17:AP11407');
```

```
% RawData{245}(1:6,7) =[1.2655;13;21;31;41;52];
% RawData{246} = xlsread('Fresh Ovine_JMS_2.xlsx', '01-06-14', 'AT17:AY12000');
% RawData{246}(1:6,7) =[2.111;13;22;31;41;52];
%
% %% Loaded in 01/29/14
%
% RawData{247} = xlsread('Fresh Ovine_JMS_2.xlsx', '01-28-14', 'A17:F11300');
% RawData{247}(1:6,7) =[0.9125;13;21;33;41;52];
% RawData{248} = xlsread('Fresh Ovine_JMS_2.xlsx', '01-28-14', 'J17:O11099');
% RawData{248}(1:6,7) =[2.2185;13;22;33;41;52];
% RawData{249} = xlsread('Fresh Ovine_JMS_2.xlsx', '01-28-14', 'S17:X11216');
% RawData{249}(1:6,7) =[0.7781;13;21;33;41;52];
% RawData{250} = xlsread('Fresh Ovine_JMS_2.xlsx', '01-28-14', 'AB17:AG11303');
% RawData{250}(1:6,7) =[2.3606;13;22;33;41;52];
% RawData{251} = xlsread('Fresh Ovine_JMS_2.xlsx', '01-28-14', 'AK17:AP11062');
% RawData{251}(1:6,7) =[0.5825;13;21;33;41;52];
% RawData{252} = xlsread('Fresh Ovine_JMS_2.xlsx', '01-28-14', 'AT17:AY11411');
% RawData{252}(1:6,7) =[2.3345;13;22;33;41;52];
% RawData{253} = xlsread('Fresh Ovine_JMS_2.xlsx', '01-28-14', 'BC17:BH11264');
% RawData{253}(1:6,7) =[0.6867;13;21;33;41;52];
% RawData{254} = xlsread('Fresh Ovine_JMS_2.xlsx', '01-28-14', 'BL17:BQ11773');
% RawData{254}(1:6,7) =[2.3751;13;22;33;41;52];
%
```

```
%
% RawData{255} = xlsread('Fresh Ovine_JMS_2.xlsx', '01-29-14', 'A17:F10988');
% RawData{255}(1:6,7) =[0.6638;13;21;32;41;52];
% RawData{256} = xlsread('Fresh Ovine_JMS_2.xlsx', '01-29-14', 'J17:O11924');
% RawData{256}(1:6,7) =[2.0613;13;22;32;41;52];
% RawData{257} = xlsread('Fresh Ovine_JMS_2.xlsx', '01-29-14', 'S17:X10917');
% RawData{257}(1:6,7) =[0.7027;13;21;32;41;52];
% RawData{258} = xlsread('Fresh Ovine_JMS_2.xlsx', '01-29-14', 'AB17:AG11881');
% RawData{258}(1:6,7) =[2.6438;13;22;32;41;52];
%
% %% Loaded in 02/04/14
%
% RawData{259} = xlsread('Fresh Ovine_JMS_2.xlsx', '02-03-14', 'A17:F4506');
% RawData{259}(1:6,7) =[0.1729;11;24;31;42;52];
% RawData{260} = xlsread('Fresh Ovine_JMS_2.xlsx', '02-03-14', 'J17:O11975');
% RawData{260}(1:6,7) =[0.2994;11;21;31;41;52];
% RawData{261} = xlsread('Fresh Ovine_JMS_2.xlsx', '02-03-14', 'S17:X11006');
% RawData{261}(1:6,7) =[0.5563;11;22;31;41;52];
% RawData{262} = xlsread('Fresh Ovine_JMS_2.xlsx', '02-03-14', 'AB17:AG15514');
% RawData{262}(1:6,7) =[0.3875;11;21;31;41;52];
% RawData{263} = xlsread('Fresh Ovine_JMS_2.xlsx', '02-03-14', 'AK17:AP10987');
% RawData{263}(1:6,7) =[0.5736;11;22;31;41;52];
%
% RawData{264} = xlsread('Fresh Ovine_JMS_2.xlsx', '02-04-14', 'A17:F12634');
```

```
% RawData{264}(1:6,7) =[0.7139;13;21;32;41;52];
% RawData{265} = xlsread('Fresh Ovine_JMS_2.xlsx', '02-04-14', 'J17:O12128');
% RawData{265}(1:6,7) =[2.0267;13;22;32;41;52];
% RawData{266} = xlsread('Fresh Ovine_JMS_2.xlsx', '02-04-14', 'S17:X15129');
% RawData{266}(1:6,7) =[0.7403;13;21;32;41;52];
% RawData{267} = xlsread('Fresh Ovine_JMS_2.xlsx', '02-04-14', 'AB17:AG11959');
% RawData{267}(1:6,7) =[2.1161;13;22;32;41;52];
%
% %% Loaded in 03/24/14
%
% RawData{268} = xlsread('Fresh Ovine_JMS_2.xlsx', '03-17-14', 'A17:F1979');
% RawData{268}(1:6,7) =[0.389;11;21;31;41;52];
% RawData{269} = xlsread('Fresh Ovine_JMS_2.xlsx', '03-17-14', 'J17:O1458');
% RawData{269}(1:6,7) =[0.924;11;22;31;41;52];
% RawData{270} = xlsread('Fresh Ovine_JMS_2.xlsx', '03-17-14', 'S17:X2269');
% RawData{270}(1:6,7) =[0.4043;11;21;31;41;52];
% RawData{271} = xlsread('Fresh Ovine_JMS_2.xlsx', '03-17-14', 'AB17:AG1410');
% RawData{271}(1:6,7) =[0.9831;11;22;31;41;52];
%
% RawData{272} = xlsread('Fresh Ovine_JMS_2.xlsx', '03-18-14', 'A17:F2596');
% RawData{272}(1:6,7) =[2.0241;13;22;31;41;52];
% RawData{273} = xlsread('Fresh Ovine_JMS_2.xlsx', '03-18-14', 'J17:O2578');
% RawData{273}(1:6,7) =[0.9924;13;21;31;41;52];
% RawData{274} = xlsread('Fresh Ovine_JMS_2.xlsx', '03-18-14', 'S17:X2633');
% RawData{274}(1:6,7) =[2.1286;13;22;31;41;52];
% RawData{275} = xlsread('Fresh Ovine_JMS_2.xlsx', '03-18-14', 'AB17:AG2652');
% RawData{275}(1:6,7) =[0.9297;13;21;31;41;52];
% RawData{276} = xlsread('Fresh Ovine_JMS_2.xlsx', '03-18-14', 'AK17:AP2467');
% RawData{276}(1:6,7) =[3.959;13;27;31;43;52];

% %% Loaded in 04/05/14
%
% RawData{277} = xlsread('Fresh Ovine_JMS_2.xlsx', '04-05-14', 'A17:F1720');
% RawData{277}(1:6,7) =[0.3728;12;21;33;41;52];
% RawData{278} = xlsread('Fresh Ovine_JMS_2.xlsx', '04-05-14', 'J17:O2656');
% RawData{278}(1:6,7) =[0.7684;12;22;33;41;52];
% RawData{279} = xlsread('Fresh Ovine_JMS_2.xlsx', '04-05-14', 'S17:X1634');
% RawData{279}(1:6,7) =[0.3755;12;21;33;41;52];
% RawData{280} = xlsread('Fresh Ovine_JMS_2.xlsx', '04-05-14', 'AB17:AG1290');
% RawData{280}(1:6,7) =[0.7036;12;22;33;41;52];
% RawData{281} = xlsread('Fresh Ovine_JMS_2.xlsx', '04-05-14', 'AK17:AP1891');
% RawData{281}(1:6,7) =[0.7403;13;21;33;41;52];
% RawData{282} = xlsread('Fresh Ovine_JMS_2.xlsx', '04-05-14', 'AT17:AY1411');
% RawData{282}(1:6,7) =[1.9333;13;22;33;41;52];
% RawData{283} = xlsread('Fresh Ovine_JMS_2.xlsx', '04-05-14', 'BC17:BH1826');
% RawData{283}(1:6,7) =[0.8748;13;21;33;41;52];
```

```
% RawData{284} = xlsread('Fresh Ovine_JMS_2.xlsx', '04-05-14', 'BL17:BQ1667');
% RawData{284}(1:6,7) =[2.0559;13;22;33;41;52];
%
% RawData{285} = xlsread('Fresh Ovine_JMS_2.xlsx', '04-05-14', 'BU17:BZ7986');
% RawData{285}(1:6,7) =[0.2018;13;23;32;42;52];
% RawData{286} = xlsread('Fresh Ovine_JMS_2.xlsx', '04-05-14', 'CD17:CI73747');
% RawData{286}(1:6,7) =[0.2166;13;23;32;42;52];

%% Loaded in 06/06/14

% RawData{287} = xlsread('New_Ovine_Data.xlsx', '6-4-14', 'A17:F432');
% RawData{287}(1:6,7) =[0.185;13;25;31;42;51];
% RawData{288} = xlsread('New_Ovine_Data.xlsx', '6-4-14', 'J17:O426');
% RawData{288}(1:6,7) =[0.1614;13;25;31;42;51];
% RawData{289} = xlsread('New_Ovine_Data.xlsx', '6-4-14', 'S17:X487');
% RawData{289}(1:6,7) =[0.1818;13;25;31;42;51];

% RawData{290} = xlsread('New_Ovine_Data.xlsx', '6-5-14', 'A17:F429');
% RawData{290}(1:6,7) =[0.1411;12;25;31;42;51];
% RawData{291} = xlsread('New_Ovine_Data.xlsx', '6-5-14', 'J17:O517');
% RawData{291}(1:6,7) =[0.1459;12;25;31;42;51];
% RawData{292} = xlsread('New_Ovine_Data.xlsx', '6-5-14', 'S17:X415');
% RawData{292}(1:6,7) =[0.1561;12;25;31;42;51];
% RawData{293} = xlsread('New_Ovine_Data.xlsx', '6-5-14', 'AB17:AG605');
% RawData{293}(1:6,7) =[0.1497;12;25;31;42;51];
% RawData{294} = xlsread('New_Ovine_Data.xlsx', '6-5-14', 'AK17:AP521');
% RawData{294}(1:6,7) =[0.1529;12;25;31;42;51];
% RawData{295} = xlsread('New_Ovine_Data.xlsx', '6-5-14', 'AT17:AY467');
% RawData{295}(1:6,7) =[0.0903;12;25;31;42;51];
% RawData{296} = xlsread('New_Ovine_Data.xlsx', '6-5-14', 'BC17:BH472');
% RawData{296}(1:6,7) =[0.1562;12;25;31;42;51];

% RawData{297} = xlsread('New_Ovine_Data.xlsx', '6-5-14', 'BL17:BQ2014');
% RawData{297}(1:6,7) =[0.6897;12;21;31;41;52];
% RawData{298} = xlsread('New_Ovine_Data.xlsx', '6-5-14', 'BU17:BZ2089');
% RawData{298}(1:6,7) =[0.9916;12;22;31;41;52];
% RawData{299} = xlsread('New_Ovine_Data.xlsx', '6-5-14', 'CD17:CI2261');
% RawData{299}(1:6,7) =[0.3495;12;21;31;41;52];
% RawData{300} = xlsread('New_Ovine_Data.xlsx', '6-5-14', 'CM17:CR2274');
% RawData{300}(1:6,7) =[0.9267;12;22;31;41;52];
% RawData{301} = xlsread('New_Ovine_Data.xlsx', '6-5-14', 'CV17:DA2182');
% RawData{301}(1:6,7) =[0.6006;12;21;31;41;52];
% RawData{302} = xlsread('New_Ovine_Data.xlsx', '6-5-14', 'DE17:DJ1897');
% RawData{302}(1:6,7) =[1.0707;12;22;31;41;52];
% RawData{303} = xlsread('New_Ovine_Data.xlsx', '6-5-14', 'DN17:DS2131');
% RawData{303}(1:6,7) =[0.4069;12;21;31;41;52];
```

```
% RawData{304} = xlsread('New_Ovine_Data.xlsx', '6-5-14', 'DW17:EB2050');
% RawData{304}(1:6,7) =[0.9513;12;22;31;41;52];


%% SAVING

% save('RawData','RawData')
```

APPENDIX B

MATLAB CODE FOR SCLERAL ANALYSIS AND PLOTTING

% SCLERA_ANALYSIS
% This code calls in the uploaded 'RawData' and analyzes the relaxation and pull-to-failure data separately.

```
clear all; close all; clc;
load('RawData.mat')
load('Norm_Relax_Sclera.mat')
load('Norm_Pull_Sclera.mat')
load('A.mat')

RawData_Sclera = 0;
DriftCorr_Sclera = 0;
NormalizedRelaxation_Sclera = 0;
RelaxationFit_Sclera = 0;
NormalizedPull_Sclera = 0;
PullFail_Sclera = 0;

zeroline = zeros(length(RawData{1}(:,1)),1);

% skip = [139 141];

% Trials where tissue does not fail
% skip = [141 158 159 160 164 166 167 173 175 177 179 180 181 182 183 185 202 ...
%     203 205 206 207 208 209 214 216 222 223 224 225 237 238 239 240 247 248 249
250 251 252 253 254 255 257 261 263];

% SKIP = ones(length(RawData),1);
% for i = 1:length(skip)
%     SKIP(skip(i),1) = 0;
% end

for i = 1:length(RawData);

%     if SKIP(i,1) == 1
if isempty(RawData{i})

elseif  i > 0

      RAW_SCLERA=RawData;

      if RawData{i}(5,7) == 41

         %%% Shifting by "zero load"
         if RawData{i}(end,1)>1000
            time = round(RawData{i}(:,1)*10)./10;
            tlow = find(time==79,1,'first');
```

```
    tup = find(time==81,1,'first');
    tstart = find(RawData{i}(:,2)==min(RawData{i}(tlow:tup,2)));
    load_zero{i}(:,1)=RawData{i}(:,2)-RawData{i}(tstart(1),2);
else
    time = round(RawData{i}(:,1)*10)./10;
    tlow = find(time==19,1,'first');
    tup = find(time==82,1,'first');
    tstart = find(RawData{i}(:,2)==min(RawData{i}(tlow:tup,2)));
    load_zero{i}(:,1)=RawData{i}(:,2)-RawData{i}(tstart(1),2);
end

%%% DRIFT CORRECTING
if RawData{i}(end,1)>1000
    if RawData{i}(6,7)==51
        time = round(RawData{i}(:,1)*10)./10;
        time1=RawData{i}(:,1);
        load_0 = load_zero{i}(:,1);
        t_corr = find(time==985,1,'first');
        slope = load_0(t_corr)/time1(t_corr);
        load_d = load_0 - time1.*slope;
    else
        load_d=load_zero{i}(:,1);
    end
else
    load_d=load_zero{i}(:,1);
end

RawData{i}(:,2)=load_d;
%RawData{i}(:,2)=load_zero{i}(:,1);
RawData{i}(:,3)=RawData{i}(:,2)/(3*RawData{i}(1,7));
RawData{i}(:,6)=RawData{i}(:,4)/6;

%%% NEW CORRECTED VARIABLE
ScleraCorr{i}(:,1) = RawData{i}(:,1);
ScleraCorr{i}(:,2) = RawData{i}(:,2);
ScleraCorr{i}(:,3) = RawData{i}(:,3);
ScleraCorr{i}(:,4) = RawData{i}(:,4);
ScleraCorr{i}(:,5) = RawData{i}(:,5);
ScleraCorr{i}(:,6) = RawData{i}(:,6);
ScleraCorr{i}(:,7) = RawData{i}(:,7);

if RawData_Sclera==1
    figure(1)
    plot(RawData{1}(:,1),zeroline,'--k','LineWidth',2)
    hold on
    plot(RAW_SCLERA{i}(:,1),RAW_SCLERA{i}(:,2),'--b','tag',sprintf('trial =
```

```
%d',i))
            xlabel('Time (s)')
            ylabel('Load (N)')
            outputString= sprintf('Raw Scleral Data');
            title(outputString)
        elseif RawData_Sclera==0
        end

        datacursormode on
        dcm = datacursormode(gcf);
        set(dcm,'UpdateFcn',@myupdatefcn)

        if DriftCorr_Sclera==1
            figure(2)
            plot(RawData{1}(:,1),zeroline,'--k','LineWidth',2)
            hold on
            plot(ScleraCorr{i}(:,1),ScleraCorr{i}(:,2),'b','tag',sprintf('trial = %d',i))
            xlabel('Time (s)')
            ylabel('Load (N)')
            outputString= sprintf('Corrected Scleral Data');
            title(outputString)
        elseif DriftCorr_Sclera==0
        end

        datacursormode on
        dcm = datacursormode(gcf);
        set(dcm,'UpdateFcn',@myupdatefcn)

        %%% ISOLATING RELAXATION DATA AND PULL-TO-FAILURE DATA
        if RawData{i}(end,1) > 1000
            t = round(ScleraCorr{i}(:,1)*10)./10;
            tlowerlim = find(t==70);
            tupperlim = find(t==1000);
            tstart = find(ScleraCorr{i}(:,5)==max(ScleraCorr{i}(tlowerlim:tupperlim,5)));
            tend = find(t==980,1,'last');
            tstart2 = find(ScleraCorr{i}(:,5)==0,1,'last');
            tend2 = find(ScleraCorr{i}(:,5),1,'last');
            Norm_Relax_Sclera{i}(:,1:3) = [ScleraCorr{i}(tstart:tend,1)-
ScleraCorr{i}(tstart(1),1),ScleraCorr{i}(tstart:tend,2),ScleraCorr{i}(tstart:tend,3)];
            Norm_Relax_Sclera{i}(:,4:7) =
[ScleraCorr{i}(tstart:tend,4),ScleraCorr{i}(tstart:tend,5),ScleraCorr{i}(tstart:tend,6),Scle
raCorr{i}(1:length(tstart:tend),7)];

            if NormalizedRelaxation_Sclera==1
                figure(3)
```

```
plot(Norm_Relax_Sclera{i}(:,1),Norm_Relax_Sclera{i}(:,3),'r','tag',sprintf('trial = %d',i))
            hold on
            xlabel('Time (s)')
            ylabel('Stress (MPa)')
            outputString= sprintf('Normalized Sclera Stress Relaxation Data');
            title(outputString)
        elseif NormalizedRelaxation_Sclera==0
        end

        datacursormode on
        dcm = datacursormode(gcf);
        set(dcm,'UpdateFcn',@myupdatefcn)

        [sclera_coeffs{i} stressfit{i}] =
curvefit(Norm_Relax_Sclera{i}(:,1),Norm_Relax_Sclera{i}(:,3));
        clc

        Norm_Pull_Sclera{i}(:,1:3) = [ScleraCorr{i}(tstart2:tend2,1)-
ScleraCorr{i}(tstart2(1),1),ScleraCorr{i}(tstart2:tend2,2)-
ScleraCorr{i}(tstart2(1),2),ScleraCorr{i}(tstart2:tend2,3)-ScleraCorr{i}(tstart2(1),3)];
        Norm_Pull_Sclera{i}(:,4:7) =
[ScleraCorr{i}(tstart2:tend2,4),ScleraCorr{i}(tstart2:tend2,5),ScleraCorr{i}(tstart2:tend2,
6),ScleraCorr{i}(1:length(tstart2:tend2),7)];

    else
        t = round(ScleraCorr{i}(:,1)*10)./10;
        tstart2 = find(ScleraCorr{i}(:,5)<0,1,'last');
        tend2 = find(ScleraCorr{i}(:,5),1,'last');

        sclera_coeffs{i} = zeros(7,1);

        Norm_Pull_Sclera{i}(:,1:3) = [ScleraCorr{i}(tstart2:tend2,1)-
ScleraCorr{i}(tstart2(1),1),abs(ScleraCorr{i}(tstart2:tend2,2)-
ScleraCorr{i}(tstart2,2)),abs(ScleraCorr{i}(tstart2:tend2,3)-ScleraCorr{i}(tstart2(1),3))];
        Norm_Pull_Sclera{i}(:,4:7) =
[ScleraCorr{i}(tstart2:tend2,4),ScleraCorr{i}(tstart2:tend2,5),ScleraCorr{i}(tstart2:tend2,
6),ScleraCorr{i}(1:length(tstart2:tend2),7)];
    end

    if NormalizedPull_Sclera==1
        figure(4)
        plot(Norm_Pull_Sclera{i}(:,1),Norm_Pull_Sclera{i}(:,2),'g','tag',sprintf('trial =
%d',i))
        hold on
        plot(Norm_Pull_Sclera{i}(:,1),Norm_Pull_Sclera{i}(:,6),'-.k')
        xlabel('Time (s)')
```

```
            ylabel('Load (N)')
            outputString= sprintf('Normalized Scleral Pull-to-failure Data');
            title(outputString)
        elseif NormalizedPull_Sclera==0
        end
        datacursormode on
        dcm = datacursormode(gcf);
        set(dcm,'UpdateFcn',@myupdatefcn)

        if PullFail_Sclera==1
            figure(5)
            plot(Norm_Pull_Sclera{i}(:,6),Norm_Pull_Sclera{i}(:,3),'g','tag',sprintf('trial =
%d',i))
            hold on
            xlabel('Strain (mm/mm)')
            ylabel('Stress (MPa)')
            outputString= sprintf('Pull-to-failure Stress/Strain');
            title(outputString)
        elseif PullFail_Sclera==0

            datacursormode on
            dcm = datacursormode(gcf);
            set(dcm,'UpdateFcn',@myupdatefcn)

        end
    end
  end
end

%% PLOTTING RELAXATION CURVE FITS

% for i = 1:length(sclera_coeffs)
%     if isempty(sclera_coeffs{i})
%     else
%         A(i,:) = [sclera_coeffs{i}(1,1) sclera_coeffs{i}(2,1) sclera_coeffs{i}(3,1)
sclera_coeffs{i}(4,1) sclera_coeffs{i}(5,1) sclera_coeffs{i}(6,1) sclera_coeffs{i}(7,1)];
%         if RelaxationFit_Sclera == 1
%             figure
%
plot(Norm_Relax_Sclera{i}(:,1),Norm_Relax_Sclera{i}(:,3),'.r',Norm_Relax_Sclera{i}(:
,1),stressfit{i},'b')
%             xlabel('time','FontSize',24,'FontName','Times New Roman')
%             ylabel('Stress (MPa)','FontSize',24,'FontName','Times New Roman')
%             set(gca,'FontSize',24,'FontName','Times New Roman')
%             legend('Exp','Model')
%             outputString = sprintf('stress relaxation, trial = %d',i);
```

```
%            title(outputString)
%            xlim([-50,900])
%            outputString= sprintf('R^2 = %d',sclera_coeffs{i}(7));
%            text(300,sclera_coeffs{i}(6),outputString)
%        elseif RelaxationFit_Sclera == 0
%        end
%    end
% end

% hold on
% % title('Normalized stress-strain curves')
% ylabel('Stress (MPa)','FontSize',24,'FontName','Times New Roman')
% xlabel('Strain (mm/mm)','FontSize',24,'FontName','Times New Roman')
% set(gca,'FontSize',24,'FontName','Times New Roman')
% % xlim([0,1])

% saveas(figure,outputTitle);

%% Plotting trials that dip below zero
% for i=1:length(Norm_Relax_Sclera)
%     if isempty(Norm_Relax_Sclera{i})
%     else
%         time = round(Norm_Relax_Sclera{i}(:,1)*10)./10;
%         t = find(time==30,1,'first');
%         early_stress=Norm_Relax_Sclera{i}(t,3);
%         end_stress=Norm_Relax_Sclera{i}(end,3);
%         %         if end_stress>early_stress
%         if end_stress<0
%             plot(Norm_Relax_Sclera{i}(:,1),Norm_Relax_Sclera{i}(:,3),'tag',sprintf('trial
= %d',i))
%             hold on
%         else
%         end
%         datacursormode on
%         dcm = datacursormode(gcf);
%         set(dcm,'UpdateFcn',@myupdatefcn)
%     end
% end

%% SAVING
% save('Norm_Relax_Sclera','Norm_Relax_Sclera')
% save('Norm_Pull_Sclera','Norm_Pull_Sclera')
% save('A','A')
% save('ScleraCorr','ScleraCorr')

%% IN COMMAND WINDOW, TYPE DESIRED TRIAL AND DATA WILL BE
```

INDICATED ON GRAPH AS A THICKER LINE
% prompt = 'Enter trial #:';
% trial = input(prompt)
% plot(Norm_Relax_Sclera{trial}(:,1),Norm_Relax_Sclera{trial}(:,3),'--k','LineWidth',2)
% outputString = sprintf('trial # = %d',trial);
% stress_end=find(Norm_Relax_Sclera{trial}(end,3));
%
text(Norm_Relax_Sclera{trial}(stress_end,1),Norm_Relax_Sclera{trial}(stress_end,3),ou
tputString)

%%

% PLOTTING PULL-TO-FAILURE DATA – AGE AND REGION
% This code calls in the normalized pull-to-failure data and plots all raw trials, as well as, averaged values across age groups and region

%%% Variables:
%%% StressAtStrain_averaged:
%%% Row 1 --> PRE | ANTERIOR
%%% Row 2 --> INFANT | ANTERIOR
%%% Row 3 --> ADULT | ANTERIOR
%%% Row 4 --> PRE | POSTERIOR
%%% Row 5 --> INFANT | POSTERIOR
%%% Row 6 --> ADULT | POSTERIOR

clear; close all; clc;

load Norm_Pull_Sclera.mat

%% CHOOSE PLOTTING OPTIONS
% PAUSE (1) OR NO PAUSE (0)
% LIST TRIAL (1) OR NO LIST TRIAL (0)

skip = [141 158 159 160 164 166 167 173 175 177 179 180 181 182 183 185 202 ...
203 204 205 206 207 208 209 214 216 222 223 224 225 237 238 239 240 247 248 249
250 251 252 253 254 255 257 261 263];

PauseOrNo = 0;
ListTrialOrNo = 0;

wait = 0.5; % pause s

%% PLOTTING RAW TRIALS & CATEGORIZATION

figure(1)

```
hold on
% title('Average stress-strain over age and region')
ylabel('Stress (MPa)','FontSize',24,'FontName','Times New Roman')
xlabel('Strain (mm/mm)','FontSize',24,'FontName','Times New Roman')
set(gca,'FontSize',24,'FontName','Times New Roman')
%axis([-50,1000,-0.25,3])

figure(2)
hold on
% title('Normalized stress-strain curves')
ylabel('Stress (MPa)','FontSize',24,'FontName','Times New Roman')
xlabel('Strain (mm/mm)','FontSize',24,'FontName','Times New Roman')
set(gca,'FontSize',24,'FontName','Times New Roman')
xlim([0,1])

% % SELECTING TIME POINTS TO TAKE AVERAGE
% strainpts = 0:0.01:0.23;
strainpts = 0:0.01:1;
% strainpts(end) = [];
% strainpts = floor(strainpts*100)./100;

% FILLING IN SKIP MATRIX
SKIP = ones(length(Norm_Pull_Sclera),1);
for i = 1:length(skip)
   SKIP(skip(i),1) = 0;
end

% CATEGORIZING ACROSS AGE GROUPS AND REGION
countPreA = 0;
countInfantA = 0;
countAdultA = 0;
countPreP = 0;
countInfantP = 0;
countAdultP = 0;

countAll = 0;

%%
for i = 1:length(Norm_Pull_Sclera);

   if  isempty(Norm_Pull_Sclera{i}) || SKIP(i,1) == 0

      % Keep this if you want to see average pull data for HIGH STRAIN across age and
region (PMT < 6 hours)
   %elseif Norm_Pull_Sclera{i}(7,7)>0 && Norm_Pull_Sclera{i}(7,7)<360 &&
Norm_Pull_Sclera{i}(4,7)==31 && Norm_Pull_Sclera{i}(6,7)==51
```

```
    % Keep this if you want to see average pull data for LOW STRAIN across age and
region
   elseif Norm_Pull_Sclera{i}(4,7)==31 && Norm_Pull_Sclera{i}(6,7)==52

    countAll = countAll+1;

    for j = 1:length(strainpts)
        k = strainpts(j);
        [~, ind] = min(abs(Norm_Pull_Sclera{i}(:,6) - k));
        StressAtStrain{i}(j,1) = Norm_Pull_Sclera{i}(ind(1),3);
    end

        % 1 PRE | ANTERIOR
    if Norm_Pull_Sclera{i}(2,7) == 11 && Norm_Pull_Sclera{i}(3,7) == 21
        StressAtStrain_grouped{1}(i,:) = StressAtStrain{i}(:,1);
        hPreA =
plot(Norm_Pull_Sclera{i}(:,6),Norm_Pull_Sclera{i}(:,3),'LineWidth',1,'LineStyle','-
','Color','b','tag',sprintf('trial = %d',i));
        countPreA = countPreA +1;

        % 2 INFANT | ANTERIOR
    elseif Norm_Pull_Sclera{i}(2,7) == 12 && Norm_Pull_Sclera{i}(3,7) == 21
        StressAtStrain_grouped{2}(i,:) = StressAtStrain{i}(:,1);
        hInfantA =
plot(Norm_Pull_Sclera{i}(:,6),Norm_Pull_Sclera{i}(:,3),'LineWidth',1,'LineStyle','-
','Color','r','tag',sprintf('trial = %d',i));
        countInfantA = countInfantA +1;

        % 3 ADULT | ANTERIOR
    elseif Norm_Pull_Sclera{i}(2,7) == 13 && Norm_Pull_Sclera{i}(3,7) == 21
        StressAtStrain_grouped{3}(i,:) = StressAtStrain{i}(:,1);
        hAdultA =
plot(Norm_Pull_Sclera{i}(:,6),Norm_Pull_Sclera{i}(:,3),'LineWidth',1,'LineStyle','-
','Color','g','tag',sprintf('trial = %d',i));
        countAdultA = countAdultA +1;

        % 4 PRE | POSTERIOR
    elseif Norm_Pull_Sclera{i}(2,7) == 11 && Norm_Pull_Sclera{i}(3,7) == 22
        StressAtStrain_grouped{4}(i,:) = StressAtStrain{i}(:,1);
        hPreP =
plot(Norm_Pull_Sclera{i}(:,6),Norm_Pull_Sclera{i}(:,3),'LineWidth',1,'LineStyle','--
','Color','b','tag',sprintf('trial = %d',i));
        countPreP = countPreP +1;

        % 5 INFANT | POSTERIOR
```

```
        elseif Norm_Pull_Sclera{i}(2,7) == 12 && Norm_Pull_Sclera{i}(3,7) == 22
            StressAtStrain_grouped{5}(i,:) = StressAtStrain{i}(:,1);
            hInfantP =
plot(Norm_Pull_Sclera{i}(:,6),Norm_Pull_Sclera{i}(:,3),'LineWidth',1,'LineStyle','--
','Color','r','tag',sprintf('trial = %d',i));
            countInfantP = countInfantP +1;

            % 6 ADULT | POSTERIOR
        elseif Norm_Pull_Sclera{i}(2,7) == 13 && Norm_Pull_Sclera{i}(3,7) == 22
            StressAtStrain_grouped{6}(i,:) = StressAtStrain{i}(:,1);
            hAdultP =
plot(Norm_Pull_Sclera{i}(:,6),Norm_Pull_Sclera{i}(:,3),'LineWidth',1,'LineStyle','--
','Color','g','tag',sprintf('trial = %d',i));
            countAdultP = countAdultP +1;

        end
        datacursormode on
        dcm = datacursormode(gcf);
        set(dcm,'UpdateFcn',@myupdatefcn)
    end

    %%% Graphing Options
    if ListTrialOrNo == 1;
        outputText = sprintf('trial = %d',i);
        text(90,Norm_Pull_Sclera{i}(end,1),outputText)
    end
    if PauseOrNo == 1;
        pause(wait)
    end
end

%%%%%%%%%
countPreASt = sprintf('Pre Ant (N=%.f)',countPreA);
countInfantASt = sprintf('Infant Ant (N=%.f)',countInfantA);
countAdultASt = sprintf('Adult Ant (N=%.f)',countAdultA);
countPrePSt = sprintf('Pre Post (N=%.f)',countPreP);
countInfantPSt = sprintf('Infant Post (N=%.f)',countInfantP);
countAdultPSt = sprintf('Adult Post (N=%.f)',countAdultP);

figure(1)
legend([hPreA,hPreP,hInfantA,hInfantP,hAdultA,hAdultP],{'Pre-term, Anterior','Pre-
term, Posterior','Infant, Anterior','Infant, Posterior','Adult, Anterior','Adult,
Posterior'},'Location','NorthEast');
legend([hPreA,hPreP,hInfantA,hInfantP,hAdultA,hAdultP],{countPreASt,countPrePSt,co
untInfantASt,countInfantPSt,countAdultASt,countAdultPSt},'Location','NorthEast');
```

```
%% AVERAGE ACROSS AGE GROUPS AND REGION
for i = 1:length(StressAtStrain_grouped)

    % Eliminate rows of zeroes
    count = 0;
    delete0 = [];
    for j = 1:length(StressAtStrain_grouped{i}(:,1))
        if StressAtStrain_grouped{i}(j,2) == 0
            delete0(count+1) = j;
            count = count +1;
        end
    end
    StressAtStrain_grouped{i}(delete0,:) = [];

    % Averaging
    StressAtStrain_averaged(i,:) = mean(StressAtStrain_grouped{i},1);
    %StressAtStrain_std(i,:) = std(StressAtStrain_grouped{i},0,1);

end

%% PLOTTING AVERAGED STRESS

% Plot line to connect
plot(strainpts,StressAtStrain_averaged(1,:),'b')
plot(strainpts,StressAtStrain_averaged(2,:),'r')
plot(strainpts,StressAtStrain_averaged(3,:),'g')
plot(strainpts,StressAtStrain_averaged(4,:),'b')
plot(strainpts,StressAtStrain_averaged(5,:),'r')
plot(strainpts,StressAtStrain_averaged(6,:),'g')

% Plot marker
hPreA = plot(strainpts,StressAtStrain_averaged(1,:),'LineStyle','x','Color','b','MarkerSize',
12);
hInfantA =
plot(strainpts,StressAtStrain_averaged(2,:),'LineStyle','x','Color','r','MarkerSize', 12);
hAdultA =
plot(strainpts,StressAtStrain_averaged(3,:),'LineStyle','x','Color','g','MarkerSize', 12);
hPreP = plot(strainpts,StressAtStrain_averaged(4,:),'LineStyle','o','Color','b','MarkerSize',
12);
hInfantP =
plot(strainpts,StressAtStrain_averaged(5,:),'LineStyle','o','Color','r','MarkerSize', 12);
hAdultP =
plot(strainpts,StressAtStrain_averaged(6,:),'LineStyle','o','Color','g','MarkerSize', 12);

% Plot errorbars
% errorbar(strainpts,StressAtStrain_averaged(1,:),StressAtStrain_std(1,:),'b')
```

```
% errorbar(strainpts,StressAtStrain_averaged(2,:),StressAtStrain_std(2,:),'r')
% errorbar(strainpts,StressAtStrain_averaged(3,:),StressAtStrain_std(3,:),'g')
% errorbar(strainpts,StressAtStrain_averaged(4,:),StressAtStrain_std(4,:),'b')
% errorbar(strainpts,StressAtStrain_averaged(5,:),StressAtStrain_std(5,:),'r')
% errorbar(strainpts,StressAtStrain_averaged(6,:),StressAtStrain_std(6,:),'g')

figure(2)
legend([hPreA,hPreP,hInfantA,hInfantP,hAdultA,hAdultP],{'Pre-term, Anterior','Pre-
term, Posterior','Infant, Anterior','Infant, Posterior','Adult, Anterior','Adult,
Posterior'},'Location','NorthWest');

A = [];
count = 0;
for i = 1:length(StressAtStrain)
   for j = 1:length(strainpts)
      if isempty(StressAtStrain{i})
         A(j+count,2) = NaN;
         A(j+count,3) = NaN;
         A(j+count,1) = i;
         A(j+count,4) = NaN;
         A(j+count,5) = NaN;
      else
         A(j+count,2) = strainpts(j);
         A(j+count,3) = StressAtStrain{i}(j,1);
         A(j+count,1) = i;
         A(j+count,4) = Norm_Pull_Sclera{i}(2,7);
         A(j+count,5) = Norm_Pull_Sclera{i}(3,7);
      end
   end
   count = count+length(strainpts);
end

%%
% We are limited by our low capacity load cell. Not all tissues fail when tested at low-
strain
% Maximum stresses of all trials at the lowest strain (so to compare peak stresses at same
strain)
% for i = 1:length(StressAtStrain)
%    if isempty(StressAtStrain{i})
%       else Max_StressAtStrain(i,:)=[StressAtStrain{i}(24,1)];
%    end
% end

%% IN COMMAND WINDOW, TYPE DESIRED TRIAL AND DATA WILL BE
INDICATED ON GRAPH AS A THICKER LINE
% prompt = 'Enter trial #:';
```

```
% trial = input(prompt)
% plot(Norm_Pull_Sclera{trial}(:,6),Norm_Pull_Sclera{trial}(:,3),'--k','LineWidth',2)
% outputString = sprintf('trial # = %d',trial);
% stress_max=find(Norm_Pull_Sclera{trial}(:,3)==max(Norm_Pull_Sclera{trial}(:,3)));
%
text(Norm_Pull_Sclera{trial}(stress_max,6),Norm_Pull_Sclera{trial}(stress_max,3),outp
utString)


%%%%%%%%%%%%%%%%%%%%%%%%%%%%%%%%%%%%%%%%%%%%%%%%%%%%%%%%%%%%%%%%
```

% PLOTTING PULL-TO-FAILURE DATA – STORAGE CONDITION

% This code calls in the normalized pull-to-failure data and plots all raw trials, as well as, averaged values across condition groups and region

```
%%% Variables:
%%% StressAtStrain_averaged:
%%% Row 1 --> FRESH | ANTERIOR
%%% Row 2 --> FROZEN | ANTERIOR
%%% Row 3 --> FIXED | ANTERIOR
%%% Row 4 --> FRESH | POSTERIOR
%%% Row 5 --> FROZEN | POSTERIOR
%%% Row 6 --> FIXED | POSTERIOR

clear; close all; clc;

load Norm_Pull_Sclera.mat

%% CHOOSE PLOTTING OPTIONS
% PAUSE (1) OR NO PAUSE (0)
% LIST TRIAL (1) OR NO LIST TRIAL (0)
%
skip = [141 158 159 160 164 166 167 173 175 177 179 180 181 182 183 185 202 ...
   203 205 206 207 208 209 214 216 222 223 224 225 237 238 239 240 247 248 249 250
251 252 253 254 255 257 261 263];

PauseOrNo = 0;
ListTrialOrNo = 0;

wait = 0.5; % pause s

%% PLOTTING RAW TRIALS & CATEGORIZATION

figure(1)
hold on
```

```
% title('Average stress-strain over condition and regions')
ylabel('Stress (MPa)','FontSize',24,'FontName','Times New Roman')
xlabel('Strain (mm/mm)','FontSize',24,'FontName','Times New Roman')
set(gca,'FontSize',24,'FontName','Times New Roman')
%axis([-50,1000,-0.25,3])

figure(2)
hold on
title('Normalized stress-strain curves')
ylabel('Stress (MPa)','FontSize',24,'FontName','Times New Roman')
xlabel('Strain (mm/mm)','FontSize',24,'FontName','Times New Roman')
set(gca,'FontSize',24,'FontName','Times New Roman')
xlim([0,2])
% axis([0,2,0,3.5])

% SELECTING TIME POINTS TO TAKE AVERAGE
% strainpts = 0:0.005:0.1;
strainpts = 0:0.01:1;

% FILLING IN SKIP MATRIX
SKIP = ones(length(Norm_Pull_Sclera),1);
for i = 1:length(skip)
   SKIP(skip(i),1) = 0;
end

% CATEGORIZING ACROSS AGE GROUPS AND REGION
countFreshA = 0;
countFrozenA = 0;
countFixedA = 0;
countFreshP = 0;
countFrozenP = 0;
countFixedP = 0;

countAll = 0;

%%
for i = 1:length(Norm_Pull_Sclera);

   if  isempty(Norm_Pull_Sclera{i}) || SKIP(i,1) == 0

      % Keep this if you want to see average pull data for INFANT across region and
storage condition
   elseif Norm_Pull_Sclera{i}(2,7) == 11 && Norm_Pull_Sclera{i}(6,7) == 52 ||
Norm_Pull_Sclera{i}(2,7) == 12 && Norm_Pull_Sclera{i}(6,7) == 52

      % Keep this if you want to see average pull data for ADULT across region and
```

```
storage condition
   %elseif Norm_Pull_Sclera{i}(2,7) == 13 && Norm_Pull_Sclera{i}(6,7) == 52

      countAll = countAll+1;
      for j = 1:length(strainpts)
         k = strainpts(j);
         [~, ind] = min(abs(Norm_Pull_Sclera{i}(:,6) - k));
         StressAtStrain{i}(j,1) = Norm_Pull_Sclera{i}(ind(1),3);
      end

         % 1 FRESH | ANTERIOR
      if Norm_Pull_Sclera{i}(4,7) == 31 && Norm_Pull_Sclera{i}(3,7) == 21
         StressAtStrain_grouped{1}(i,:) = StressAtStrain{i}(:,1);
         hFreshA =
plot(Norm_Pull_Sclera{i}(:,6),Norm_Pull_Sclera{i}(:,3),'LineWidth',1,'LineStyle','-
','Color','g','tag',sprintf('trial = %d',i));
         countFreshA = countFreshA +1;

         % 2 FROZEN | ANTERIOR
      elseif Norm_Pull_Sclera{i}(4,7) == 32 && Norm_Pull_Sclera{i}(3,7) == 21
         StressAtStrain_grouped{2}(i,:) = StressAtStrain{i}(:,1);
         hFrozenA =
plot(Norm_Pull_Sclera{i}(:,6),Norm_Pull_Sclera{i}(:,3),'LineWidth',1,'LineStyle','-
','Color','b','tag',sprintf('trial = %d',i));
         countFrozenA = countFrozenA +1;

         % 3 FIXED | ANTERIOR
      elseif Norm_Pull_Sclera{i}(4,7) == 33 && Norm_Pull_Sclera{i}(3,7) == 21
         StressAtStrain_grouped{3}(i,:) = StressAtStrain{i}(:,1);
         hFixedA =
plot(Norm_Pull_Sclera{i}(:,6),Norm_Pull_Sclera{i}(:,3),'LineWidth',1,'LineStyle','-
','Color','r','tag',sprintf('trial = %d',i));
         countFixedA = countFixedA +1;

         % 4 FRESH | POSTERIOR
      elseif Norm_Pull_Sclera{i}(4,7) == 31 && Norm_Pull_Sclera{i}(3,7) == 22
         StressAtStrain_grouped{4}(i,:) = StressAtStrain{i}(:,1);
         hFreshP =
plot(Norm_Pull_Sclera{i}(:,6),Norm_Pull_Sclera{i}(:,3),'LineWidth',1,'LineStyle','--
','Color','g','tag',sprintf('trial = %d',i));
         countFreshP = countFreshP+1;

         % 5 FROZEN | POSTERIOR
      elseif Norm_Pull_Sclera{i}(4,7) == 32 && Norm_Pull_Sclera{i}(3,7) == 22
         StressAtStrain_grouped{5}(i,:) = StressAtStrain{i}(:,1);
         hFrozenP =
```

```
plot(Norm_Pull_Sclera{i}(:,6),Norm_Pull_Sclera{i}(:,3),'LineWidth',1,'LineStyle','--
','Color','b','tag',sprintf('trial = %d',i));
        countFrozenP = countFrozenP +1;

        % 6 FIXED | POSTERIOR
      elseif Norm_Pull_Sclera{i}(4,7) == 33 && Norm_Pull_Sclera{i}(3,7) == 22
        StressAtStrain_grouped{6}(i,:) = StressAtStrain{i}(:,1);
        hFixedP =
plot(Norm_Pull_Sclera{i}(:,6),Norm_Pull_Sclera{i}(:,3),'LineWidth',1,'LineStyle','--
','Color','r','tag',sprintf('trial = %d',i));
        countFixedP = countFixedP+1;

      end
      datacursormode on
      dcm = datacursormode(gcf);
      set(dcm,'UpdateFcn',@myupdatefcn)
   end

   %%% Graphing Options
   if ListTrialOrNo == 1;
      outputText = sprintf('trial = %d',i);
      text(90,Norm_Pull_Sclera{i}(end,1),outputText)
   end

   if PauseOrNo == 1;
      pause(wait)
   end
end
%%%%%%%%%
countFreshASt = sprintf('Fresh Ant (N=%.f)',countFreshA);
countFrozenASt = sprintf('Frozen Ant (N=%.f)',countFrozenA);
countFixedASt = sprintf('Fixed Ant (N=%.f)',countFixedA);
countFreshPSt = sprintf('Fresh Post (N=%.f)',countFreshP);
countFrozenPSt = sprintf('Frozen Post (N=%.f)',countFrozenP);
countFixedPSt = sprintf('Fixed Post (N=%.f)',countFixedP);

figure(1)
legend([hFreshA,hFreshP,hFrozenA,hFrozenP,hFixedA,hFixedP],{'Fresh,
Anterior','Fresh, Posterior','Frozen, Anterior','Frozen, Posterior','Fixed, Anterior','Fixed,
Posterior'},'Location','NorthEast');
legend([hFreshA,hFreshP,hFrozenA,hFrozenP,hFixedA,hFixedP],{countFreshASt,count
FreshPSt,countFrozenASt,countFrozenPSt,countFixedASt,countFixedPSt},'Location','No
rthEast');
%% AVERAGE ACROSS AGE GROUPS AND REGION
for i = 1:length(StressAtStrain_grouped)
```

```
    % Eliminate rows of zeroes
    count = 0;
    delete0 = [];
    for j = 1:length(StressAtStrain_grouped{i}(:,1))
        if StressAtStrain_grouped{i}(j,2) == 0
            delete0(count+1) = j;
            count = count +1;
        end
    end
    StressAtStrain_grouped{i}(delete0,:) = [];

    % Averaging
    StressAtStrain_averaged(i,:) = mean(StressAtStrain_grouped{i},1);
    %StressAtStrain_std(i,:) = std(StressAtStrain_grouped{i},1,1);

end

%% PLOTTING AVERAGED STRESS

% Plot line to connect
plot(strainpts,StressAtStrain_averaged(1,:),'g')
plot(strainpts,StressAtStrain_averaged(2,:),'b')
plot(strainpts,StressAtStrain_averaged(3,:),'r')
plot(strainpts,StressAtStrain_averaged(4,:),'g')
plot(strainpts,StressAtStrain_averaged(5,:),'b')
plot(strainpts,StressAtStrain_averaged(6,:),'r')

% Plot marker
hFreshA =
plot(strainpts,StressAtStrain_averaged(1,:),'LineStyle','x','Color','g','MarkerSize', 12);
hFrozenA =
plot(strainpts,StressAtStrain_averaged(2,:),'LineStyle','x','Color','b','MarkerSize', 12);
hFixedA =
plot(strainpts,StressAtStrain_averaged(3,:),'LineStyle','x','Color','r','MarkerSize', 12);
hFreshP =
plot(strainpts,StressAtStrain_averaged(4,:),'LineStyle','o','Color','g','MarkerSize', 12);
hFrozenP =
plot(strainpts,StressAtStrain_averaged(5,:),'LineStyle','o','Color','b','MarkerSize', 12);
hFixedP =
plot(strainpts,StressAtStrain_averaged(6,:),'LineStyle','o','Color','r','MarkerSize', 12);

% Plot errorbars
%    errorbar(strainpts,StressAtStrain_averaged(1,:),StressAtStrain_std(1,:),'c')
%    errorbar(strainpts,StressAtStrain_averaged(2,:),StressAtStrain_std(2,:),'m')
%    errorbar(strainpts,StressAtStrain_averaged(3,:),StressAtStrain_std(3,:),'y')
%    errorbar(strainpts,StressAtStrain_averaged(4,:),StressAtStrain_std(4,:),'b')
```

```
%     errorbar(strainpts,StressAtStrain_averaged(5,:),StressAtStrain_std(5,:),'r')
%     errorbar(strainpts,StressAtStrain_averaged(6,:),StressAtStrain_std(6,:),'g')

figure(2)
legend([hFreshA,hFreshP,hFrozenA,hFrozenP,hFixedA,hFixedP],{'Fresh,
Anterior','Fresh, Posterior','Frozen, Anterior','Frozen, Posterior','Fixed, Anterior','Fixed,
Posterior'},'Location','NorthEast');


A = [];
count = 0;
for i = 1:length(StressAtStrain)
   for j = 1:length(strainpts)
      if isempty(StressAtStrain{i})
         A(j+count,2) = NaN;
         A(j+count,3) = NaN;
         A(j+count,1) = i;
         A(j+count,4) = NaN;
         A(j+count,5) = NaN;
      else
         A(j+count,2) = strainpts(j);
         A(j+count,3) = StressAtStrain{i}(j,1);
         A(j+count,1) = i;
         A(j+count,4) = Norm_Pull_Sclera{i}(2,7);
         A(j+count,5) = Norm_Pull_Sclera{i}(3,7);
      end
   end
   count = count+length(strainpts);
end

%% IN COMMAND WINDOW, TYPE DESIRED TRIAL AND DATA WILL BE
INDICATED ON GRAPH AS A THICKER LINE
% prompt = 'Enter trial #:';
% trial = input(prompt)
% plot(Norm_Pull_Sclera{trial}(:,6),Norm_Pull_Sclera{trial}(:,3),'--k','LineWidth',2)
% outputString = sprintf('trial # = %d',trial);
% stress_max=find(Norm_Pull_Sclera{trial}(:,3)==max(Norm_Pull_Sclera{trial}(:,3)));
%
text(Norm_Pull_Sclera{trial}(stress_max,6),Norm_Pull_Sclera{trial}(stress_max,3),outp
utString)
%%%%%%%%%%%%%%%%%%%%%%%%%%%%%%%%%%%%%%%%%%%%%%%%%%%%%%%%
```

% PLOTTING STRESS-RELAXATION DATA – AGE AND REGION

% This code calls in the normalized relaxation data and plots all raw trials, as well as, averaged values across age groups and region

```
%%% Variables:
%%% StressAtTime_averaged:
%%% Row 1 --> PRE | ANTERIOR
%%% Row 2 --> INFANT | ANTERIOR
%%% Row 3 --> ADULT | ANTERIOR
%%% Row 4 --> PRE | POSTERIOR
%%% Row 5 --> INFANT | POSTERIOR
%%% Row 6 --> ADULT | POSTERIOR

clear; close all; clc;

load Norm_Relax_Sclera.mat

%% CHOOSE PLOTTING OPTIONS
% PAUSE (1) OR NO PAUSE (0)
% LIST TRIAL (1) OR NO LIST TRIAL (0)

% skip = [139 140 142 145 182 206];
% skip = [139 141 142 144 143 145 182 206 150 151];

% skip = [139 142 144 145];
% skip = [139 141 142 143 144 145];
% skip = [141 158 159 160 164 166 167 173 175 177 179 180 181 182 183 185 202 ...
%     203 205 206 207 208 209 214 216 222 223 224 225 237 238 239 240 247 248 249
250 251 252 253 254 255 257 261 263];

% skip = [144 145 139 142 143 159 161 166 171 173 176 177 190 192 214 216 228 230
232 233 234 243 244 245 246 256 258 260 262 263 265 267];

PauseOrNo = 0;
ListTrialOrNo = 0;

wait = 0.5; % pause s

%% PLOTTING RAW TRIALS & CATEGORIZATION

figure(1)
hold on
% title('Average stress relaxation over age and regions')
ylabel('Stress (MPa)','FontSize',24,'FontName','Times New Roman')
xlabel('Time (s)','FontSize',24,'FontName','Times New Roman')
set(gca,'FontSize',24,'FontName','Times New Roman')
%axis([-50,1000,-0.25,3])

figure(2)
```

```
hold on
% title('Normalized stress relaxation curves')
ylabel('Stress (MPa)','FontSize',24,'FontName','Times New Roman')
xlabel('Time (s)','FontSize',24,'FontName','Times New Roman')
set(gca,'FontSize',24,'FontName','Times New Roman')
% axis([-50,1000,-0.25,2.05])

% SELECTING TIME POINTS TO TAKE AVERAGE
timepts = logspace(0,3,8);              % Logarithmic time points

% FILLING IN SKIP MATRIX
% SKIP = ones(length(Norm_Relax_Sclera),1);
% for i = 1:length(skip)
%     SKIP(skip(i),1) = 0;
% end

% CATEGORIZING ACROSS AGE GROUPS AND REGION
countPreA = 0;
countInfA = 0;
countMatA = 0;
countPreP = 0;
countInfP = 0;
countMatP = 0;

countAll = 0;

%%
for i = 1:length(Norm_Relax_Sclera);

   if  isempty(Norm_Relax_Sclera{i}) %|| SKIP(i,1) == 0

      % Keep this if you want to see average relaxation data for HIGH STRAIN across
age and region (PMT < 6 hours)
   elseif Norm_Relax_Sclera{i}(7,7)>1 && Norm_Relax_Sclera{i}(7,7)<360 &&
Norm_Relax_Sclera{i}(4,7)==31 && Norm_Relax_Sclera{i}(6,7)==51

      % Keep this if you want to see average relaxation data for LOW STRAIN across age
and region
   %elseif Norm_Relax_Sclera{i}(4,7)==31 && Norm_Relax_Sclera{i}(6,7)==52

      countAll = countAll+1;
      TrialsUsed(countAll,1) = i;
      TrialsUsed(countAll,2:3) = [Norm_Relax_Sclera{i}(2,7)
Norm_Relax_Sclera{i}(3,7)];

      for j = 1:length(timepts)
```

```
            k = timepts(j);
            [~, ind] = min(abs(Norm_Relax_Sclera{i}(:,1) - k));
            StressAtTime{i}(j,1) = Norm_Relax_Sclera{i}(ind(1),3);
        end


        % 1 PRE | ANTERIOR
        if Norm_Relax_Sclera{i}(2,7) == 11 && Norm_Relax_Sclera{i}(3,7) == 21
            StressAtTime_grouped{1}(i,:) = StressAtTime{i}(:,1);
            hPreA =
plot(Norm_Relax_Sclera{i}(:,1),Norm_Relax_Sclera{i}(:,3),'LineWidth',1,'LineStyle','-
','Color','b','tag',sprintf('trial = %d',i));
            countPreA = countPreA +1;

            % 2 INFANT | ANTERIOR
        elseif Norm_Relax_Sclera{i}(2,7) == 12 && Norm_Relax_Sclera{i}(3,7) == 21
            StressAtTime_grouped{2}(i,:) = StressAtTime{i}(:,1);
            hInfantA =
plot(Norm_Relax_Sclera{i}(:,1),Norm_Relax_Sclera{i}(:,3),'LineWidth',1,'LineStyle','-
','Color','r','tag',sprintf('trial = %d',i));
            countInfA = countInfA +1;

            % 3 ADULT | ANTERIOR
        elseif Norm_Relax_Sclera{i}(2,7) == 13 && Norm_Relax_Sclera{i}(3,7) == 21
            StressAtTime_grouped{3}(i,:) = StressAtTime{i}(:,1);
            hAdultA =
plot(Norm_Relax_Sclera{i}(:,1),Norm_Relax_Sclera{i}(:,3),'LineWidth',1,'LineStyle','-
','Color','g','tag',sprintf('trial = %d',i));
            countMatA = countMatA +1;

            % 4 PRE | POSTERIOR
        elseif Norm_Relax_Sclera{i}(2,7) == 11 && Norm_Relax_Sclera{i}(3,7) == 22
            StressAtTime_grouped{4}(i,:) = StressAtTime{i}(:,1);
            hPreP =
plot(Norm_Relax_Sclera{i}(:,1),Norm_Relax_Sclera{i}(:,3),'LineWidth',1,'LineStyle','--
','Color','b','tag',sprintf('trial = %d',i));
            countPreP = countPreP+1;

            % 5 INFANT | POSTERIOR
        elseif Norm_Relax_Sclera{i}(2,7) == 12 && Norm_Relax_Sclera{i}(3,7) == 22
            StressAtTime_grouped{5}(i,:) = StressAtTime{i}(:,1);
            hInfantP =
plot(Norm_Relax_Sclera{i}(:,1),Norm_Relax_Sclera{i}(:,3),'LineWidth',1,'LineStyle','--
','Color','r','tag',sprintf('trial = %d',i));
            countInfP = countInfP +1;
```

```
            % 6 ADULT | POSTERIOR
        elseif Norm_Relax_Sclera{i}(2,7) == 13 && Norm_Relax_Sclera{i}(3,7) == 22
            StressAtTime_grouped{6}(i,:) = StressAtTime{i}(:,1);
            hAdultP =
plot(Norm_Relax_Sclera{i}(:,1),Norm_Relax_Sclera{i}(:,3),'LineWidth',1,'LineStyle','--
','Color','g','tag',sprintf('trial = %d',i));
            countMatP = countMatP+1;

        end
        datacursormode on
        dcm = datacursormode(gcf);
        set(dcm,'UpdateFcn',@myupdatefcn)
    end

    %%% Graphing Options
    if ListTrialOrNo == 1;
        outputText = sprintf('trial = %d',i);
        text(90,Norm_Relax_Sclera{i}(end,1),outputText)
    end
    if PauseOrNo == 1;
        pause(wait)
    end
    %%%%%%%%%

end
countPreASt = sprintf('Pre-term A (N=%.f)',countPreA);
countInfASt = sprintf('Infant A (N=%.f)',countInfA);
countMatASt = sprintf('Mature A (N=%.f)',countMatA);
countPrePSt = sprintf('Pre-term P (N=%.f)',countPreP);
countInfPSt = sprintf('Infant P (N=%.f)',countInfP);
countMatPSt = sprintf('Mature P (N=%.f)',countMatP);

figure(1)
%legend([hPreA,hPreP,hInfantA,hInfantP,hAdultA,hAdultP],{'Pre-term, Anterior','Pre-
term, Posterior','Infant, Anterior','Infant, Posterior','Adult, Anterior','Adult,
Posterior'},'Location','NorthEast');
legend([hPreA,hPreP,hInfantA,hInfantP,hAdultA,hAdultP],{countPreASt,countPrePSt,co
untInfASt,countInfPSt,countMatASt,countMatPSt},'Location','NorthEast');

%% AVERAGE ACROSS AGE GROUPS AND REGION
for i = 1:length(StressAtTime_grouped)

    % Eliminate rows of zeroes
    count = 0;
    delete0 = [];
    for j = 1:length(StressAtTime_grouped{i}(:,1))
```

```
        if StressAtTime_grouped{i}(j,1) == 0
            delete0(count+1) = j;
            count = count +1;
        end
    end
    StressAtTime_grouped{i}(delete0,:) = [];

    % Averaging
    StressAtTime_averaged(i,:) = mean(StressAtTime_grouped{i},1);
    StressAtTime_std(i,:) = std(StressAtTime_grouped{i},1,1);

end

%% PLOTTING AVERAGED STRESS

% Plot line to connect
plot(timepts,StressAtTime_averaged(1,:),'b')
plot(timepts,StressAtTime_averaged(2,:),'r')
plot(timepts,StressAtTime_averaged(3,:),'g')
plot(timepts,StressAtTime_averaged(4,:),'b')
plot(timepts,StressAtTime_averaged(5,:),'r')
plot(timepts,StressAtTime_averaged(6,:),'g')

% Plot marker
hPreA = plot(timepts,StressAtTime_averaged(1,:),'LineStyle','x','Color','b','MarkerSize',
12);
hInfantA =
plot(timepts,StressAtTime_averaged(2,:),'LineStyle','x','Color','r','MarkerSize', 12);
hAdultA =
plot(timepts,StressAtTime_averaged(3,:),'LineStyle','x','Color','g','MarkerSize', 12);
hPreP = plot(timepts,StressAtTime_averaged(4,:),'LineStyle','o','Color','b','MarkerSize',
12);
hInfantP = plot(timepts,StressAtTime_averaged(5,:),'LineStyle','o','Color','r','MarkerSize',
12);
hAdultP = plot(timepts,StressAtTime_averaged(6,:),'LineStyle','o','Color','g','MarkerSize',
12);

% Plot errorbars
%    errorbar(timepts,StressAtTime_averaged(1,:),StressAtTime_std(1,:),'b')
%    errorbar(timepts,StressAtTime_averaged(2,:),StressAtTime_std(2,:),'r')
%    errorbar(timepts,StressAtTime_averaged(3,:),StressAtTime_std(3,:),'g')
%    errorbar(timepts,StressAtTime_averaged(4,:),StressAtTime_std(4,:),'b')
%    errorbar(timepts,StressAtTime_averaged(5,:),StressAtTime_std(5,:),'r')
%    errorbar(timepts,StressAtTime_averaged(6,:),StressAtTime_std(6,:),'g')

figure(2)
```

```
legend([hPreA,hPreP,hInfantA,hInfantP,hAdultA,hAdultP],{'Pre-term, Anterior','Pre-
term, Posterior','Infant, Anterior','Infant, Posterior','Mature, Anterior','Mature,
Posterior'},'Location','NorthEast');


A = [];
count = 0;
for i = 1:length(StressAtTime)
   for j = 1:length(timepts)
      if isempty(StressAtTime{i})
         A(j+count,2) = NaN;
         A(j+count,3) = NaN;
         A(j+count,1) = i;
         A(j+count,4) = NaN;
         A(j+count,5) = NaN;
      else
         A(j+count,2) = timepts(j);
         A(j+count,3) = StressAtTime{i}(j,1);
         A(j+count,1) = i;
         A(j+count,4) = Norm_Relax_Sclera{i}(2,7);
         A(j+count,5) = Norm_Relax_Sclera{i}(3,7);
      end
   end
   count = count+8;
end

%% IN COMMAND WINDOW, TYPE DESIRED TRIAL AND DATA WILL BE
INDICATED ON GRAPH AS A THICKER LINE
% prompt = 'Enter trial #:';
% trial = input(prompt)
% plot(Norm_Relax_Sclera{trial}(:,1),Norm_Relax_Sclera{trial}(:,3),'--k','LineWidth',2)
% outputString = sprintf('trial # = %d',trial);
% stress_end=find(Norm_Relax_Sclera{trial}(end,3));
%
text(Norm_Relax_Sclera{trial}(stress_end,1),Norm_Relax_Sclera{trial}(stress_end,3),ou
tputString)


%%%%%%%%%%%%%%%%%%%%%%%%%%%%%%%%%%%%%%%%%%%%%%%%%%%%%%%%
```

% PLOTTING STRESS-RELAXATION DATA – STORAGE CONDITION

% This code calls in the normalized relaxation data and plots all raw trials, as well as, averaged values across condition groups and region

%%% Variables:

```
%%% StressAtTime_averaged:
%%% Row 1 --> FRESH | ANTERIOR
%%% Row 2 --> FROZEN | ANTERIOR
%%% Row 3 --> FIXED | ANTERIOR
%%% Row 4 --> FRESH | POSTERIOR
%%% Row 5 --> FROZEN | POSTERIOR
%%% Row 6 --> FIXED | POSTERIOR

clear; close all; clc;

load Norm_Relax_Sclera.mat

%% CHOOSE PLOTTING OPTIONS
% PAUSE (1) OR NO PAUSE (0)
% LIST TRIAL (1) OR NO LIST TRIAL (0)

% skip = [139 142 143 144 145];
% skip = [139 140 142 145];
% skip = [139 140 142 143 144 145];
% skip = [139 140 142 145 182 206];
% skip = [139 140 142 143 144 145 182 206];
% skip = [141 158 159 160 164 166 167 173 175 177 179 180 181 182 183 185 202 ...
%     203 205 206 207 208 209 214 216 222 223 224 225 237 238 239 240 247 248 249
250 251 252 253 254 255 257 261 263];
% skip = [143 144 145];

skip = [144 145 139 140 142 143 159 161 166 171 173 176 177 190 192 214 216 228
230 232 233 234 243 244 245 246 256 258 260 262 263 265 267];


PauseOrNo = 0;
ListTrialOrNo = 0;

wait = 0.5; % pause s

%% PLOTTING RAW TRIALS & CATEGORIZATION

figure(1)
hold on
% title('Average stress relaxation over condition and regions')
ylabel('Stress (MPa)','FontSize',24,'FontName','Times New Roman')
xlabel('Time (s)','FontSize',24,'FontName','Times New Roman')
set(gca,'FontSize',24,'FontName','Times New Roman')
% axis([0,1050,-0.005,0.08])

figure(2)
```

```
hold on
title('Normalized stress relaxation curves')
ylabel('Stress (MPa)','FontSize',24,'FontName','Times New Roman')
xlabel('Time (s)','FontSize',24,'FontName','Times New Roman')
set(gca,'FontSize',24,'FontName','Times New Roman')
% axis([-50,1000,-0.25,2.05])

% % SELECTING TIME POINTS TO TAKE AVERAGE
timepts = logspace(0,3,8);              % Logarithmic time points

% FILLING IN SKIP MATRIX
SKIP = ones(length(Norm_Relax_Sclera),1);
for i = 1:length(skip)
   SKIP(skip(i),1) = 0;
end

% CATEGORIZING ACROSS AGE GROUPS AND REGION
countFreshA = 0;
countFrozenA = 0;
countFixedA = 0;
countFreshP = 0;
countFrozenP = 0;
countFixedP = 0;

countAll = 0;

%%
for i = 1:length(Norm_Relax_Sclera);

   if isempty(Norm_Relax_Sclera{i}) || SKIP(i,1) == 0

   elseif Norm_Relax_Sclera{i}(5,7)==41

      % Keep this if you want to see average relaxation data for INFANT across region
and storage condition
      %if Norm_Relax_Sclera{i}(2,7) == 11 && Norm_Relax_Sclera{i}(6,7) == 52 ||
Norm_Relax_Sclera{i}(2,7) == 12 && Norm_Relax_Sclera{i}(6,7) == 52

      % Keep this if you want to see average relaxation data for ADULT across region
and storage condition
      if Norm_Relax_Sclera{i}(2,7) == 13 && Norm_Relax_Sclera{i}(6,7) == 52

      countAll = countAll+1;
      for j = 1:length(timepts)
         k = timepts(j);
         [~, ind] = min(abs(Norm_Relax_Sclera{i}(:,1) - k));
```

```
        StressAtTime{i}(j,1) = Norm_Relax_Sclera{i}(ind(1),3);
    end

        % 1 FRESH | ANTERIOR
    if Norm_Relax_Sclera{i}(4,7) == 31 && Norm_Relax_Sclera{i}(3,7) == 21
        StressAtTime_grouped{1}(i,:) = StressAtTime{i}(:,1);
        hFreshA =
plot(Norm_Relax_Sclera{i}(:,1),Norm_Relax_Sclera{i}(:,3),'LineWidth',1,'LineStyle','-
','Color','g','tag',sprintf('trial = %d',i));
        countFreshA = countFreshA +1;

        % 2 FROZEN | ANTERIOR
    elseif Norm_Relax_Sclera{i}(4,7) == 32 && Norm_Relax_Sclera{i}(3,7) == 21
        StressAtTime_grouped{2}(i,:) = StressAtTime{i}(:,1);
        hFrozenA =
plot(Norm_Relax_Sclera{i}(:,1),Norm_Relax_Sclera{i}(:,3),'LineWidth',1,'LineStyle','-
','Color','b','tag',sprintf('trial = %d',i));
        countFrozenA = countFrozenA +1;

        % 3 FIXED | ANTERIOR
    elseif Norm_Relax_Sclera{i}(4,7) == 33 && Norm_Relax_Sclera{i}(3,7) == 21
        StressAtTime_grouped{3}(i,:) = StressAtTime{i}(:,1);
        hFixedA =
plot(Norm_Relax_Sclera{i}(:,1),Norm_Relax_Sclera{i}(:,3),'LineWidth',1,'LineStyle','-
','Color','r','tag',sprintf('trial = %d',i));
        countFixedA = countFixedA +1;

        % 4 FRESH | POSTERIOR
    elseif Norm_Relax_Sclera{i}(4,7) == 31 && Norm_Relax_Sclera{i}(3,7) == 22
        StressAtTime_grouped{4}(i,:) = StressAtTime{i}(:,1);
        hFreshP =
plot(Norm_Relax_Sclera{i}(:,1),Norm_Relax_Sclera{i}(:,3),'LineWidth',1,'LineStyle','--
','Color','g','tag',sprintf('trial = %d',i));
        countFreshP = countFreshP+1;

        % 5 FROZEN | POSTERIOR
    elseif Norm_Relax_Sclera{i}(4,7) == 32 && Norm_Relax_Sclera{i}(3,7) == 22
        StressAtTime_grouped{5}(i,:) = StressAtTime{i}(:,1);
        hFrozenP =
plot(Norm_Relax_Sclera{i}(:,1),Norm_Relax_Sclera{i}(:,3),'LineWidth',1,'LineStyle','--
','Color','b','tag',sprintf('trial = %d',i));
        countFrozenP = countFrozenP +1;

        % 6 FIXED | POSTERIOR
    elseif Norm_Relax_Sclera{i}(4,7) == 33 && Norm_Relax_Sclera{i}(3,7) == 22
        StressAtTime_grouped{6}(i,:) = StressAtTime{i}(:,1);
```

```
            hFixedP =
plot(Norm_Relax_Sclera{i}(:,1),Norm_Relax_Sclera{i}(:,3),'LineWidth',1,'LineStyle','--
','Color','r','tag',sprintf('trial = %d',i));
            countFixedP = countFixedP+1;
         end

      datacursormode on
      dcm = datacursormode(gcf);
      set(dcm,'UpdateFcn',@myupdatefcn)

      end

      %%% Graphing Options
      if ListTrialOrNo == 1;
         outputText = sprintf('trial = %d',i);
         text(90,Norm_Relax_Sclera{i}(end,1),outputText)
      end

      if PauseOrNo == 1;
         pause(wait)
      end
      %%%%%%%%%
   end
end
countFreshASt = sprintf('Fresh Ant (N=%.f)',countFreshA);
countFrozenASt = sprintf('Frozen Ant (N=%.f)',countFrozenA);
countFixedASt = sprintf('Fixed Ant (N=%.f)',countFixedA);
countFreshPSt = sprintf('Fresh Post (N=%.f)',countFreshP);
countFrozenPSt = sprintf('Frozen Post (N=%.f)',countFrozenP);
countFixedPSt = sprintf('Fixed Post (N=%.f)',countFixedP);

figure(1)
legend([hFreshA,hFreshP,hFrozenA,hFrozenP,hFixedA,hFixedP],{'Fresh,
Anterior','Fresh, Posterior','Frozen, Anterior','Frozen, Posterior','Fixed, Anterior','Fixed,
Posterior'},'Location','NorthEast');
legend([hFreshA,hFreshP,hFrozenA,hFrozenP,hFixedA,hFixedP],{countFreshASt,count
FreshPSt,countFrozenASt,countFrozenPSt,countFixedASt,countFixedPSt},'Location','No
rthEast');

   %% AVERAGE ACROSS AGE GROUPS AND REGION
   for i = 1:length(StressAtTime_grouped)

      % Eliminate rows of zeroes
      count = 0;
      delete0 = [];
      for j = 1:length(StressAtTime_grouped{i}(:,1))
```

```
        if StressAtTime_grouped{i}(j,1) == 0
            delete0(count+1) = j;
            count = count +1;
        end
    end
    StressAtTime_grouped{i}(delete0,:) = [];

    % Averaging
    StressAtTime_averaged(i,:) = mean(StressAtTime_grouped{i},1);
    StressAtTime_std(i,:) = std(StressAtTime_grouped{i},1,1);
end

%% PLOTTING AVERAGED STRESS

% Plot line to connect
plot(timepts,StressAtTime_averaged(1,:),'g')
plot(timepts,StressAtTime_averaged(2,:),'b')
plot(timepts,StressAtTime_averaged(3,:),'r')
plot(timepts,StressAtTime_averaged(4,:),'g')
plot(timepts,StressAtTime_averaged(5,:),'b')
plot(timepts,StressAtTime_averaged(6,:),'r')

% Plot marker
hFreshA =
plot(timepts,StressAtTime_averaged(1,:),'LineStyle','x','Color','g','MarkerSize', 12);
hFrozenA =
plot(timepts,StressAtTime_averaged(2,:),'LineStyle','x','Color','b','MarkerSize', 12);
hFixedA =
plot(timepts,StressAtTime_averaged(3,:),'LineStyle','x','Color','r','MarkerSize', 12);
hFreshP =
plot(timepts,StressAtTime_averaged(4,:),'LineStyle','o','Color','g','MarkerSize', 12);
hFrozenP =
plot(timepts,StressAtTime_averaged(5,:),'LineStyle','o','Color','b','MarkerSize', 12);
hFixedP =
plot(timepts,StressAtTime_averaged(6,:),'LineStyle','o','Color','r','MarkerSize', 12);

%    % Plot errorbars
%    errorbar(timepts,StressAtTime_averaged(1,:),StressAtTime_std(1,:),'g')
%    errorbar(timepts,StressAtTime_averaged(2,:),StressAtTime_std(2,:),'b')
%    errorbar(timepts,StressAtTime_averaged(3,:),StressAtTime_std(3,:),'r')
%    errorbar(timepts,StressAtTime_averaged(4,:),StressAtTime_std(4,:),'g')
%    errorbar(timepts,StressAtTime_averaged(5,:),StressAtTime_std(5,:),'b')
%    errorbar(timepts,StressAtTime_averaged(6,:),StressAtTime_std(6,:),'r')

figure(2)
legend([hFreshA,hFreshP,hFrozenA,hFrozenP,hFixedA,hFixedP],{'Fresh,
```

```
Anterior','Fresh, Posterior','Frozen, Anterior','Frozen, Posterior','Fixed, Anterior','Fixed,
Posterior'},'Location','NorthEast');


   A = [];
   count = 0;
   for i = 1:length(StressAtTime)
      for j = 1:length(timepts)
         if isempty(StressAtTime{i})
            A(j+count,2) = NaN;
            A(j+count,3) = NaN;
            A(j+count,1) = i;
            A(j+count,4) = NaN;
            A(j+count,5) = NaN;
            A(j+count,6) = NaN;
         else
            A(j+count,2) = timepts(j);
            A(j+count,3) = StressAtTime{i}(j,1);
            A(j+count,1) = i;
            A(j+count,4) = Norm_Relax_Sclera{i}(2,7);
            A(j+count,5) = Norm_Relax_Sclera{i}(3,7);
            A(j+count,6) = Norm_Relax_Sclera{i}(4,7);
         end
      end
      count = count+8;
   end

%% IN COMMAND WINDOW, TYPE DESIRED TRIAL AND DATA WILL BE
INDICATED ON GRAPH AS A THICKER LINE
% prompt = 'Enter trial #:';
% trial = input(prompt)
% plot(Norm_Relax_Sclera{trial}(:,1),Norm_Relax_Sclera{trial}(:,3),'--k','LineWidth',2)
% outputString = sprintf('trial # = %d',trial);
% stress_end=find(Norm_Relax_Sclera{trial}(end,3));
%
text(Norm_Relax_Sclera{trial}(stress_end,1),Norm_Relax_Sclera{trial}(stress_end,3),ou
tputString)
```

APPENDIX C

MATLAB CODE FOR RETINAL ANALYSIS AND PLOTTING

```
% RETINAANALYSIS_PLOTTING
% This code calls in the uploaded 'RawData' and analyzes the retina pull-to-failure data

%%% Variables:
%%% RawData{trial} = [time(s) load(N) Stress(MPa) Extension(mm) Strain(%)
Strain(mm/mm) TestParameters]
%%% RetinaPullFail{trial} = [time(s) load(N) Stress(Mpa) Extension(mm) Strain(%)
Strain(mm/mm) TestParameters]
%%% NormPull_Retina{trial} = [time(s) load(N) Stress(MPa) Extension(mm) Strain(%)
Strain(mm/mm) TestParameters]

clear; clc; close all;
load('RawData.mat')
%% SHOW FIGURE OPTIONS
Raw_Retina = 1;
NormalizedPull_Retina = 1;
Plotting_Retina = 1;

zeroline = zeros(length(RawData{1}(:,1)),1);

for i = 1:length(RawData);
if isempty(RawData{i})

   % Keep this set to 42 to ensure only retinal trials are being analyzed
elseif RawData{i}(5,7) == 42

      [RetinaPullFail{i}(:,3), RetinaPullFail{i}(:,6)] =
Retina_DataCalcs(RawData{i}(:,2),RawData{i}(1,7),RawData{i}(:,4));
      RetinaPullFail{i}(:,1) = RawData{i}(:,1);
      RetinaPullFail{i}(:,2) = RawData{i}(:,2);
      RetinaPullFail{i}(:,4) = RawData{i}(:,4);
      RetinaPullFail{i}(:,5) = RawData{i}(:,5);
      RetinaPullFail{i}(:,7) = RawData{i}(:,7);

      clear t tlowerlim tupperlim tstart tend

      if RetinaPullFail{i}(end,1) > 1000
         t = round(RetinaPullFail{i}(:,1)*10)./10;
         %tlowerlim = find(t==1040);
         %tupperlim = find(RetinaPullFail{i}(:,1),1,'last');
         %tstart = find(RetinaPullFail{i}(tlowerlim:tupperlim,5)==0,1,'last');
         tstart = find(RetinaPullFail{i}(:,5)==0,1,'last');
         tend = find(RetinaPullFail{i}(:,5),1,'last');
      else%if RawData{i}(:,1) < 1000
         t = round(RetinaPullFail{i}(:,1)*10)./10;
         tlowerlim = find(t==21);
```

```
        tupperlim = find(RetinaPullFail{i}(:,1),1,'last');
        tstart = find(RetinaPullFail{i}(:,5)>1.01,1,'first');
        tend = find(RetinaPullFail{i}(:,5),1,'last');
%           time = round(RawData{i}(:,1)*10)./10;
%           tlow = find(time==19,1,'first');
%           tup = find(time==20,1,'first');
%           tstart = find(RawData{i}(:,2)==min(RawData{i}(tlow:tup,2)));
%           RawData{i}(:,2)=RawData{i}(:,2)-RawData{i}(tstart(1),2);
    end

    % Normalized data as a new variable
    NormPull_Retina{i}(:,1:3) = [RetinaPullFail{i}(tstart:tend,1)-
RetinaPullFail{i}(tstart(1),1),abs(RetinaPullFail{i}(tstart:tend,2)-
RetinaPullFail{i}(tstart,2)),abs(RetinaPullFail{i}(tstart:tend,3)-
RetinaPullFail{i}(tstart,3))];
    NormPull_Retina{i}(:,4:7) =
[RetinaPullFail{i}(tstart:tend,4),RetinaPullFail{i}(tstart:tend,5),RetinaPullFail{i}(tstart:t
end,6),RetinaPullFail{i}(1:length(tstart:tend),7)];

    % Plotting normalized retinal data
    if NormalizedPull_Retina == 1
        figure(1)
        plot(NormPull_Retina{i}(:,6),NormPull_Retina{i}(:,3),'k')
        hold on
        xlabel('Strain (mm/mm)')
        ylabel('Stress (MPa)')
        % outputString = sprintf('Normalized Retinal pull-to-failure data, trial = %d',i);
        % title(outputString)
        % xlim([0,10])
    elseif NormalizedPull_Retina == 0
    end

    % Plotting by age, direction, strain, and condition
    if Plotting_Retina == 1
        figure(2)
        % line([0 0], [0 0.07],'Color','k')

        % Preterm, Parallel
        if NormPull_Retina{i}(2,7) == 11 && NormPull_Retina{i}(3,7) == 24
            plot(NormPull_Retina{i}(:,6),NormPull_Retina{i}(:,3),'-c','tag',sprintf('trial =
%d',i))
            hold on
            datacursormode on
            dcm = datacursormode(gcf);
            set(dcm,'UpdateFcn',@myupdatefcn)
        % Preterm, Perpendicular
```

```
        elseif NormPull_Retina{i}(2,7) == 11 && NormPull_Retina{i}(3,7) == 25
            plot(NormPull_Retina{i}(:,6),NormPull_Retina{i}(:,3),'--b','tag',sprintf('trial =
%d',i))
            hold on
            datacursormode on
            dcm = datacursormode(gcf);
            set(dcm,'UpdateFcn',@myupdatefcn)
        % Infant, Parallel
        elseif NormPull_Retina{i}(2,7) == 12 && NormPull_Retina{i}(3,7) == 24
            plot(NormPull_Retina{i}(:,6),NormPull_Retina{i}(:,3),'-m','tag',sprintf('trial =
%d',i))
            hold on
            datacursormode on
            dcm = datacursormode(gcf);
            set(dcm,'UpdateFcn',@myupdatefcn)
        % Infant, Perpendicular
        elseif NormPull_Retina{i}(2,7) == 12 && NormPull_Retina{i}(3,7) == 25
            plot(NormPull_Retina{i}(:,6),NormPull_Retina{i}(:,3),'--r','tag',sprintf('trial =
%d',i))
            hold on
            datacursormode on
            dcm = datacursormode(gcf);
            set(dcm,'UpdateFcn',@myupdatefcn)
        % Adult, Parallel
        elseif NormPull_Retina{i}(2,7) == 13 && NormPull_Retina{i}(3,7) == 24
            plot(NormPull_Retina{i}(:,6),NormPull_Retina{i}(:,3),'-y','tag',sprintf('trial =
%d',i))
            hold on
            datacursormode on
            dcm = datacursormode(gcf);
            set(dcm,'UpdateFcn',@myupdatefcn)
        % Adult, Perpendicular
        elseif NormPull_Retina{i}(2,7) == 13 && NormPull_Retina{i}(3,7) == 25
            plot(NormPull_Retina{i}(:,6),NormPull_Retina{i}(:,3),'--g','tag',sprintf('trial =
%d',i))
            hold on
            datacursormode on
            dcm = datacursormode(gcf);
            set(dcm,'UpdateFcn',@myupdatefcn)
        % Preterm, ?
        elseif NormPull_Retina{i}(2,7) == 11 && NormPull_Retina{i}(3,7) == 23
            plot(NormPull_Retina{i}(:,6),NormPull_Retina{i}(:,3),'.c','tag',sprintf('trial =
%d',i))
            hold on
            datacursormode on
            dcm = datacursormode(gcf);
```

```
            set(dcm,'UpdateFcn',@myupdatefcn)
        % Preterm, None
        elseif NormPull_Retina{i}(2,7) == 11 && NormPull_Retina{i}(3,7) == 26
            plot(NormPull_Retina{i}(:,6),NormPull_Retina{i}(:,3),'.b','tag',sprintf('trial =
%d',i))
            hold on
            datacursormode on
            dcm = datacursormode(gcf);
            set(dcm,'UpdateFcn',@myupdatefcn)
        % Infant, ?
        elseif NormPull_Retina{i}(2,7) == 12 && NormPull_Retina{i}(3,7) == 23
            plot(NormPull_Retina{i}(:,6),NormPull_Retina{i}(:,3),'+m','tag',sprintf('trial =
%d',i))
            hold on
            datacursormode on
            dcm = datacursormode(gcf);
            set(dcm,'UpdateFcn',@myupdatefcn)
        % Infant, None
        elseif NormPull_Retina{i}(2,7) == 12 && NormPull_Retina{i}(3,7) == 26
            plot(NormPull_Retina{i}(:,6),NormPull_Retina{i}(:,3),'+r','tag',sprintf('trial =
%d',i))
            hold on
            datacursormode on
            dcm = datacursormode(gcf);
            set(dcm,'UpdateFcn',@myupdatefcn)
        % Adult, ?
        elseif NormPull_Retina{i}(2,7) == 13 && NormPull_Retina{i}(3,7) == 23
            plot(NormPull_Retina{i}(:,6),NormPull_Retina{i}(:,3),'xy','tag',sprintf('trial =
%d',i))
            hold on
            datacursormode on
            dcm = datacursormode(gcf);
            set(dcm,'UpdateFcn',@myupdatefcn)
        % Adult, None
        elseif NormPull_Retina{i}(2,7) == 13 && NormPull_Retina{i}(3,7) == 26
            plot(NormPull_Retina{i}(:,6),NormPull_Retina{i}(:,3),'xg','tag',sprintf('trial =
%d',i))
            hold on
            datacursormode on
            dcm = datacursormode(gcf);
            set(dcm,'UpdateFcn',@myupdatefcn)
        end
        xlabel('Strain (mm/mm)')
        ylabel('Stress (MPa)')
        % xlim([0,10])
    elseif Plotting_Retina == 0
```

```
        end
    end
end

%%
% if Raw_Retina == 1
%     for i = 1:length(RawData);
%         if RawData{i}(5,7) == 42
%             figure(3)
%             plot(RawData{i}(:,1),RawData{i}(:,2))
%             hold on
%             xlabel('Time (s)')
%             ylabel('Load (N)')
% %               outputString = sprintf('Normalized Retinal pull-to-failure data, trial = %d',i);
% %               title(outputString)
%         end
%     end
% elseif Raw_Retina == 0
% end

%% SAVING
% save('NormPull_Retina','NormPull_Retina')


%%%%%%%%%%%%%%%%%%%%%%%%%%%%%%%%%%%%%%%%%%%%%%%%%%%%%%%%%%%%%%%%
```

% PLOTTING PULL-TO-FAILURE DATA – AGE AND RATE

% This code calls in the normalized pull-to-failure data and plots all raw trials, as well as, averaged values across age groups and strain-rate

```
%%% Variables:
%%% StressAtStrain_averaged:
%%% Row 1 --> PRE
%%% Row 2 --> INFANT
%%% Row 3 --> ADULT

clear; close all; clc;

load NormPull_Retina.mat

%% CHOOSE PLOTTING OPTIONS

% PAUSE (1) OR NO PAUSE (0)
% LIST TRIAL (1) OR NO LIST TRIAL (0)
```

```
skip = [130 131];

PauseOrNo = 0;
ListTrialOrNo = 0;

wait = 0.5; % pause s

%%
% FILLING IN SKIP MATRIX
SKIP = ones(length(NormPull_Retina),1);
for i = 1:length(skip)
   SKIP(skip(i),1) = 0;
end

%% PLOTTING RAW TRIALS & CATEGORIZATION

figure(1)
hold on
% title('Average stress-strain over age and region')
ylabel('Stress (MPa)','FontSize',24,'FontName','Times New Roman')
xlabel('Strain (mm/mm)','FontSize',24,'FontName','Times New Roman')
set(gca,'FontSize',24,'FontName','Times New Roman')
%axis([-50,1000,-0.25,3])
xlim([0,1])

figure(2)
hold on
% title('Normalized stress-strain curves')
ylabel('Stress (MPa)','FontSize',24,'FontName','Times New Roman')
xlabel('Strain (mm/mm)','FontSize',24,'FontName','Times New Roman')
set(gca,'FontSize',24,'FontName','Times New Roman')
xlim([0,1])

% % SELECTING TIME POINTS TO TAKE AVERAGE
% strainpts = 0:0.01:0.23;
strainpts = 0:0.01:3;
% strainpts(end) = [];
% strainpts = floor(strainpts*100)./100;

% CATEGORIZING ACROSS AGE GROUPS AND REGION
countPre = 0;
countAdult = 0;

countAll = 0;

%%
```

```
for i = 1:length(NormPull_Retina);

   if  isempty(NormPull_Retina{i}) || SKIP(i,1) == 0

      % Keep this if you want to see average pull data for HIGH STRAIN across age
   elseif NormPull_Retina{i}(4,7)==31 && NormPull_Retina{i}(6,7)==51

      % Keep this if you want to see average pull data for LOW STRAIN across age and
region
   %elseif NormPull_Retina{i}(4,7)==31 && NormPull_Retina{i}(6,7)==52

      countAll = countAll+1;

      for j = 1:length(strainpts)
         k = strainpts(j);
         [~, ind] = min(abs(NormPull_Retina{i}(:,6) - k));
         StressAtStrain{i}(j,1) = NormPull_Retina{i}(ind(1),3);
      end

         % IMMATURE
      if NormPull_Retina{i}(2,7) == 11 || NormPull_Retina{i}(2,7) == 12
         StressAtStrain_grouped{1}(i,:) = StressAtStrain{i}(:,1);
         hPre =
plot(NormPull_Retina{i}(:,6),NormPull_Retina{i}(:,3),'LineWidth',1,'LineStyle','-
','Color','b','tag',sprintf('trial = %d',i));
         countPre = countPre +1;
         % MATURE
      elseif NormPull_Retina{i}(2,7) == 13
         StressAtStrain_grouped{2}(i,:) = StressAtStrain{i}(:,1);
         hAdult =
plot(NormPull_Retina{i}(:,6),NormPull_Retina{i}(:,3),'LineWidth',1,'LineStyle','-
','Color','r','tag',sprintf('trial = %d',i));
         countAdult = countAdult +1;
      end

      datacursormode on
      dcm = datacursormode(gcf);
      set(dcm,'UpdateFcn',@myupdatefcn)
   end

   %%% Graphing Options
   if ListTrialOrNo == 1;
      outputText = sprintf('trial = %d',i);
      text(90,NormPull_Retina{i}(end,1),outputText)
   end
   if PauseOrNo == 1;
```

```
        pause(wait)
    end
end

%%%%%%%%%

countPreSt = sprintf('Preterm (N=%.f)',countPre);
countAdultSt = sprintf('Adult (N=%.f)',countAdult);

figure(1)
legend([hPre,hAdult],{'Immature','Mature'},'Location','NorthWest');
%legend([hPre,hAdult],{countPreSt,countAdultSt},'Location','NorthEast');


%% AVERAGE ACROSS AGE GROUPS AND REGION
for i = 1:length(StressAtStrain_grouped)

    % Eliminate rows of zeroes
    count = 0;
    delete0 = [];
    for j = 1:length(StressAtStrain_grouped{i}(:,1))
        if StressAtStrain_grouped{i}(j,233) == 0 && StressAtStrain_grouped{i}(j,38) == 0
&& StressAtStrain_grouped{i}(j,230) == 0 && StressAtStrain_grouped{i}(j,225) == 0
            delete0(count+1) = j;
            count = count +1;
        end
    end
    StressAtStrain_grouped{i}(delete0,:) = [];

    % Averaging
    StressAtStrain_averaged(i,:) = mean(StressAtStrain_grouped{i},1);
    StressAtStrain_std(i,:) = std(StressAtStrain_grouped{i},0,1);

end

%% PLOTTING AVERAGED STRESS

% Plot line to connect
plot(strainpts,StressAtStrain_averaged(1,:),'b')
plot(strainpts,StressAtStrain_averaged(2,:),'r')

% Plot marker
hPre = plot(strainpts,StressAtStrain_averaged(1,:),'LineStyle','x','Color','b','MarkerSize',
12);
hAdult = plot(strainpts,StressAtStrain_averaged(2,:),'LineStyle','x','Color','r','MarkerSize',
12);
```

```
% Plot errorbars
% errorbar(strainpts,StressAtStrain_averaged(1,:),StressAtStrain_std(1,:),'b')
% errorbar(strainpts,StressAtStrain_averaged(2,:),StressAtStrain_std(3,:),'g')

figure(2)
legend([hPre,hAdult],{'Immature','Mature'},'Location','NorthWest');


A = [];
count = 0;
for i = 1:length(StressAtStrain)
   for j = 1:length(strainpts)
      if isempty(StressAtStrain{i})
         A(j+count,2) = NaN;
         A(j+count,3) = NaN;
         A(j+count,1) = i;
         A(j+count,4) = NaN;
         A(j+count,5) = NaN;
      else
         A(j+count,2) = strainpts(j);
         A(j+count,3) = StressAtStrain{i}(j,1);
         A(j+count,1) = i;
         A(j+count,4) = NormPull_Retina{i}(2,7);
         A(j+count,5) = NormPull_Retina{i}(3,7);
      end
   end
   count = count+length(strainpts);
end

%%
% We are limited by our low capacity load cell. Not all tissues fail when tested at low-
strain
% Maximum stresses of all trials at the lowest strain (so to compare peak stresses at same
strain)
% for i = 1:length(StressAtStrain)
%     if isempty(StressAtStrain{i})
%         else Max_StressAtStrain(i,:)=[StressAtStrain{i}(24,1)];
%     end
% end

%% IN COMMAND WINDOW, TYPE DESIRED TRIAL AND DATA WILL BE
INDICATED ON GRAPH AS A THICKER LINE
% prompt = 'Enter trial #:';
% trial = input(prompt)
```

```
% plot(NormPull_Retina{trial}(:,6),NormPull_Retina{trial}(:,3),'--k','LineWidth',2)
% outputString = sprintf('trial # = %d',trial);
% stress_max=find(NormPull_Retina{trial}(:,3)==max(NormPull_Retina{trial}(:,3)));
%
text(NormPull_Retina{trial}(stress_max,6),NormPull_Retina{trial}(stress_max,3),output
String)


%%%%%%%%%%%%%%%%%%%%%%%%%%%%%%%%%%%%%%%%%%%%%%%%%%%%%%%%%%%%%%%%
```

% PLOTTING PULL-TO-FAILURE DATA – STORAGE CONDITION

```
% This code calls in the normalized pull-to-failure data and plots all raw trials, as well as,
averaged values across storage groups and region

%%% Variables:
%%% StressAtStrain_averaged:
%%% Row 1 --> Fresh
%%% Row 2 --> INFANT
%%% Row 3 --> Frozen

clear; close all; clc;

load NormPull_Retina.mat

%% CHOOSE PLOTTING OPTIONS
% PAUSE (1) OR NO PAUSE (0)
% LIST TRIAL (1) OR NO LIST TRIAL (0)

PauseOrNo = 0;
ListTrialOrNo = 0;

wait = 0.5; % pause s

%% PLOTTING RAW TRIALS & CATEGORIZATION

figure(1)
hold on
% title('Average stress-strain over age and region')
ylabel('Stress (MPa)','FontSize',24,'FontName','Times New Roman')
xlabel('Strain (mm/mm)','FontSize',24,'FontName','Times New Roman')
set(gca,'FontSize',24,'FontName','Times New Roman')
%axis([-50,1000,-0.25,3])
xlim([0,1])

figure(2)
```

```
hold on
% title('Normalized stress-strain curves')
ylabel('Stress (MPa)','FontSize',24,'FontName','Times New Roman')
xlabel('Strain (mm/mm)','FontSize',24,'FontName','Times New Roman')
set(gca,'FontSize',24,'FontName','Times New Roman')
xlim([0,1])

% % SELECTING TIME POINTS TO TAKE AVERAGE
% strainpts = 0:0.01:0.23;
strainpts = 0:0.01:3;
% strainpts(end) = [];
% strainpts = floor(strainpts*100)./100;

% CATEGORIZING ACROSS AGE GROUPS AND REGION
countFresh = 0;
countFrozen = 0;
countFixed = 0;

countAll = 0;




%%
for i = 1:length(NormPull_Retina);

   if  isempty(NormPull_Retina{i}) || NormPull_Retina{i}(6,7)==51%% || i==131 ||
i==130 || i==126 || i==127

      % Keep this if you want to see average pull data for IMMATURE across
      % storage condition at LOW STRAIN
   elseif NormPull_Retina{i}(2,7)==11 || NormPull_Retina{i}(2,7)==12


%       % Keep this if you want to see average pull data for MATURE across
%       % storage condition at LOW STRAIN
   %elseif NormPull_Retina{i}(2,7)==13 && NormPull_Retina{i}(6,7)==52

      countAll = countAll+1;

      for j = 1:length(strainpts)
         k = strainpts(j);
         [~, ind] = min(abs(NormPull_Retina{i}(:,6) - k));
         StressAtStrain{i}(j,1) = NormPull_Retina{i}(ind(1),3);
      end
```

```
            % FRESH
        if NormPull_Retina{i}(4,7) == 31
            StressAtStrain_grouped{1}(i,:) = StressAtStrain{i}(:,1);
            hFresh =
plot(NormPull_Retina{i}(:,6),NormPull_Retina{i}(:,3),'LineWidth',1,'LineStyle','-
','Color','g','tag',sprintf('trial = %d',i));
            countFresh = countFresh +1;
            % FROZEN
        elseif NormPull_Retina{i}(4,7) == 32
            StressAtStrain_grouped{2}(i,:) = StressAtStrain{i}(:,1);
            hFrozen =
plot(NormPull_Retina{i}(:,6),NormPull_Retina{i}(:,3),'LineWidth',1,'LineStyle','-
','Color','b','tag',sprintf('trial = %d',i));
            countFrozen = countFrozen +1;
            % FIXED
        elseif NormPull_Retina{i}(4,7) == 33
            StressAtStrain_grouped{3}(i,:) = StressAtStrain{i}(:,1);
            hFixed =
plot(NormPull_Retina{i}(:,6),NormPull_Retina{i}(:,3),'LineWidth',1,'LineStyle','-
','Color','r','tag',sprintf('trial = %d',i));
            countFixed = countFixed +1;
        end

        datacursormode on
        dcm = datacursormode(gcf);
        set(dcm,'UpdateFcn',@myupdatefcn)
    end

    %%% Graphing Options
    if ListTrialOrNo == 1;
        outputText = sprintf('trial = %d',i);
        text(90,NormPull_Retina{i}(end,1),outputText)
    end
    if PauseOrNo == 1;
        pause(wait)
    end
end

%%%%%%%%%

countFreshSt = sprintf('Freshterm (N=%.f)',countFresh);
countFrozenSt = sprintf('Frozen (N=%.f)',countFrozen);

figure(1)
legend([hFresh,hFrozen,hFixed],{'Fresh','Frozen','Fixed'},'Location','NorthWest');
%legend([hFresh,hFrozen],{countFreshSt,countFrozenSt},'Location','NorthEast');
```

```
%% AVERAGE ACROSS AGE GROUPS AND REGION
for i = 1:length(StressAtStrain_grouped)

   % Eliminate rows of zeroes
   count = 0;
   delete0 = [];
   for j = 1:length(StressAtStrain_grouped{i}(:,1))
      if StressAtStrain_grouped{i}(j,233) == 0 && StressAtStrain_grouped{i}(j,230) ==
0 && StressAtStrain_grouped{i}(j,225) == 0
         delete0(count+1) = j;
         count = count +1;
      end
   end
   StressAtStrain_grouped{i}(delete0,:) = [];

   % Averaging
   StressAtStrain_averaged(i,:) = mean(StressAtStrain_grouped{i},1);
   StressAtStrain_std(i,:) = std(StressAtStrain_grouped{i},0,1);

end

%% PLOTTING AVERAGED STRESS

% Plot line to connect
plot(strainpts,StressAtStrain_averaged(1,:),'g')
plot(strainpts,StressAtStrain_averaged(2,:),'b')
plot(strainpts,StressAtStrain_averaged(3,:),'r')

% Plot marker
hFresh =
plot(strainpts,StressAtStrain_averaged(1,:),'LineStyle','x','Color','g','MarkerSize', 12);
hFrozen =
plot(strainpts,StressAtStrain_averaged(2,:),'LineStyle','x','Color','b','MarkerSize', 12);
hFixed = plot(strainpts,StressAtStrain_averaged(3,:),'LineStyle','x','Color','r','MarkerSize',
12);


% Plot errorbars
% errorbar(strainpts,StressAtStrain_averaged(1,:),StressAtStrain_std(1,:),'b')
% errorbar(strainpts,StressAtStrain_averaged(2,:),StressAtStrain_std(3,:),'g')

figure(2)
legend([hFresh,hFrozen,hFixed],{'Fresh','Frozen','Fixed'},'Location','NorthWest');
```

```
A = [];
count = 0;
for i = 1:length(StressAtStrain)
   for j = 1:length(strainpts)
      if isempty(StressAtStrain{i})
         A(j+count,2) = NaN;
         A(j+count,3) = NaN;
         A(j+count,1) = i;
         A(j+count,4) = NaN;
         A(j+count,5) = NaN;
      else
         A(j+count,2) = strainpts(j);
         A(j+count,3) = StressAtStrain{i}(j,1);
         A(j+count,1) = i;
         A(j+count,4) = NormPull_Retina{i}(2,7);
         A(j+count,5) = NormPull_Retina{i}(3,7);
      end
   end
   count = count+length(strainpts);
end

%%
% We are limited by our low capacity load cell. Not all tissues fail when tested at low-
strain
% Maximum stresses of all trials at the lowest strain (so to compare peak stresses at same
strain)
% for i = 1:length(StressAtStrain)
%     if isempty(StressAtStrain{i})
%         else Max_StressAtStrain(i,:)=[StressAtStrain{i}(24,1)];
%     end
% end

%% IN COMMAND WINDOW, TYPE DESIRED TRIAL AND DATA WILL BE
INDICATED ON GRAPH AS A THICKER LINE
% prompt = 'Enter trial #:';
% trial = input(prompt)
% plot(NormPull_Retina{trial}(:,6),NormPull_Retina{trial}(:,3),'--k','LineWidth',2)
% outputString = sprintf('trial # = %d',trial);
% stress_max=find(NormPull_Retina{trial}(:,3)==max(NormPull_Retina{trial}(:,3)));
%
text(NormPull_Retina{trial}(stress_max,6),NormPull_Retina{trial}(stress_max,3),output
String)
```

APPENDIX D

SCLERA AND RETINA DATA

Table 20: Sclera data for material property evaluation with age, region, and strain-rate.

Age	A/P	Thick. (mm)	Strain	τ1 (sec)	σ1 (MPa)	τ2 (sec)	σ2 (MPa)	σi (MPa)	σe (MPa)	εtoe	E (MPa)	σult (MPa)	εult
Pre	Ant	0.4238	Low							0.14	21.91	5.76	0.41
Pre	Ant	0.2952	Low							0.95	70.21	19.17	0.52
Pre	Ant	0.4815	Low							0.20	12.20	4.82	0.62
Pre	Ant	0.5426	Low							0.17	18.51	5.34	0.47
Pre	Ant	0.2994	Low							0.10	8.54	2.08	0.38
Pre	Ant	0.3875	Low							0.09	11.23	2.38	0.31
Pre	Ant	0.3890	Low							0.19	7.57	2.50	0.56
Pre	Ant	0.4043	Low							0.16	12.64	3.54	0.43
Pre	Ant	0.3998	High	267.87	0.94	17.58	1.22	3.18	1.02	0.25	27.26	6.63	0.55
Pre	Ant	0.3366	High	261.15	0.56	9.96	0.98	2.58	1.03	0.22	24.41	4.51	0.49
Pre	Ant	0.3725	High	222.82	0.25	7.69	0.57	1.23	0.41	0.21	17.07	2.85	0.41
Pre	Ant	0.4243	High	484.70	0.04	14.53	0.07	0.14	0.02	0.40	13.71	3.88	0.65
Pre	Post	0.7015	Low							0.23	24.82	6.95	0.56
Pre	Post	0.9215	Low							0.26	16.27	4.36	0.53
Pre	Post	0.7213	Low							0.25	20.05	4.70	0.78
Pre	Post	0.5563	Low							0.21	16.78		
Pre	Post	0.5736	Low							0.20	13.15		
Pre	Post	0.9240	Low							0.32	14.34	3.40	0.50
Pre	Post	0.9831	Low							0.26	15.13	3.70	0.49
Pre	Post	0.5218	High	276.86	0.28	12.77	0.40	1.23	0.55	0.19	16.11	2.64	0.34
Pre	Post	0.7540	High	283.07	0.55	15.23	0.84	2.37	0.98	0.21	36.64	5.76	0.38
Pre	Post	0.4945	High	229.25	0.46	9.24	0.77	1.82	0.59	0.25	24.96	5.17	0.48
Pre	Post	0.9259	High	212.96	0.24	7.60	0.46	1.02	0.31	0.26	15.44	3.69	0.52
Pre	Post	0.8452	High	217.49	0.10	8.14	0.25	0.52	0.17	0.25	14.58	3.55	0.55
Inf	Ant	0.7965	Low							0.14	15.86		
Inf	Ant	0.8195	Low							0.14	12.57		
Inf	Ant	0.5911	Low							0.15	17.56	2.64	0.29
Inf	Ant	0.6782	Low							0.14	11.54		
Inf	Ant	0.5473	Low							0.14	3.86	1.43	0.48
Inf	Ant	0.3862	Low							0.06	4.85	1.28	0.39
Inf	Ant	0.6897	Low							0.13	6.99	2.27	0.44
Inf	Ant	0.3495	Low							0.16	8.91	2.66	0.51
Inf	Ant	0.6006	Low							0.10	4.62	1.70	0.45
Inf	Ant	0.4069	Low							0.10	9.05	2.65	0.38
Inf	Ant	0.3452	High	190.63	0.36	3.90	1.02	1.77	0.38	0.25	21.66	3.59	0.89
Inf	Ant	0.4954	High	212.85	0.45	6.22	0.84	1.99	0.69	0.24	28.26	5.12	0.50
Inf	Ant	0.7533	High	197.71	0.21	6.12	0.57	1.14	0.37	0.23	13.08	2.42	0.60
Inf	Ant	0.7330	High	219.05	0.21	9.79	0.35	0.89	0.33	0.25	12.52	2.60	0.49
Inf	Ant	0.7338	High	199.55	0.23	7.71	0.41	0.99	0.35	0.24	11.47	2.98	0.52

Table 20: Continued.

Age	A/P	Thick. (mm)	Strain	τ1 (sec)	σ1 (MPa)	τ2 (sec)	σ2 (MPa)	σi (MPa)	σe (MPa)	εtoe	E (MPa)	σult (MPa)	εult
Inf	Ant	0.4206	High	213.22	0.34	5.48	0.82	1.70	0.54	0.25	20.74	4.52	0.54
Inf	Ant	0.4413	High	202.60	0.42	6.79	0.82	1.98	0.74	0.23	22.71	5.40	0.53
Inf	Ant	0.3763	High	284.19	0.21	13.02	0.30	0.76	0.25	0.24	13.74	2.39	0.45
Inf	Ant	0.4047	High	7.34	0.03	1008.3	0.04	0.07	0.00	0.43	17.75	4.61	0.69
Inf	Post	1.9689	Low							0.22	4.57		
Inf	Post	1.8812	Low							0.10	3.87	0.72	0.27
Inf	Post	1.0557	Low							0.20	13.63		
Inf	Post	0.9705	Low							0.16	16.58		
Inf	Post	1.4254	Low							0.17	3.13	0.50	0.31
Inf	Post	1.5260	Low							0.22	6.55		
Inf	Post	0.9916	Low							0.26	13.65	4.44	0.56
Inf	Post	0.9267	Low							0.14	9.81	3.42	0.52
Inf	Post	1.0707	Low							0.34	10.95	3.59	0.69
Inf	Post	0.9513	Low							0.21	10.75	3.48	0.50
Inf	Post	1.2727	High	180.13	0.19	5.37	0.45	0.93	0.29	0.25	13.58	2.40	0.47
Inf	Post	0.7652	High	203.67	0.41	9.88	0.65	1.56	0.50	0.26	36.11	8.10	0.54
Inf	Post	1.0108	High	251.21	0.22	15.65	0.30	0.76	0.24	0.26	23.56	4.99	0.53
Inf	Post	1.2139	High	241.79	0.15	10.44	0.26	0.56	0.15	0.31	14.62	5.03	0.64
Inf	Post	1.4700	High	223.57	0.09	11.31	0.14	0.30	0.07	0.30	15.68	4.60	0.58
Inf	Post	1.2535	High	245.99	0.15	11.28	0.22	0.51	0.14	0.32	19.13	6.32	0.67
Inf	Post	1.1603	High	205.18	0.19	10.29	0.28	0.63	0.16	0.32	22.26	6.55	0.62
Inf	Post	1.1975	High	299.68	0.08	14.70	0.08	0.20	0.04	0.30	18.49	4.55	0.57
Inf	Post	1.2533	High	287.53	0.03	15.16	0.04	0.08	0.02	0.33	15.01	5.32	0.71
Adu	Ant	0.7685	Low							0.08	30.89	8.81	0.41
Adu	Ant	0.7417	Low							0.06	29.75		
Adu	Ant	0.7929	Low							0.06	5.10	0.69	0.69
Adu	Ant	0.8528	Low							0.02	4.72	0.67	0.77
Adu	Ant	1.4295	Low							0.04	2.74	0.53	0.25
Adu	Ant	1.2655	Low							0.02	1.89	0.09	0.11
Adu	Ant	0.9924	Low							0.10	5.04	1.34	0.38
Adu	Ant	0.9297	Low							0.07	1.25	0.51	1.07
Adu	Ant	0.9631	High	96.92	0.17	1.40	0.76	1.24	0.31	0.23	13.61	1.42	0.51
Adu	Ant	0.6677	High	46.93	0.29	1.15	1.26	1.85	0.29	0.23	14.67	1.72	0.51
Adu	Ant	1.0018	High	67.91	0.04	1.46	0.18	0.29	0.06	0.23	2.35	0.32	0.53
Adu	Ant	0.7118	High	42.62	0.13	0.88	0.64	0.86	0.08	0.24	4.83	0.88	0.83
Adu	Ant	0.9052	High	240.54	0.09	7.41	0.19	0.43	0.15	0.23	14.50	2.29	0.42
Adu	Ant	1.1092	High	229.51	0.09	8.63	0.17	0.38	0.13	0.24	15.17	3.16	0.47
Adu	Ant	0.7209	High	96.81	0.07	1.58	0.23	0.43	0.13	0.24	7.96	0.60	0.49
Adu	Ant	0.8310	High	167.02	0.13	3.32	0.49	1.04	0.42	0.24	13.93	1.88	0.53

Table 20: Continued.

Age	A/P	Thick. (mm)	Strain	τ1 (sec)	σ1 (MPa)	τ2 (sec)	σ2 (MPa)	σi (MPa)	σe (MPa)	εtoe	E (MPa)	σult (MPa)	εult
Adu	Post	2.1424	Low							0.12	2.89	1.59	0.64
Adu	Post	2.1435	Low							0.18	13.63	3.13	0.47
Adu	Post	2.8413	Low							0.21	0.44	0.15	0.65
Adu	Post	2.3421	Low							0.11	0.60	0.20	0.47
Adu	Post	2.0204	Low							0.10	0.60	0.15	0.37
Adu	Post	2.1110	Low							0.08	0.39	0.07	0.27
Adu	Post	2.0241	Low							0.04	0.75	0.22	0.42
Adu	Post	2.1286	Low							0.22	0.59	0.25	0.61
Adu	Post	1.9569	High	107.63	0.04	4.24	0.10	0.19	0.04	0.23	2.91	0.90	1.03
Adu	Post	1.7867	High	105.06	0.04	3.09	0.12	0.21	0.05	0.23	2.39	0.27	0.38
Adu	Post	1.5264	High	140.50	0.02	6.90	0.07	0.14	0.04	0.24	1.84	0.39	0.56
Adu	Post	2.3137	High	123.25	0.02	6.37	0.05	0.11	0.04	0.26	1.45	0.43	0.74
Adu	Post	2.1650	High	151.12	0.03	4.58	0.06	0.12	0.03	0.23	1.31	0.17	0.41
Adu	Post	2.2898	High	778.50	0.03	15.63	0.05	0.10	0.02	0.33	13.08	3.82	0.61
Adu	Post	2.2641	High	239.05	0.03	11.40	0.05	0.10	0.02	0.32	21.56	5.79	0.60
Adu	Post	2.6904	High	46.49	0.02	1.25E6	-1.64	0.03	1.65	0.28	0.29	0.21	1.08
Adu	Post	2.5946	High	85.71	0.05	2.93	0.10	0.20	0.05	0.25	2.69	0.36	0.47

Table 21: Retina data for material property evaluation with age and strain-rate.

Age	Thickness (mm)	Strain-rate	ε_{toe} (mm/mm)	E (MPa)	σ_{ult} (MPa)	ε_{ult} (mm/mm)
Immature	0.1884	Low	0.072666667	0.002071336	0.001592357	0.700766667
Immature	0.1538	Low	0.042833333	0.0055937	0.004334634	0.967916667
Immature	0.1864	Low	0.023883333	0.005151671	0.003576538	0.692983333
Immature	0.2203	Low	0.091966667	0.042361358	0.004690573	0.925016667
Immature	0.1487	Low	0.047683333	0.002916864	0.004259135	1.42435
Immature	0.2141	Low	0.853433333	0.00037845	0.001245524	2.5162
Immature	0.1993	Low	0.101533333	0.002960248	0.00167252	0.783483333
Immature	0.1729	Low	0.124283333	0.00403129	0.002506266	0.707866667
Immature	0.1356	High	0.0587	0.032963443	0.034660767	1.829016667
Immature	0.1523	High	0.049383333	0.013974174	0.017071569	1.159383333
Immature	0.1241	High	0.03795	0.031383592	0.037335482	1.498133333
Immature	0.0878	High	0.0683	0.04361731	0.053151101	1.628233333
Immature	0.1411	High	0.080316667	0.001562605	0.001181195	0.630233333
Immature	0.1459	High	0.290283333	0.002138384	0.001827736	0.9602
Immature	0.1561	High	0.040016667	0.021366552	0.004270767	0.4101
Immature	0.1497	High	0.14005	0.003476381	0.003340013	1.060283333
Immature	0.1529	High	0.240133333	0.002064751	0.002180074	1.17025
Immature	0.0903	High	0.490066667	0.002261419	0.002583979	1.250066667

Table 21: Continued.

Age	Thickness (mm)	Strain-rate	ε_{toe} (mm/mm)	E (MPa)	σ_{ult} (MPa)	ε_{ult} (mm/mm)
Immature	0.1562	High	0.240283333	0.00145276	0.001067008	0.86025
Mature	0.1991	Low	0.064816667	0.003761806	0.002176461	0.556766667
Mature	0.1715	Low	0.068516667	0.002457178	0.003304179	1.206016667
Mature	0.2079	Low	0.055666667	0.005079401	0.005611672	1.217366667
Mature	0.2156	Low	0.23315	0.006395432	0.002782931	0.515133333
Mature	0.204	Low	0.80065	0.02519842	0.017810458	1.208433333
Mature	0.211	Low	0.515716667	0.065505481	0.038704581	0.9935
Mature	0.15129	Low	0.039316667	0.033074829	0.018066847	1.061533333
Mature	0.14506	Low	0.178983333	0.001149583	0.00206811	1.476216667
Mature	0.1182	High	0.058383333	0.002835327	0.006051392	2.718633333
Mature	0.1512	High	0.058116667	0.028462192	0.05026455	2.9382
Mature	0.1485	High	0.068333333	0.035317594	0.042424242	1.568333333
Mature	0.2093	High	0.278483333	0.059293322	0.042681956	1.048316667
Mature	0.1523	High	0.088133333	0.024195373	0.05704918	3.248216667
Mature	0.185	High	0.080166667	0.012681666	0.006306306	0.720233333
Mature	0.1614	High	0.04	0.004458915	0.002478315	0.520083333
Mature	0.1818	High	0.509933333	0.001455202	0.001466813	1.29005

Table 22: Sclera data for postmortem time study.

Age	A/P	Thick. (mm)	PMT (hrs)	τ1 (sec)	σ1	τ2	σ2	σi	σe	εtoe	E	σult	εult
Pre	Ant	0.3998	0-6	267.87	0.94	17.58	1.22	3.18	1.02	0.25	27.26	6.63	0.55
Pre	Ant	0.3366	0-6	261.15	0.56	9.96	0.98	2.58	1.03	0.22	24.41	4.51	0.49
Pre	Ant	0.3725	0-6	222.82	0.25	7.69	0.57	1.23	0.41	0.21	17.07	2.85	0.41
Pre	Ant	0.4243	0-6	484.70	0.04	14.53	0.07	0.14	0.02	0.40	13.71	3.88	0.65
Pre	Ant	0.3437	6-12	274.15	0.26	5.15	0.69	1.64	0.68	0.23	17.00	3.44	0.47
Pre	Ant	0.3782	6-12	193.62	0.39	3.25	1.21	2.53	0.92	0.22	23.49	4.15	0.55
Pre	Ant	0.3774	6-12	261.61	0.19	6.20	0.49	1.10	0.43	0.23	14.75	3.21	0.48
Pre	Ant	0.3437	6-12	219.51	0.34	4.10	0.98	2.01	0.68	0.24	18.76	4.37	0.52
Pre	Ant	0.311	6-12	55.27	0.37	1.11	1.60	2.78	0.81	0.24	10.85	1.65	0.57
Pre	Ant	0.4022	6-12	65.87	0.08	1.49E6	-1.07	0.16	1.16	0.26	0.70	0.26	0.62
Pre	Ant	0.216	12-24	139.80	0.29	4.68	1.12	1.66	0.25	0.25	4.10	1.51	0.71
Pre	Ant	0.3685	12-24	108.42	0.07	3.04	0.23	0.37	0.08	0.23	1.14	0.31	0.91
Pre	Ant	0.3723	12-24	79.42	0.07	1.62E6	-0.97	0.16	1.06	0.24	1.06	0.13	0.47
Pre	Ant	0.3815	12-24	21.44	0.07	5883.41	-0.04	0.10	0.08	0.25	0.45	0.13	0.57
Pre	Ant	0.7044	12-24	260.52	0.06	4.93	0.14	0.25	0.05	0.25	3.20	0.79	0.96
Pre	Ant	0.3316	12-24	1500.58	0.10	35.56	0.14	0.25	0.01	0.37	11.59	3.86	0.73
Pre	Ant	0.4661	12-24	233.94	0.07	7.84	0.11	0.25	0.07	0.28	10.02	3.26	0.60

Table 22: Continued.

Age	A/P	Thick. (mm)	PMT (hrs)	τ1 (sec)	σ1	τ2	σ2	σi	σe	εtoe	E	σult	εult
Pre	Ant	0.3576	12-24	221.60	0.18	6.16	0.58	1.05	0.30	0.24	13.17	2.21	0.50
Pre	Ant	0.4282	12-24	232.64	0.06	5.23	0.18	0.29	0.06	0.24	2.55	1.27	1.07
Pre	Ant	0.4596	>24	227.35	0.10	8.26	0.23	0.48	0.15	0.26	11.34	2.92	0.54
Pre	Ant	0.3441	>24	229.61	0.25	4.41	0.65	1.32	0.42	0.21	11.81	2.26	0.43
Pre	Ant	0.3436	>24	224.98	0.11	5.72	0.27	0.57	0.19	0.21	7.29	1.08	0.38
Pre	Ant	0.4018	>24	212.43	0.15	5.74	0.37	0.78	0.26	0.24	10.76	2.04	0.45
Pre	Ant	0.3796	>24	323.41	0.25	6.68	0.57	1.09	0.27	0.24	7.26	1.14	0.84
Pre	Post	0.5218	0-6	276.86	0.28	12.77	0.40	1.23	0.55	0.19	16.11	2.64	0.34
Pre	Post	0.754	0-6	283.07	0.55	15.23	0.84	2.37	0.98	0.21	36.64	5.76	0.38
Pre	Post	0.4945	0-6	229.25	0.46	9.24	0.77	1.82	0.59	0.25	24.96	5.17	0.48
Pre	Post	0.9259	0-6	212.96	0.24	7.60	0.46	1.02	0.31	0.26	15.44	3.69	0.52
Pre	Post	0.8452	0-6	217.49	0.10	8.14	0.25	0.52	0.17	0.25	14.58	3.55	0.55
Pre	Post	0.7071	6-12	196.99	0.21	6.58	0.46	0.82	0.15	0.23	28.89	9.23	0.60
Pre	Post	0.733	6-12	205.82	0.47	6.58	0.91	1.84	0.47	0.25	22.13	4.32	0.56
Pre	Post	0.588	6-12	211.37	0.56	7.03	0.97	2.15	0.62	0.25	32.26	6.72	0.50
Pre	Post	1.0184	6-12	79.71	0.05	2.26	0.13	0.24	0.06	0.24	1.80	0.37	0.78
Pre	Post	0.999	6-12	103.11	0.05	2.73	0.18	0.33	0.10	0.23	3.72	0.69	0.52
Pre	Post	0.6112	12-24	237.62	0.04	9.23	0.11	0.19	0.05	0.26	1.16	0.42	0.69
Pre	Post	1.0703	12-24	11.98	0.01	160.22	0.00	0.02	0.01	0.28	0.32	0.14	0.88
Pre	Post	0.9483	12-24	293.49	0.01	6.41	0.01	0.02	0.01	0.23	0.21	0.06	1.28
Pre	Post	1.1386	12-24	272.16	0.07	7.63	0.13	0.35	0.15	0.25	4.60	1.35	0.54
Pre	Post	1.0666	12-24	81.18	0.06	1.45E6	-1.83	0.10	1.86	0.25	1.37	0.48	0.83
Pre	Post	0.8160	12-24	77.19	0.14	1.04E6	-3.71	0.18	3.76	0.24	9.17	2.07	0.47
Pre	Post	1.0627	12-24	243.86	0.07	10.67	0.09	0.21	0.05	0.31	13.31	3.01	0.53
Pre	Post	1.0512	12-24	253.99	0.11	15.66	0.13	0.34	0.10	0.28	11.11	2.93	0.54
Pre	Post	1.0754	>24	14.95	0.07	1.50E6	43.90	0.14	-43.84	0.29	12.27	3.36	0.57
Pre	Post	1.0008	>24	219.85	0.04	8.91	0.08	0.16	0.04	0.28	6.52	1.95	0.59
Pre	Post	0.9182	>24	242.22	0.06	8.47	0.14	0.30	0.10	0.24	5.88	1.54	0.52
Pre	Post	1.141	>24	243.45	0.02	8.93	0.05	0.09	0.03	0.37	11.87	3.39	0.62
Pre	Post	0.9612	>24	34.82	0.02	3.12	0.03	0.08	0.03	0.27	1.23	0.36	0.84
Inf	Ant	0.3452	0-6	190.63	0.36	3.90	1.02	1.77	0.38	0.25	21.66	3.59	0.89
Inf	Ant	0.4954	0-6	212.85	0.45	6.22	0.84	1.99	0.69	0.24	28.26	5.12	0.50
Inf	Ant	0.7533	0-6	197.71	0.21	6.12	0.57	1.14	0.37	0.23	13.08	2.42	0.60
Inf	Ant	0.733	0-6	219.05	0.21	9.79	0.35	0.89	0.33	0.25	12.52	2.60	0.49
Inf	Ant	0.7338	0-6	199.55	0.23	7.71	0.41	0.99	0.35	0.24	11.47	2.98	0.52
Inf	Ant	0.4206	0-6	213.22	0.34	5.48	0.82	1.70	0.54	0.25	20.74	4.52	0.54
Inf	Ant	0.4413	0-6	202.60	0.42	6.79	0.82	1.98	0.74	0.23	22.71	5.40	0.53
Inf	Ant	0.3763	0-6	284.19	0.21	13.02	0.30	0.76	0.25	0.24	13.74	2.39	0.45
Inf	Ant	0.4047	0-6	7.34	0.03	1008.29	0.04	0.07	0.00	0.43	17.75	4.61	0.69

Table 22: Continued.

Age	A/P	Thick. (mm)	PMT (hrs)	τ1 (sec)	σ1	τ2	σ2	σi	σe	εtoe	E	σult	εult
Inf	Ant	0.4282	12-24	1639005	14.64	24.57	0.06	0.17	-14.53	0.26	2.82	1.38	0.74
Inf	Ant	0.3614	12-24	56.16	0.18	2.99	0.55	0.90	0.17	0.25	12.64	1.41	0.37
Inf	Post	1.2727	0-6	180.13	0.19	5.37	0.45	0.93	0.29	0.25	13.58	2.40	0.47
Inf	Post	0.7652	0-6	203.67	0.41	9.88	0.65	1.56	0.50	0.26	36.11	8.10	0.54
Inf	Post	1.0108	0-6	251.21	0.22	15.65	0.30	0.76	0.24	0.26	23.56	4.99	0.53
Inf	Post	1.2139	0-6	241.79	0.15	10.44	0.26	0.56	0.15	0.31	14.62	5.03	0.64
Inf	Post	1.47	0-6	223.57	0.09	11.31	0.14	0.30	0.07	0.30	15.68	4.60	0.58
Inf	Post	1.2535	0-6	245.99	0.15	11.28	0.22	0.51	0.14	0.32	19.13	6.32	0.67
Inf	Post	1.1603	0-6	205.18	0.19	10.29	0.28	0.63	0.16	0.32	22.26	6.55	0.62
Inf	Post	1.1975	0-6	299.68	0.08	14.70	0.08	0.20	0.04	0.30	18.49	4.55	0.57
Inf	Post	1.2533	0-6	287.53	0.03	15.16	0.04	0.08	0.02	0.33	15.01	5.32	0.71
Inf	Post	1.7943	12-24	104.53	0.05	5.10	0.05	0.13	0.04	0.19	3.06	0.78	0.45
Inf	Post	1.8312	12-24	174.12	0.10	12.09	0.14	0.37	0.13	0.25	9.13	2.02	0.60
Adu	Ant	0.9631	0-6	96.92	0.17	1.40	0.76	1.24	0.31	0.23	13.61	1.42	0.51
Adu	Ant	0.6677	0-6	46.93	0.29	1.15	1.26	1.85	0.29	0.23	14.67	1.72	0.51
Adu	Ant	1.0018	0-6	67.91	0.04	1.46	0.18	0.29	0.06	0.23	2.35	0.32	0.53
Adu	Ant	0.7118	0-6	42.62	0.13	0.88	0.64	0.86	0.08	0.24	4.83	0.88	0.83
Adu	Ant	0.9052	0-6	240.54	0.09	7.41	0.19	0.43	0.15	0.23	14.50	2.29	0.42
Adu	Ant	1.1092	0-6	229.51	0.09	8.63	0.17	0.38	0.13	0.24	15.17	3.16	0.47
Adu	Ant	0.8015	12-24	347.86	0.04	11.16	0.08	0.17	0.05	0.23	12.30	1.83	0.42
Adu	Ant	1.0058	12-24	236.60	0.05	9.62	0.08	0.19	0.05	0.34	12.84	3.28	0.57
Adu	Ant	1.364	12-24	299.52	0.02	13.01	0.04	0.08	0.02	0.31	10.14	3.65	0.67
Adu	Ant	0.9295	12-24	93.97	0.02	3.60	0.06	0.11	0.03	0.24	1.11	0.31	0.70
Adu	Ant	1.0936	12-24	159.64	0.09	3.43	0.33	0.51	0.09	0.25	4.06	1.27	0.79
Adu	Ant	0.8081	12-24	156.39	0.13	4.16	0.49	1.10	0.48	0.23	17.87	2.97	0.66
Adu	Ant	0.6685	12-24	199.49	0.19	7.20	0.68	1.06	0.19	0.27	7.24	3.31	0.72
Adu	Ant	1.277	>24	158.88	0.01	7.87	0.02	0.04	0.01	0.37	8.78	2.77	0.65
Adu	Ant	0.7112	>24	251.68	0.16	13.57	0.22	0.54	0.16	0.25	11.90	3.70	0.67
Adu	Ant	0.9785	>24	321.47	0.13	17.08	0.17	0.48	0.18	0.23	20.15	3.53	0.46
Adu	Ant	0.7209	>24	96.81	0.07	1.58	0.23	0.43	0.13	0.24	7.96	0.60	0.49
Adu	Ant	0.831	>24	167.02	0.13	3.32	0.49	1.04	0.42	0.24	13.93	1.88	0.53
Adu	Post	1.9569	0-6	107.63	0.04	4.24	0.10	0.19	0.04	0.23	2.91	0.90	1.03
Adu	Post	1.7867	0-6	105.06	0.04	3.09	0.12	0.21	0.05	0.23	2.39	0.27	0.38
Adu	Post	1.5264	0-6	140.50	0.02	6.90	0.07	0.14	0.04	0.24	1.84	0.39	0.56
Adu	Post	2.3137	0-6	123.25	0.02	6.37	0.05	0.11	0.04	0.26	1.45	0.43	0.74
Adu	Post	2.165	0-6	151.12	0.03	4.58	0.06	0.12	0.03	0.23	1.31	0.17	0.41
Adu	Post	2.2898	0-6	778.50	0.03	15.63	0.05	0.10	0.02	0.33	13.08	3.82	0.61
Adu	Post	2.2641	0-6	239.05	0.03	11.40	0.05	0.10	0.02	0.32	21.56	5.79	0.60
Adu	Post	1.6485	12-24	476.10	0.03	13.59	0.05	0.11	0.03	0.28	9.48	2.76	0.58

Table 22: Continued.

Age	A/P	Thick. (mm)	PMT (hrs)	τ1 (sec)	σ1	τ2	σ2	σi	σe	εtoe	E	σult	εult
Adu	Post	1.7947	12-24	259.25	0.02	9.25	0.05	0.10	0.03	0.26	9.31	2.68	0.56
Adu	Post	2.1396	12-24	201.06	0.01	7.44	0.02	0.05	0.02	0.24	10.17	2.34	0.49
Adu	Post	2.941	12-24	124.06	0.02	5.17	0.04	0.08	0.02	0.25	0.88	0.36	0.70
Adu	Post	2.1362	12-24	122.44	0.03	5.45	0.08	0.15	0.04	0.24	1.62	0.50	0.66
Adu	Post	2.5011	12-24	1464739	-2.56	60.25	0.02	0.03	2.58	0.33	1.25	0.57	0.90
Adu	Post	1.9211	>24	202.45	0.03	8.04	0.06	0.17	0.08	0.22	12.61	2.58	0.49
Adu	Post	2.3274	>24	251.45	0.12	15.03	0.17	0.41	0.12	0.25	18.69	4.72	0.53
Adu	Post	1.4954	>24	160.04	0.02	12.54	0.04	0.09	0.03	0.32	16.58	4.75	0.61
Adu	Post	2.6904	>24	46.49	0.02	1.25E6	-1.64	0.03	1.65	0.28	0.29	0.21	1.08
Adu	Post	2.5946	>24	85.71	0.05	2.93	0.10	0.20	0.05	0.25	2.69	0.36	0.47

Table 23: Sclera data for storage condition study.

Age	Storage	A/P	Thick. (mm)	Strain-rate	ε_{toe} (mm/mm)	E (Mpa)	σ_{ult} (Mpa)	ε_{ult} (mm/mm)
Pre	Ant	Fresh	0.4238	Low	0.14	21.91	5.76	0.41
Pre	Ant	Fresh	0.2952	Low	0.95	70.21	19.17	0.52
Pre	Ant	Fresh	0.4815	Low	0.20	12.20	4.82	0.62
Pre	Ant	Fresh	0.5426	Low	0.17	18.51	5.34	0.47
Pre	Ant	Fresh	0.2994	Low	0.10	8.54	2.08	0.38
Pre	Ant	Fresh	0.3875	Low	0.09	11.23	2.38	0.31
Pre	Ant	Fresh	0.389	Low	0.19	7.57	2.50	0.56
Pre	Ant	Fresh	0.4043	Low	0.16	12.64	3.54	0.43
Pre	Ant	Fixed	0.3371	Low	0.11	33.16		
Pre	Ant	Fixed	0.2396	Low	0.13	48.99		
Pre	Ant	Fixed	0.3003	Low	0.02	16.60	2.39	0.17
Pre	Ant	Fixed	0.2592	Low	0.12	46.43		
Pre	Ant	Fixed	0.2612	Low	0.11	55.20	6.69	0.19
Pre	Ant	Fixed	0.2783	Low	0.11	48.10		
Pre	Ant	Fixed	0.3319	Low	0.12	39.37		
Pre	Post	Fresh	0.7015	Low	0.23	24.82	6.95	0.56
Pre	Post	Fresh	0.9215	Low	0.26	16.27	4.36	0.53
Pre	Post	Fresh	0.7213	Low	0.25	20.05	4.70	0.78
Pre	Post	Fresh	0.5563	Low	0.21	16.78		
Pre	Post	Fresh	0.5736	Low	0.20	13.15		
Pre	Post	Fresh	0.924	Low	0.32	14.34	3.40	0.50
Pre	Post	Fresh	0.9831	Low	0.26	15.13	3.70	0.49
Pre	Post	Fixed	0.54	Low	0.08	32.05		
Pre	Post	Fixed	0.5281	Low	0.10	33.47		
Pre	Post	Fixed	0.7347	Low	0.10	20.76		

Table 23: Continued.

Age	Storage	A/P	Thick. (mm)	Strain-rate	ε_{toe} (mm/mm)	E (Mpa)	σ_{ult} (Mpa)	ε_{ult} (mm/mm)
Pre	Post	Fixed	0.7131	Low	0.09	23.05		
Pre	Post	Fixed	0.5283	Low	0.08	34.39		
Pre	Post	Fixed	0.6802	Low	0.08	28.54		
Pre	Post	Fixed	0.6762	Low	0.13	24.69		
Pre	Post	Fixed	0.6645	Low	0.13	27.16		
Infant	Ant	Fresh	0.7965	Low	0.14	15.86		
Infant	Ant	Fresh	0.8195	Low	0.14	12.57		
Infant	Ant	Fresh	0.5911	Low	0.15	17.56	2.64	0.29
Infant	Ant	Fresh	0.6782	Low	0.14	11.54		
Infant	Ant	Fresh	0.5473	Low	0.14	3.86	1.43	0.48
Infant	Ant	Fresh	0.3862	Low	0.06	4.85	1.28	0.39
Infant	Ant	Fresh	0.6897	Low	0.13	6.99	2.27	0.44
Infant	Ant	Fresh	0.3495	Low	0.16	8.91	2.66	0.51
Infant	Ant	Fresh	0.6006	Low	0.10	4.62	1.70	0.45
Infant	Ant	Fresh	0.4069	Low	0.10	9.05	2.65	0.38
Infant	Ant	Frozen	0.6236	Low	0.24	4.50	2.13	0.70
Infant	Ant	Frozen	0.7703	Low	0.11	6.14	1.37	0.31
Infant	Ant	Frozen	0.4359	Low	0.12	6.72	2.11	0.44
Infant	Ant	Frozen	0.4426	Low	0.14	8.18	3.00	0.54
Infant	Ant	Frozen	0.49	Low	0.11	11.68	2.60	0.45
Infant	Ant	Frozen	0.6521	Low	0.04	3.36	1.10	0.42
Infant	Ant	Frozen	0.5472	Low	0.07	4.51	1.46	0.76
Infant	Ant	Frozen	0.8541	Low	0.09	4.78	1.00	0.69
Infant	Ant	Fixed	0.6332	Low	0.07	27.98		
Infant	Ant	Fixed	0.4373	Low	0.14	22.64		
Infant	Ant	Fixed	3728	Low	0.11	41.11	8.96	0.31
Infant	Ant	Fixed	0.3755	Low	0.08	47.82	13.49	0.37
Infant	Post	Fresh	1.9689	Low	0.22	4.57		
Infant	Post	Fresh	1.8812	Low	0.10	3.87	0.72	0.27
Infant	Post	Fresh	1.0557	Low	0.20	13.63		
Infant	Post	Fresh	0.9705	Low	0.16	16.58		
Infant	Post	Fresh	1.4254	Low	0.17	3.13	0.50	0.31
Infant	Post	Fresh	1.526	Low	0.22	6.55		
Infant	Post	Fresh	0.9916	Low	0.26	13.65	4.44	0.56
Infant	Post	Fresh	0.9267	Low	0.14	9.81	3.42	0.52
Infant	Post	Fresh	1.0707	Low	0.34	10.95	3.59	0.69
Infant	Post	Fresh	0.9513	Low	0.21	10.75	3.48	0.50
Infant	Post	Frozen	0.9193	Low	0.22	9.47		
Infant	Post	Frozen	1.3212	Low	0.36	6.70		

Table 23: Continued.

Age	Storage	A/P	Thick. (mm)	Strain-rate	ε_{toe} (mm/mm)	E (Mpa)	σ_{ult} (Mpa)	ε_{ult} (mm/mm)
Infant	Post	Frozen	1.3482	Low	0.22	9.16		
Infant	Post	Frozen	1.2898	Low	0.27	8.27		
Infant	Post	Frozen	2.2681	Low	0.11	1.01	0.31	0.41
Infant	Post	Frozen	2.2515	Low	0.30	1.61	0.58	0.64
Infant	Post	Frozen	2.3884	Low	0.21	0.75	0.44	0.79
Infant	Post	Frozen	2.5043	Low	0.30	1.13	0.28	0.49
Infant	Post	Fixed	0.8787	Low	0.06	25.87		
Infant	Post	Fixed	0.9664	Low	0.08	21.43		
Infant	Post	Fixed	0.784	Low	0.08	53.27	14.10	0.33
Infant	Post	Fixed	0.7036	Low	0.10	58.69	13.65	0.31
Adult	Ant	Fresh	0.7685	Low	0.08	30.89	8.81	0.41
Adult	Ant	Fresh	0.7417	Low	0.06	29.75		
Adult	Ant	Fresh	0.7929	Low	0.06	5.10	0.69	0.69
Adult	Ant	Fresh	0.8528	Low	0.02	4.72	0.67	0.77
Adult	Ant	Fresh	1.4295	Low	0.04	2.74	0.53	0.25
Adult	Ant	Fresh	1.2655	Low	0.02	1.89	0.09	0.11
Adult	Ant	Fresh	0.9924	Low	0.10	5.04	1.34	0.38
Adult	Ant	Fresh	0.9297	Low	0.07	1.25	0.51	1.07
Adult	Ant	Frozen	0.6638	Low	0.07	31.72		
Adult	Ant	Frozen	0.7027	Low	0.09	20.74		
Adult	Ant	Frozen	0.7139	Low	0.06	9.85	2.28	0.57
Adult	Ant	Frozen	0.7403	Low	0.06	5.48	1.19	0.52
Adult	Ant	Fixed	0.7825	Low	0.09	25.77		
Adult	Ant	Fixed	0.6431	Low	0.09	28.99		
Adult	Ant	Fixed	0.9125	Low	0.05	23.22		
Adult	Ant	Fixed	0.7781	Low	0.05	28.82		
Adult	Ant	Fixed	0.5825	Low	0.05	45.67		
Adult	Ant	Fixed	0.6867	Low	0.04	29.31		
Adult	Ant	Fixed	0.7403	Low	0.04	37.09	6.71	0.24
Adult	Ant	Fixed	0.8748	Low	0.07	57.62	12.66	0.29
Adult	Post	Fresh	2.1424	Low	0.12	2.89	1.59	0.64
Adult	Post	Fresh	2.1435	Low	0.18	13.63	3.13	0.47
Adult	Post	Fresh	2.8413	Low	0.21	0.44	0.15	0.65
Adult	Post	Fresh	2.3421	Low	0.11	0.60	0.20	0.47
Adult	Post	Fresh	2.0204	Low	0.10	0.60	0.15	0.37
Adult	Post	Fresh	2.111	Low	0.08	0.39	0.07	0.27
Adult	Post	Fresh	2.0241	Low	0.04	0.75	0.22	0.42
Adult	Post	Fresh	2.1286	Low	0.22	0.59	0.25	0.61
Adult	Post	Frozen	2.0613	Low	0.10	1.24	0.27	0.32

Table 23: Continued.

Age	Storage	A/P	Thick. (mm)	Strain-rate	ε_{toe} (mm/mm)	E (Mpa)	σ_{ult} (Mpa)	ε_{ult} (mm/mm)
Adult	Post	Frozen	2.6438	Low	0.17	0.72	0.28	0.54
Adult	Post	Frozen	2.0267	Low	0.13	1.21	0.32	0.41
Adult	Post	Frozen	2.1161	Low	0.14	0.79	0.20	0.37
Adult	Post	Fixed	1.8588	Low	0.02	10.00		
Adult	Post	Fixed	1.5507	Low	0.06	14.71		
Adult	Post	Fixed	2.2185	Low	0.12	8.32		
Adult	Post	Fixed	2.3606	Low	0.07	6.77		
Adult	Post	Fixed	2.3345	Low	0.05	8.64		
Adult	Post	Fixed	2.3751	Low	0.05	8.29		
Adult	Post	Fixed	1.9333	Low	0.10	30.35	8.27	0.34
Adult	Post	Fixed	2.0559	Low	0.10	42.69	6.18	0.22

Table 24: Retina data for storage condition study.

Age	Storage	Thickness	Strain-rate	ε_{toe} (mm/mm)	E (MPa)	σ_{ult} (MPa)	ε_{ult} (mm/mm)
Immature	Fresh	0.1884	Low	0.0727	0.0021	0.0016	0.7008
Immature	Fresh	0.1538	Low	0.0428	0.0056	0.0043	0.9679
Immature	Fresh	0.1864	Low	0.0239	0.0052	0.0036	0.6930
Immature	Fresh	0.2203	Low	0.0920	0.0424	0.0047	0.9250
Immature	Fresh	0.1487	Low	0.0477	0.0029	0.0043	1.4244
Immature	Fresh	0.2141	Low	0.8534	0.0004	0.0012	2.5162
Immature	Fresh	0.1993	Low	0.1015	0.0030	0.0017	0.7835
Immature	Fresh	0.1729	Low	0.1243	0.0040	0.0025	0.7079
Immature	Frozen	0.2566	Low	0.0765	0.0010	0.0014	2.4693
Immature	Frozen	0.2163	Low	0.4665	0.0009	0.0023	2.5906
Immature	Frozen	0.1589	Low	0.1296	0.0013	0.0025	1.6532
Immature	Fixed	0.225	Low	0.1735	0.0285	0.0138	0.5504
Immature	Fixed	0.21	Low	0.1172	0.0200	0.0084	0.5116
Immature	Fixed	0.2148	Low	0.1213	0.0104	0.0078	0.7163
Immature	Fixed	0.20204	Low	0.1746	0.0102	0.0051	0.6577
Immature	Fixed	0.2407	Low	0.1107	0.0224	0.0061	0.3143
Immature	Fixed	0.2184	Low	0.1121	0.0559	0.0249	0.4821
Immature	Fixed	0.203	Low	0.1918	0.0217	0.0143	0.9143
Immature	Fixed	0.1314	Low	0.1785	0.1094	0.0482	0.5921
Immature	Fixed	0.2227	Low	0.0715	0.0333	0.0084	0.3035
Immature	Fixed	0.2744	Low	0.1635	0.0237	0.0072	0.3560
Immature	Fixed	0.2366	Low	0.1382	0.0440	0.0121	0.3024
Mature	Fresh	0.1991	Low	0.0648	0.0038	0.0022	0.5568
Mature	Fresh	0.1715	Low	0.0685	0.0025	0.0033	1.2060

Table 24: Continued.

Age	Storage	Thickness	Strain-rate	ε_{toe} (mm/mm)	E (MPa)	σ_{ult} (MPa)	ε_{ult} (mm/mm)
Mature	Fresh	0.2079	Low	0.0557	0.0051	0.0056	1.2174
Mature	Fresh	0.2156	Low	0.2332	0.0064	0.0028	0.5151
Mature	Fresh	0.204	Low	0.8007	0.0252	0.0178	1.2084
Mature	Fresh	0.211	Low	0.5157	0.0655	0.0387	0.9935
Mature	Fresh	0.15129	Low	0.0393	0.0331	0.0181	1.0615
Mature	Fresh	0.14506	Low	0.1790	0.0011	0.0021	1.4762
Mature	Frozen	0.1629	Low	0.0979	0.0022	0.0038	2.1273
Mature	Frozen	0.1317	Low	0.9460	0.0012	0.0006	1.3102
Mature	Fixed	0.2141	Low	0.1919	0.0612	0.0286	0.5602
Mature	Fixed	0.2398	Low	0.1087	0.0912	0.0599	0.6234
Mature	Fixed	0.1225	Low	0.1918	0.0935	0.0441	0.5562
Mature	Fixed	0.1966	Low	0.2446	0.1773	0.0665	0.5349
Mature	Fixed	0.1642	Low	0.1608	0.0605	0.0337	0.6313

APPENDIX E

DATA TABLES FOR MATERIAL MODELING AND CONVERGENCE STUDY

Table 25: Normalized shear modulus was computed form the average stress relaxation response for the anterior and posterior sclera. These data were used to define the scleral viscoelastic material responses.

Anterior		Posterior	
Time (sec)	Shear Modulus	Time (sec)	Shear Modulus
1	1	1	1
2.68	0.8677	2.68	0.8872
7.20	0.7419	7.20	0.7651
19.31	0.6374	19.31	0.6483
51.79	0.5517	51.79	0.5437
138.95	0.4757	138.95	0.4470
372.76	0.4074	372.76	0.3640
1000	0.3542	1000	0.3033

Table 26: The stress-strain responses for the anterior and posterior sclera were used to define the scleral hyperelastic material responses.

Anterior		Posterior	
Stress (MPa)	Strain (mm/mm)	Stress (MPa)	Strain (mm/mm)
0	0	0.0000	0
0.0034	0.01	0.0009	0.01
0.0060	0.02	0.0022	0.02
0.0122	0.03	0.0032	0.03
0.0198	0.04	0.0053	0.04
0.0311	0.05	0.0078	0.05
0.0438	0.06	0.0112	0.06
0.0624	0.07	0.0165	0.07
0.0884	0.08	0.0244	0.08
0.1213	0.09	0.0350	0.09
0.1556	0.1	0.0490	0.1
0.2026	0.11	0.0686	0.11
0.2601	0.12	0.0964	0.12
0.3374	0.13	0.1348	0.13
0.4377	0.14	0.1873	0.14
0.5679	0.15	0.2600	0.15
0.7210	0.16	0.3526	0.16
0.8970	0.17	0.4686	0.17
1.0788	0.18	0.5982	0.18
1.2605	0.19	0.7400	0.19
1.4354	0.2	0.8843	0.2

Table 27: Normalized shear modulus was computed form the average creep response for the vitreous. These data were used to define the vitreous viscoelastic material response.

Vitreous	
Time (sec)	Shear Modulus
1	1
1.09854	1.0445
1.20679	1.09207
1.32571	1.13227
1.45635	1.17554
1.59986	1.21482
1.75751	1.2361
1.9307	1.25889
2.12095	1.27343
2.32995	1.28567
2.55955	1.29176
2.81177	1.30403
3.08884	1.33447
3.39322	1.40141
3.72759	1.47719
4.09491	1.55211
4.49843	1.59896
4.94171	1.63785
5.42868	1.68186
5.96362	1.74129
6.55129	1.82232
7.19686	1.88906
7.90604	1.95112
8.68511	2.02633
9.54095	2.11113
10.4811	2.18797
11.514	2.27181
12.6486	2.35029
13.895	2.44949
15.2642	2.54269
16.7683	2.64752
18.4207	2.74647
20.2359	2.85785
22.23	2.97484
24.4205	3.09024
26.827	3.22871
29.4705	3.35487
32.3746	3.47991
35.5648	3.61728
39.0694	3.77636
42.9193	3.91861
47.1487	4.12467
51.7947	4.282
56.8987	4.47049
62.5055	4.65481
68.6649	4.8589
75.4312	5.05315
82.8643	5.29394
91.0298	5.39585

Table 28: A pressure-dependent function was applied to the bottom surface of the ocular model.

Time (sec)	Pressure (MPa)
0	0
0.25	0.000293629
0.5	0.000715528
0.75	0.001137426
1	0.001559325
1.25	0.001981224
1.5	0.002403122
1.75	0.002825021
2	0.00324692

Table 29: Average of top 5% of Lagrangian strains output from FE analysis.

Anterior				
Seed Size	*# Elem.'s*	*Max.Prin.*	*E11*	*E22*
0.1	29120	0.021589	0.019342	0.012369
0.2	9461	0.024997	0.014332	0.017477
0.4	2632	0.024769	0.013254	0.018596
0.6	1168	0.025273	0.012731	0.018682
0.8	552	0.025121	0.011816	0.018308
1	368	0.024093	0.009831	0.017855
Posterior				
Seed Size	*# Elem.'s*	*Max.Prin.*	*E11*	*E22*
0.1	20216	0.025052	0.014576	0.017191
0.2	3493	0.025018	0.014484	0.017229
0.4	1016	0.024829	0.013459	0.018571
0.6	432	0.025344	0.012834	0.018375
0.8	240	0.025192	0.011881	0.018186
1	160	0.024181	0.009872	0.017865